

Investigating Semi-Volatile Organic Compound Emissions from Light-Duty Vehicles

Contract No. 12-318

Prepared for the California Air Resources Board

Principal Investigators

Professor Allen H. Goldstein
Department of Environmental Science, Policy and Management
330 Hilgard Hall, University of California
Berkeley, CA 94720-3114
(510) 643-3788, ahg@nature.berkeley.edu

Professor Allen Robinson
Department of Mechanical Engineering
5000 Forbes Ave, Carnegie Mellon University
Pittsburgh, PA 15213
(412) 268-3657 alr@andrew.cmu.edu

Associate Professor Jesse Kroll
Department of Civil and Environmental Engineering
Room 48-323 Parsons Laboratory, Massachusetts Institute of Technology
Cambridge, MA 02139
617-258-8850 jhkroll@mit.edu

Contributing Researchers

Dr. Greg Drozd, UC Berkeley
Dr. Yunliang Zhao, Carnegie Mellon University
Georges Saliba, Carnegie Mellon University
Dr. Rawad Saleh, Carnegie Mellon University
Dr. Albert Presto, Carnegie Mellon University

February 20, 2017

DISCLAIMER

The statements and conclusions in this Report are those of the contractor and not necessarily those of the California Air Resources Board. The mention of commercial products, their source, or their use in connection with material reported herein is not to be construed as actual or implied endorsement of such products.

ACKNOWLEDGEMENTS

The project team expresses their sincere gratitude to ARB and are very thankful for their support, particularly Hector Maldonado. We also thank all the staff at the Haagen-Smit Laboratory in El Monte, California, for their work with us on the vehicle emission testing.

TABLE OF CONTENTS

Disclaimer.....	i
Acknowledgments.....	ii
Table of Contents.....	iii
List of Figures.....	v
List of Tables.....	viii
1. EXECUTIVE SUMMARY.....	12
1.1 Background.....	12
1.2 Objectives and Methods.....	12
1.3 Results	13
1.4 Conclusions	15
2. INTRODUCTION.....	17
2.1 Background.....	17
2.2 Objectives and Approach.....	20
2.2 References	22
3. MEASUREMENTS	24
3.1 Test Fleet, Fuel and Test Cycle	26
3.2 Measurements of Primary Emissions	28
3.2.1 Measurements of Primary Gases	28
3.2.2 Measurements of Particulate Matter	28

3.2.3 Speciation of NMOG	30
3.2.4 Time resolved measurements of VOC	30
3.2.5 Sampling of IVOCs and SVOCs.....	31
3.2.6 Sampling of IVOCs and SVOCs.....	33
3.2.8 Engine Oil Analysis.....	35
3.2.7 Emission Factors.....	36
3.2.3 Photo-oxidation Experiments.....	36
3.3 References	40
4. High time-resolution measurements of speciated tailpipe emissions from motor vehicles: trends with emission control technology, cold start effects, and speciation...	43
4.1 Introduction	43
4.2 Results and discussion	45
4.2.1 Overall Fleet emissions	45
4.2.1.1 Total Hydrocarbons	45
4.2.1.2 BTEX Compounds	46
4.2.1.3 Differences in BTEX Between Fuel and Exhaust.....	49
4.2.1.4 Incomplete Combustion Products	50
4.2.1.5 Overall VOC Composition.....	51
4.3 Time Resolved Measurements.....	54
4.3.1 Non-oxygenated/Fuel Derived Emissions.....	54
4.3.2 Incomplete Combustion Products.....	57
4.4 Cold Start Emissions	57
4.5 Environmental Implications.....	60
4.6 References.....	62
5. Comparison of GDI and PFI Vehicles	67

5.1 Introduction	67
5.2 Fleet Overview.....	69
5.3 Real Time Measurements	70
5.4 Emission Factors	71
5.5 Results	71
5.5.1 Gas and Particle Phase Emissions.....	71
5.5.2 Particle number emissions and size distributions.....	77
5.5.3.VOC Speciation.....	79
5.5.4 Cold-start versus hot-stabilized emissions.....	82
5.6 Potential Climate Impacts	85
6 References	87
6. Detailed Speciation of IVOC and SVOC: Cold Start Effects and Sources	91
6.1 Introduction	91
6.2 Results and Discussion.....	94
6.2.1 IVOC Emissions	94
6.2.2 IVOC Emissions and Overall Composition.....	94
6.2.3 Relationship Between THC and IVOC Emissions.....	97
6.2.4 Cold Start Effects on IVOC Emissions.....	98
6.2.5 Volatility of IVOC Emissions.....	99
6.2.6 Characterization of IVOC-SRA.....	100
6.2.7 Characterization of Primary Organic Aerosol Emissions.....	103
6.3 Atmospheric Implications.....	104
6.4 References	105
7. Reducing Secondary Organic Aerosol Formation from Gasoline Vehicle Exhaust: Precursors and NO_x Effects.....	110

7.1 Introduction	110
7.2 Results and Discussion.....	113
7.3 Atmospheric Implications.....	124
7.4 References.....	124
8. SUMMARY AND RECOMMENDATIONS.....	127
8.1 Summary	110
8.2 Recommendation on Future Work.....	113
Glossary of Symbols and Acronyms.....	130
Appendices.....	132
Appendix A.....	132
Appendix B.....	153
Appendix C.....	198
Appendix A.....	202

LIST OF FIGURES

Figure 3.1. Experimental setup	24
Figure 4.1. Total hydrocarbon emissions for the complete UC drive protocol.	48
Figure 4.2. The BTEX composition for exhaust from gasoline vehicles.	50
Figure 4.3. Total PTR-MS signal for bag 1 averaged by vehicle class.	54
Figure 4.4 Time resolved PTR-MS measurements of benzene, acetaldehyde, and aliphatic compounds.	56
Figure 4.5. γ values, based on the UC test protocol.	58
Figure 5.1. Distance-based emission factors for a) THC, b) CO, and c) NO _x (as NO ₂)	73
Figure 5.2. PM mass, median EC, and median OM distance-based emission factors (mg/mi) for different vehicle classes. OM:NMOG ratio.	74
Figure 5.3. Average number size distribution for the entire UC cycle of four GDI vehicles	78
Figure 5.4. Detailed speciation of non-methane VOCs.	81
Figure 5.5. Number of miles of hot-stabilized operation to equal cold-start emissions.	84
Figure 6.1. Two-dimensional gas chromatogram.	95
Figure 6.2. The total IVOC emissions for each vehicle class.	96
Figure 6.3. The fraction of IVOC in THC for the complete UC test.	98
Figure 6.4. Comparison of IVOC emission factors for cold-start and combined operation.	100
Figure 6.5. The volatility of IVOC emissions is shown as a function of n-alkane equivalent retention time on the first column.	101
Figure 6.6. Classification of IVOC-SRA across all vehicle classes.	102
Figure 6.7. Composition of POA according to carbon number, double bond equivalents, and branching. Also shown is the used motor oil.	103
Figure 7.1. Emissions and SOA production data from photo-oxidation experiments with diluted gasoline-vehicle emissions.	114

Figure 7.2 Median mass fractions of major NMOG components, Median estimated effective SOA yields, effective SOA yields	116
Figure 7.3. Effective SOA yield as a function of the initial NMOG:NO _x .	121
Figure 7.4. Comparison of distribution of predicted-to-measured SOA for high- and low-NO _x simulations.	123
Figure A1. Comparisons of cold-start total BTEX , benzene , and acetaldehyde emissions as measured by PTR-MS and GC-FID.	150
Figure A2. BTEX emission factors for all vehicle classes for bag 1 (a), bag 2 (b), and bag 3 (c) of the UC protocol, as measured by PTR-MS.	150
Figure A3. Emissions of ketones and aldehydes, measured by LC-MS in mg/mile.	151
Figure A4. BTEX emissions normalized to NMOG emissions.	151
Figure A5. Average mass spectra for all classes of vehicles	152
Figure B1: Fuel economy expressed in miles per gallon (MPG) as a function of vehicle categories.	153
Figure B2: Experimental repeatability for gas-phase species including NO, CO ₂ , CO, and THC.	154
Figure B3: Particle emission factors for: EC, OC, OC:EC ratio, and fraction of speciated particulate matter (PM) to gravimetric PM.	155
Figure B4: Fraction of EC, OC, and sum of ions in total speciated PM as a function of vehicle categories.	156
Figure B5: Composition of primary organic aerosol (POA) as a function of emission certification and engine technology.	157
Figure B6: Scatter plot of particle volume versus gravimetric PM mass for five PFI vehicles	157
Figure B7: Particle number mobility size distributions emission factors for a typical experiment.	158
Figure B8: Average fraction of methane, speciated non-methane volatile organic compounds and unspeciated VOCs.	159

Figure B9: Detailed composition of speciated VOCs as a percentage of total organic gas for methane, C2-C6 paraffins, C7-C12 paraffins, olefins/naphthenes, cyclic olefins, polycyclic naphthenes, single-ring aromatics, polycyclic aromatics, and oxygenated compounds	160
Figure B10: Unspeciated VOCs as a percentage of speciated non-methane organic gas (NMOG), as a function of vehicle class.	161
Figure B11. BTEX emission factors as a function of vehicle categories.	161
Figure B12: Cold-start importance for different gas-phase pollutants as a function of emission certification and engine technology	162
Figure B13: Comparison of filter EC and SP2 refractory BC (rBC) mass concentrations for all vehicle tested in the 2014 campaign.	163
Figure B14: Scatter plot of filter measured organic mass fuel-based emission factors versus AMS measured primary organic aerosol (POA) fuel-based emission factors.	163
Figure B15: CO ₂ and EC distance-based emission factors for vehicles equipped with PFI and GDI engines.	164
Figure B16: Monte Carlo simulation using data from Figure B13.	165
Figure C1. Correlation of IVOC and THC emissions	197
Figure D7.1. Fraction of total oxygenated compounds in NMOG as a function of the fraction of the residual NMOG.	214
Figure D7.3. Time series of gases during chamber experiments.	215
Figure D7.4. NMOG and SOA precursor emission factors for all tested vehicles.	217
Figure D7.5. POA emission factors for all tested vehicles.	218
Figure D7.6. SOA production calculated using different approaches to correct for vapor wall losses in a photo-oxidation experiment for a ULEV vehicle.	219

List of Tables

Table A1. Vehicle and test information for the current study.	135
Table A2. Composition of calibration standard for PTR-MS, concentrations in pbb.	135
Table A3. Test information for current study: total volume, CO, CO ₂ , and THC.	136
Table A4. Test information for current study: BTEX, ethane, and n-pentane.	140
Table A5. BTEX Composition Data from a previous study ¹ used in combination with current data for Figure 4.2.	142
Table A6. Vehicle data and emissions from a previous study ¹ used in combination with current data for for Figure 4.4.	144
Table A7. Vehicle data and emissions from a previous study ¹ used in combination with current data for Figure 4.6.	146
Table A8. Contribution of cold start for US drivers assuming driving patterns similar to the UC protocol.	148
Table A9. Gasoline composition analysis.	149
Table B1: Number of vehicles in each certification category for all vehicles reported	166
Table B2 : Emissions Standards, FTP-75 (g/mi), 50,000 miles/5 years	166
Table B3: Gasoline fuel property and composition analysis	167
Table B4: List of gasoline vehicles from 2014 campaign used in this study	168
Table B5: List of gasoline vehicles used in previous campaigns	169
Table B6: Light-duty gasoline vehicle emissions. Gas phase emissions in (g/mi), particle phase emissions (mg/mi)	171
Table B7: Light-duty gasoline vehicle speciated VOC emissions	196
Table C1: IVOC volatility and classification	
Table D7.1: Summary of the fleet and measurements	220
Table D7.2a: Summary of the surrogate compounds and SOA yields	224
Table D7.2a: Summary of the surrogate compounds and SOA yields	224

1. EXECUTIVE SUMMARY

Background: Organic aerosols (OA) are a major component of fine particulate matter (PM_{2.5}) in all regions of California. OA is directly emitted but is also generated in the atmosphere from reactions of gas-phase precursors that form low-volatility products (secondary organic aerosol, or SOA). SOA is often dominant, even in urban areas. Light-duty vehicles are a major source of air pollutants in urban areas, but their contribution to SOA is uncertain. SOA precursor emissions from newer (LEV-2) gasoline vehicles are substantially lower than older vehicles (LEV-1 or Pre LEV), but smog chamber studies suggest the SOA formation has not been proportionally reduced. California recently adopted LEVIII emissions standards to be phased-in for 2015-2025 models. These new super ultralow emitting vehicles (SULEV) are certified to the most stringent tailpipe emissions standards. It has been proposed that ARB's SULEV standard may effectively control the emissions that lead to SOA, but this has not been directly tested. In addition, the tightening of vehicle fuel economy standards has led to the widespread adoption of gasoline direct injection (GDI) engines. GDI's have higher primary particulate matter emissions, but their contribution to SOA formation is not known.

Objectives and Methods: The objective of this project was to quantify semivolatile and intermediate volatility organic compound (IVOC & SVOC) emissions and SOA formation from a small fleet of in-use vehicles, including SULEVs, GDI, late model larger non-SULEVs, and non-gasoline powered vehicles. Chassis dynamometer tests were done at the ARB Haagen-Smit Laboratory with a comprehensive set of

measurements to quantify the primary emissions, including standard gases, PM mass, PM speciation (ions, OC/EC), SVOCs, and comprehensive speciation of volatile organic compounds (VOCs) including high time resolution for some VOCs using a proton transfer reaction mass spectrometer (PTR-MS). During a subset of the experiments, dilute exhaust was transferred into a smog chamber to quantify SOA formation under urban-like conditions. The combination of measurements and smog chamber experiments enable the evaluation of the effectiveness of the LEVIII standards for reducing motor vehicle emission contributions to ambient PM. We used multiple different complementary techniques to measure SVOC emissions, including state-of-the-art new instruments: a high resolution aerosol mass spectrometer (AMS) to measure particle-phase SVOC; a real-time instrument to quantify gas-and-particle SVOCs with 10-28 carbon atoms; and quartz filter and Tenax TA sorbent samples analyzed via thermal desorption and comprehensive two-dimensional GC with high resolution time of flight mass spectrometry (TD-GCxGC/HR-TOFMS).

Results: Tailpipe emissions of regulated gas-phase pollutants (THC, CO, and NO_x) are lower from vehicles that meet more stringent emissions standards. In addition, there are no statistically significant differences in the composition of the speciated organics, including benzene, toluene, ethylbenzene, and xylenes (BTEX), between port-fuel injection (PFI) and GDI engine technologies. For vehicles certified to the same emissions standards, GDI engines had, on average, a factor of two higher particulate matter (PM) mass emissions compared to PFI engines. The difference is due to higher elemental carbon emissions from GDI vehicles. PM mass emissions from newer SULEV-certified GDIs are lower than older ULEV-certified GDIs suggesting improvements in

GDI engine design. For our test fleet, the 16% decrease in CO₂ emissions from GDI vehicles was much greater than the potential climate forcing associated with higher EC emissions; thus, switching from PFI to GDI vehicles will likely lead to a reduction in net global warming. Real-time measurements were used to investigate the relative importance of cold-start versus hot-stabilized emissions. Hot-stabilized emissions have varying importance depending on species and may require a driving distance of 200 miles to equal the emissions from a single cold start. THC emissions are most sensitive to cold-start, followed by NO_x, CO and POA; elemental carbon emissions are the least sensitive to cold-start. Detailed quantification and characterization of IVOC emissions shows Tier 0 vehicles have about a factor of 10 higher emissions than PZEV vehicles, the composition of IVOC is relatively consistent across vehicle technologies, and 60% of IVOC mass is attributed to aromatic compounds. IVOC contribute, on average, 3% of THC emissions. Cold start IVOC emissions are between 2-6 times that of hot-running emissions, showing a weaker cold start effect compared to VOCs. Predictions of potential SOA formation based solely on single ring aromatics and IVOC emissions give a consistent effective SOA yield of 10% across all vehicle categories, suggesting that the composition of emissions does not drive changes in SOA formation across vehicle classes. SVOC are emitted mainly as POA, have the same composition as the vehicles motor oil, correlate well with OC/EC measurements, and are dominated by cyclic aliphatic compounds. We investigated SOA formation from dilute, ambient-level exhaust from a subset of the fleet using a smog chamber. We measured lower SOA formation from newer vehicles that meet more stringent emissions standards than from older vehicles. SULEV vehicles had the lowest SOA production, comparable to that measured

during dynamic blank experiments when the chamber was only filled with dilution air. Therefore, the gradual replacement of vehicles with newer vehicles that meet more stringent emissions standards should lead to lower SOA levels in California. However, we found a strongly nonlinear relationship between SOA formation and the VOC-to-NO_x ratio with the effective SOA yield for exhaust from gasoline vehicles a factor of 8 higher at low NO_x conditions. SOA formation from gasoline vehicle exhaust can be explained if one accounts for all precursors (VOCs, IVOCs, and SVOCs) and NO_x effects. The strong NO_x dependence also appears to explain higher effective yields measured from newer vehicles reported by previous studies. We investigated the implications of the strong NO_x dependence for the Los Angeles area. Although organic gas emissions from gasoline vehicles are expected to fall by almost 80% in Los Angeles over the next two decades, we predict there will be little to no reduction in SOA production from vehicle exhaust due to the rising atmospheric VOC-to-NO_x ratio. This highlights the importance of an integrated emission control policies for NO_x and organic gases.

Conclusions: The major conclusions of this work are that SULEV-certified vehicles have lower emissions and dramatically lower SOA production than vehicles meeting less-stringent emissions standards. SOA formation from gasoline vehicle exhaust can be quantitatively explained if one accounts for all precursors (VOCs, IVOCs, and SVOCs) and NO_x effects. However, the strong NO_x dependence of SOA formation means that there may be little to no reduction in SOA production from vehicle exhaust due to the rising atmospheric VOC-to-NO_x ratio. Recommendations for future study include characterization of the effects of different drive cycles on emissions and SOA production; characterization of emissions and SOA production from high-mileage

SULEV-certified vehicles; quantification of emissions from non-vehicular sources such as petroleum based consumer products that are highly utilized in urban areas; quantification of SOA formation, including NO_x effects, from a comprehensive set of IVOCs, including different alkyl-benzenes; and incorporation of new emissions (especially IVOC and SVOC) into inventories and models.

2. INTRODUCTION

2.1 Background

Los Angeles and other parts of California are designated non-attainment for fine particulate matter (PM_{2.5}). Organic aerosols (OA) are a major component of PM_{2.5} in all regions of California; however, its sources are not well understood. OA is directly emitted to the atmosphere (primary organic aerosol or POA) from a large number of sources (e.g., fossil fuel combustion, biomass combustion). It is also generated in the atmosphere from reactions of gas-phase precursors that form low-volatility products (secondary organic aerosol, or SOA). Multiple field studies indicate that SOA contributes the dominant fraction of OA, even in heavily urbanized areas such as the Los Angeles Basin [1-6]. However, the sources of these SOA precursors are not well understood.

Light-duty vehicles are a major source of air pollutants in urban areas such as Los Angeles. Both field and experimental studies suggest that their emissions are a major source of SOA precursors and ultimately ambient PM_{2.5}. For example, members of this research team recently conducted experiments in collaboration with ARB to quantify the SOA formation from a fleet of vehicles recruited from the California in-use fleet (15 gasoline and 5 diesel). Substantial SOA formation was measured in both dilute diesel and gasoline vehicle exhaust. This SOA could not be explained by traditional aerosol chemistry models, but was linked to unspiciated emissions of semivolatile organic compounds (SVOC). Although hydrocarbon emissions from newer (LEV-2) gasoline vehicles are substantial lower than older (LEV-1 or Pre LEV), there was not a

proportional reduction in the measured SOA formation. Recent analysis of the CalNex dataset also suggests that gasoline vehicle exhaust may be a major contributor to SOA in the Los Angeles basin [7], but this result remains controversial and requires further study.

California recently adopted the LEVIII emissions standards which are to be phased-in over the 2015-2025 model years. It has been proposed that vehicles certified to the ARB's super ultralow emitting vehicle (SULEV) standards may be effective in controlling the emissions that lead to SOA. SULEVs are certified to the most stringent tailpipe emissions standards (e.g., 10 mg/mile NMOG for LEV-2 and 20 mg/mi for NMOG + NO_x for LEVIII) with a durability requirement of 150,000 miles. During our previous study we randomly procured and tested a single SULEV (out of 25 LEV-2 vehicles); this vehicle had very low tailpipe emissions, but smog chamber experiments were not conducted to quantify the SOA formation. In addition, it is not certain to what extent this trend extends to the entire in-use fleet, including larger vehicles such as SUVs and pickup trucks, which may be subject to less stringent standards as part of the LEVIII regulation.

The objective of this contract was to quantify the SVOC emissions and SOA formation from a small fleet of in-use vehicles, including SULEV technology vehicles (new, low mileage vehicles and end-of/past-end-of useful life mileage), gasoline direct injection vehicles, late model larger, non-SULEV vehicles, and non-gasoline powered vehicles. The project was based on conducting chassis dynamometer tests to characterize the SVOC emissions and SOA formation from a fleet of in-use vehicles at the ARB Haagen-Smit Laboratory. The overall project design leverages expertise of ARB

scientists, University of California Berkeley, Carnegie Mellon University, and the Massachusetts Institute of Technology.

The fleet was chosen to specifically investigate the potential effectiveness of the new LEV_{III} standards at reducing SVOC emissions and SOA formation from motor vehicles. During every test, a comprehensive set of measurements were performed to quantify the primary emissions, including standard gases, PM mass, PM speciation (ions, OC/EC), SVOCs, and comprehensive speciation of volatile organic compounds (VOCs). During a subset of the experiments, dilute exhaust was also transferred into a smog chamber to quantify the secondary organic aerosol (SOA) formation under urban-like conditions. The combination of the speciated VOC measurements, comprehensive SVOC measurements and smog chamber experiments enable the evaluation of the effectiveness of the latest standards (LEV_{III}) for reducing the contribution of motor vehicle emissions to ambient PM.

We also used multiple different techniques to measure SVOC emissions. The measurements represent different (though complementary) approaches, including state-of-the-art instruments. A high resolution aerosol mass spectrometer (AMS) was used to measure particle-phase SVOC emissions directly from the CVS. The second estimate is the difference between the measured NMOG emissions and the sum of speciated organics smaller than 10 carbons. The third approach is a real-time instrument developed by the Kroll group at MIT in partnership with Aerodyne Research. It is similar to an AMS, except that it employs a cryogenic inlet that quantitatively collects both gas-and-particle SVOCs with 10-28 carbon atoms. Finally, researchers from UC Berkeley collected quartz filter and Tenax TA sorbent samples for analysis via thermal desorption and

comprehensive two-dimensional GC with high resolution time of flight mass spectrometry (TD-GCxGC/HR-TOFMS). We combined results from each of these approaches to comprehensively characterize vehicle emissions from the chassis dynamometer tests.

The SOA formation from a subset of the test fleet was also investigated using a portable smog chamber. A suite of real-time instrumentation was used to characterize the evolution of the gas and particle phase emissions inside the chamber. The data from the smog chamber experiments were corrected for wall losses to quantify the mass of SOA formation in each experiment.

2.2 Objectives and Approach

This was a collaborative research project between UC Berkeley, Carnegie Mellon University, MIT, and the California Air Resources Board to:

1. Characterize SVOC and other pollutant emissions from a small (~ 25) fleet of in-use vehicles (light- and medium-duty) operated over hot- and cold-start test cycles. Approximately half of this fleet was super ultra-low emission vehicle (SULEV) technology passenger cars – half late-model, low-mileage vehicles and half high-mileage end-of-useful-life vehicles. The remainder of the fleet was late-model-year, non-SULEV vehicles of various ages and emissions standards and non-gasoline powered vehicles.
2. Evaluate the performance of different techniques to quantify SVOC emissions.

3. Quantify the SOA formation from dilute emissions from a subset of vehicles inside a smog chamber under urban-like conditions; and
4. Measure SVOC emissions and SOA formation from SULEV certified vehicles, both for new as well as older SULEVs at the end of their useful lives.

The project involved chassis dynamometer tests for the characterization of SVOC and other emissions and SOA formation from a fleet of in-use vehicles at the ARB Haagen-Smit Laboratory. The approach used followed the same framework as used by our previous ARB/CRC/EPA supported Linking-Tailpipe-to-Ambient project. The overall project design leverages vehicle testing expertise of ARB scientists, SVOC measurements of the Robinson, Goldstein and Kroll groups, and smog chamber expertise of the Robinson and Kroll groups. Vehicles were recruited from the in-use California fleet and operated with commercial fuels over standard test cycles. The experiments included comprehensive characterization of the primary emissions: standard gases, PM mass, PM speciation (ions, OC/EC, and molecular markers), SVOCs, and comprehensive organic speciation. We also evaluate and compare different techniques to measure VOC and SVOC emissions. Smog chamber experiments were conducted with dilute exhaust to measure secondary organic aerosol (SOA) formation under urban-like conditions. The combination of the detailed SVOC measurements and smog chamber experiments enable the evaluation of the effectiveness of the latest standards (LEVIII) for reducing the contribution of motor vehicle emissions to ambient PM.

Specific Tasks completed during this project:

Task 1 Vehicle Testing Campaign Preparation and Execution

Task 2 Measurements of VOC/IVOC/SVOC/PM

Task 3 Measurements of SOA

Task 4 Data Analysis

Task 5 Final Report

The report includes a chapter (3) describing the site for vehicle testing, vehicle selection, measurements of vehicle emissions, and smog chamber SOA experiments. Subsequent chapters describe results and interpretation including (4) High time-resolution measurements of speciated tailpipe emissions from motor vehicles including trends with emission control technology, cold start effects, and speciation; (5) Emissions and climate impact of Gasoline Direct Injection (GDI) and Port Fuel Injection (PFI) engines; (6) Comprehensive characterization of IVOC and SVOC emissions; (7) Reducing SOA formation from gasoline vehicle exhaust focusing on precursors and NO_x effects; and a final chapter (8) that summarizes conclusions and recommendations.

2.3 References

1. Zhang, Q., et al., Hydrocarbon-like and oxygenated organic aerosols in Pittsburgh: insights into sources and processes of organic aerosols. *Atmospheric Chemistry and Physics*, 2005. **5**: p. 3289-3311.
2. Zhang, Q., et al., Ubiquity and dominance of oxygenated species in organic aerosols in anthropogenically-influenced Northern Hemisphere midlatitudes. *Geophysical Research Letters*, 2007. **34**(L13801): p. doi:10.1029/2007GL029979.
3. Subramanian, R., et al., Insights into the primary-secondary and regional-local contributions to organic aerosol and PM_{2.5} mass in Pittsburgh, Pennsylvania. *Atmospheric Environment*, 2007. **41**(35): p. 7414-7433.
4. Shrivastava, M.K., et al., Sources of organic aerosol: Positive matrix factorization of molecular marker data and comparison of results from different source apportionment models. *Atmospheric Environment*, 2007. **41**: p. 9353–9369.
5. Docherty, K.S., et al., Apportionment of Primary and Secondary Organic Aerosols in Southern California during the 2005 Study of Organic Aerosols in

- Riverside (SOAR-1). *Environmental Science & Technology*, 2008. **42**(20): p. 7655-7662.
6. Sheesley, R.J., et al., Trends in secondary organic aerosol at a remote site in Michigan's upper peninsula. *Environmental Science & Technology*, 2004. **38**(24): p. 6491-6500.
 7. Bahreini, R., et al., Gasoline emissions dominate over diesel in formation of secondary organic aerosol mass. *Geophysical Research Letters*, 2012. **39**(6): p. L06805.

Chapter 3

3. Measurements

Tailpipe emissions from a fleet of on-road vehicles and their SOA production have been investigated during dynamometer testing at the California Air Resources Board's (CARB) Haagen-Smit Laboratory. The test fleet consisted of 20 on-road gasoline vehicles, spanning a wide range of model years and after treatment technologies. All of these vehicles were tested for primary emissions. A subset of these vehicles ($n=14$) was also tested for SOA formation in a smog chamber. Figure 3.1 shows the experimental setup and summarizes the measurements conducted in this study. Table 3.1 compiles information about the vehicle test fleet and test cycles. Detailed description of the experimental setup and procedure has been provided elsewhere [Gordon *et al.*, 2014; May *et al.*, 2014]. Only a brief discussion is provided here.

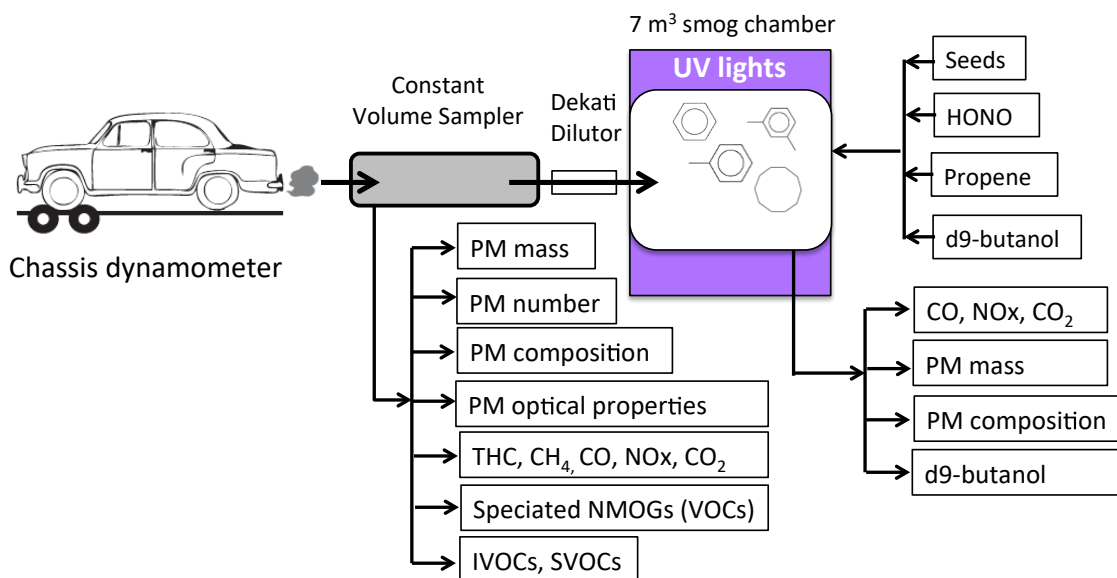


Figure 3.1 Schematic of the experimental setup and summary of measurements

Table 3.1. Test fleet and test cycle.

Test ID	Vehicle#	Vehicle Class	Model Year	Engine displacement (L)	Emission Standard	Fuel Economy (mpg)*	Test Cycle
1038708	20	PC	2012	2	SULEV	23.76	UC
1038722	20	PC	2012	2	SULEV	27.88	UB1B
1038723	30	PC	2014	3.5	L2SUL	19.85	UC
1038724	31	PC	2012	2.4	SULEV	20.75	UC
1038745	1	PC	2013	1.6	PZEV	20.59	UC
1038747	23	PC	2013	1.4	PZEV	36.72	UC
1038749	20	PC	2012	2	SULEV	38.32	MAC 4
1038750	30	PC	2014	3.5	L2SUL	19.07	UC
1038755	24	PC	2012	2.5	PZEV	35.17	UC
1038757	31	PC	2012	2.4	SULEV	21.11	UC
1038760	24	PC	2012	2.5	PZEV	34.39	UC
1038763	24	PC	2012	2.5	PZEV	35.41	UB1B
1038797	23	PC	2013	1.4	PZEV	32.35	UC
1038799	31	PC	2012	2.4	SULEV	32.18	MAC 4
1038801	35	PC	2013	1.6	ULEV	27.51	UC
1038820	35	PC	2013	1.6	ULEV	27.84	UC
1038821	18	PC	2008	3.9	L2LEV	15.80	UC
1038822	36	PC	2013	1.6	L2ULV	23.66	UC
1038823	37	PC	2013	2	ULEV	18.65	UC
1038824	4	LDT	2013	5.3	ULEV	12.78	UC
1038825	38	PC	2012	1.6	L2LEV	24.48	UC
1038827	27	PC	2013	2	L2ULV	26.32	UC
1038848	18	PC	2008	3.9	L2LEV	15.76	UC
1038849	18	PC	2008	3.9	L2LEV	15.21	UC
1038850	36	PC	2013	1.6	L2ULV	23.48	UC
1038853	21	PC	2014	2.4	PZEV	6.84	UC
1038854	21	PC	2014	2.4	PZEV	36.72	MAC 4
1038862	28	PC	2013	3.6	L2SUL	16.86	UC
1038864	5	PC	2007	1.3	L2SUL	31.95	UC
1038867	29	PC	2012	2.4	PZEV	21.55	UC
1038868	21	PC	2014	2.4	PZEV	22.50	UC
1038869	28	PC	2013	3.6	L2SUL	16.55	UC
1038870	9	M3	2003	5.4	LEV	16.83	MAC 4
1038871	9	M3	2003	5.4	LEV	17.55	MAC 4

Test ID	Vehicle#	Vehicle Class	Model Year	Engine displacement (L)	Emission Standard	Fuel Economy (mpg)*	Test Cycle
1038885	5	PC	2007	1.3	L2SUL	34.18	UC
1038891	9	M3	2003	5.4	LEV	11.43	UC
1038901	14	PC	1990	3.8	TIER0	17.65	UC
1038902	14	PC	1990	3.8	TIER0	24.40	MAC 4
1038909	37	PC	2013	2	ULEV	19.42	UC
1038911	9	M3	2003	5.4	LEV	11.12	UC
1038912	14	PC	1990	3.8	TIER0	17.48	UC
1038915	37	PC	2013	2	ULEV	18.71	UC
1038916	37	PC	2013	2	ULEV	30.86	MAC 4
1038917	4	LDT	2013	5.3	ULEV	12.93	UC
1038918	4	LDT	2013	5.3	ULEV	12.62	UC
1038919	4	LDT	2013	5.3	ULEV	19.98	MAC 4
1038920	21	PC	2014	2.4	PZEV	23.39	UC
1038922	15	M3	1990	5.0	TIER1	17.06	MAC 4
1038945	4	LDT	2013	5.3	ULEV	12.60	UC
1038947	36	PC	2013	1.6	L2ULV	23.81	UC
1038952	28	PC	2013	3.6	L2SUL	17.57	UC

*measured during the test cycle.

3.1 Test Fleet, Fuel and Test Cycle

For discussion, the 20 tested vehicles were categorized into four groups based on emission certification standards as 2 Pre-LEV vehicles (Tier0 and Tier1), 3 LEV vehicles (transitional low emission vehicles and low emission vehicles) and 5 ULEV vehicles (Ultra-low emission vehicles) and 10 SULEV vehicles (Super ultra-low and partial zero emission vehicles). The number of tests was greater than the number of vehicles because of repeated tests for some of the vehicles. The SULEV category includes both port and direct injection vehicles. SULEV vehicles meet the most stringent emissions standard under the California LEV II regulations and comparable to the fleet average emission factor (NMOG+NO_x) under the California LEV III regulations in model year 2015.

Our categorization reflects reductions in emissions due to the tightening of emissions standards. Our recruitment of vehicles not only enabled us to investigate the emissions from on-road gasoline vehicles during the phase-in period and implantation of California LEV III regulations by testing ULEV and SULEV vehicles. Furthermore, our vehicle fleet provided an opportunity to compare results from our present study with published results, which focused on Pre-LEV, LEV and ULEV vehicles, to systematically examine the effectiveness of increasingly stringent emission regulations at reducing both primary organic emissions and their SOA formation.

All vehicles were tested using the same California commercial summer gasoline fuel. The fuel composition is presented in Table A9.

All vehicles were tested over a cold-start Unified Cycle (UC). A subset of vehicles was also tested over the model arterial cycle 4 (MAC4) and US06 to investigate the emissions of vehicles under different driving conditions. The UC is designed to simulate the driving in the Sothern California. The UC consists of three bags, similar to the Federal Test Procedure (FTP)-75, but is a more aggressive cycle with higher speeds, higher acceleration, fewer stops and less idling time. In comparison to the cold-start UC, both the MAC4 and UB1B only have one bag and are hot-start cycles with much higher average speeds (55.2 mph for the MAC4 and 48.1 mph for UB1B versus 22.4 mph for UC).

3.2 Measurements of Primary Emissions.

The entire exhaust from a gasoline vehicle during each test was diluted in a constant volume sampler (CVS, Horiba-7200 SLE) using clean air treated by high efficient particulate filters, nominally following the procedures outlined in Code of Federal Regulations Title 40, Chapter 1, Subchapter C, Part 86 [USGPO, 2014]. Comprehensive characterization of primary emissions was carried out by directly sampling the dilute exhaust from the CVS using an AVL-AMA 4000 system (EC/OC, PM mass, water-soluble ions, metals, THC, CH₄, NO_x, CO₂ and CO, speciated NMOG) and customized sampling systems (IVOCs, SVOCs, PM number size distributions, and optical properties of PM) (Figure 3.1).

3.2.1 Measurements of Gases

Gas-phase organics were measured by flame ionization detection (FID), methane by gas chromatography (GC)-FID, NO_x by chemiluminescence and CO and CO₂ by nondispersive infrared detection. The gas-phase organics include both hydrocarbons and oxygenated compounds. Therefore, for discussion, we define the organics measured by FID as organic gases. Non-methane organic gases (NMOG) were defined as the difference between total organic gases and methane. However, one should note that the amount of oxygenated compounds measured by FID was underestimated [Scanlon and Willis, 1985] because the FID was calibrated with a methane/propane blend. The gas-phase measurements were made by UC phase and corrected for background concentrations in the dilution air.

3.2.2 Measurements of Particulate Matter

Particle-phase emissions were collected using three filter trains operating in parallel. Train 1 contains a single Teflon filter (47 nm, Paul-Gelman, Teflo R2PJ047) that was used to determine gravimetric PM mass [CARB, 2011a]. Train 2 contains two quartz filters (47 nm, Paul-Gelman, Tissuquartz 2500 QAOUP) in series. Train 3 contains a Teflon filter followed by a quartz filter for artifact corrections. Teflon filters in Train 1 were analyzed by ion chromatography for water soluble anions (chloride, nitrate and sulfate) and cations (sodium, ammonium, potassium, magnesium and calcium) [CARB, 2011b]. All quartz filters were analyzed for organic and elemental carbon (OC and EC) [CARB, 2011c]. Teflon filters were pre- and post- weighted in a temperature and humidity controlled room to determine gravimetric PM mass emissions [CARB, 2011a].

Real-time measurements of PM were also performed during this campaign in addition to off-line filter measurements. Particle number distributions from 5.2 and 523 nm, were measured by directly sampling from the CVS using a fast response Engine Exhaust Particle Sizer (EEPS, TSI Inc.) [Ayala and Herner, 2005].

A Single Particle Soot Photometer (SP2, Droplet Measurements Techniques Inc.) [Moteki and Kondo, 2010; Schwarz et al., 2006] was used to measure real-time refractory black carbon (rBC) mass and number concentrations inside the CVS. The SP2 was calibrated prior to the campaign using Fullerene soot [Gysel et al., 2011].

The nonrefractory submicron particle mass and chemical composition were measured by a high-resolution time-of-flight aerosol mass spectrometer (HR-tof-AMS, Aerodyne, Inc., MA).

3.2.3 Speciation analysis of NMOG

Speciation analysis of NMOG was performed for most tests. The dilute exhaust was sampled from the CVS into Tedlar[®] bags and analyzed by GC using CARB test methods MLD 102 and 103[Maddox, 2007]. More than 200 species were quantified, which spanned the carbon number range of 2 to 12 and covered the major classes of hydrocarbons, including straight-alkanes (*n*-alkanes), branched alkanes (*b*-alkanes), alkenes, cycloalkanes, single-ring aromatic compounds. For discussion, we define these speciated NMOG as speciated volatile organic compounds (VOCs). The difference between total NMOG and speciated VOCs during each test was defined as unspeciated NMOG. Oxygenated compounds, including alcohols, aldehydes and ketones, were quantified using the CARB test methods MLD 101 and 104[CARB, 2005; 2006].

3.2.4 Time resolved measurements of VOC

Diluted exhaust was sampled from the CVS into a proton transfer reaction mass spectrometer (PTR-MS) using a heated 1/2 in. diameter transfer line made of passivated stainless steel followed by an unheated, 1/8 in. diameter passivated steel tube. Prior to the PTR-MS the emissions were further diluted by a factor of 10-100 using filtered air. This second stage of dilution was required to ensure that the reagent H₃O⁺ ions were not significantly depleted in the PTR-MS. The PTR-MS measured gas-phase compounds with a quadrupole mass analyzer (Ionicon Analytik). A 6 second scan was used to cover all masses from 21-140. Monitoring the signal for water clusters (i.e. humidity) showed that the instrument responded faithfully to engine activity, as water is always produced from combustion.

The PTR-MS was calibrated using a custom mix of standard gases (Scott-Marin Gases) and a custom built calibration unit with a platinum catalyst to provide VOC-free air for accurate dilution of the standard. Measurements during drive cycles were background subtracted and quantified. The PTR-MS data generally agreed to within 30-40% of standard GC/LC measurements by ARB, described above (Figure A1). Due to sample analysis considerations, the dataset for PTR-MS, which is obtained in real-time, included more experiments (48) than the GC-FID measurements (13).

3.2.5 Sampling and analysis IVOCs and SVOCs

IVOC and SVOC were sampled similarly to previous studies. [May et al .2014, Zhao 2016] Emissions were sampled through two sample trains of a single connection to the CVS. The first train consisted of a Teflon filter (47 mm, Pall-Gelman, Teflo R2PJ047) followed by a quartz filter (47 mm, Pall-Gelman, Tissuquartz 2500 QAOUP) in series. The second train consisted of a quartz filter followed by two sets of Tenax-TA sorbent tubes (Gerstel). The first set of sorbent tubes was connected in parallel to the sampling line. One of these tubes was used to collect gaseous emissions during the cold start phase of operation, and the other tube was used to sample emissions during the combined hot-running and hot start phases. The second set of sorbent tubes was connected in series to the sampling line to collect total UC test emissions. The flow rate through each train was 47 L min^{-1} . This sampling train was housed in a heated enclosure ($47 \pm 5 \text{ }^\circ\text{C}$) mimicking the CFR86 protocol.

Dynamic blanks were collected for both filters and adsorbent tubes when the CVS was operated on dilution air, without vehicle exhaust, for the same period as a standard driving cycle. Prior to sampling, the quartz filters were pre-fired at $550 \text{ }^\circ\text{C}$ in air for at

least 12 h and adsorbent tubes were thermally regenerated at 320 °C in the helium flow to reduce their organic background. After sampling, the quartz filters and adsorbent tubes were stored at -24 °C until analysis.

Both sorbent tubes and filters were analyzed using thermal desorption gas chromatography with mass spectrometry. Filters were subsampled for organic analysis using punches (0.4 cm²) that were then loaded into a thermal desorption and autosampler system (TDS3 and TDSA2; Gerstel Inc.) and heated to 300 °C under helium flow to transfer to a nitrogen cooled inlet for cryo-focusing on a quartz wool inlet liner (CIS4, Gerstel, Inc.) at -25 °C. Sorbent tubes were desorbed in a similar manner, but heating only up to 275°C. Injection into the GC column was achieved by rapid heating of the cooled injection system (CIS) (10 °C s⁻¹) up to 320 °C under a flow of helium. Analytes were separated in two chromatographic dimensions (2D-GC) using an Agilent 7890 GC equipped with a non-polar primary column (60 m × 0.25 mm × 250 μm Rxi-5Sil-MS, Restek) and a secondary column (1 m Rtx-200, Restek) using a flow rate of 2 mL min⁻¹ helium. The GC temperature program was 40 °C with 5 min hold, 3.5 °C min⁻¹ up to 320 °C, and a final hold at 320 °C for 10 min. Following GC separation, analytes were ionized using standard electron impact ionization (EI) and a vacuum-ultraviolet (VUV) photon beam at 10.5 eV.[Isaacman et al. 2012] Analytes were detected using a time-of-flight (ToF) mass spectrometer (TOFWERK) operated in positive mode with a resolving power of $m/\Delta m \approx 4000$. Data were collected at 100 Hz and signal averaged to 0.5 Hz. The ion source was operated at the reduced temperature of 170 °C to minimize fragmentation with VUV ionization and 270 °C with EI ionization to better maintain volatilization of the GC effluent. The VUV photon flux of $\sim 10^{16}$ photons cm⁻²·s was

generated by the Chemical Dynamics Beamline 9.0.2 of the Advanced Light Source at Lawrence Berkeley National Laboratory.

3.2.5 Quantification of IVOC and SVOC

Our calibration methods for quantification of samples analyzed with GV-VUV-MS are based on the method used in Worton et al. 2015, Isaacman et al. 2012, and Chan et al 2013. The molecular ion signals for linear, branched, cyclic, and aromatic hydrocarbons under VUV ionization are used as the basis for quantification. Sensitivity of the molecular ion for any given compound is a function of its thermal transfer efficiency, ionization efficiency, and degree of fragmentation. For molecules with a given carbon number, the molecular ion signal increases with increasing number of double bond equivalency (NDBE) because of reduced fragmentation. Authentic standards of more than 80 compounds were used for calibration; these included n-alkanes, branched alkanes, n-alkyl cyclohexanes, n-alkyl benzenes, hopanes, steranes, PAHs, and alkylated PAHs. These species were selected to span both carbon number and NDBE ranges of the diesel samples. This yields NDBE-specific calibration curves for NDBE = 0, 1, 4, and 7+ due to limited availability of authentic standards for the other NDBE's. The previous work referenced has shown that intermediate NDBE sensitivities can be interpolated.

Thermal transfer efficiency is not linear with carbon number because early and late eluting components have lower efficiency for transfer than intermediate eluting components. A series of perdeuterated n-alkanes (even carbon numbers from C8-C34) was added as an internal standard to all samples to generate a relationship between thermal transfer and retention time.

Total analytical uncertainty includes contributions from transfer efficiency, structural differences in fragmentation within a NDBE class, and uncertainties in calibration curves. The uncertainty in calibrating response to mass, determined from calibration curves of authentic standards, was structurally and mass- dependent with larger uncertainties for lower NDBE species and smaller mass fractions. The total analytical uncertainty was < 40% for all species at mass fractions above 0.1%, increasing to <70% at mass fractions below 0.01%. Blanks run without any sample injection showed that background levels were negligible compared with observed levels of analytes in the samples. Repeat analyses showed analytical precision was < 25% for each compound class.

The quantification of IVOC is similar to that of Zhao et al. (2016), except adapted for 2D-GC methods. Slightly different methods were applied to quantify the material that fell into three categories: aliphatic, single ring aromatics (SRA), and polar material. All three classes of compounds were quantified by either direct calibration with known standards or relating the total ion chromatogram (TIC) signals to calibration standards of similar volatility and polarity. For example, n-alkanes were directly quantified, but compounds nearby in terms of polarity and volatility (i.e. branched alkanes) were quantified by relating their TIC signal to that of the nearest n-alkane. To this end, volatility bins were defined that are evenly spaced with their centers corresponding to the n-alkanes. In 2D-GC, the TIC signal corresponds to a “blob”, or a region in volatility and polarity retention space, thus the TIC blobs were quantified using the calibration for the available standard of similar polarity in the same volatility bin. The GC-Image software package was used to create blobs from the generated 2D chromatograms.

IVOC single ring aromatics (IVOC-SRA) were quantified slightly differently than the polar and aliphatic material. We used characteristic fragmentation patterns to gain further information on the isomeric composition of the IVOC-SRA. The TIC chromatograms were decomposed into selected ion chromatograms (SIC) using the main fragments indicative of SRA (m/z 57, 71, 77, 83, 91, 92, 105, 106, 117, 118, 119, 120, 131, 133, 134, 144, 145, 147, 148). Blobs were then generated from each SIC, and these single ion blobs were re-combined to create new pseudo-TIC blobs that contained only these selected ions. In this way, the original chromatograms become much cleaner, and the mass spectra for the reconstructed pseudo-TIC blobs can generally be classified into one of several categories defined by the substituents attached to the benzene ring: straight-chain (a-alkyl), di-substituted, poly-substituted, groups tertiary at the C1 positions (similar to isopropyl), branched compounds (such as tert butyl), unsaturated compounds (such as tetralins), and general compounds that are identified as clearly aromatic but do not readily fit into one of the other categories. The general category may include compounds that so nearly co-elute, that blob decomposition does not help to resolve them. Rules for categorization were derived from the mass spectra for all SRA compounds with between 11 and 16 carbons in the NIST library.

3.2.6 Engine Oil Analysis

Engine oil samples were taken for nearly all vehicles and stored in sealed glass containers at -24°C until analysis. Samples were diluted (50:1) in chloroform (Sigma-Aldrich, HPLC grade). Analytes were separated using an Agilent 7890 GC equipped with a non-polar column ($60\text{ m} \times 0.25\text{ mm} \times 250\text{ }\mu\text{m}$ Rxi-5Sil-MS, Restek). The diluted samples were directly injected into the heated GC inlet. The GC temperature program was the

same as above for IVOC and SVOC analysis. The quantification was nearly identical to the GC-VUV-MS analysis described above, except for the method of ionization. A soft electron-impact ion source (Markes Select-eV Time of Flight MS) was used in place of the VUV ionization source. The data in both cases are quite similar, except that slightly higher fragmentation occurs in the Select-eV case and aromatic compounds do not follow the linear trend in ionization observed with VUV ionization. Aromatic compounds were quantified using the same TIC calibration with volatility binning as described above for the polar compounds using regular electron impact ionization.

3.2.7 Emission Factors

Emissions are presented using emission factors, as mass emitted per mass of fuel consumed, using a mass balance approach:

$$EF_i = \Delta m_i \frac{x_c}{\Delta CO_2 + \Delta CO + \Delta THC}$$

ΔCO_2 , ΔCO , and ΔTHC are the background-corrected concentrations of CO_2 , CO , and THC . The fuel had a carbon mass fraction, x_c of 0.82. Δm_i is the measured background corrected concentration of species i . Measured fuel consumption per mile for each test is provided in the supporting information for conversion to distance-based emission factors.

3.3 Photo-oxidation Experiments

Photo-oxidation experiments were conducted for 14 vehicles, a subset of total tested vehicles, including 1 Pre-LEV, 3 LEV, 3 ULEV and 7 SULEV (Table S1). All photo-oxidation experiments were conducted with exhaust emitted from vehicles operated during the cold-start UC cycle.

The photo-oxidation experiments of dilute exhaust were conducted using the Carnegie Mellon's mobile chamber. This mobile chamber is a 7 m³ Teflon[®] bag suspended in a metal frame [Hennigan et al., 2011] and was located indoors during this study. Before each experiment, the chamber was flushed overnight using clean air treated by silica gel, HEPA filters and activated charcoal in series and with the chamber UV lights (Model F40BL UVA, General Electric) turned on.

The dilute exhaust was drawn from the CVS and injected into the chamber by a Dekati[®] diluter through silcosteel[®] stainless steel tubing. Both the diluter and transfer line were electrically heated and maintained at ~47°C, matching the CVS and the filter and Tenax collection temperature. For eleven of these experiments we only filled the chamber during the period of the first UC bag. For the rest of these experiments we filled the chamber through the entire UC, except for the 10-min hot-soak period. The NMOG emissions occur dominantly during the period of the first UC bag. The concentration of NMOGs in the chamber was approximately the same between the first UC bag and the entire UC, especially for experiments for SULEV vehicles.

Following the injection of the dilute exhaust, we generated ammonium sulfate seed particles using a constant-output atomizer (TSI, model 3075) followed by a diffusion dryer and a neutralizer and subsequently injected them into the chamber. These seed particles provide a sink for condensable vapors, reducing losses to the chamber walls; we also used them to determine the particle wall losses during each experiment

Nitrous acid (HONO) was used as a hydroxyl radical (OH) source. We added HONO into the chamber by bubbling clean air through a solution prepared by mixing 0.1 M NaNO₂ and 0.05 M H₂SO₄ with a volume ratio of 1:2. A known amount of butanol-d₉ (Cambridge Isotope Laboratories, MA) was added to determine the OH concentration. Propene was also added to adjust the NMOG to NO_x ratio (NMOG:NO_x) to a typical urban level of ~3:1 ppbC/ppb NO_x [Gordon et al., 2014]. However, the interference of HONO on chemiluminescence NO_x measurements [Dunlea et al., 2007] led to addition of excess propene in the beginning of experiments. As a result, the initial NMOG:NO_x varied substantially by vehicle class, although in all cases the NMOG:NO_x would have been around 3 following the complete photolysis of HONO. In this work the amount of NMOG used to calculate the initial NMOG:NO_x was the sum of NMOG in the exhaust, propene, and d₉-butanol added to the chamber. The amount of NO_x used to calculate the initial NMOG:NO_x was the NO measured by the NO_x monitor. Consequently, the NMOG:NO_x values we employed in our analysis and calculations are empirical and should be applied in other applications with caution; however, the strong empirical correlations support our conclusion. After all gases and particles were injected and mixed, the UV lights were switched on to initiate the photo-oxidation reactions.

The temporal evolution of particles and gases in the chamber was characterized by a suite of instruments. The particle number and volume in the chamber were measured using a scanning mobility particle sizer (SMPS, TSI classifier model 3080, CPC model 3772 or 3776). The nonrefractory submicron particle mass and chemical composition were measured by a high-resolution time-of-flight aerosol mass spectrometer (HR-ToF-AMS,

Aerodyne, Inc., MA). CO₂ was measured by a LI-820 monitor (Li-COR Biosciences, NE); NO_x, CO and O₃ was measured by API-Teledyne T200, T300 and 400A analyzers, respectively. The concentration of butanol-d₉ was measured by proton transfer reaction-mass spectrometry (Ionicon, Austria).

A small number of VOCs (e.g. single ring aromatics) was measured in real time the chamber using the PTR-MS. Concentrations NMOG species in the chamber was not directly measured. Instead, the initial NMOG concentration in the chamber was calculated based on the NMOG concentration measured in the CVS and the dilution ratio determined by CO₂ measured in the CVS and the chamber concurrently. The dilution ratio determined by CO₂ was confirmed by measurements of CO and NO_x. The decay of total NMOGs was unknown, but reacted speciated VOCs, IVOCs and SVOCs can be predicted based on their initial concentration and OH exposure derived from the decay of butanol-d₉ or aromatics when butanol-d₉ was not added.

Both particle and organic vapor wall losses were estimated in order to determine the SOA production. In the present study, the organic vapors were assumed to maintain equilibrium with both suspended and wall-bound particles [Gordon et al., 2014; Hildebrandt et al., 2009]. Therefore, the SOA production (C_{SOA} , $\mu\text{g}/\text{m}^3$) over a period of photo-oxidation was calculated by:

$$C_{SOA}(t) = \left(\frac{C_{OA,sus}(t)}{C_{seed,sus}(t)} - \frac{C_{OA,sus}(t=0)}{C_{seed,sus}(t=0)} \right) \times C_{seed,sus}(t=0)$$

Where $C_{OA,sus}(t)$ and $C_{seed,sus}(t)$ are the concentrations of suspended OA and seed particles (ammonium sulfate); $t=0$ refers to the time when the UV lights were switched on. The

$C_{\text{OA,sus}}(t)$ -to- $C_{\text{seed,sus}}(t)$ ratio was directly measured by HR-tof-AMS. The contribution of POA to suspended OA was determined by the $C_{\text{OA,sus}}(t=0)$ -to- $C_{\text{seed,sus}}(t=0)$ ratio multiplied by $C_{\text{seed,sus}}(t=0)$. The concentration of $C_{\text{seed,sus}}(t=0)$ was calculated based on the particle volume measured by SMPS and the $C_{\text{OA,sus}}(t=0)$ -to- $C_{\text{seed,sus}}(t=0)$ ratio measured by HR-tof-AMS. An inorganic density of 1.77 g/cm^3 [Hildebrandt et al., 2009] and an organic density of 1.0 g/cm^3 [Tkacik et al., 2014] were used to distinguish ammonium sulfate from primary OA and convert the volume to the mass.

In addition to experiments with dilute exhaust, photo-oxidation experiments were also conducted when the CVS was operated on clean air (no exhaust) for the same period as a standard UC. The addition of HONO, ammonium sulfate seeds, d_9 -butanol and propene followed the same procedure described above. Gases and particles were characterized using the same array of instruments. The SOA formation during these experiments was defined as dynamic blanks. The dynamic blanks were converted to emission factors using the average carbon emission across all tests. The dynamic blanks likely overestimate the SOA production from background organics because operating CVS on clean air promotes evaporation of organics condensed on the CVS walls [May et al., 2013].

3.3 References:

Ayala, A., and J. D. Herner (2005), Transient Ultrafine Particle Emission Measurements with a New Fast Particle Aerosol Sizer for a Trap Equipped Diesel Truck,, SAE Technical Paper 2005-01-3800, 2005,.

CARB (2005), California Air Resources Board Procedure for the Analysis of Automotive Exhaust for Methanol and Ethanol. MLD 101.
<http://www.arb.ca.gov/testmeth/slb/exhaust.htm>, edited.

CARB (2006), California Air Resources Board Determination of Aldehyde and Ketone Compounds in Automotive Source Samples by High Performance Liquid Chromatography MLD104. <http://www.arb.ca.gov/testmeth/slb/exhaust.htm>, edited.

CARB (2011a), California Air Resources Board SOP No. MLD145: Procedure for the Determination of Particulate Matter (PM) on Filters. http://www.arb.ca.gov/testmeth/slb/sop145v5_1.pdf, edited.

CARB (2011b), California Air Resources Board SOP No. MLD142: Procedure for the Analysis of Particulate Anions and Cations in Motor Vehicle Exhaust by Ion Chromatography. <http://www.arb.ca.gov/testmeth/slb/sop142v2-0.pdf>, edited.

CARB (2011c), California Air Resources Board SOP No. MLD139: Procedure for Organic Carbon and Elemental Carbon (OC/EC) Analysis of Vehicular Exhaust Particulate Matter (PM) on Quartz Filters. http://www.arb.ca.gov/testmeth/slb/sop139v1_1.pdf, edited.

Dunlea, E. J., et al. (2007), Evaluation of nitrogen dioxide chemiluminescence monitors in a polluted urban environment, *Atmos. Chem. Phys.*, 7(10), 2691-2704.

Gordon, T. D., et al. (2014), Secondary organic aerosol formation exceeds primary particulate matter emissions for light-duty gasoline vehicles, *Atmos. Chem. Phys.*, 14(9), 4661-4678.

Gysel, M., M. Laborde, J. S. Olfert, R. Subramanian, and A. J. Grohn (2011), Effective density of Aquadag and fullerene soot black carbon reference materials used for SP2 calibration, *Atmospheric Measurement Techniques*, 4(12), 2851-2858.

Hennigan, C. J., et al. (2011), Chemical and physical transformations of organic aerosol from the photo-oxidation of open biomass burning emissions in an environmental chamber, *Atmos. Chem. Phys.*, 11(15), 7669-7686.

Hildebrandt, L., N. M. Donahue, and S. N. Pandis (2009), High formation of secondary organic aerosol from the photo-oxidation of toluene, *Atmos. Chem. Phys.*, 9(9), 2973-2986.

Isaacman, G., Wilson, K. R., Chan, A. W. H., Worton, D. R., Kimmel, J. R., Nah, T., Hohaus, T., Gonin, M., Kroll, J. H., Worsnop, D. R., Goldstein, A. H. Improved resolution of hydrocarbon structures and constitutional isomers in complex mixtures using gas chromatography-vacuum ultraviolet-mass spectrometry. *Anal. Chem.* 2012, 84, 2335-2342.

Maddox, C. (2007), California Air Resources Board Procedure for the Determination of C2 to C12 Hydrocarbons in Automotive Exhaust Samples by Gas Chromatography. Standard Operating Procedure No. MLD 102/103 Version 2.2. <http://www.arb.ca.gov/testmeth/slb/sop102-103v2-2.pdf>, edited.

May, A. A., A. A. Presto, C. J. Hennigan, N. T. Nguyen, T. D. Gordon, and A. L. Robinson (2013), Gas-Particle Partitioning of Primary Organic Aerosol Emissions: (2) Diesel Vehicles, *Environ. Sci. Technol.*, 47(15), 8288-8296.

- May, A. A., et al. (2014), Gas- and particle-phase primary emissions from in-use, on-road gasoline and diesel vehicles, *Atmos. Environ.*, 88, 247-260.
- Moteki, N., and Y. Kondo (2010), Dependence of Laser-Induced Incandescence on Physical Properties of Black Carbon Aerosols: Measurements and Theoretical Interpretation, *Aerosol Sci. Technol.*, 44(8), 663-675.
- Scanlon, J. T., and J. T. Willis (1985), Calculation of Flame Ionization Detector Relative Response Factors Using the Effective Carbon Number Concept, *J. Chromatogr. Sci.*, 23(333-340).
- Schwarz, J. P., et al. (2006), Single-particle measurements of midlatitude black carbon and light-scattering aerosols from the boundary layer to the lower stratosphere, *J. Geophys. Res.*, 111(D16).
- Tkacik, D. S., et al. (2014), Secondary Organic Aerosol Formation from in-Use Motor Vehicle Emissions Using a Potential Aerosol Mass Reactor, *Environ. Sci. Technol.*, 48(19), 11235-11242.
- USGPO (2014), U.S. Government Publishing Office, Electronic Code of Federal Regulations: Title 40, Chapter 1, Subchapter C, Part 86: Control of Emissions From New and In-use Highway Vehicles and Engines., edited, <http://www.ecfr.gov/cgi-bin/text-idx?SID=c56ff4e0ab7f442c7e8babf29cc6e4c2&mc=true&node=pt40.19.86&rgn=div5>.
- Zhao, Y.; Nguyen, N. T.; Presto, A. A.; Hennigan, C. J.; May, A. A.; Robinson, A. L. Intermediate Volatility Organic Compound Emissions from On-Road Diesel Vehicles: Chemical Composition, Emission Factors, and Estimated Secondary Organic Aerosol Production. *Environ. Sci. Technol.* **2015**, 49 (19), 11516–11526.

Chapter 4

This chapter has been adapted from the published article:

Drozd, G.T., Y. Zhao, G. Saliba, B. Frodin, C. Maddox, R.J. Weber, M-C.O. Chang, H. Maldonado, S. Sardar, A.L. Robinson, A.H. Goldstein, Time resolved measurements of speciated tailpipe emissions from motor vehicles: trends with emission control technology, cold start effects, and speciation, *Environmental Science & Technology*, DOI: 10.1021/acs.est.6b04513, Articles ASAP, 2016.

4. Time resolved measurements of speciated tailpipe emissions

4.1. Introduction

US emissions standards for vehicles have decreased by over a factor of 20 in the past twenty years.¹ To meet these standards, engine and emissions control technologies have advanced to decrease both the magnitude of driving emissions and duration of cold start emissions of hydrocarbons and criteria pollutants. Reduction of vehicle emissions, particularly non-methane organic gases (NMOG), will continue to be a major focus for improving air quality in the US. Major innovations to reduce vehicle emissions have been improved measurement and control systems as well as improved sensors components and actuators. Advances in these three areas continue to be the important routes to lowering vehicle emissions, and a major outcome has been to further compress emissions to distinct events during vehicle operation (e.g. engine start and hard acceleration). Correlating emissions and engine activity thus requires characterization of emissions with increasingly higher time resolution. In addition, the complex nature of secondary

pollutant formation, such as ozone and secondary organic aerosol (SOA), requires detailed speciation of a wide range of NMOG compounds.

Controlled vehicle testing clearly shows that cold starts dominate emissions, because the catalyst is not fully active, allowing unburned and incompletely combusted material to pass through exhaust after-treatment systems^{2,3} The ratio of total emissions from cold start to per-mile hot-stabilized emissions (γ) can be used as a metric of the relative impact of cold start emissions.⁴ Values of γ for NMOG may reach hundreds of miles, meaning that emissions are dominated by cold starts for any distance shorter than this. Cool-starts, which occur when the engine is somewhere between ambient and hot-stabilized temperature are also common. Cool-start emissions may reach 20% of cold start emissions after a soak-time (time between a cold-start and the next engine start) of just 1 hour.⁵ While this is true for properly operating vehicles, on-road tests suggest during hot-stabilized operation emissions are dominated from a limited number of high emitting vehicles with catastrophic failure of their emissions controls.⁶⁻¹⁰

Health impacts of vehicle emissions are strongly tied to emissions composition. Toxicity of emissions and their contribution to secondary pollutants (e.g. ozone and PM_{2.5}) depend on the particular species that are emitted, such as the BTEX (benzene, toluene, and xylenes) compounds and oxygenated species such as acetaldehyde. Due to the difficulty in sampling actual vehicle exhaust, fuel composition may be used to approximate exhaust composition. This approach is useful for fuel-based estimates of emissions and laboratory experiments on secondary pollutant formation, allowing the use of a readily available precursor mixture, but exhaust composition can differ from fuel composition and varies with driving conditions¹¹⁻¹³ Detailed composition measurements

of actual exhaust are thus required and must be continually be updated as new emissions controls systems are implemented to meet new emissions standards.

To address the issues stated above, rapid and comprehensive measurements of speciated NMOG emissions are needed, especially as cold-start emissions continue to shorten. Currently 1 Hz measurements have been made for gas species including the BTEX compounds, small carbonyls, acids, and some nitrogen containing compounds using FTIR and/or chemical ionization mass spectrometry (CIMS), but high time resolution studies of vehicle emissions are limited and not routine.¹⁴⁻²¹ While routine real-time measurements include CO₂, CO, and HC; here we focus on high-time resolution of a range of individual NMOG species to give broader insight into the changing effects of new emissions control technologies and project future vehicle fleet emissions, both in terms of species profiles and identifying future needs in emissions controls. This paper presents measurements of a wide range of individual NMOGs in tailpipe emissions during chassis dynamometer testing of gasoline vehicles recruited from the Southern California fleet to determine the effects of control technologies on both emissions time-profiles and their speciation.

4.2. Results and Discussion

4.2.1 Overall Fleet Emissions

4.2.1.1. Total Hydrocarbons

As expected, the total hydrocarbon (THC) emissions for the full UC drive protocol have decreased significantly in accordance with stricter vehicle emissions standards. The results for our fleet augmented by previous measurements² are shown in Fig 1 as box-

and-whisker plots. Note the logarithmic scale. The number of vehicles included is 8 for the combined SULEV and PZEV vehicles, the other classes include 11 or 12 vehicles. From Tier 0 (pre-LEV) to SULEV and PZEV vehicles, the decreases in median THC emissions are a factor of 40.

4.2.1.2 BTEX Compounds

Benzene emissions as measured by PTR-MS for our test fleet show strong reductions for vehicles with newer emissions controls. This data is shown in the lower left section of Figure 4.1 for the UC drive protocol. There is a clear decreasing trend for cold-start (bag 1) emissions, which includes the first 300 seconds after engine start. Appendix A, Figure A2 shows this data for all BTEX compounds. The oldest Tier 0 vehicle has emissions that are between 13 (benzene) to 20 (toluene and xylenes) higher than the PZEV vehicles that meet much stricter emissions standards. While the current study has only a single Tier 0 vehicle, this vehicle had emissions similar to other Tier 0 vehicles in a previous study with a larger number of vehicles.¹³ Both control system technology and its condition contribute to these decreases in emissions. For hot-stabilized operations (bag 2), there is much less of a trend with vehicle technology/condition, and most of the emissions in bag 2 are associated with hard accelerations. Hot-start (bag 3) emissions are again highest for the Tier 0 vehicle. The high hot-start emissions for one of the LEVII vehicles strongly suggest emissions controls that are in poor condition. This is also supported by the fact that this part of the drive cycle does not have hard accelerations. Looking across technologies we see that even the LEV I vehicle (certified to a less strict standard) has lower emissions than this LEV II vehicle in both bags 2 and 3. These observations suggest that the bag 3 emissions from the LEV II vehicle are most likely due to a poorly

functioning catalyst. Vehicles in the PZEV and SULEV class show slightly increased emissions during bag 2, indicating that hard acceleration and high fuel delivery can overwhelm even new technology catalysts when they are hot, but they do not show very low emissions during hot-start. The Tier 0 and LEV II vehicle with high emissions will be discussed in further detail below, as indicators of how the future vehicle fleet will be affected by aging vehicles with poorly functioning emissions controls.

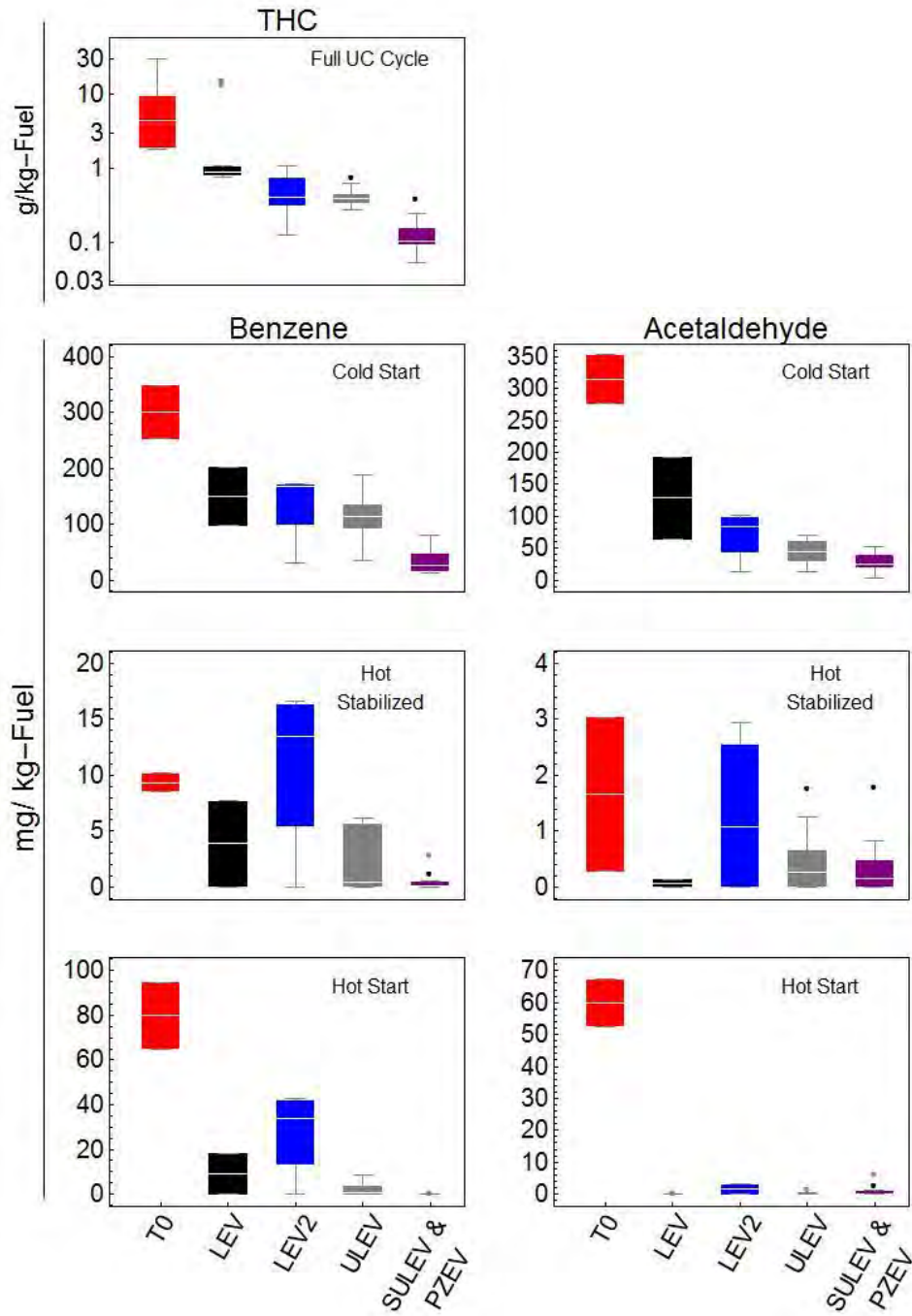


Figure 4.1. Total hydrocarbon emissions for the complete UC drive protocol. Includes data for Tier 0, Tier I, and Tier II vehicles from a previous study¹³, (top panels). Benzene (lower left) and acetonitrile (lower right) emission factors for each phase of the UC protocol for all vehicle classes as measured by PTR-MS for the current study only. The central white lines on the box plots are median values; the edges of the boxes are the 25th and 75th percentiles; the whiskers extend to the most extreme data not considered outliers; black points are determined to be outliers.

4.2.1.3 Differences in BTEX Composition Between Exhaust and Fuel

The relationship between the unburned gasoline and tailpipe exhaust composition can be important for modeling emissions, secondary pollutant formation, and source apportionment. A metric for the similarity between exhaust and fuel, particularly for predicting formation of SOA, is the fraction of total BTEX from its 3 constituents: benzene, toluene, and the xylenes. Figure 4.2 shows that exhaust from all vehicle classes spanning over 20 model years have a similar BTEX composition, including data from previous work.² Compared to the fuel composition, the exhaust has distinctly higher proportions of benzene and lower proportions of xylenes compared to unburned fuel. For benzene, toluene, and xylenes, the average fractions by vehicle class are within the range (0.21-0.27), (0.33-0.4), and (0.37-0.41). No trend in the exhaust BTEX composition was observed moving from older to newer technologies. For the purposes of converting fuel usage data to actual emissions data, we recommend that the BTEX composition in the fuel can be multiplied by factors of 5, 1, and 0.6 for benzene, toluene, and (xylenes+ethyl benzene) to approximate the BTEX composition of emissions. This increase in benzene, known to result from catalytic converter effects, and these multipliers are similar to previous results for gasoline vehicles.^{13,30,31} The BTEX compounds are important SOA precursors and air toxics, so accurate representation of this class of compounds is important in atmospheric modeling of SOA and human exposure. It appears that emissions controls exhibit a fairly constant BTEX profile, so although the exhaust composition is different from the initial fuel, it is nonetheless fairly constant for a given fuel input.

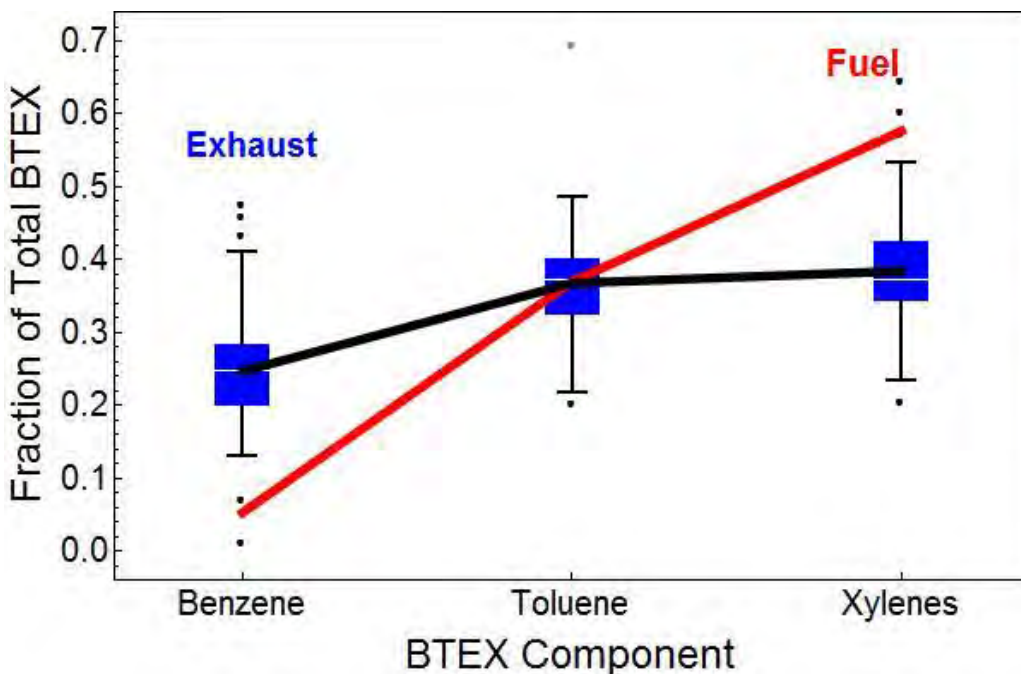


Figure 4.2. The BTEX composition for exhaust from gasoline vehicles in this study and an earlier study², both performed at the ARB Hagen-Smit Laboratory with the UC drive protocol. The xylenes category includes ethyl benzene. Exhaust data includes vehicles from all classes with number of vehicles in parentheses. (T0(15), LEV I(20), LEV II(27), ULEV(5), SULEV(6), PZEV(6)).

4.2.1.4 Incomplete Combustion Products

Gas-phase products from incomplete combustion of fuel are emitted in addition to unburned fuel. The lower right section of Figure 4.1 shows results for bag-integrated PTR-MS measurements of acetaldehyde, which is readily detected using PTR-MS and not present in fuel. The trend for cold-starts is as expected; exhaust emissions drop significantly with newer control technologies. Hot-stabilized emissions are 1-2 orders of magnitude below bag 1 emissions. The Tier 0 and LEV II vehicles have the highest acetaldehyde emissions during hot stabilized operation. While ULEV and SULEV vehicles can emit as much as these older vehicles, median acetaldehyde emissions decrease with newer technologies during hot stabilized operation. During hot-start, the

Tier-0 and LEV II vehicle stand out with the highest bag 3 acetonitrile emissions, while the other classes had hot-start acetonitrile emissions below 1 mg/kg-Fuel. Notably, the outliers in the SULEV and PZEV classes are hybrid vehicles. These PTR-MS results show that cold-starts can be expected to dominate emissions of incomplete combustion products, even for poorly functioning vehicles.

Other ketone and aldehyde emissions were dominated by acetone and formaldehyde. This was true across all vehicle classes and ages. These emissions, as measured using DNPH cartridges followed by analysis by HPLC, are shown in Appendix A, Figure A2. The number of vehicles included is limited for these oxygenated species: PZEV(4), SULEV(3), ULEV(7), LEV II(2), LEV I(1), Tier-0(1). Emissions of these unsaturated ketones and aldehydes decrease dramatically for vehicles that meet newer emissions standards. Methacrolein and acrolein were detected in nearly all vehicle classes, with acrolein not detected in ULEV or PZEV vehicles (See Appendix A, Figure A3). A notable exception is methacrolein during hot starts, where the LEV II vehicle has emissions as high as the Tier-0 vehicle. The PZEV vehicle that had detectable methacrolein during bag 2 was the only hybrid PZEV vehicle tested. Propionaldehyde was a minor contributor for Tier 0 to ULEV vehicles, and only for cold-starts. Other ketones and aldehydes that were monitored but had emissions near or below reporting limits included methyl-ethyl-ketone, butyraldehyde, hexanal, valeraldehyde, and crotonaldehyde.

4.2.1.5 Overall VOC Composition

The varying composition of exhaust by vehicle class was assessed, in part, by comparing the mass fraction of BTEX compounds in NMOG emissions. These data are shown in

Appendix A, Figure A4. For cold start emissions, benzene and toluene are a similar fraction of NMOG mass across all vehicle classes, centering on a value of 0.04 mg/mg-THC. Xylenes + ethyl-benzene to THC ratios for cold-start emissions declined slightly for vehicles meeting stricter emissions standards, with medians decreasing by about 20% between Tier-0 and LEV I vehicles and those meeting stricter standards. The upper quartile for vehicles meeting LEV II and stricter certifications was also below the median of the Tier 0 and LEV I vehicles. Hot-stabilized emissions showed some enhancement of BTEX composition for vehicles meeting stricter certifications. Hot-start emissions showed significant fractions of benzene for vehicles up to ULEV, with values between 0.01 and 0.05 mg/mg-THC, while SULEV and PZEV vehicles showed almost no benzene emissions. Toluene and xylenes + ethyl benzene hot-start fractions declined with stricter emissions control systems. Because cold-start emissions are dominated by unburned fuel and all vehicles used the same fuel, it is not surprising that BTEX emissions as a fraction of THC emissions do not vary significantly across control technologies. Conversion of larger alkyl benzene compounds to benzene is known to occur, and it appears that newer technologies (catalysts) behave similarly to older technologies in this respect.³¹⁻³³

The average mass spectra observed by PTR-MS are shown in Appendix A, Figure A5 for each vehicle class studied. Figure 4.4 shows the total PTR-MS signal broken into 5 chemical categories: alkanes, BTEX, speciated alkenes, speciated oxygenated compounds, and compounds that have parent/fragment masses without explicit identification (unknown). The alkanes signal is mainly derived from ionization by O_2^+ and subsequent fragmentation, and the speciated compounds, including BTEX, are

measured via H_3O^+ ionization.³⁴ The mass fragments in the unknown category have been separated into even and odd masses. Odd mass fragments, except the well-known alkane fragments, are associated with ions from H_3O^+ ionization. Even masses in the unknown category may either undergo H_3O^+ ionization and contain nitrogen or be associated with O_2^+ or NO^+ ionization.

Alkanes are generally 30-40% of total PTRMS signal; the BTEX compounds are 20-40%; and other speciated compounds are typically 20-30%. The unknown category is generally less than about 10% of the total PTR-MS signal. The majority of the unknown compounds appear at odd masses attributable to H_3O^+ ionization and their sensitivity will thus be similar to speciated oxygenated compounds. This suggests that the mass of unidentified compounds is generally less than 30% of speciated oxygenated compounds and about 15-25% of BTEX compounds. Previous studies have suggested the potential for newer vehicles to have mixes of exhaust gases that are more potent SOA precursors, per total mass of emissions, than older vehicles.²³ If vehicle exhaust composition, rather than total mass of emissions, were becoming a dominant factor for vehicle-derived SOA, future regulations would need to target specific compounds or classes of compounds. If any change in potency for SOA formation has occurred, our results do not suggest it is related to changes in VOC emissions, though variation in lower volatility emissions is possible. Our overall VOC composition measurements show similar VOC composition for all vehicle classes.

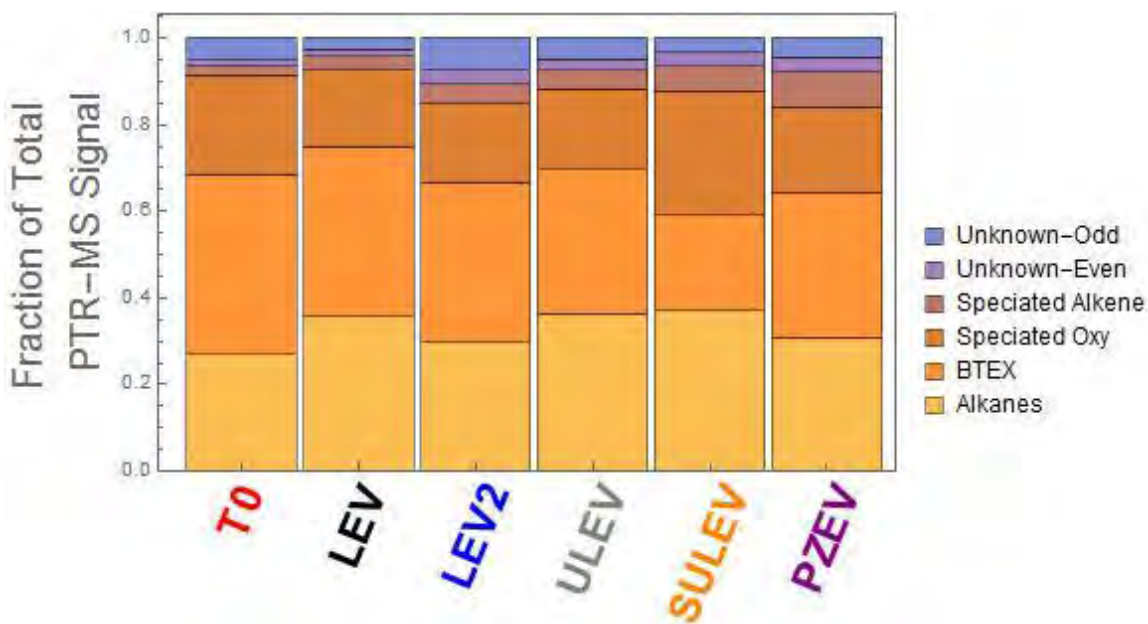


Figure 4.3. Total PTR-MS signal for bag 1 averaged by vehicle class and divided into chemical categories. The unknown category has been sub-divided into even and odd masses, showing dominance of odd-masses.

4.3 Time Resolved Measurements

4.3.1 Non-oxygenated/Fuel-Derived Emissions

Time resolved emissions, as measured by PTR-MS, are shown in Figure 4.4 for benzene (m/z 79, blue), acetaldehyde (m/z 45, red), and aliphatics (m/z 57, black), normalized to their maximum signals. The drive cycle speed trace is in shown gray. Figure 4.4a shows emissions from the vehicle that met the least stringent emission standard (T0, 1990); 4b, a moderate-age, medium-emissions vehicle (LEV II, 2008); and 4c, a new vehicle that meets the strictest emissions standard (PZEV, 2013). The peak benzene concentrations in the CVS are shown in blue with the corresponding benzene signal trace. The benzene emissions data show that newer and advanced emissions control systems reduce both the peak concentration of emissions and the duration of emissions spikes throughout the drive cycle. The PTR-MS time-traces for aliphatics (m/z 57) show a similar trend.

Both benzene and aliphatic emissions have roughly the same temporal profile. Emissions occur almost exclusively during engine start, whether hot or cold, and during hard acceleration. Emissions during start events occur because the exhaust catalyst has not reached the light-off temperature at which hydrocarbons are oxidized (largely to CO₂ & H₂O) and the engine is running fuel-rich. The engine will run rich to ensure volatilization of enough fuel for combustion, because prior to warm-up fuel will not evaporate efficiently on the timescale of the engine combustion cycle. Because the catalyst has minimal effect prior to warm-up, the decrease in peak magnitudes for newer vehicles is largely attributed to more efficient fuel delivery programs, aided in part by better engine sensors (temperature and oxygen). Fuel delivery early in the cold-start phase appears to decrease emissions by roughly a factor of 6, judging from peak CVS concentrations (3200 – 500ppb). The duration of the emissions during cold start depends on time to catalyst light-off. Figure 4.4 shows that older vehicles require up to 250 seconds for full catalyst efficiency, while new vehicles reach full conversion of hydrocarbons in close to 45 seconds. The reductions in duration and peak emissions are both approximately a factor of five to six. This suggests that improvements in both processes contribute significantly to reductions in cold start emissions.

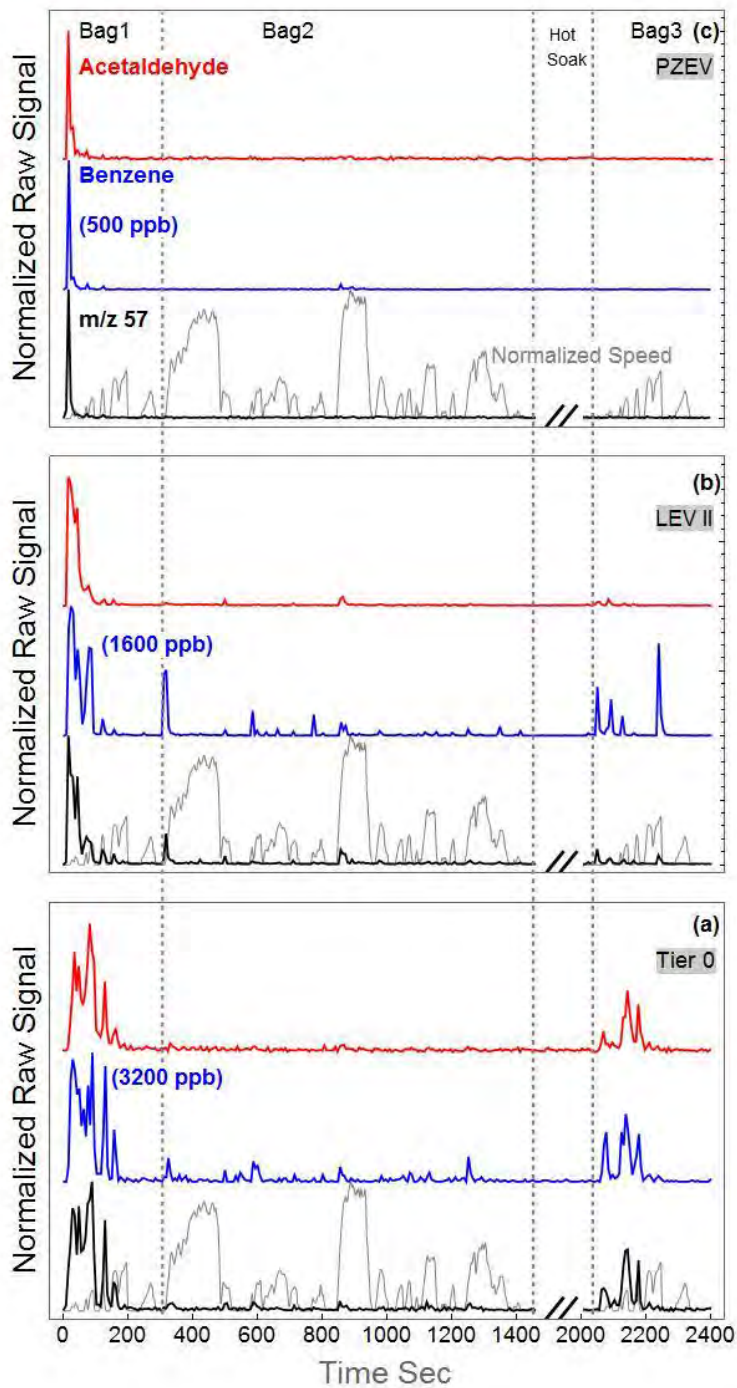


Figure 4.4. Time resolved PTR-MS measurements of benzene (m/z 79, blue), acetaldehyde (m/z 45, red), and aliphatic compounds (m/z 57, black) for a PZEV (c), a malfunctioning LEV II vehicle (b), and a Tier 0 vehicle (a) for the UC testing protocol. Data are normalized to peak signal for each species. Values for the peak concentrations of benzene are shown in blue. The drive trace is shown in gray, with a maximum speed of 67 mph.

4.3.2 Incomplete Combustion Emissions

Species formed from incomplete combustion (e.g. acetaldehyde) generally have a similar temporal profile to the fuel components (BTEX and hydrocarbons). However malfunctioning vehicles such as the LEV II vehicle, with high hot-stabilized and hot-start emissions of incomplete combustion compounds, have different time profiles (Fig. 4). The PZEV vehicle shows a short burst during cold-start for both benzene and acetaldehyde, with nearly overlapping traces. The LEV II vehicle shows a slightly longer initial burst for both benzene and acetaldehyde followed by near-zero acetaldehyde emissions and further bursts of benzene emissions. Emissions for other incomplete combustion products monitored by PTR-MS (e.g. acetonitrile, isoprene, styrene) show the same temporal pattern as acetaldehyde. The oldest vehicle (T0), which had significant hot- and cold-start emissions, had the same trend for all observable compounds. The emissions from the LEV II vehicle indicate a poorly functioning catalyst. The LEV II emission burst at ~300 seconds is due to hard acceleration, when excess fuel is delivered to the engine. At this point in the drive cycle, both the engine and the catalyst are warm, and we can assume combustion is near-optimal, minimizing the output of acetaldehyde. The differing time profiles for incomplete combustion compounds and fuel-derived compounds are further evidence of poorly functioning emissions controls. These results suggest that emissions factors for aging vehicles will vary by species and how they are formed.

4.4 Cold-Start Emissions

The importance of cold-starts from all vehicles to the total in-use fleet emissions has been clearly demonstrated in dynamometer tests.^{4,5,35,36} On-road tests suggest that extreme

emissions from a small portion of vehicles that have emissions control systems in catastrophic failure may outweigh the emissions from all other vehicles on the road, including cold-start emissions. This is possible because these vehicles emit continuously, even after the engine and catalyst are hot. The vehicle fleet tested here had a wide range of cars, including a very old vehicle (24 yrs, Tier 0), a poorly functioning and moderately aged vehicle (6yrs, LEV II), and multiple brand new vehicles that meet the most stringent emission standards (<1yr, PZEV). We combine our new data with data from previous measurement campaigns to project how the future vehicle fleet will be affected by cold-start emissions.

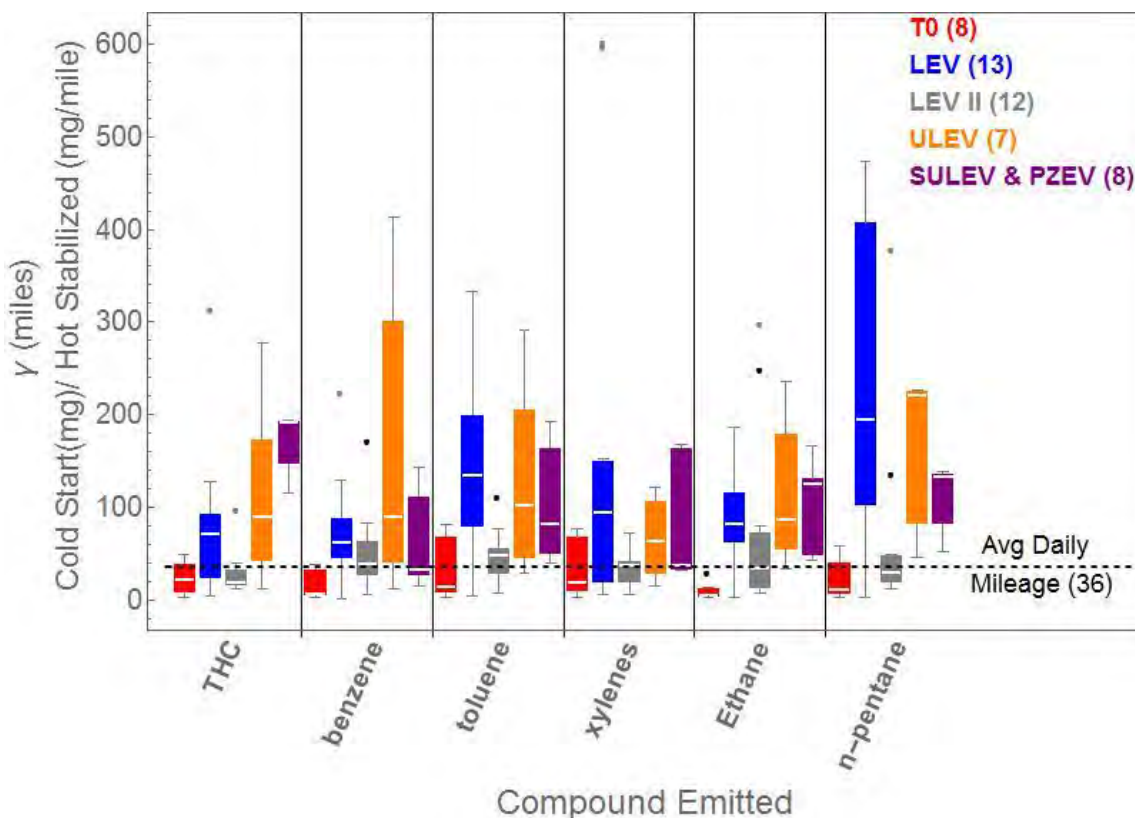


Figure 4.5. γ values, based on the UC test protocol, are shown for a range of species and vehicle classes. The dashed line emphasizes that the median values for most vehicle classes and types of compounds are above 36 miles, the average total daily mileage among US drivers.

The ratio of total cold start emissions to the hot-stabilized emissions per mile, γ , gives the number of miles a vehicle would need to travel between cold-starts before hot-stabilized emissions would exceed cold-start emissions.⁴ The cold-start emissions used in this analysis are the emissions during the first 300 seconds of operation (full bag 1 of UC). In Figure 4.5 we compare γ for all vehicle classes tested for a range of chemical species, including THC, benzene, toluene, xylenes, ethane, and n-pentane. The speciated data are from GC measurements. Measurements for Tier 0, LEV I, and LEVII vehicles include both new measurements and those from previous studies.¹³

Median values of γ for NMOG are almost always greater than 30 miles, except for the oldest Tier 0 vehicles. THC emissions have a striking trend in γ values, increasing nearly an order of magnitude to reach 200+ miles for the newest emissions controls. BTEX and selected hydrocarbons (ethane and n-pentane) show less of a trend in γ with vehicle emissions certification, but emissions standards specify reductions in the magnitude of THC over the full driving protocol, so technologies are not necessarily expected to specifically control for cold start emissions and specific species. A typical commuter will have two cold starts, one for each direction of their commute. Accounting for both cold starts, a commuter would need to travel more than 60 miles for hot running emissions to equal total cold start emissions. In the US, the average total driving distance is 36 miles per day, with fewer than 10% of trips more than 50 miles in length.³⁷ Furthermore, vehicles with ages 20 years or greater, which encompasses Tier 0 vehicles, comprise less than 10% of the US passenger car fleet.³⁸ This means that cold-start emissions of most NMOG species dominate total-trip emissions in the US for a majority of the in-use fleet.

We present results for several scenarios of the contribution of cold start emissions to average driving trip emissions in Appendix A, Table A7. The average trip length as of the most recent transportation survey data, commute or otherwise, is 11.8 miles.³⁷ Including γ values across all vehicle classes, the average contribution of cold-start emissions to total commute emissions, for all species emitted, is more than 90%. Using the lower quartile instead of the average, cold-start emissions will still be above 70% of average commute emissions. Excepting mountainous areas, which will have elevated hot stabilized emissions, the scenarios where long distances are driven will likely have lower incidences of hard acceleration, effectively making γ values even higher. The worst case vehicles, which are all Tier 0 or Tier I vehicles, have around 10-20% of emissions due to cold starts. These vehicles are either already in the far end of the vehicle age distribution (20+ years) or soon will be. These vehicles are also not contained in the lower quartile of the respective classes. This suggests that vehicles strongly dominated by hot-stabilized emissions are less than 3% of the current in-use fleet. The above analysis relies on the ability of the UC test to reflect real-world driving (aggressiveness, length of soak periods, ambient temperature, etc.). Within the limit of the UC cycle representing US driving patterns, specifically commuting, the majority of the in-use fleet is already dominated by cold starts, and only a few percent of the fleet will have significant hot-stabilized emissions compared to cold start emissions in the next several years.

4.5 Environmental Implications

NMOG emissions from vehicles will continue to decrease beyond the significant reductions shown above. New LEV III regulations will require emissions reductions of about 75% in the sum of NMOG and NO_x in the coming decade. The work shown here

guides expectations in the composition and temporal and spatial trends these further reductions will have on emissions. Future emissions for all species from nearly all vehicles will be dominated by cold starts, occurring as a short burst that decreases in both magnitude and duration. These trends are now supported over a wide range of vehicle makes and years by combining new measurements and reanalysis of previous measurements. Newer vehicles can be expected to have their emissions further compressed into discrete events, namely cold starts and hard accelerations, and the current fleet, as vehicles are retired, will have this same trajectory. Warm-up times are already in the range of 30-40 seconds at moderate temperatures of about 70°F in dynamometer tests, so an increase of just 10 seconds, easily caused by near freezing temperatures, is significant. This sensitivity to ambient temperature is likely to increase for newer technologies with shorter overall warm up times. The last 20+ years of innovation in emissions controls technology have not significantly changed the composition of NMOG emissions, as evidenced by the mass fraction of BTEX in the total emissions and the general mass spectra observed in the PTR-MS. This is true for both unburned fuel compounds and oxidized compounds not found in fuel. Emissions of all NMOG compound classes have the same dependence on engine activity for properly functioning vehicles, though poorly functioning vehicles may show emissions that have compositions more strongly dependent on driving conditions. In addition, the change in the BTEX profile from fuel to exhaust has also remained fairly constant with advances in emissions control technology. The total of our observations suggest that future NMOG vehicle emissions will likely not have drastic changes in composition and will become much more spatially and temporally correlated with cold starts, and the main emissions

from vehicles will become increasingly located where people live in the morning and where they work in the evening. Total emissions and exposure to VOC emissions from mobile sources, including toxic compounds such as benzene, will continue to decrease.

4.6 References

- (1) Propper, R.; Wong, P.; Bui, S.; Austin, J.; Vance, W.; Alvarado, Á.; Croes, B.; Luo, D. Ambient and Emission Trends of Toxic Air Contaminants in California. *Environ. Sci. Technol.* **2015**, 49 (19), 11329–11339.
- (2) May, A. A.; Nguyen, N. T.; Presto, A. A.; Gordon, T. D.; Lipsky, E. M.; Karve, M.; Gutierrez, A.; Robertson, W. H.; Zhang, M.; Brandow, C.; et al. Gas- and particle-phase primary emissions from in-use, on-road gasoline and diesel vehicles. *Atmos. Environ.* **2014**, 88, 247–260.
- (3) George, I. J.; Hays, M. D.; Herrington, J. S.; Preston, W.; Snow, R.; Faircloth, J.; George, B. J.; Long, T.; Baldauf, R. W. Effects of Cold Temperature and Ethanol Content on VOC Emissions from Light-Duty Gasoline Vehicles. *Environ. Sci. Technol.* **2015**, 49 (21), 13067–13074.
- (4) Weilenmann, M.; Favez, J. Y.; Alvarez, R. Cold-start emissions of modern passenger cars at different low ambient temperatures and their evolution over vehicle legislation categories. *Atmos. Environ.* **2009**, 43 (15), 2419–2429.
- (5) Favez, J. Y.; Weilenmann, M.; Stilli, J. Cold start extra emissions as a function of engine stop time: Evolution over the last 10 years. *Atmos. Environ.* **2009**, 43 (5), 996–1007.
- (6) Bishop, G. A.; Schuchmann, B. G.; Stedman, D. H.; Lawson, D. R. Multispecies remote sensing measurements of vehicle emissions on Sherman Way in Van Nuys, California. *J.*

- Air Waste Manage. Assoc. **2012**, 62 (10), 1127–1133.
- (7) Bishop, G. A.; Stedman, D. H. A decade of on-road emissions measurements. *Environ. Sci. Technol.* **2008**, 42 (5), 1651–1656.
- (8) Kirchstetter, T. W.; Singer, B. C.; Harley, R. A.; Kendall, G. R.; Traverse, M. Impact of california reformulated gasoline on motor vehicle emissions. 1. Mass emission rates. *Environ. Sci. Technol.* **1999**, 33 (2), 318–328.
- (9) Heeb, N. V.; Forss, A. M.; Weilenmann, M. Pre- and post-catalyst-, fuel-, velocity- and acceleration-dependent benzene emission data of gasoline-driven EURO-2 passenger cars and light duty vehicles. *Atmos. Environ.* **2002**, 36 (30), 4745–4756.
- (10) Weilenmann, M. F.; Soltic, P.; Hausberger, S. The cold start emissions of light-duty-vehicle fleets: A simplified physics-based model for the estimation of CO₂ and pollutants. *Sci. Total Environ.* **2013**, 444, 161–176.
- (11) Gentner, D.; Isaacman, G. Elucidating secondary organic aerosol from diesel and gasoline vehicles through detailed characterization of organic carbon emissions. *Proc. Natl. Acad. Sci. U. S. A.* **2012**, 109 (45), 18318–18323.
- (12) McDonald, B. C.; Goldstein, A. H.; Harley, R. A. Long-term trends in California mobile source emissions and ambient concentrations of black carbon and organic aerosol. *Environ. Sci. Technol.* **2015**, 49 (8), 5178–5188.
- (13) May, A. A.; Nguyen, N. T.; Presto, A. A.; Gordon, T. D.; Lipsky, E. M.; Karve, M.; Gutierrez, A.; Robertson, W. H.; Zhang, M.; Brandow, C.; et al. Gas- and particle-phase primary emissions from in-use, on-road gasoline and diesel vehicles. *Atmos. Environ.* **2014**, 88, 247–260.

- (14) Heeb, N. V.; Forss, A. M.; Bach, C.; Reimann, S.; Herzog, A.; Jäckle, H. W. A comparison of benzene, toluene and C2-benzenes mixing ratios in automotive exhaust and in the suburban atmosphere during the introduction of catalytic converter technology to the Swiss Car Fleet. *Atmos. Environ.* **2000**, 34 (19), 3103–3116.
- (15) Heeb, N. Velocity-dependent emission factors of benzene, toluene and C2-benzenes of a passenger car equipped with and without a regulated 3-way catalyst. *Atmos. Environ.* **2000**, 34 (7), 1123–1137.
- (16) Mohn, J.; Forss, A. M.; Bruhlmann, S.; Zeyer, K.; Luscher, R.; Emmenegger, L.; Novak, P.; Heeb, N. Time-resolved ammonia measurement in vehicle exhaust. *Int. J. Environ. Pollut.* **2004**, 22 (3), 342–356.
- (17) Reyes, F.; Grutter, M.; Jazcilevich, a.; González-Oropeza, R. Analysis of non-regulated vehicular emissions by extractive FTIR spectrometry: tests on a hybrid car in Mexico City. *Atmos. Chem. Phys. Discuss.* **2006**, 6 (4), 5773–5796.
- (18) Wentzell, J. J. B.; Liggio, J.; Li, S. M.; Vlasenko, A.; Staebler, R.; Lu, G.; Poitras, M. J.; Chan, T.; Brook, J. R. Measurements of gas phase acids in diesel exhaust: A relevant source of HNCO? *Environ. Sci. Technol.* **2013**, 47 (14), 7663–7671.
- (19) Brady, J. M.; Crisp, T. A.; Collier, S.; Kuwayama, T.; Forestieri, S. D.; Perraud, V.; Zhang, Q.; Kleeman, M. J.; Cappa, C. D.; Bertram, T. H. Real-time emission factor measurements of isocyanic acid from light duty gasoline vehicles. *Environ. Sci. Technol.* **2014**, 48 (19), 11405–11412.
- (20) Sentoff, K. M.; Robinson, M. K.; Holmén, B. a. Second-by-Second Characterization of Cold-Start Gas-Phase and Air Toxic Emissions from a Light-Duty Vehicle. *Transp. Res. Rec. J. Transp. Res. Board* **2010**, 2158 (1), 95–104.

- (21) Moussa, S. G.; Leithead, A.; Li, S.-M.; Chan, T. W.; Wentzell, J. J. B.; Stroud, C.; Zhang, J.; Lee, P.; Lu, G.; Brook, J. R.; et al. Emissions of hydrogen cyanide from on-road gasoline and diesel vehicles. *Atmos. Environ.* **2016**, 131, 185–195.
- (22) Robert, M. a; VanBergen, S.; Kleeman, M. J.; Jakober, C. A. Size and composition distributions of particulate matter emissions: part 1--light-duty gasoline vehicles. *J. Air Waste Manage. Assoc.* **2007**, 57 (12), 1414–1428.
- (23) Gordon, T. D.; Presto, A. A.; May, A. A.; Nguyen, N. T.; Lipsky, E. M.; Donahue, N. M.; Gutierrez, A.; Zhang, M.; Maddox, C.; Rieger, P.; et al. Secondary organic aerosol formation exceeds primary particulate matter emissions for light-duty gasoline vehicles. *Atmos. Chem. Phys.* **2014**, 14 (9), 4661–4678.
- (24) Pang, Y.; Fuentes, M.; Rieger, P. Trends in the emissions of Volatile Organic Compounds (VOCs) from light-duty gasoline vehicles tested on chassis dynamometers in Southern California. *Atmos. Environ.* **2014**, 83, 127–135.
- (25) Gordon, T. D.; Presto, A. A.; Nguyen, N. T.; Robertson, W. H.; Na, K.; Sahay, K. N.; Zhang, M.; Maddox, C.; Rieger, P.; Chattopadhyay, S.; et al. Secondary organic aerosol production from diesel vehicle exhaust: Impact of aftertreatment, fuel chemistry and driving cycle. *Atmos. Chem. Phys.* **2014**, 14 (9), 4643–4659.
- (26) Gordon, T. D.; Tkacik, D. S.; Presto, A. A.; Zhang, M.; Jathar, S. H.; Nguyen, N. T.; Massetti, J.; Truong, T.; Cicero-Fernandez, P.; Maddox, C.; et al. Primary gas- and particle-phase emissions and secondary organic aerosol production from gasoline and diesel off-road engines. *Environ. Sci. Technol.* **2013**, 47 (24), 14137–14146.
- (27) California Air Resources Board. California Air Resources Board, 2001. SOP No. MLD119: Procedure for the Direct Determination of Total Non-methane Hydrocarbons

and Methane in Motor Vehicle Exhaust Using Cryogenic Preconcentration and Flame Ionization Detection[WWWDocument]. URL.

<https://www.arb.ca.gov/testmeth/slb/sop119.pdf>.

- (28) California Air Resources Board. No Title. Calif. Air Resour. Board, 2007. SOP No. MLD102/103 Proced. Determ. C2 to C12 Hydrocarb. Automot. exhaust samples by gas Chromatogr. [WWW Doc. URL <http://www.arb.ca.gov/testmeth/slb/sop102-103v2-2.pdf>].
- (29) California Air Resources Board. No Title. Calif. Air Resour. Board, 2006. SOP No. 104 Stand. Oper. Proced. Determ. aldehyde ketone Compd. Automot. source samples by high Perform. Liq. Chromatogr. [WWW Doc. URL <http://www.arb.ca.gov/testmet>].
- (30) Dearth, M. A.; Gierczak, C. A.; Siegl, W. O. Online measurement of benzene and toluene in dilute vehicle exhaust by mass- spectrometry. *Environ. Sci. Technol.* **1992**, 26 (8), 1573–1580.
- (31) Bruehlmann, S.; Forss, A.-M.; Steffen, D.; Heeb, N. V. Benzene: a secondary pollutant formed in the three-way catalyst. *Environ. Sci. Technol.* **2005**, 39 (1), 331–338.
- (32) Heeb, N. V.; Forss, A. M.; Saxer, C. J.; Wilhelm, P. Methane, benzene and alkyl benzene cold start emission data of gasoline-driven passenger cars representing the vehicle technology of the last two decades. *Atmos. Environ.* **2003**, 37 (37), 5185–5195.
- (33) Saxer, C. J.; Forss, A. M.; Rudy, C.; Heeb, N. V. Benzene, toluene and C2-benzene emissions of 4-stroke motorbikes: Benefits and risks of the current TWC technology. *Atmos. Environ.* **2006**, 40 (31), 6053–6065.
- (34) Omar Amador-Muñoz; Misztal, P. K.; Weber, R.; Worton, D. R.; Zhang, H.; Drozd, G.; Goldstein, A. H. Sensitive detection of n-alkanes using a mixed ionization mode Proton-Transfer Reaction – Mass Spectrometer. *Aerosol Meas. Tech.* In press.

- (35) Chan, T. W.; Meloche, E.; Kubsh, J.; Brezny, R.; Rosenblatt, D.; Rideout, G. Impact of Ambient Temperature on Gaseous and Particle Emissions from a Direct Injection Gasoline Vehicle and its Implications on Particle Filtration. *SAE Int. J. Fuels Lubr.* **2013**, 6, 350–371.
- (36) Dardiotis, C.; Martini, G.; Marotta, A.; Manfredi, U. Low-temperature cold-start gaseous emissions of late technology passenger cars. *Appl. Energy* **2013**, 111, 468–478.
- (37) United States Department of Transportation Bureau of Transportation Statistics. *Transportation Statistics Annual Report*. **2015**.
- (38) U.S. Department of Transportation Federal Highway Administration and Federal Transit Administration. *2013 Status of the Nation's Highways, Bridges and Transit: Conditions and Performance*. **2014**, 1–482.

Chapter 5

5. Comparison of GDI and PFI Vehicles

5.1. Introduction

Vehicle tailpipe emissions are an important source of urban air pollution ¹⁻³. To reduce these emissions, vehicles have been required to meet increasingly strict emissions standards for particulate matter mass (PM), carbon monoxide (CO), total hydrocarbons (THC), and nitrogen oxides (NO_x = nitric oxide NO + nitrogen oxide NO₂) over the last several decades. This has pushed the automotive industry to improve both engine design and after-treatment technologies.

The United States recently increased the Corporate Average Fuel Economy (CAFE) standards ⁴. Gasoline direct injection (GDI) engines have higher fuel economy compared to the more widely used port fuel injection (PFI) engines ⁵. As a result, the market share of GDI engines has increased dramatically over the past decade and is expected to reach 50% of new gasoline vehicles sold in 2016 ^{6,7}. Widespread adoption of new engine technologies raises potential concerns about changes in emissions.

Recent studies have compared particulate number and mass emissions ⁷⁻¹², gas-phase emissions ^{13,14} and exhaust composition ^{7,13,15} between PFI and GDI vehicles. However, many of these studies have only considered very small fleets of a few vehicles, which makes it difficult to draw robust conclusions given the vehicle-to-vehicle variability in tailpipe emissions ². PFI and GDI equipped vehicles must meet the same emissions standards. However, these standards only apply to regulated pollutant metrics. For example, the standards limit the THC mass emissions, but not their composition. Potential changes in the THC composition can have important effects on ozone and secondary organic aerosol (SOA) formation ^{16,17}. Detailed volatile organic compounds

(VOC) speciation of GDI engine emissions database are limited in the literature, and include older studies¹³ and studies with a limited number of compounds reported^{7,14,15}. In addition, PM emissions from PFI engine equipped vehicles are well below existing standards creating the potential for back sliding. Previous studies have shown that GDI engines have higher overall PM emissions^{7,10-12}, and higher particle number emissions^{6,18} than PFI equipped vehicles. However, few studies^{6,10} have tested GDI vehicles meeting the most stringent emission standards: Super ultra-low emitting vehicles (SULEV) and partial-zero emitting vehicles (PZEV).

In this study we present a comprehensive emissions database of GDI and PFI equipped light duty gasoline vehicles tested on a chassis dynamometer over the cold-start unified cycle (UC). Measurements include gas- and particle-phase emissions, including particle number, size distributions, and speciated VOC emissions. We use the data to investigate ozone and SOA formation potential and the importance of cold-start emissions. Finally, we analyze the potential climate effects of switching a PFI to a GDI fleet.

5.2. Fleet overview

In addition to the fleet listed in Table 3.1, in this chapter we report tailpipe emission data from eighty-two light duty gasoline vehicles – nineteen vehicles tested in 2014 combined with previously published data for sixty-three vehicles previously reported². The same protocols were used in both test campaigns.

For discussion, the vehicles are grouped based on engine technology (PFI or GDI) and emission standard: Tier1 (median model year: 1991); LEV (including LEV1 vehicles with median model year: 1999 and LEV2 vehicles with median model year: 2008);

ULEV (including ULEV and L2ULV; median model year: 2010); SULEV (median model year: 2013) as shown in Table S1. The SULEV category also includes vehicles certified as Partial Zero Emission Vehicles (PZEV) which must meet the same tailpipe emissions standard as SULEV vehicles. All SULEV PFI vehicles tested in the 2014 campaign were equipped with a hybrid engine technology.

For all gas- and particle- phase reported emissions (with the exception of NO_x), vehicles certified as LEV (LEV1 and LEV2) were grouped together, since these vehicles meet the same emissions standards for the reported pollutants (see Table S2). For NO_x, LEV1 and ULEV categories were grouped as LEV1; LEV2 and L2ULV vehicles were grouped as LEV2 (Table S2).

To test for statistical significance between two groups, we performed a Wilcoxon non-parametric rank-sum test (suitable for small datasets) with a significance threshold of $\alpha=0.05$. Tests of statistical significance were performed when there were at least five vehicles in each group.

5.3. Real-time Measurements

Real-time measurements were made during the 2014 campaign. Particle number distributions (from 6.4 to 523 nm) were measured by directly sampling from the CVS using a fast response Engine Exhaust Particle Sizer (EEPS, TSI Inc.)¹⁹.

A Single Particle Soot Photometer (SP2, Droplet Measurements Techniques Inc.)^{20,21} was used to measure real-time refractory black carbon (rBC) concentrations from diluted tailpipe emissions. rBC and EC are operationally defined²², and both terms refer to light-absorbing carbon.

The nonrefractory submicron particle mass and chemical composition were measured by a high-resolution time-of-flight aerosol mass spectrometer (HR-tof-AMS, Aerodyne, Inc., MA).

5.4. Emission factors

Gas- and particle-phase emissions are reported as distance-based emission factors (mass of pollutant emitted per mile driven). The mass of pollutant emitted was calculated as the product of the pollutant concentration measured in the CVS times the total volume of air that passed through the CVS. We also report the measured fuel efficiency for each test (Table S6) so the distance based emission factors (Table S6) can be converted to fuel-based ones.

Emission factors for gas-phase pollutants are corrected for background concentrations measured in the dilution air upstream of the mixing section of the CVS. Background PM and EC mass concentrations measured during dynamic blank experiments (CVS was operated only on dilution air i.e., no exhaust) were below detection limit. However, reported OC emission factors are not background corrected because the dynamic blank OC levels (average \pm one standard deviation of $15.4 \pm 1.9 \mu\text{g}\cdot\text{m}^{-3}$) exceeded the OC mass collected on filters during tests of very low emitting vehicles (the lowest mass concentration collected on filter corresponded to $11.2 \mu\text{g}\cdot\text{m}^{-3}$), due to organics desorbing from the CVS walls².

5.5. Results

5.5.1. Gas- and particle-phase emissions

Emissions of THC, CO, and NO_x (as NO₂) are plotted in Figure 5.1 (the data are given in Table S6 in SI). The distribution of emissions among the set of vehicles within a given vehicle class are shown using box-whisker plots, with the exception the LEV GDI category (N=2) for which the box shows the full range of emissions. For vehicles tested multiple times, we report the average emission factors over all tests, in order to examine the vehicle-to-vehicle variability. Experimental repeatability is shown in Figure S2 in the SI; test-to-test variability of the same vehicle was < 1% for CO₂ and had an inter-quartile range of 45% for other pollutants.

There is significant vehicle-to-vehicle variability in emissions within each class, with the data exhibiting relative standard deviation ranging from 100% to 300%. Emissions appear to be somewhat more variable for newer vehicles. Similar vehicle-to-vehicle variability was observed for GDI and PFI vehicles.

As expected, Figure 5.1 shows lower tailpipe emissions of regulated pollutants (THC, CO, and NO_x (as NO₂)) from vehicles that meet more stringent emissions standards. Although Tier1 and LEV vehicles meet the same CO emissions standards (Table S2), these two categories were separated to illustrate the advances in both engine and catalyst technology, which decreased CO distance-based emission factors by a factor of three from an average of 12.0 ± 13.3 g/mi for Tier1 PFIs to 3.9 ± 5.2 g/mi for LEV PFIs ($p = 0.0003$), Figure 5.1b. The large decrease in NO_x emissions between LEV1 to LEV2 vehicles, shown in Figure 5.1c, mirrors the sharp reduction in NO_x emissions standards (whereas, for example, CO emission standard was unchanged, see Table S1). We found no statistically significant differences in gas-phase emissions of ULEV certified GDIs (N=5) and PFIs (N=17).

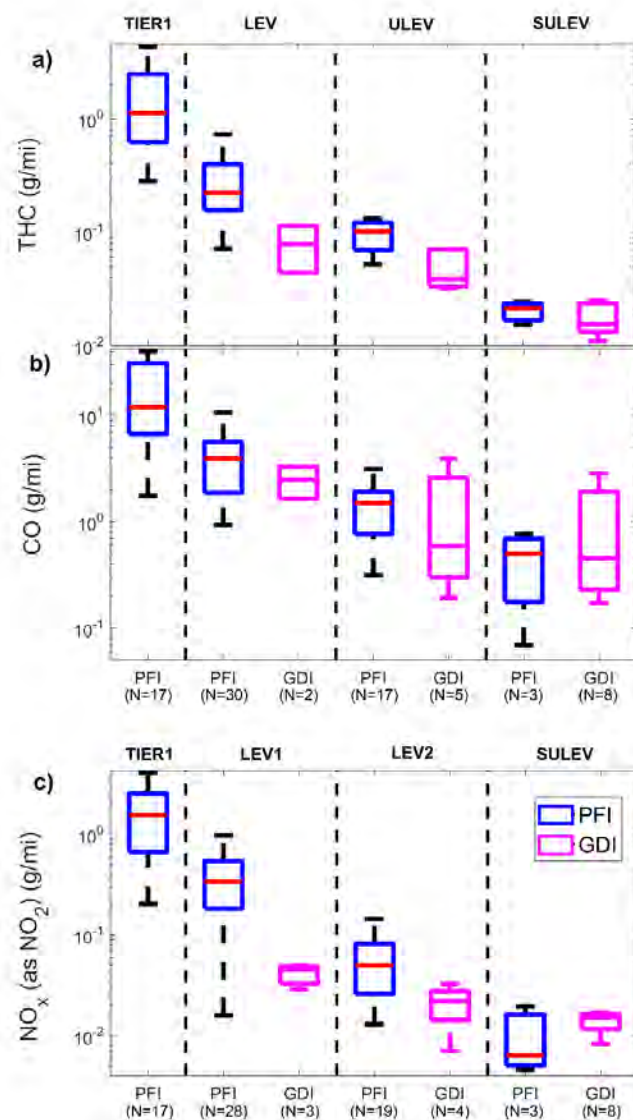


Figure 5.1. Distance-based emission factors for a) THC, b) CO, and c) NO_x (as NO₂) for different vehicle classes. The data are shown as box and whiskers to illustrate vehicle-to-vehicle variability in emissions for each class (with the box representing the 25th to 75th interval and the horizontal line indicating the median). Blue and magenta box-whiskers represent data from PFI and GDI equipped vehicles respectively. Vehicles are grouped based on emission certification standard. Dashed vertical lines indicate different emission standards.

Figure 5.2a shows PM emission factors for all vehicle categories (data are given in Table S6 in SI). We obtained good PM mass closure for all the vehicles tested, with 61% of the data having a ratio of speciated PM to gravimetric PM between 0.8 and 1.2 (Figure S3). The gravimetric PM mass emissions are shown using box-whisker plots to illustrate

the vehicle-to-vehicle variability for each vehicle class; also shown are the median EC and particulate organic mass (OM), defined as OC multiplied by 1.2 organic-matter-to-organic-carbon ratio, which is representative of fresh vehicle emissions²³. Box-whiskers plots for EC and OC are shown in the SI, Figure S3.

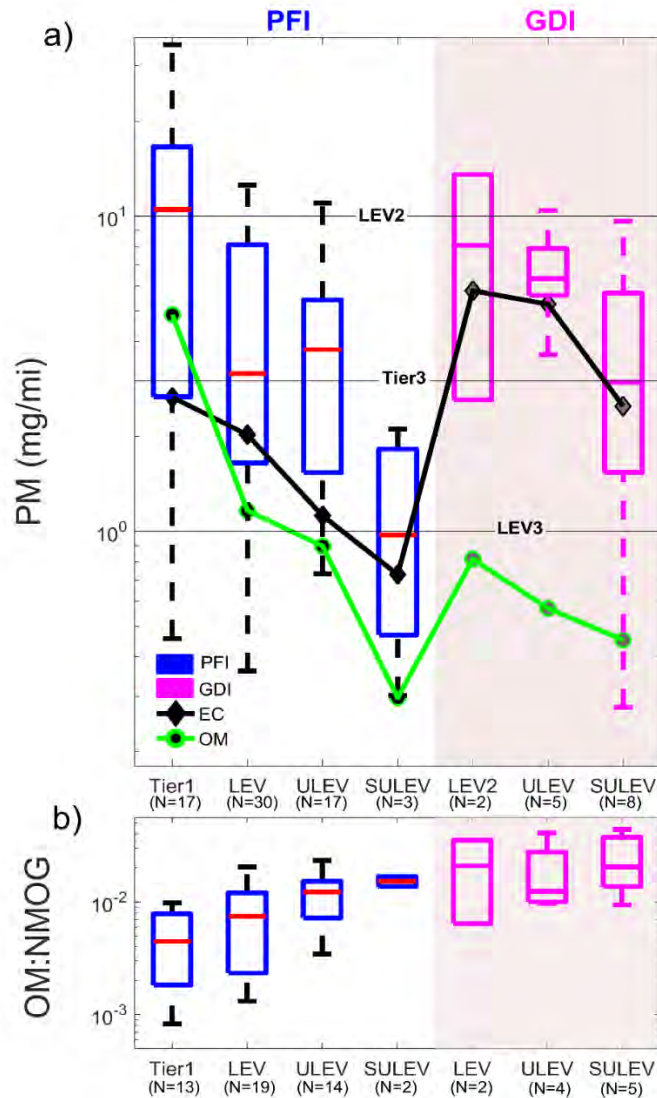


Figure 5.2. (a) PM mass (shown in box whiskers), median EC (black diamond data points) and median OM (green circle data points) distance-based emission factors (mg/mi) for different vehicle classes. Horizontal lines indicate PM emission standards (current PM LEV2 regulation of 10 mg/mi and future, Tier3 and LEV3, PM regulations of 3 mg/mi and 1 mg/mi respectively) for reference. (b) OM:NMOG ratio of different vehicle classes (OM is the organic mass collected on a quartz filter; NMOG is non-methane organic gases). Blue and magenta box-whiskers correspond to PFI and GDI

equipped vehicles respectively. Vehicles are grouped based on emission certification standard.

For most of the tested vehicles, PM emission factors are lower than the current standard of 10 mg/mi, even though they were tested on the more aggressive UC cycle. However, new Federal (Tier3) and California (LEV3) standards limit PM mass emissions to 3 mg/mi and 1 mg/mi respectively (to be enforced starting 2018).

We measured higher PM mass emissions from GDI vehicles certified as LEV2 or newer (N=15) compared to PFI vehicles certified as LEV2 or newer (N=30): median emissions of 4.2 ± 3.7 mg/mi versus 2.6 ± 2.9 mg/mi ($p=0.05$). Similarly, PM distance-based emission factors from ULEV GDI vehicles are about a factor of two higher than ULEV PFI vehicles (median PM emissions of 6.3 ± 2.4 versus 3.8 ± 3.0 mg/mi). In fact, the average PM mass fuel-based emission factors from ULEV GDI engines are only 10% lower than the median PM mass emission factors from 25+ years old Tier1 PFI engines. In contrast, newer SULEV GDIs have lower PM mass emissions (3.0 ± 3.1 mg/mi) compared to ULEV GDIs (6.3 ± 2.4 mg/mi) indicating reduced PM emissions from newer GDI engine technology, and the spray-guided GDI SULEV vehicle had PM emission factors of 0.7 mg/mi already below the LEV3 PM standards. However, additional reductions in PM emissions from GDI engines will likely be needed to meet the stricter LEV3 and Tier 3 standards. In contrast to SULEV GDIs, all SULEV PFI vehicles tested appear to meet both the Tier3 and LEV3 PM standard (assuming PM mass emissions from the UC are a factor of two higher than from the FTP²⁴).

The PM composition data indicate that EC drives the variation in PM mass emissions. We measured a five-fold increase in median EC emission factors for GDI vehicles compared to PFI vehicles (5.3 ± 1.9 mg/mi versus 1.1 ± 2.4 mg/mi) that meet the ULEV

standard. This is similar to previously reported increase in BC emission factors between PFI and GDI vehicles ²⁵. For vehicles certified as SULEV, we measured a threefold increase in median EC emission factors (2.5 ± 2.4 mg/mi for GDI vehicles versus 0.8 ± 0.6 mg/mi for PFI vehicles). This is smaller than the 3 to 17 fold increase in BC emissions from two PZEV GDI vehicles compared to a single L2ULV PFI vehicle reported in ¹⁰ based on the FTP.

In contrast to EC, all newer vehicles have lower OC emissions. However, the median OC emissions of PFI vehicles (certified as LEV2 or newer, N=30) is about a factor of two larger compared to GDI vehicles (N=15): 0.7 ± 0.6 mg/mi versus 0.4 ± 0.2 mg/mi ($p=0.009$). The steady decrease in OC emission factors (due to better catalyst converters) means that EC dominates PM emissions from newer vehicles (Figure S4) with EC contributing more than 80% of speciated PM mass for GDI vehicles. The PM composition of GDI emissions is similar to diesel engines not equipped with diesel particulate filters ^{2,26}, indicating that EC emissions from GDI engines are largely uncoated with organics (Figure S4). Therefore widespread adoption of GDI vehicles will dramatically reduce the utility of EC as a marker for diesel exhaust in urban environment ^{26,27}.

Composition of primary organic aerosols (POA) emitted from vehicle tailpipe was measured using the AMS, and the data exhibited good correlation with filter collected OM (Figure S14). Composition of POA did not depend on emission certification and on engine technology, as shown in Figure S5.

Figure 5.2b plots the ratio of OM measured using quartz filters to the non-methane organic gas (NMOG) – OM:NMOG. The majority of the organics collected on quartz

filters are semivolatile organics, both particle-phase organics plus some organic vapors ². Therefore the OM:NMOG is an indicator of the ratio of the emissions of semivolatile-to-gas-phase organics.

The median OM:NMOG ratio for all vehicles tested is 0.009 ± 0.01 , indicating that emissions of gas-phase organics dominate those of semivolatile organics. However, the OM:NMOG ratio increases steadily by a factor of more than four moving towards tighter emission certification from a median value of 0.004 ± 0.003 for TIER1 PFIs to 0.02 ± 0.01 for SULEV GDIs (OM contribution increased from 0.4% to 2% of NMOG emissions). Therefore, newer vehicles have relatively higher semivolatile organic emissions. This indicates that catalytic converters more efficiently remove more volatile organic compounds compared to the lower volatility organics collected by quartz filters.

5.5.2. Particle number emissions and size distributions

Figure 5.3 shows measured particle number and size distributions from four GDIs (two ULEVs and two SULEVs) and five PFIs (two SULEVs – hybrids –, a single ULEV, LEV and Tier1). Particle number emissions were only measured available during the 2014 campaign. Figure S6 shows a scatter plot of gravimetric PM mass versus integrated particle volume (calculated from integrating the EEPS particle mobility distribution) for GDI and PFI equipped vehicles. Gravimetric PM mass increases linearly with particle mobility-based volume, regardless of engine technology, leading an average effective particle density (slope) of 0.73 g/cm^3 ($0.38 - 1.09 \text{ g/cm}^3$ 95% confidence interval, $R^2 = 0.78$), consistent with the effective density of freshly emitted EC particles ²⁸.

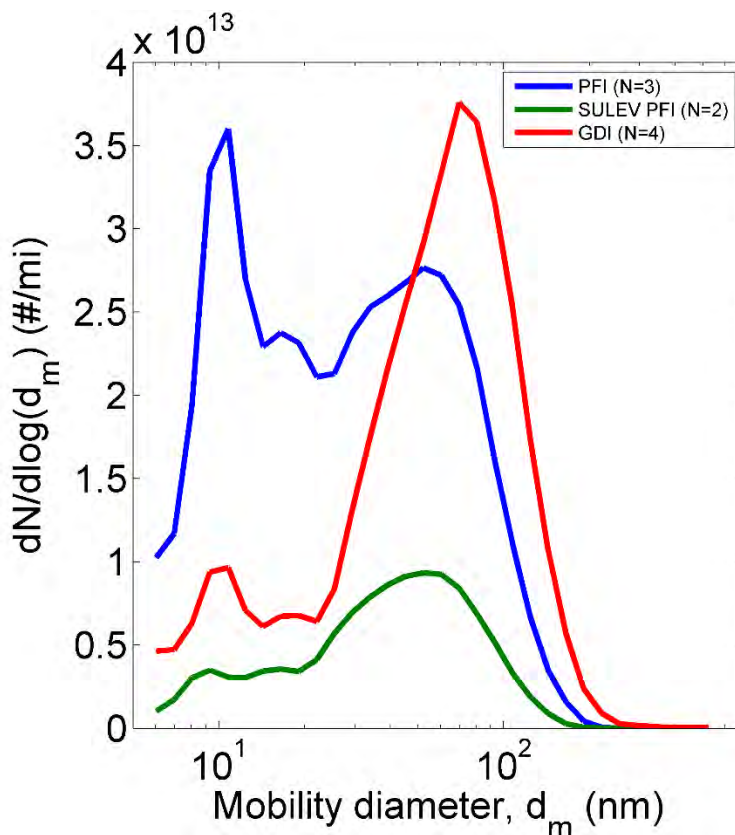


Figure 5.3. Average number size distribution for the entire UC cycle of four GDI vehicles (two ULEVs and two SULEVs; solid red line), 5 PFI vehicles (two SULEVs, one ULEV, LEV and Tier1; solid blue line) and 2 newer hybrid PFI vehicles (two SULEVs; dashed yellow line).

Particle number emissions exhibited significant vehicle-to-vehicle variability. For this test fleet, the GDI vehicles (N=4) had a higher average total particle number emission factor of $(2.4 \pm 1.6) \times 10^{13}$ #/mi ($3.2 \times 10^{13} \pm 4.9 \times 10^{12}$ #/mi excluding the spray-guided GDI) compared to $(6.5 \pm 7.4) \times 10^{12}$ #/mi for PFI vehicles (N=5). In fact the spray-guided GDI had total number emission factor of 1.0×10^{11} #/mi, much lower than wall-guided GDIs. The difference in particle number emission factor between PFI and GDI vehicles is smaller than the order of magnitude increase reported by ¹⁸. However, Braisher et al.¹⁸ compared emissions data using a smaller fleet – two GDI equipped vehicles and a single

PFI equipped vehicle, tested on a cold-start NEDC cycle and using a 5% ethanol blend fuel.

There are important differences in the PM size distributions of GDI and PFI emissions, which must be accounted for when comparing total number emissions. Figure 5.3 shows size distributions averaged over the entire UC for GDI vehicles and two different groups of PFI vehicles (SULEV certified and all other PFI). For most vehicles, the measured number distribution was bimodal with a nucleation mode of ~ 10 nm and an EC mode ~50-90 nm, consistent with previous studies^{6,7,29,30}.

Figure 5.3 indicates that GDI emissions are characterized by: 1) an EC mode mobility diameter that is shifted to larger sizes compared to that of PFI vehicles (mode mobility diameter of ~80 nm for GDIs versus ~ 50 nm for PFIs, regardless of emission certification), and 2) Modestly higher particle number in the EC mode; average of $(2.8 \pm 1.4) \times 10^{13}$ #/mi for GDIs versus an average of $(2.1 \pm 3.0) \times 10^{13}$ #/mi for all PFIs. Both of these factors contribute to higher PM mass emissions from GDI vehicles compared to PFI vehicles. Non-hybrid PFI vehicles have higher particle number emissions in the nucleation mode compared to GDI vehicles; $(9.9 \pm 8.1) \times 10^{12}$ #/mi versus $(3.5 \pm 2.8) \times 10^{12}$ #/mi for PFI and GDI vehicles respectively and for particles with mobility diameter smaller than 20 nm. This is likely related to the differences in particle surface area. GDI vehicles have much higher EC emissions (particle surface area) than PFI vehicles. EC serves as a sink for condensable vapors, suppressing nucleation³¹. A challenge is that nucleation is sensitive to dilution conditions³², making it difficult to extrapolate number emissions data measured in a CVS into the real world. Differences sampling conditions may also contribute to the differences in number emissions reported here and by Braisher

et al¹⁸. In contrast, SULEV PFIs have a nucleation mode that is significantly suppressed compared to other non-SULEV PFIs (sevenfold decrease in particle number).

5.5.3.VOC Speciation

The impact of vehicle emissions on ozone and secondary organic aerosol formation (SOA) depends on the speciation of volatile organic compound (VOC) emissions. Individual VOCs are also air toxics. Although previous studies have reported detailed VOC composition of gasoline vehicle emissions^{2,33}, limited data are found in the literature^{7,13} about a direct and comparison of VOC composition from PFI and GDI vehicles.

Figure 5.4 shows the average composition of speciated non-methane VOCs (206 identified compounds) for all vehicle categories. VOC composition data are listed in Table S7 in SI, and the vehicle-to-vehicle variability in VOC composition is shown in Figure S9 and S10. The data are shown in the following categories: C2-C6 straight/branched paraffins, C7-C12+ straight/branched paraffins, olefins/naphthenes, poly-cyclic olefins, single-ring aromatics, poly-cyclic aromatics, alkynes, and oxygenated (dominated by formaldehyde and acetaldehyde). There were no major differences in VOC composition between vehicle class regardless of engine technology, with the exception of relatively higher contributions of oxygenated compounds from SULEV GDIs compared to other vehicle categories (~25% versus ~5% of speciated non-methane VOCs) and therefore lower contribution from olefins/naphthenes and single-ring aromatics.

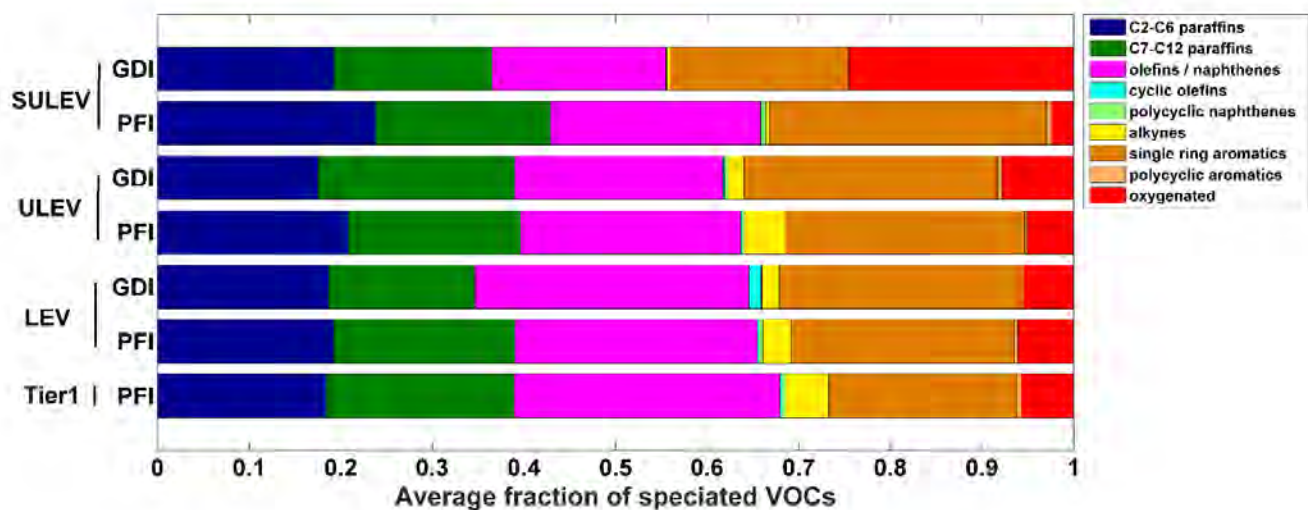


Figure 5.4. Detailed speciation of non-methane VOCs. Across all vehicle categories the VOC speciation emission profile is consistent with the exception of relatively higher oxygenated compound emissions from newer SULEV GDIs. Vehicles are grouped based on emission certification standard, as described in the text.

Several non-aromatic carbonyls (formaldehyde, acetaldehyde, and acrolein) and single-ring aromatics are classified as priority mobile source air toxics (MSATs)³⁴. Emission factors for benzene, toluene, ethylbenzene, and xylenes (BTEX) are shown in Figure S11 in the SI for different vehicle categories. BTEX emissions mirror THC emissions (Figure 5.1) with lower emissions from vehicles meeting more stringent emissions. There are negligible ethylbenzene emissions from newer vehicles. Zimmerman et al. (2016) reports elevated emissions of BTEX from a single GDI vehicle compared to the Toronto fleet. We found no statistically significant difference in BTEX compounds emission factors between GDI and PFI engine emissions for our larger GDI vehicle fleet.

Acetaldehyde and formaldehyde dominate the mass of oxygenated compounds. SULEV GDIs have two times higher formaldehyde emission factors compared to ULEV

GDI; 2.1 ± 3.6 mg/mi for SULEV GDIs versus 1.2 ± 0.7 mg/mi for ULEV GDIs. However, the large variability in formaldehyde emissions from the SULEV category is due to a single vehicle having large formaldehyde emissions.

To quantify the effects of switching engine technologies (GDI vs. PFI) on ozone and SOA production, we calculate both the ozone and SOA formation potentials using VOC composition data. Ozone formation potential ($\text{g O}_3/\text{g VOC}$) is an estimate of the maximum amount of ozone formed from a given amount of reacted VOC. We calculated this potential maximum incremental reactivity (MIR) values (available at <http://www.oal.ca.gov/CCR.htm>³⁵). VOC emissions from PFI and GDI vehicles have essentially the same median ozone formation potential 3.0 ± 1.2 versus 2.8 ± 1.2 $\text{g O}_3/\text{g VOC}$ ($p=0.7$) for all vehicles certified as LEV2 or newer this is in agreement with findings from Kirchstetter et al¹⁶ and Cole et al¹³.

We calculated the SOA formation potential using the high NO_x mass-yield data in CMAQv4.7³⁶ for speciated VOCs and the mass-yield data from Jathar et al.³⁷ for unspeciated VOCs. The calculations assume an organic mass concentration of $5 \mu\text{g}/\text{m}^3$. Both technologies have essentially the same SOA formation potential with a median SOA mass-yield ($\text{mg SOA}/\text{mg VOC}$) of $6.5\% \pm 2.9$ and $6.9\% \pm 2.4$ ($p=0.8$) for all PFI and GDI vehicles certified as LEV2 or newer respectively.

5.5.4. Cold-start versus hot-stabilized emissions

Cold-start contributes disproportionately to vehicle emissions, because the catalytic converter has not reached its operating temperature^{33,38,39}. We quantify the importance of cold-start using the ratio (γ).

$$\gamma = \frac{m_x^{bag1}}{EF_x^{bag2}} \quad (1)$$

where m_x^{bag1} is the total mass of emissions of pollutant x in UC bag 1 (cold start) and EF_x^{bag2} is the distance-based emissions factors of pollutant x in UC bag 2 (hot-stabilized operations). UC bag 1 is first 5 min of the test cycle; it corresponds to the first 1.2 miles of driving. Therefore, γ represents the number of miles of hot-stabilized driving required to match cold-start (bag 1) emissions from the UC cycle.

Figure 5.5 plots γ values for gas-phase: THC, and CO and NOx and particle phase: POA, rBC, and particle number. The THC γ are shown using a box-whisker plot to illustrate vehicle-to-vehicle variability. γ values for other components exhibit similar variability; only median values for these pollutants in Figure 5.5 to reduce clutter, and box-whiskers for individual components are shown in Figure S12 in the SI. As a reference, the daily average trip length in the US is 9.7 miles⁴⁰. Therefore if gamma is greater than 9.7 miles it means that cold-start emissions exceed those of hot stabilized operations.

Figure 5.5 shows that the importance of cold-start varies by pollutant and emission certification standard, but not engine technology. Cold-start is more important for THC emissions than for other pollutants (e.g. for all vehicles, median $\gamma = 41$ mi for THC versus median $\gamma = 8.1$ mi for CO and $\gamma = 6$ mi for NOx; standard deviations are not reported due to the significant variability in the data). The data exhibited significant scatter as illustrated in Figure 5.5. The median THC γ is four times the daily average trip length of 9.7 miles in the US. Cold-start THC emissions are even more important for newer vehicles; the median THC is $\gamma = 15$ mi for 25+ year-old Tier 1 vehicles versus median $\gamma = 100$ mi for newer SULEV vehicles. Therefore, within the limit of the UC

cycle representing US driving patterns, specifically commuting, cold starts dominate the THC emissions for the majority of the, and only a few percent of the fleet will have significant hot-stabilized emissions compared to cold start emissions in the next several years. This underscores the importance of continued focus at reducing cold-start emissions.

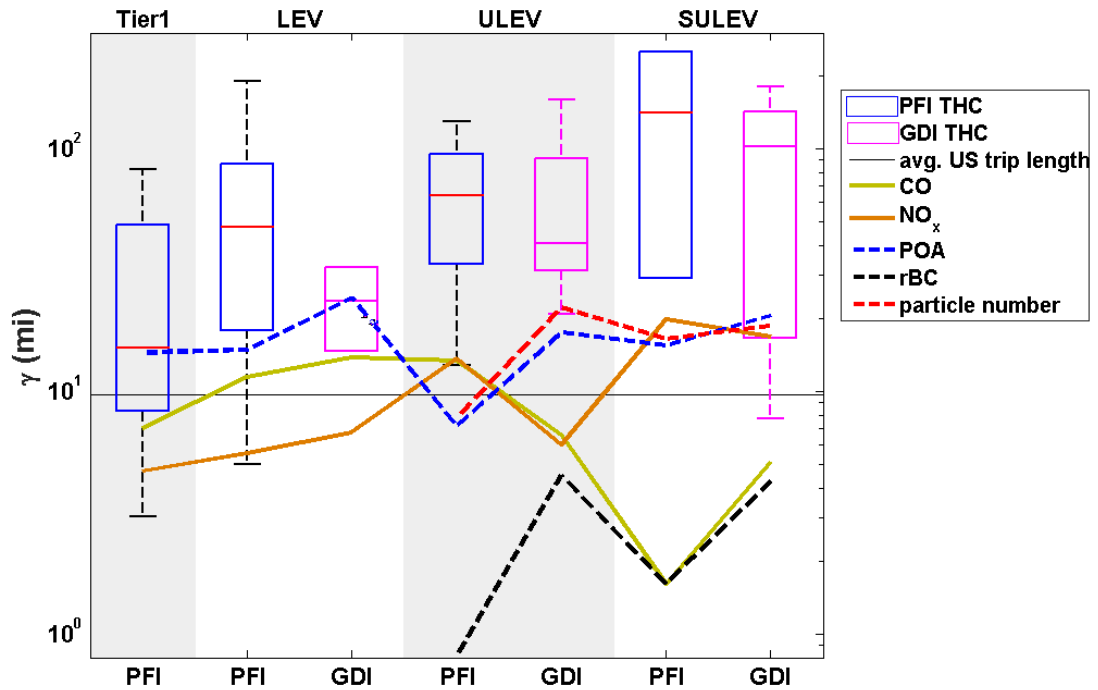


Figure 5.5. Number of miles of hot-stabilized operations (UC bag 2) to equal cold-start (UC bag 1) emissions for different vehicle categories. Values of γ for THC are shown as box whiskers to illustrate vehicle-to-vehicle variability in emissions. Blue and magenta colors for box-whiskers correspond to GDI and PFI engines respectively. Colored solid lines correspond to γ values for CO and NOx. Colored dashed lines correspond to γ values for POA, rBC, and particle number. For reference the U.S average trip length is 9.7 miles, and is shown as the horizontal solid line. Vehicles are grouped based on emission certification standard. The alternating shaded regions indicate different certification standards.

In comparison to THC, cold-start emissions are less important for other gas-phase emissions such as CO and NOx. The median γ for CO and NOx is less than the daily

average trip length in the US. Therefore, both cold-start and hot-stabilized operations likely make significant contributions to real-world emissions for these pollutants. The average γ values for CO decreases as we move towards newer vehicles, from $\gamma = 32$ mi for ULEV vehicles to $\gamma = 4.5$ mi for newer SULEV vehicles. Unlike THC and CO, there is no clear trend in γ with emission certification standard for NO_x.

Figure 5.5 also shows γ values for POA, rBC (or EC) and particle number. EC drives the trends in PM emissions by vehicle class and engine technology (Figure 5.2a). Cold-start is less important for EC than gaseous pollutants. For our fleet, median EC $\gamma = 4$ mi for GDI vehicles $\gamma = 1$ mi for PFI vehicles, indicating cold-start and hot-stabilized operations have similar EC emission factors for PFI vehicles. EC emissions are not controlled by the catalytic converter and therefore not dependent on catalyst warm up. Cold-start is more important for GDI vehicles than for PFI vehicles (median γ EC of 4 versus 1 mile). In contrast to EC, γ values for POA dependent little on engine technology and emission certification (median $\gamma = 17.1 \pm 9.1$ mi for all vehicles, Figure 5.5). Similarly to POA, median γ values for particle number follow closely γ trends for γ POA.

γ values for the major SOA precursors (sum of single-ring aromatics and unspciated VOCs), BTEX, and air toxics (formaldehyde and acetaldehyde) are shown in Figure S12. Emissions of these species largely mirror those of the THC, i.e., increased importance of cold-start emissions from newer vehicles. However, this is not true for all organics. For example, primary fuel compounds in the C7-C12+ paraffin category, and a majority of single ring aromatic compounds (not including BTEX) have undefined γ values due to undetectable emissions during the hot-stabilized phase. In addition cold-start emissions

for formaldehyde are less important for newer vehicles, as shown by the decrease γ from a median $\gamma = 22$ mi for LEV vehicles to $\gamma = 4$ mi for SULEV GDI vehicles.

5.6. Potential climate impacts

Higher fuel efficiency is a major motivation for the widespread adoption of GDI vehicles. For our fleet, the GDI vehicles had on average 57 g/mi (10 g/mi – 104 g/mi; 95% confidence interval, Figure S15) lower CO₂ emissions than PFI vehicles, which corresponds to a 14.5% (2% – 31%; 95% confidence interval) increase in fuel economy. This suggests a potentially important climate benefit. However, GDI vehicles have higher EC emissions. Black carbon (BC, or EC) is the most potent light-absorber component in anthropogenic PM emissions²⁶ and can have significant warming impact on the overall energy balance of the earth^{41,42}. Therefore, the climate benefit depends not only on increases in fuel efficiency, but also on changes in BC emissions.

In this section, we examine the potential climate implications of the tradeoff between increased EC emissions from GDI vehicles potentially offsetting the lower CO₂ emissions compared to PFI vehicles. Using emission factors for EC and CO₂ from all PFI and GDI vehicles, we investigated the climate tradeoffs between lower CO₂ emissions and higher BC emission factors. We compare the net atmospheric CO₂ addition or removal from replacing a PFI engine by a GDI engine, by converting EC emissions to equivalent CO₂ (CO_{2-e}).

$$\text{Net CO}_2 = \Delta\text{EC} * GWP_{BC} \frac{\text{gCO}_{2-e}}{\text{gBC}} - \Delta\text{CO}_2 \quad (2)$$

Where ΔEC indicates the measured increase in EC emissions, ΔCO_2 indicates the measured decrease in CO₂ distance-based emission factor. EC emissions are converted to

a CO₂ equivalent basis using the BC global warming potential (GWP_{BC}, 3200 gCO₂-e/gBC for a 20 year horizon period and 900 gCO₂-e/gBC for a 100 year horizon period)

26

We evaluated equation (2) by randomly sampling emissions data from our fleet of GDI and PFI vehicles 100,000 times using a Monte Carlo simulation. We calculated that increases in the fuel economy of PFI vehicles of 1.6% (0.5% – 2.4%; 95% confidence interval) and 0.5% (0.14% – 0.67%; 95% confidence interval) are sufficient to offset warming from increased EC emissions from GDIs over a 20 year and a 100 year horizon periods respectively. This is much lower than the measured 14.5% increase in fuel economy between PFI and GDI vehicles. Therefore, there is a net climate benefit associated with switching from PFI to GDI vehicles ²⁵. However, the increased BC emissions reduce the potential climate benefits of switching to higher efficiency GDI vehicles by 10-20%.

Supplemental Information Available

References

1. Worton, D. R. *et al.* Lubricating oil dominates primary organic aerosol emissions from motor vehicles. *Environ. Sci. Technol.* **48**, 3698–3706 (2014).
2. May, A. A. *et al.* Gas- and particle-phase primary emissions from in-use, on-road gasoline and diesel vehicles. *Atmos. Environ.* **88**, 247–260 (2014).
3. Borbon, A. *et al.* Emission ratios of anthropogenic volatile organic compounds in northern mid-latitude megacities: Observations versus emission inventories in Los Angeles and Paris. *J. Geophys. Res. Atmos.* **118**, 2041–2057 (2013).
4. NHTSA. *United States Department of Transportation, CORPORATE AVERAGE FUEL ECONOMY FOR MY 2011-2015 PASSENGER CARS and LIGHT TRUCKS.* (2010).
5. Zhao, F., Lai, M. C. & Harrington, D. L. Automotive spark-ignited direct-injection gasoline engines. *Prog. Energy Combust. Sci.* **25**, 437–562 (1999).
6. Zhang, S. & McMahon, W. Particulate Emissions for LEV II Light-Duty Gasoline Direct Injection Vehicles. *SAE Int. J. Fuels Lubr.* **5**, 637–646 (2012).
7. Zimmerman, N. *et al.* Field Measurements of Gasoline Direct Injection Emission Factors: Spatial and Seasonal Variability. *Environ. Sci. Technol.* **50**, 2035–43

- (2016).
8. Zhang, S. & McMahon, W. Particulate Emissions for LEV II Light-Duty Gasoline Direct Injection Vehicles. *SAE Int. J. Fuels Lubr.* **5**, (2012).
 9. Fushimi, A. *et al.* Chemical composition and source of fine and nanoparticles from recent direct injection gasoline passenger cars: Effects of fuel and ambient temperature. *Atmos. Environ.* **124**, 77–84 (2016).
 10. Bahreini, R. *et al.* Characterizing emissions and optical properties of particulate matter from PFI and GDI light-duty gasoline vehicles. *J. Aerosol Sci.* **90**, 144–153 (2015).
 11. Khalek, I. A., Bougher, T. & Jetter, J. J. Particle Emissions from a 2009 Gasoline Direct Injection Engine Using Different Commercially Available Fuels. *SAE Int. J. Fuels Lubr.* **3**, 623–637 (2010).
 12. Liang, B. *et al.* Comparison of PM emissions from a gasoline direct injected (GDI) vehicle and a port fuel injected (PFI) vehicle measured by electrical low pressure impactor (ELPI) with two fuels: Gasoline and M15 methanol gasoline. *J. Aerosol Sci.* **57**, 22–31 (2013).
 13. Cole, R. L., Poola, R. B. & Sekar, R. Exhaust Emissions of a Vehicle with a Gasoline Direct-Injection Engine. *SAE Tech. Pap.* (1998). doi:10.4271/982605
 14. Myung, C. L. *et al.* Comparative study of regulated and unregulated toxic emissions characteristics from a spark ignition direct injection light-duty vehicle fueled with gasoline and liquid phase LPG (liquefied petroleum gas). *Energy* **44**, 189–196 (2012).
 15. Storey, J. M. *et al.* Novel Characterization of GDI Engine Exhaust for Gasoline and Mid-Level Gasoline-Alcohol Blends. *SAE Int. J. Fuels Lubr.* **7**, 571–579 (2014).
 16. Kirchstetter, T. W., Singer, B. C., Harley, R. A., Kendall, G. R. & Hesson, J. M. Impact of California reformulated gasoline on motor vehicle emissions. 2. Volatile organic compound speciation and reactivity. *Environ. Sci. Technol.* **33**, 329–336 (1999).
 17. Odum, J. R., Jungkamp, T. P., Griffin, R. J., Flagan, R. C. & Seinfeld, J. H. The atmospheric aerosol-forming potential of whole gasoline vapor. *Science* **276**, 96–99 (1997).
 18. Braisher, M., Stone, R. & Price, P. Particle Number Emissions from a Range of European Vehicles. *Soc. Automot. Eng.* (2010). doi:10.4271/2010-01-0786
 19. Ayala, A. & Herner, J. D. Transient Ultrafine Particle Emission Measurements with a New Fast Particle Aerosol Sizer for a Trap Equipped Diesel Truck. *SAE Tech. Pap.* **2005-01-38**, (2005).
 20. Schwarz, J. P. *et al.* Single-particle measurements of midlatitude black carbon and light-scattering aerosols from the boundary layer to the lower stratosphere. *J. Geophys. Res.* **111**, D16207 (2006).
 21. Moteki, N. & Kondo, Y. Dependence of Laser-Induced Incandescence on Physical Properties of Black Carbon Aerosols: Measurements and Theoretical Interpretation. *Aerosol Science and Technology* **44**, 663–675 (2010).
 22. Andreae, M. O. & Gelencsér, A. Black carbon or brown carbon? The nature of light-absorbing carbonaceous aerosols. *Atmos. Chem. Phys.* **6**, 3419–3463 (2006).
 23. Turpin, B. J. & Lim, H.-J. Species Contributions to PM_{2.5} Mass Concentrations:

- Revisiting Common Assumptions for Estimating Organic Mass. *Aerosol Sci. Technol.* **35**, 602–610 (2001).
24. Robert, M. a, VanBergen, S., Kleeman, M. J. & Jakober, C. A. Size and composition distributions of particulate matter emissions: part 1--light-duty gasoline vehicles. *J. Air Waste Manage. Assoc.* **57**, 1414–1428 (2007).
 25. Zimmerman, N., Wang, J. M., Jeong, C.-H., Wallace, J. S. & Evans, G. J. Assessing the Climate Trade-Offs of Gasoline Direct Injection Engines. *Environ. Sci. Technol.* acs.est.6b01800 (2016). doi:10.1021/acs.est.6b01800
 26. Bond, T. C. *et al.* Bounding the role of black carbon in the climate system: A scientific assessment. *J. Geophys. Res. Atmos.* **118**, 5380–5552 (2013).
 27. NIOSH. NIOSH. Elemental carbon (diesel particulate): Method 5040. *NIOSH Man. Anal. Methods 4th ed.*, National Institute for Occupational Safety and Health (1996).
 28. Schnitzler, E. G., Dutt, A., Charbonneau, A. M., Olfert, J. S. & Jørgen, W. Soot aggregate restructuring due to coatings of secondary organic aerosol derived from aromatic precursors. *Environ. Sci. Technol.* **48**, 14309–14316 (2014).
 29. Peckham, M. S., Finch, a., Campbell, B., Price, P. & Davies, M. T. Study of Particle Number Emissions from a Turbocharged Gasoline Direct Injection (GDI) Engine Including Data from a Fast-Response Particle Size Spectrometer. *SAE Tech. Pap.* 1–11 (2011). doi:10.4271/2011-01-1224
 30. Karjalainen, P. *et al.* Exhaust particles of modern gasoline vehicles: A laboratory and an on-road study. *Atmos. Environ.* **97**, 262–270 (2014).
 31. Kerminen, V. M. & Wexler, A. S. The Interdependence Of Aerosol Processes And Mixing In Point-Source Plumes. *Atmos. Environ.* **29**, 361–375 (1995).
 32. Abdul-Khalek, I., Kittelson, D., Brear, F. & Kittleson, D. The Influence of Dilution Conditions on Diesel Exhaust Particle Size Distribution Measurements. **1999-01-11**, 1142–1999 (1999).
 33. Drozd, G. T. *et al.* Time resolved measurements of speciated tailpipe emissions from motor vehicles: trends with emission control technology, cold start effects, and speciation. *Environ. Sci. Technol.* acs.est.6b04513 (2016). doi:10.1021/acs.est.6b04513
 34. Federal Highway Administration, U. S. D. of T. *Transportation Air Quality Selected Facts and Figures.* (2016).
 35. Carter, W. P. L. Development of Ozone Reactivity Scales for Volatile Organic Compounds. *Air Waste* **44**, 881–899 (1994).
 36. Carlton, A. G. *et al.* Model representation of secondary organic aerosol in CMAQv4.7. *Environ. Sci. Technol.* **44**, 8553–60 (2010).
 37. Jathar, S. H. *et al.* Unspeciated organic emissions from combustion sources and their influence on the secondary organic aerosol budget in the United States. *Proc. Natl. Acad. Sci. U. S. A.* **111**, 10473–10478 (2014).
 38. George, I. J. *et al.* Effects of Cold Temperature and Ethanol Content on VOC Emissions from Light-Duty Gasoline Vehicles. *Environ. Sci. Technol.* **49**, 13067–13074 (2015).
 39. Weilenmann, M. F., Soltic, P. & Hausberger, S. The cold start emissions of light-duty-vehicle fleets: A simplified physics-based model for the estimation of CO₂ and pollutants. *Sci. Total Environ.* **444**, 161–176 (2013).

40. FHA. United States Department of Transportation, Summary of Travel Trends: 2009 National Household Travel Survey. 82 (2011). doi:FHWA-PL-11-022
41. Jacobson, M. Z. Strong radiative heating due to the mixing state of black carbon in atmospheric aerosols. *Nature* **409**, 695–697 (2001).
42. Ramanathan, V. & Carmichael, G. Global and regional climate changes due to black carbon. *Nature Geoscience* **1**, 221–227 (2008).

Chapter 6

Detailed Speciation of IVOC and SVOC: Cold Start Effects and Sources

6.1 Introduction

Tailpipe emissions from gasoline vehicles are a significant contributor to secondary organic aerosol emissions in urban areas.¹⁻⁴ Single-ring aromatics (SRA), intermediate volatility organic compounds (IVOC), and semi-volatile organic compounds (SVOC) all contribute to observed SOA formation during photo oxidation of vehicle exhaust gases.⁵⁻⁷ IVOC have recently been estimated to contribute up to half of all SOA formation from gasoline vehicles, changing the view that SRA alone dominate formation of SOA from gasoline vehicles.^{6,8-10} Because of their importance in SOA formation, IVOC and SVOC emissions require detailed characterization, both in terms of composition and dependence on vehicle engine activity.

Organic emissions in vehicle exhaust can be characterized into several groups based on volatility, expressed as an effective saturation concentration (C^*). Major categories include volatile organic compounds (VOC, $C^* > 10^6 \mu\text{g m}^{-3}$), intermediate volatility compounds (IVOC, $10^3 < C^* < 10^6 \mu\text{g m}^{-3}$), and semi-volatile organic compounds and (SVOC, $10^{-1} < C^* < 10^3 \mu\text{g m}^{-3}$). Each volatility class requires different collection and analysis techniques, resulting in different extents and methods of speciation. VOCs are commonly extensively speciated on an individual compound basis, with 100-200 specific compounds quantified.^{6,11,12} IVOC and SVOC are generally much more complex mixtures of compounds that are not readily quantified at the individual compound level. Other techniques have been applied instead that describe these lower volatility emissions

in terms of groups such as aliphatic, aromatic, cyclic, and branched.¹³⁻¹⁵ These groups represent the essential structure information to predict SOA formation, both in terms of yields of SOA and volatility to determine partitioning between the gas and particle phase.

The emissions in each of volatility group depend largely on the inputs (fuel and oil) and processing (combustion and aftertreatment). VOC emissions for gasoline vehicles are mainly attributed to unburned fuel, combustion products, and degradation products formed in the aftertreatment system. IVOC compounds likely have similar sources as VOC; this is supported by strong correlations between IVOC and total NMOG.^{13,14} SVOC are thought to be mainly derived from engine oil, and they are mainly emitted as part of the organic fraction of particulate emissions due to their lower volatility.^{15,16} The different sources for each volatility class will cause different dependencies on engine activity operations the effects of new technologies to reduce total vehicle emissions.

Since the late twentieth century, regulations have been implemented to reduce ozone and fine particulate levels in the United States. In particular regulations for ozone have led to dramatic reductions in non-methane organic gases (NMOG). A significant fraction of ambient fine particulate matter is created from photo oxidation of a subset of the organic gas emissions and formation of secondary organic aerosol (SOA).^{17,18} This fact has led to a secondary benefit in regulation total NMOG emissions from vehicles, reductions in fine particulate matter. Regulations specify the total mass of emissions, rather than targeting the volatility or individual gaseous species. SOA formation is sensitive to the composition of emissions, so future reductions in SOA formation will

depend on both reductions in total emissions and any changes in the composition of these emissions.

Past experiments involving photo oxidation of diluted vehicle exhaust in a smog chamber have shown that less SOA is formed from newer, lower-NMOG emitting gasoline vehicles that meet more stringent emissions standards than from older, higher emitting vehicles.^{19,20,7,21} However, this reduction is not proportional to the reduction in NMOG emissions, which means that the experiments imply that the yield of SOA per mass of NMOG has increased for newer vehicles.^{6,7,22} This would suggest that technologies aimed at reducing total emissions have created a more potent mix of chemicals in exhaust that leads to higher yields of SOA, despite a lower mass of emissions. If this were the case, future reductions in SOA may require targeting specific classes of NMOG compounds.

To address the issues stated above we carried out comprehensive measurements of speciated NMOG emissions. Here we focus on the IVOC and SVOC emissions from vehicles with a wide range of emissions controls technologies to give broader insight into the changing effects of new emissions control technologies and project future vehicle fleet emissions, both in terms of species profiles and identifying future needs in emissions controls. We present measurements of tailpipe emissions for a wide range NMOG classified according to characteristics that determine SOA formation (volatility and chemical structure). State-of-the-art GC analysis techniques utilizing novel ionization and analysis allowed a much higher degree of characterization than previous work. Samples were collected during chassis dynamometer testing of gasoline vehicles recruited from the Southern California fleet to determine the effects of control technologies on the

speciation of emissions and their dependence on engine state (cold-start vs. hot-running and hot start).

6.2 Results and Discussion

6.2.1 IVOC Emissions

Previous measurements for IVOC speciation are limited to older vehicle technologies and do not include vehicles meeting the strictest emissions standards. In this section we present extremely detailed composition measurements of exhaust from a wide range of vehicle classes. Complete composition data was available for the following vehicles: 4 (SULEV+PZEV), 4 ULEV, 2 LEV II, 1 Lev I, 1 Tier 0.

6.2.2 Total IVOC Emissions and Overall Composition

Vehicular IVOC emissions can be broadly grouped into three categories: aliphatic, single-ring aromatics (SRA), and polycyclic aromatic hydrocarbons (PAH). Our 2D-GC-MS analysis is particularly amenable to these categories, because separation is carried out according to both boiling point and polarity. Aliphatics, SAR, and polar compounds. compounds all generally well separated in polarity space (Figure 6.1). The aliphatic group is typically dominated by branched alkanes with small amounts of n-alkanes and cyclic alkanes. The SRA category, to be discussed in great detail below, has a number of alkyl benzene compounds with the alkyl substituents varying in the number of alkyl chains and branching. The PAH category has high fractions of naphthalene and alkylated naphthalenes, with oxidized compounds such as decanal, present in smaller amounts. It should be noted that the demarcations in the second retention time are only

guides as to identification and not strict cutoffs between each category; mass spectral information is also a major part of classification of emissions.

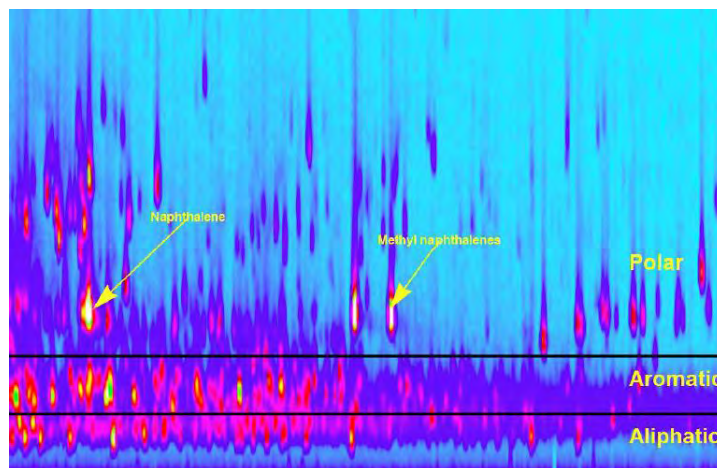


Figure 6.1. Two-dimensional gas chromatogram showing three main categories of emissions compounds: aliphatic, aromatic, and polar.

The total IVOC emissions for all vehicle classes are shown as emission factors in Figure 6.2a, displayed as the average emissions for all vehicles in each class. Emissions drop by about an order of magnitude from the vehicle with the least strict emissions controls (Tier 0) to those with most strict controls (SULEV). There is a sharp drop of about a factor of two in IVOC emissions between the LEV I and LEV II vehicles. This difference fits within the expected decreases in emissions for hydrocarbons set by the LEV II standards and mirrors the decrease in NMOG emissions. Improvements in emissions control technologies have targeted the total mass of hydrocarbons emitted. Most the mass of the emissions lies in the VOC category, so VOC are the main target for new controls. Figure 6.2a shows that as THC emissions are reduced in response to stricter standards, IVOC are reduced significantly as well. This order of magnitude drop in IVOC emissions is similar to the reduction in THC for the current vehicle test fleet. The decreases in THC noted in Chapters 4 and 5 include data from previous measurement

campaigns, and show a slightly larger decrease in THC between the oldest and newest vehicles. The relationship between THC and IVOC emissions will be discussed further below, but in general reductions in THC emissions translate to similar magnitude reductions in IVOC emissions.

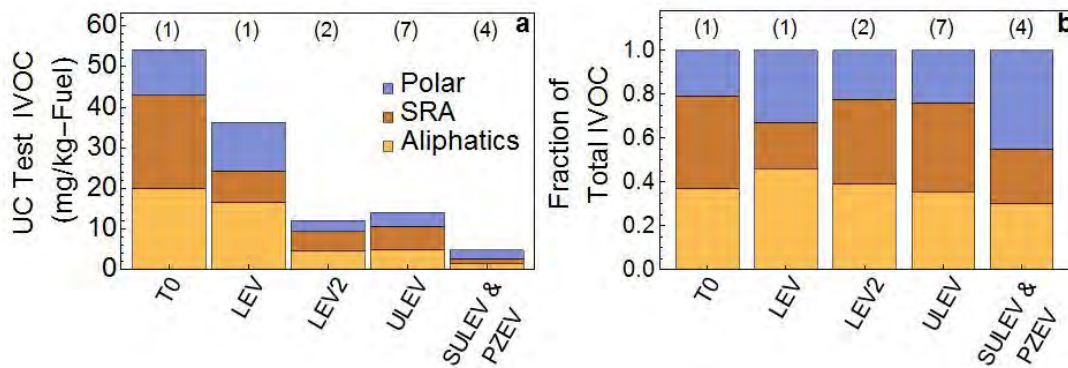


Figure 6.2. Average IVOC emissions for each vehicle class (a): aliphatic, aromatic, and polar, and the fractional composition of emissions (b) mass fractions of aliphatic (yellow), SRA (brown), and polar (blue) compounds. Number of vehicles included are noted above each class in parentheses.

Results for the overall IVOC composition are shown in Figure 6.2b. The total IVOC composition does not change dramatically with vehicle class. Aliphatics make up the most consistent fraction of IVOC emissions, at about 40%. SRA and polar compounds comprise the rest of the observed IVOC mass, generally 60%. Polar compounds are 20-30% of IVOC, except for the newest SULEV vehicles, which show a higher fraction of polar compounds. This suggests that emissions controls have become more effective at removing compounds such as aliphatics and SRA compared to more polar compounds, such as naphthalene. The polar compounds are heavily influenced by very stable naphthalene-derived compounds, and they appear to be more resistant to catalytic destruction compared to the other classes of compounds. The composition does

not change dramatically between the oldest and newest vehicles, this suggests that the ensuing oxidation chemistry after emission, and the resulting yields of ozone and SOA, are also not expected change dramatically.

6.2.3 Relationship Between THC and IVOC Emissions

The relationship between total IVOC emissions and THC emissions is important for both estimating IVOC emissions from the current extensive measurements of THC and predicting future trends in IVOC emissions. Our results for the percentage of IVOC in THC are shown in figure 6.3. IVOC are 2-4% of emissions for the full UC drive cycle. The limited number of vehicles in each class (at most 4) and the variation within each class mean a clear trend is not present, and the best fit value across all classes is 3% with an R^2 of 0.89 (Appendix C, Figure C1). This number is similar to the estimate of Zhao et al. (2016), who used similar methods to estimate that IVOC are 4% of THC emissions. The previous studies of Gentner et al. and Schauer et al. have estimated lower contributions of IVOC to THC of 1-2%.^{12,14} While a couple vehicles tested are near the 2% mark, it is clear that most vehicles emit IVOCs at levels of 3% or more of THC. This suggests some enrichment in IVOC relative to the unburned fuel..

The ratio of cold-start IVOC to cold-start THC is different from that of the full cycle. Both THC and IVOC emissions are dramatically lower during the hot operation phases (hot-running and hot-start) compared to cold-start, but IVOC emission are more consistent between all three operation phases. This results in a significant reduction in the fraction of IVOC emissions from the cold-start, compared to fraction of THC from cold-start when most THC mass is emitted. Thus the correlation of THC and IVOC is largely

derived from the cold start. Newer vehicles have IVOC emissions nearly equivalent during cold and hot operation, as shown in Figure 6.4, whereas in Chapter 3, we clearly showed that THC emissions are becoming increasingly restricted to the cold start. This difference in response to emissions controls for THC and IVOC suggests that their emissions have become less coupled with newer control technologies. This behavior warrants further study, particularly to include separate sampling of IVOC for each phase of the UC protocol, instead of combining the hot-running and hot-start phases.

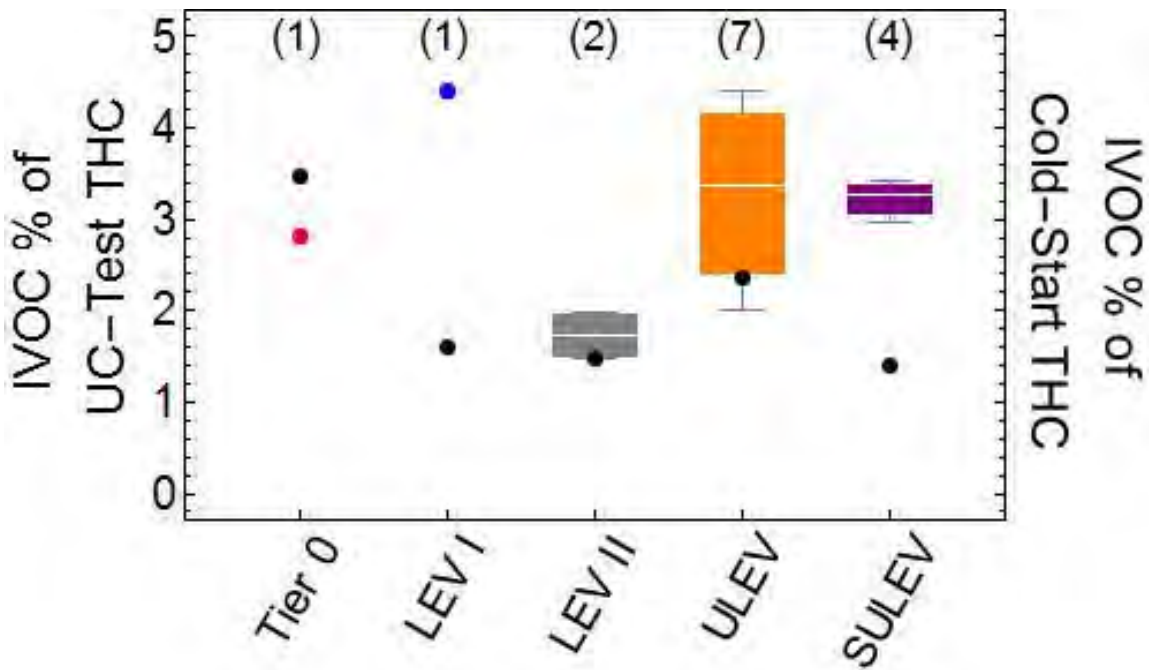


Figure 6.3. The fraction of IVOC in THC for the complete UC test as a percentage for all vehicle classes studied (bar and box-whisker charts). Also shown is this same ratio but only considering the cold start phase of the UC test (black points). Number of vehicles included is shown above each class in parentheses.

6.2.4 Cold Start Effects on IVOC Emissions

Engine state (hot vs. cold) is a critical factor in influencing assessing and predicting emissions, as shown in Chapters 4 and 5. The impact of engine state (and

aftertreatment) on IVOC emissions is shown in Figure 6.4. Emissions during cold-start are shown in blue and hot-operation emissions are shown in red. The ratio of cold:hot IVOC emissions is shown above each pair of data. It is clear that cold-start emissions are generally greater than hot-running emissions. Older emissions control technologies show a factor of 3 or greater difference between the cold-start and hot-operation emissions. These data are shown as bars, because they represent results from single vehicles in the Tier 0 and LEV I classes. Newer vehicles (LEV II, ULEV, and SULEV) show cold:hot emissions ratios between 1 and 2. This decreasing trend in the cold:hot ratio for IVOC is not the same as for VOC. Chapter 4 shows an increasing ratio of cold:hot emissions for THC mass, which is mainly VOC. This is the opposite of that observed for IVOC. Despite this difference in behavior between IVOC and THC, they still remain well correlated for the newer vehicles, shown above with IVOC as a fairly consistent fraction of THC, about 3%. While IVOC emissions have declined with similar efficiency as THC, the fraction of IVOC emissions attributed to the cold-start has been reduced. THC have continued to be well correlated with IVOC, but newer vehicles have a more complex relationship between THC and IVOC, because their dependencies on engine state appear to be diverging.

6.2.5 Volatility of IVOC Emissions

The distribution of emissions as a function of the volatility, expressed as carbon number for the equivalent n-alkane is shown Figure 6.5. Each pane shows the results from a representative vehicle in each emissions standard class and is further divided by composition of material in each bin. All the distributions peak in the n12 or n13 bins. The n12 and n13 bins also carry the overwhelming majority of PAH material, because

naphthalene and the methyl naphthalenes fall in these bins. Vehicles with emissions controls technology meeting less strict standards have somewhat broader volatility distributions and significant material in bins beyond n14. Vehicles meeting stricter emissions standards appear to converge to a similar volatility distribution, with over 90% of material in the n12 and n13 bins. The higher volatility of the IVOC for newer vehicles will lead to intrinsically lower SOA yields.

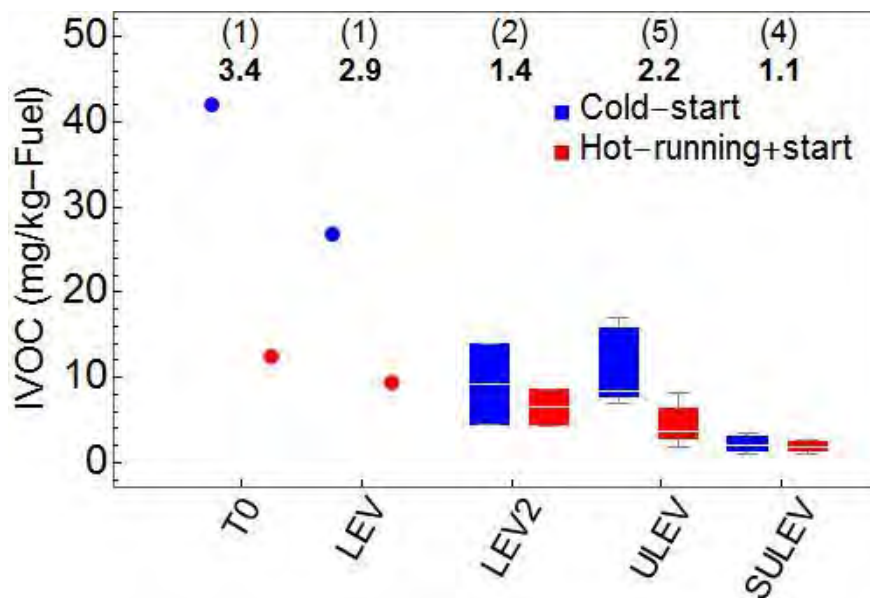


Figure 6.4. Comparison of IVOC emission factors for cold-start (blue) and combined hot-running and hot-start (red) for all vehicle classes. The ratio between the median IVOC emissions during each operating state is shown above each class. Number of vehicles included is shown above each class in parentheses.

6.2.6 Characterization of IVOC-SRA

The emissions of SRA with fewer than 10 carbons, particularly the BTEX compounds, are commonly characterized, but much less is known about the composition of larger SRA. As shown in Fig 6.2, this class of compounds is a significant fraction of the total IVOC mass for all vehicle classes. Furthermore, the IVOC-SRA have not be

studied in smog chamber but have potentially high, unmeasured yields for SOA formation.^{23–25} IVOC-SRA include alkyl benzenes with 4-5 or more carbons in addition to the basic benzene unit. We include in the SRA category compounds that have cyclic aliphatic segments, such as tetralins, because these have a single aromatic ring and elute with a similar second dimension retention time as alkyl benzenes. Standard measurements include only a handful of SRA with substituents that have 5 or more carbons. Because the number of potential isomers increases significantly with the number of substituent carbons, these larger SRA can be difficult to separate and identify uniquely. As detailed in the methods section, we utilized the separation capability of 2D-GC and diagnostic fragmentation in EI ionization to extensively characterize the SRA in the IVOC range.

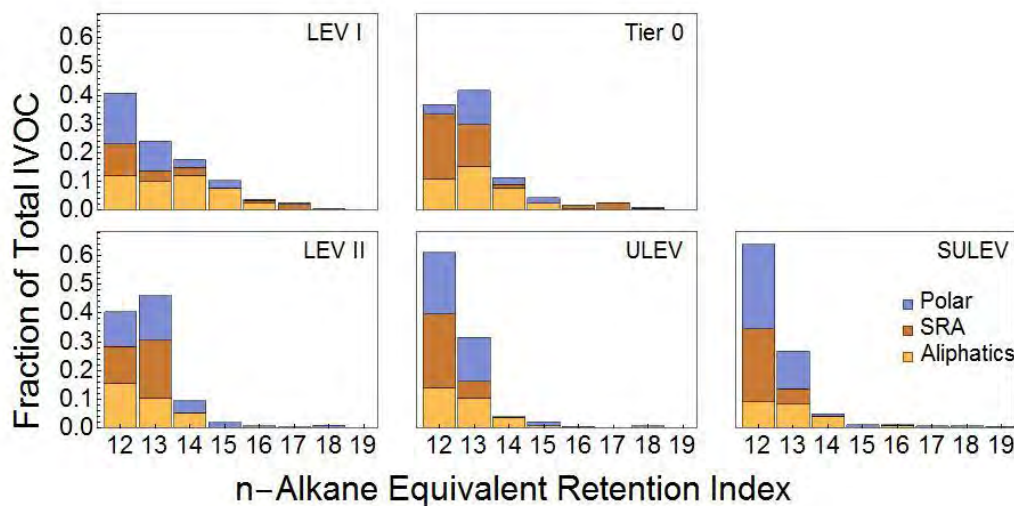


Figure 6.5. The volatility of IVOC emissions is shown as a function of n-alkane equivalent retention time on the first column, for all vehicle classes.

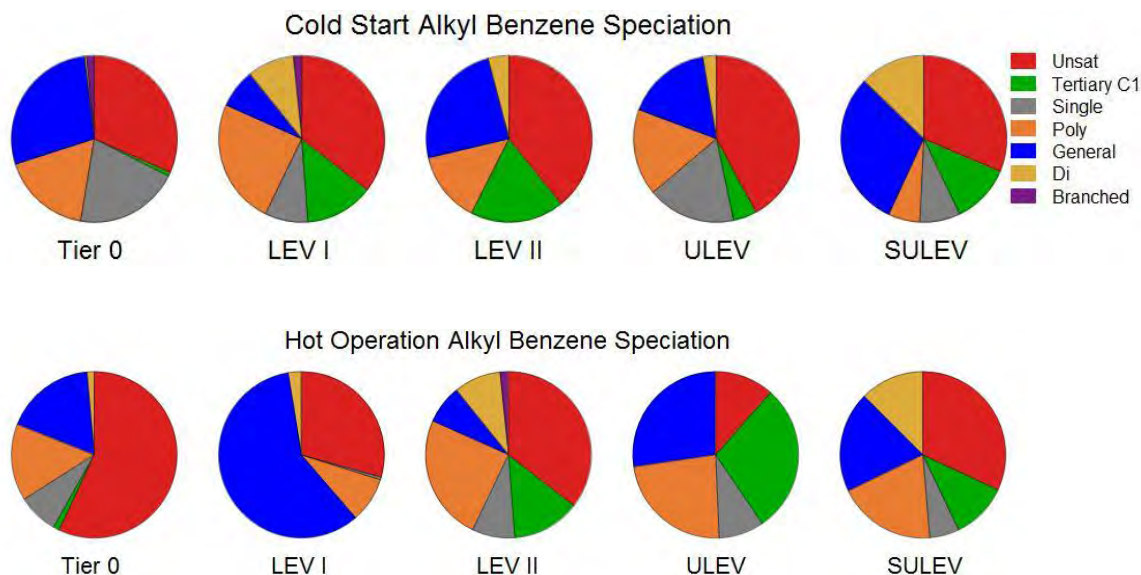


Figure 6.6. Classification of IVOC-SRA across all vehicle classes. Cold start emissions are shown in the top panel; hot-operating emissions, the bottom panel. The types of SRA are shown according to color: unsaturated (red), isopropyl (green), straight-chain (gray), poly substituted (orange), general/unclassified (blue), di-substituted (gold), multiply-branched (purple).

Figure 6.6 shows the distribution of IVOC-SRA types for all vehicle classes, for both cold-starts and hot-operation. Emissions during both engine states (and for all emissions controls categories) always have a significant fraction of unsaturated compounds, shown in red. This type of SRA is mainly composed of substituted tetralin and indane compounds. These compounds are of particular interest, because little is known about their SOA formation potential, but their yields are expected to be higher than other IVOC-SRA. Straight-chain substituted species are always less than 25% of the total IVOC-SRA. Because of the diversity in IVOC-SRA structures and their potential for varying SOA yield, n-alkyl substituents are not likely to accurately represent SOA formation from the full suite of IVOC-SRA present in vehicle exhaust. . In general there is not a clear trend in IVOC-SRA composition with vehicle emissions certification standard. Emissions during hot-operation have a distribution of IVOC-SRA that generally

also has a significant fraction of unsaturated compounds. Again, there does not appear to be a clear trend with emissions certification standard and straight chain alkyl benzenes are even less significant during hot-operation.

6.2.7 Characterization of Primary Organic Aerosol Emissions

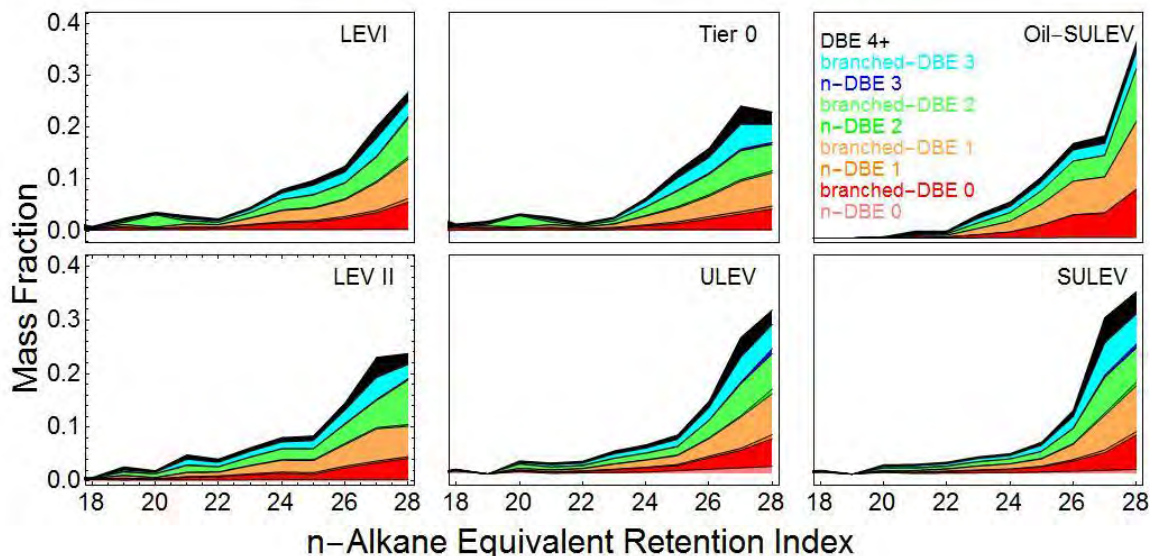


Figure 6.7. Composition of POA according to carbon number, double bond equivalents, and branching. Also shown is the used motor oil from one of the SULEV vehicles.

Total mass and the fraction of organic and elemental carbon of primary PM emissions are discussed in Chapter 5; here we focus on the composition of the organic fraction of primary aerosol (POA). Using analysis by gas chromatography with vacuum ultra violet ionization mass spectrometry (GC-VUV-MS), we characterized the POA collected on bare quartz filters according to according to degree of branching, number of cyclic rings, aromatic character, and carbon number. The results for each vehicle class are presented in Figure 6.7, along with the composition of used motor oil. The general distribution of the molecular composition of the POA is consistent with the engine lubricating oil sampled from the same vehicle. A recent study using this same analysis

method also confirmed that vehicle exhaust composition was dominated by lubricating oil.¹⁵ The majority of the POA mass, 85% or more, is composed of DBE classes 1-3, which is cyclic and polycyclic aliphatic material. Straight chain and branched linear compounds together are typically less than 10% of the total POA composition. The DBE 4+ class, including mainly aromatic compounds and PAHs, makes up the remainder. The integrated mass collected on the bare quartz filter agrees to within 35% of the mass when measured by standard protocols for OC:EC analysis (Figure D1).

6.3 Atmospheric Implications

The detailed analysis of IVOC and SVOC emissions shows a similar composition across vehicles with varying emissions control technologies. The largely consistent composition of exhaust is maintained despite different sources (e.g. fuel and lubricating oil) and dependencies on engine state. Newer vehicles show IVOC emissions that occur throughout the UC test, with less of a dependence on cold-start. SVOC emissions are clearly derived in large part from motor oil and emitted as POA. The composition of the used motor oil POA does not vary dramatically across the vehicle fleet. There is some variation in the composition of the IVOC-SRA. To the extent that the most unique material in terms of SOA production is the unsaturated portion, its fraction does not vary dramatically with vehicle class. To this point advances in emissions controls technology have thus mainly effected exactly what regulations require, they have reduced the total mass of emissions leading to pollutant formation. But we now see some indications that the correlation in THC and IVOC emissions is possibly beginning to diverge, because THC emissions are more strongly linked to cold-starts, whereas IVOC seem to be emitted more continuously across categories of engine operations.

This consistent composition of the IVOC and SVOC exhaust emissions across many vehicle classes suggests that future reductions in the total emissions of organic gases will continue to reduce SOA formation. If benzene and all larger SRA as well as the highly speciated IVOC and SVOC are taken into account, we predict effective SOA yields of ~10%. This is true across all vehicle categories, regardless of age or emissions control technology. Thus future reductions in total exhaust emissions, barring changes in oxidation chemistry, will lead to reductions in SOA formation.

6.4 References

- (1) Bahreini, R.; Middlebrook, A. M.; de Gouw, J. A.; Warneke, C.; Trainer, M.; Brock, C. A.; Stark, H.; Brown, S. S.; Dube, W. P.; Gilman, J. B.; et al. Gasoline emissions dominate over diesel in formation of secondary organic aerosol mass. *Geophys. Res. Lett.* **2012**, 39 (6), n/a-n/a.
- (2) McDonald, B. C.; Gentner, D. R.; Goldstein, A. H.; Harley, R. a. Long-Term Trends in Motor Vehicle Emissions in U.S. Urban Areas. *Environ. Sci. Technol.* **2013**, 47 (17), 10022–10031.
- (3) Jathar, S. H.; Gordon, T. D.; Hennigan, C. J.; Pye, H. O. T.; Pouliot, G.; Adams, P. J.; Donahue, N. M.; Robinson, A. L. Unspeciated organic emissions from combustion sources and their influence on the secondary organic aerosol budget in the United States. *Proc. Natl. Acad. Sci. U. S. A.* **2014**, 111 (29), 10473–10478.
- (4) May, A. A.; Nguyen, N. T.; Presto, A. A.; Gordon, T. D.; Lipsky, E. M.; Karve, M.; Gutierrez, A.; Robertson, W. H.; Zhang, M.; Brandow, C.; et al. Gas- and particle-phase primary emissions from in-use, on-road gasoline and diesel

- vehicles. *Atmos. Environ.* **2014**, 88, 247–260.
- (5) Zhao, Y.; Nguyen, N. T.; Presto, A. A.; Hennigan, C. J.; May, A. A.; Robinson, A. L. Intermediate Volatility Organic Compound Emissions from On-Road Diesel Vehicles: Chemical Composition, Emission Factors, and Estimated Secondary Organic Aerosol Production. *Environ. Sci. Technol.* **2015**, 49 (19), 11516–11526.
 - (6) Gordon, T. D.; Tkacik, D. S.; Presto, A. A.; Zhang, M.; Jathar, S. H.; Nguyen, N. T.; Massetti, J.; Truong, T.; Cicero-Fernandez, P.; Maddox, C.; et al. Primary gas- and particle-phase emissions and secondary organic aerosol production from gasoline and diesel off-road engines. *Environ. Sci. Technol.* **2013**, 47 (24), 14137–14146.
 - (7) Platt, S. M.; El Haddad, I.; Zardini, A. A.; Clairotte, M.; Astorga, C.; Wolf, R.; Slowik, J. G.; Temime-Roussel, B.; Marchand, N.; Jezek, I.; et al. Secondary organic aerosol formation from gasoline vehicle emissions in a new mobile environmental reaction chamber. *Atmos. Chem. Phys.* **2013**, 13 (18), 9141–9158.
 - (8) Odum, J. R.; Hoffmann, T.; Bowman, F.; Collins, D.; Flagan, R. C.; Seinfeld, J. H. Gas/Particle Partitioning and Secondary Organic Aerosol Yields. *Environ. Sci. Technol.* **1996**, 30 (8), 2580–2585.
 - (9) Zhao, Y.; Nguyen, N.; Presto, A.; Hennigan, C.; Robinson, A. Emissions of Intermediate- Volatility Organic Compounds (IVOCs) from On-road Vehicles Primary IVOCs Are an Important Class of SOA Precursors.
 - (10) Tkacik, D. S.; Presto, A. A.; Donahue, N. M.; Robinson, A. L. Secondary organic

- aerosol formation from intermediate-volatility organic compounds: Cyclic, linear, and branched alkanes. *Environ. Sci. Technol.* **2012**, 46 (16), 8773–8781.
- (11) May, A. A.; Presto, A. A.; Hennigan, C. J.; Nguyen, N. T.; Gordon, T. D.; Robinson, A. L. Gas-particle partitioning of primary organic aerosol emissions: (1) Gasoline vehicle exhaust. *Atmos. Environ.* **2013**, 77, 128–139.
- (12) Schauer, J. J.; Kleeman, M. J.; Cass, G. R.; Simoneit, B. R. T. Measurement of emissions from air pollution sources. 5. C1-C32 organic compounds from gasoline-powered motor vehicles. *Environ. Sci. Technol.* **2002**, 36 (6), 1169–1180.
- (13) Zhao, Y.; Nguyen, N. T.; Presto, A. A.; Hennigan, C. J.; May, A. A.; Robinson, A. L. Intermediate Volatility Organic Compound Emissions from On-Road Gasoline Vehicles and Small Off-Road Gasoline Engines. *Environ. Sci. Technol.* **2016**.
- (14) Gentner, D. R.; Isaacman, G.; Worton, D. R.; Chan, A. W. H.; Dallmann, T. R.; Davis, L.; Liu, S.; Day, D. A.; Russell, L. M.; Wilson, K. R.; et al. Elucidating secondary organic aerosol from diesel and gasoline vehicles through detailed characterization of organic carbon emissions. *Proc. Natl. Acad. Sci. U. S. A.* **2012**, 109 (45), 18318–18323.
- (15) Worton, D. R.; Isaacman, G.; Gentner, D. R.; Dallmann, T. R.; Chan, A. W. H.; Ruehl, C.; Kirchstetter, T. W.; Wilson, K. R.; Harley, R. A.; Goldstein, A. H. Lubricating oil dominates primary organic aerosol emissions from motor vehicles. *Environ. Sci. Technol.* **2014**, 48 (7), 3698–3706.
- (16) Drozd, G. T.; Miracolo, M. A.; Presto, A. A.; Lipsky, E. M.; Riemer, D. D.;

- Corporan, E.; Robinson, A. L. Particulate matter and organic vapor emissions from a helicopter engine operating on petroleum and Fischer-Tropsch fuels. *Energy and Fuels* **2012**, 26 (8), 4756–4766.
- (17) Jathar, S. H.; Miracolo, M. A.; Presto, A. A.; Donahue, N. M.; Adams, P. J.; Robinson, A. L. Modeling the formation and properties of traditional and non-traditional secondary organic aerosol: Problem formulation and application to aircraft exhaust. *Atmos. Chem. Phys.* **2012**, 12 (19), 9025–9040.
- (18) Robinson, A. L.; Donahue, N. M.; Shrivastava, M. K.; Weitkamp, E. a; Sage, A. M.; Grieshop, A. P.; Lane, T. E.; Pierce, J. R.; Pandis, S. N. Rethinking Organic Aerosols : Science (80-.). **2007**, 315, 1259–1262.
- (19) Gordon, T. D.; Presto, A. A.; Nguyen, N. T.; Robertson, W. H.; Na, K.; Sahay, K. N.; Zhang, M.; Maddox, C.; Rieger, P.; Chattopadhyay, S.; et al. Secondary organic aerosol production from diesel vehicle exhaust: Impact of aftertreatment, fuel chemistry and driving cycle. *Atmos. Chem. Phys.* **2014**, 14 (9), 4643–4659.
- (20) Liu, T.; Wang, X.; Deng, W.; Hu, Q.; Ding, X.; Zhang, Y.; He, Q.; Zhang, Z.; Lü, S.; Bi, X.; et al. Secondary organic aerosol formation from photochemical aging of light-duty gasoline vehicle exhausts in a smog chamber. *Atmos. Chem. Phys.* **2015**, 15 (15), 9049–9062.
- (21) May, A. A.; Nguyen, N. T.; Presto, A. A.; Gordon, T. D.; Lipsky, E. M.; Karve, M.; Gutierrez, A.; Robertson, W. H.; Zhang, M.; Brandow, C.; et al. Gas- and particle-phase primary emissions from in-use, on-road gasoline and diesel vehicles. *Atmos. Environ.* **2014**, 88, 247–260.

- (22) Nordin, E. Z.; Eriksson, A. C.; Roldin, P.; Nilsson, P. T.; Carlsson, J. E.; Kajos, M. K.; Hellén, H.; Wittbom, C.; Rissler, J.; Löndahl, J.; et al. Secondary organic aerosol formation from idling gasoline passenger vehicle emissions investigated in a smog chamber. *Atmos. Chem. Phys.* **2013**, 13 (12), 6101–6116.
- (23) Na, K.; Song, C.; Cocker, D. R. Formation of secondary organic aerosol from the reaction of styrene with ozone in the presence and absence of ammonia and water. *Atmos. Environ.* **2006**, 40 (10), 1889–1900.
- (24) Li, L.; Tang, P.; Nakao, S.; Kacarab, M.; Cocker, D. R. Novel Approach for Evaluating Secondary Organic Aerosol from Aromatic Hydrocarbons: Unified Method for Predicting Aerosol Composition and Formation. **2016**, No. x.
- (25) Li, L.; Tang, P.; Nakao, S.; Cocker III, D. R. Impact of molecular structure on secondary organic aerosol formation from aromatic hydrocarbon photooxidation under low NO_x conditions. *Atmos. Chem. Phys. Discuss.* **2016**, 1–40.

Chapter 7

7. Reducing Secondary Organic Aerosol Formation from Gasoline Vehicle Exhaust: Precursors and NO_x Effects

7.1 Introduction

Airborne particles pose serious health risks and strongly influence Earth's climate. Organic aerosol (OA) is a major component of fine particulate matter throughout the atmosphere. OA is comprised of primary and secondary organic aerosol (POA and SOA). SOA is formed in the atmosphere from the photo-oxidation of organic vapors (SOA precursors) and POA is directly emitted by sources. Even in urban areas SOA concentrations often exceed POA levels. Tailpipe emissions from on-road gasoline vehicles are an important source of SOA in urban environments (1-3).

Over the past several decades, increasingly stringent regulations have led to dramatic reductions in gasoline-vehicle non-methane organic gas (NMOG) emissions in the United States and elsewhere. These regulations were mainly driven to reduce ozone production, but they should also reduce SOA formation because a portion of NMOG was SOA precursors (3). However, the effectiveness of these regulations at reducing fine particulate matter exposures is not known because of large gaps in our understanding of SOA formation (4, 5).

Smog-chamber experiments with dilute exhaust have been conducted to quantify directly the SOA formation from gasoline vehicles (6-9). These experiments demonstrate that less SOA is formed from newer, lower-NMOG emitting gasoline vehicles that meet more stringent emissions standards than from older, higher emitting vehicles (6, 8, 9).

However, these experiments also reveal that exhaust from newer vehicles has, on average, higher effective SOA yields than exhaust from older vehicles (6, 8, 9). Gordon et al.(6) hypothesized that newer vehicles emit a more potent mix of SOA precursors than older vehicles. However this hypothesis has not been tested because of the complex and incompletely speciated NMOG emissions and gaps in our knowledge of SOA formation. If true, it means reduced benefits of recently promulgated even-stricter emissions standards for gasoline vehicle emissions (e.g. California LEV III regulations).

To investigate the effects of tightening vehicle emissions standards on SOA formation, we comprehensively characterized the primary emissions from 60 light-duty gasoline vehicles and performed smog chamber experiments with a subset of the fleet (25 vehicles). The number of vehicles was larger than what we have tested during this study because we have combined previously published data from May et al.(10) and Gordon et al.(6) to increase the size of the test fleet in order to reach better representative of primary emissions from gasoline vehicles and their SOA formation.

All vehicles were recruited from the California in-use fleet (Table B7.1); they spanned a wide range of model years (MY, 1988-2014), manufacturers, and emissions control technologies/standards. For discussion, the vehicles were categorized by emission certification standard. There is not a one-to-one correspondence between model year and certification standard; therefore, we also list (in parentheses) the range of vehicle MY in each category. We have four categories as: Pre-LEV vehicles (Tier0 and Tier1; MY1988-2003), LEV vehicles (transitional low emission vehicles and low emission vehicles;

MY1991-2012), ULEV vehicles (ultra-low emission vehicles; MY2003-2013) and SULEV vehicles (super ultra-low and partial emission vehicles; MY2012-2014) (Supporting Information (SI)). SULEV vehicles meet the most stringent emissions standard under the California LEV II regulations.

California is currently implementing even stricter LEV III regulations, which are being phased-in for model years 2015-2025. A comparable set of standards is implemented at the national level as the federal Tier 3 regulations between model years 2017 and 2025. SULEV emissions are comparable to those from an average LEV III vehicle in model year 2025 (11). Therefore, our results provide insight into the potential effectiveness of these regulations at reducing SOA formation from on-road gasoline vehicles.

The experiments follow the approach of Gordon et al. (6) and were described in details in Chapter 3 and Appendix#. Briefly, we tested each vehicle on a chassis dynamometer using the cold-start Unified Cycle, which simulates driving in the Southern California. We sampled the entire tailpipe emissions using a constant volume sampler (CVS) from which dilute exhaust was collected for chemical analysis. For a subset (n=25) of the vehicles, we transferred dilute exhaust from the CVS through a passivated, heated line into a 7 m³ smog chamber equipped with black lights (Model F40BL UVA, General Electric). We added HONO to the chamber as a source of OH radicals, deuterated butanol to determine the OH exposure, propene to adjust the NMOG-to-oxides-of-nitrogen ratio (NMOG:NO_x) and ammonium sulfate seeds to reduce the wall losses of condensable

vapors. These experiments corresponded to 3~13 hours of atmospheric processing at an OH concentration of 1.5×10^6 molecules cm^{-3} .

7.2 Results and Discussions

Figure 7.1 presents NMOG emissions and SOA production data from the 25 vehicles tested in the smog chamber. The term "NMOG" here refers to the non-methane organic gases measured by flame ionization detection (FID), which responds to both hydrocarbons and oxygenated compounds (12). Fig. 7.1 combines data from 14 newly tested vehicles (1 Pre-LEV, 3 LEV, 3 ULEV and 7 SULEV vehicles) with previously published data for 11 additional vehicles (3 Pre-LEV, 3 LEV, 5 ULEV vehicles) from Gordon et al. (6).

Figure 7.1A shows the NMOG emissions decreasing by 98% from the median Pre-LEV to the median SULEV vehicle, reflecting the effectiveness of tightening of emission standards. Less SOA production was measured from low-emitting vehicles (Figure 7.1B). Therefore, tightening tailpipe emissions standards reduces SOA formation from on-road gasoline vehicles. However, the reductions in SOA production are less than the decrease in NMOG emissions. For example, ULEV vehicles had about a factor of 20 lower NMOG emissions compared to Pre-LEV vehicles, but only a factor of 3 less SOA production. This raises concerns about effectiveness of new emissions standards at reducing SOA in urban areas.

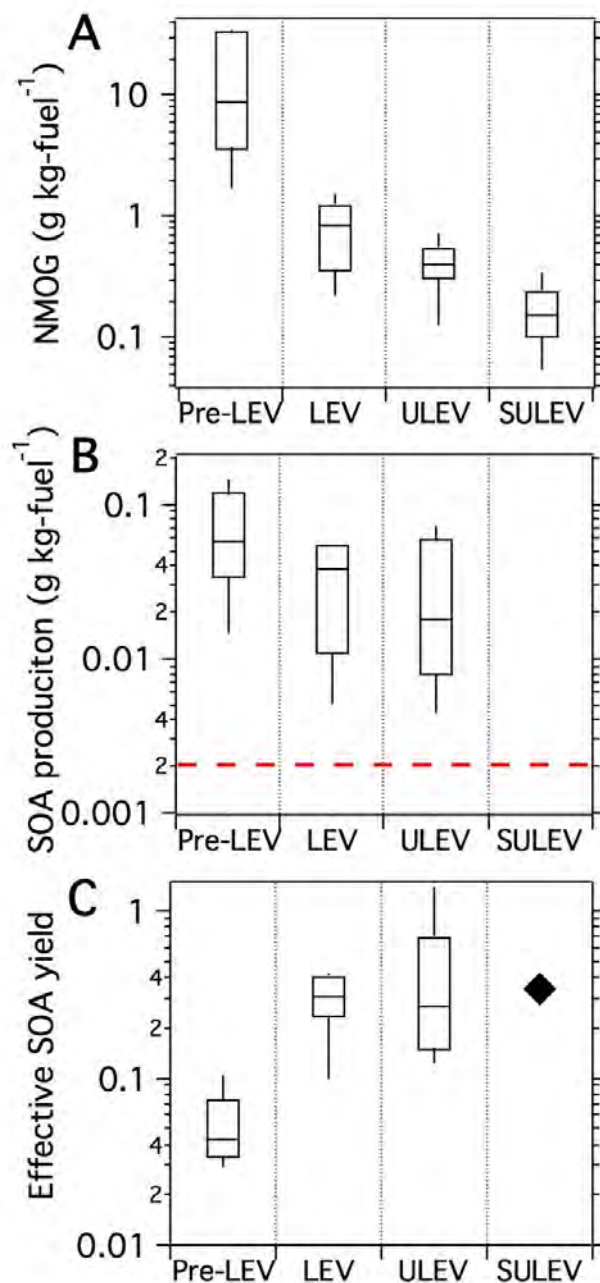


Figure 7.1. Emissions and SOA production data from photo-oxidation experiments with diluted gasoline-vehicle emissions for different vehicle classes: (A) NMOG emissions, (B) end-of-experiment SOA production and (C) effective SOA yields. The boxes represent the 75th and 25th percentiles of the data from individual vehicle tests with the centerline being the median. The whiskers are the 90th and 10th percentiles. The SOA production from SULEV was comparable to that measured during dynamic blank experiments, indicated by the dashed line in (B). The symbol in (C) indicates the upper bound of the effective SOA yields for SULEV vehicles.

SULEV vehicles had the lowest SOA production, comparable to the average SOA production (~ 2 mg-SOA/kg-fuel) measured during dynamic blank experiments when the chamber was only filled with dilution air from the CVS (no exhaust; appendix#). This complicates quantifying the SOA production from SULEV vehicles because the dynamic blank may overestimate background contamination(13). However, the data do indicate that the SOA production from SULEV vehicles is very low. Measureable SOA formation was observed from SULEV vehicles during parallel experiments conducted with an oxidation flow reactor that featured higher NMOG concentrations and higher oxidant exposures.

The trend in SOA production relative to NMOG emissions can be quantified in terms of an effective SOA yield, which is the ratio of SOA formed to reacted precursor mass (Appendix #). This accounts for experiment-to-experiment differences in the OH exposure.

Figure 7.1C plots the distribution of effective yields by vehicle class. Exhaust from newer vehicles has higher SOA yields, increasing from 0.05 ± 0.03 for Pre-LEV to 0.30 ± 0.13 for LEV and 0.48 ± 0.18 for ULEV vehicles (avg \pm stdev). We estimated an upper bound for the effective SOA yield for SULEV vehicles using the measured SOA production. This value is comparable to the effective yields for LEV and ULEV vehicles and substantially greater than Pre-LEV vehicles (Figure 7.1C). The trend in effective SOA yields by vehicle class cannot be explained by differences in OA concentrations in the smog chamber (6) or biases due to the wall losses of condensable vapors (Appendix #).

To investigate the trends in SOA formation, we comprehensively characterized the NMOG emissions (SI). In total, we quantified almost 300 individual compounds and lumped components consisting of a group of compounds with similar volatility and molecular structure, including volatile organic compounds (VOCs), intermediate volatility organic compounds (IVOCs) and semi-volatile organic compounds (SVOCs) (14, 15).

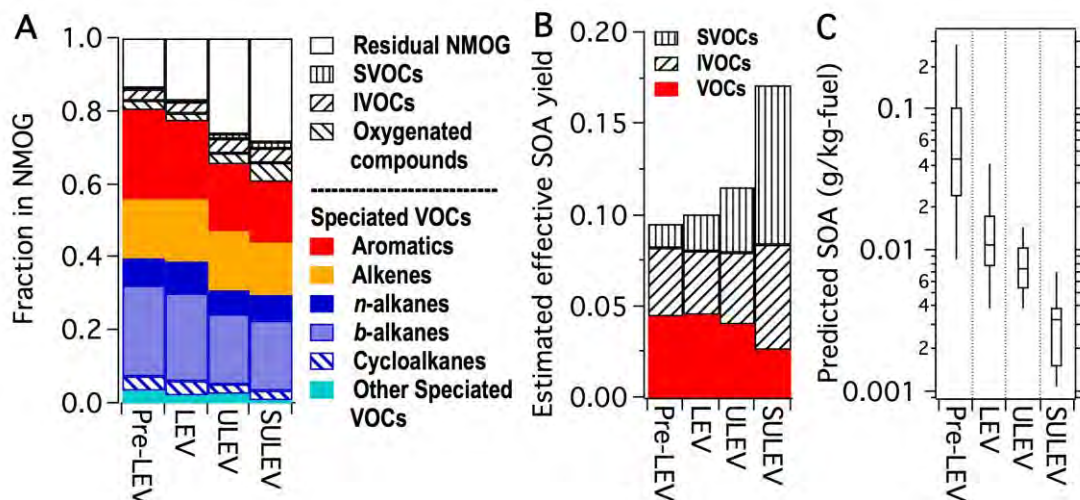


Figure 7. 2. (A) Median mass fractions of major NMOG components from all experiments by vehicle class. Speciated VOCs consisted of hydrocarbons with carbon number of 2 to 12 and oxygenated compounds with carbon number of ≤ 6 . The majority of IVOCs and SVOCs were not speciated at a molecular level. (B) Median estimated effective SOA yields and (C) distribution of predicted SOA production. The effective SOA yield and SOA production from these precursors were estimated using high- NO_x yields at an OA concentration of $10 \mu\text{g}/\text{m}^3$ and an OH concentration of 1.5×10^6 molecules/ cm^3 after 6-hour photo-oxidation. The box represents the 75th and 25th percentiles with the centerline being the median. The whiskers are the 90th and 10th percentiles.

Figure 7.2A presents the median NMOG composition for each vehicle class. Speciated VOC hydrocarbons (~ 200 species) are the largest component, contributing $74 \pm 28\%$ of the total NMOG across all tests. This includes important SOA precursors such as single-

ring aromatics ($19 \pm 9\%$ of NMOG emissions). Oxygenated VOCs with carbon number ≤ 6 , including aldehydes, ketones and alcohols, contribute about $3.6\% \pm 2.7\%$ of the NMOG emissions (Figure 7.2A). These species are likely the dominant oxygenated emissions (16), but are unlikely to be SOA precursors in these experiments because of their small molecular weight and our use of non-acidic seed particles. Finally, higher molecular weight hydrocarbons (IVOCs and SVOCs) contribute $5.3\% \pm 2.8\%$ of total NMOG (15) (Appendix#). IVOCs and SVOCs have saturation concentrations (C^*) of $300\text{-}3 \times 10^6 \mu\text{g}/\text{m}^3$ and $0.3\text{-}300 \mu\text{g}/\text{m}^3$, respectively, which correspond approximately to $C_{12}\text{-}C_{22}$ and $C_{23}\text{-}C_{32}$ n-alkanes (15, 17, 18). We characterized IVOCs and SVOCs composition by analyzing sorbent samples using GC/mass spectrometry, which enabled quantification of 57 individual compounds and 32 lumped components (15) (Appendix#).

Despite our comprehensive analysis, $26 \pm 13\%$ of the NMOG mass measured by FID remains uncharacterized (defined as the residual NMOG hereinafter) (Figure 7.2A). The most likely contributor to the residual NMOG is unidentified compounds in the C^* range of $C_2 - C_{12}$ n-alkanes (VOCs). Unlike our quantification of IVOCs and SVOCs, VOC speciation focused on a target list of compounds (Appendix#), which almost certainly does not include all species in the VOC range (19). Larger ($> C_6$) oxygenated species also likely contribute some residual NMOG, but our data indicate that the majority ($62 \pm 5\%$) of measured oxygenated emissions are C_1 and C_2 species (formaldehyde, acetaldehyde and acetone). Furthermore, there is no trend in the emissions of oxygenated organics and the residual NMOG (Fig. B7.1).

The most striking feature of Figure 7.2 is the consistency in NMOG composition across vehicle classes. The median NMOG composition for ULEV and SULEV vehicles appears to be modestly different from the other classes with somewhat lower fractional aromatic and alkane emissions (and therefore higher residual NMOG), but these differences are not statistically significant and likely due to greater uncertainty associated with lower emission rates. This consistency also exists between individual vehicles (Figure B7.2) despite the magnitude of the NMOG emissions varying by almost two orders of magnitude across the test fleet.

The consistency in the NMOG composition data appears to contrast sharply with the large variation in effective SOA yields in Figure 7.1C. However, only a portion of the NMOG emissions is SOA precursors. Figure 7.2B compares the predicted effective SOA yields under high-NO_x conditions by assuming that the characterized VOCs, IVOCs and SVOCs represent all precursors (Appendix#).

Figure 7.2B highlights the importance of IVOCs and SVOCs, which contribute only 5% of the NMOG emissions but roughly 50% of the predicted SOA. The effective SOA yields derived from composition data are predicted to increase for newer vehicles because of the increasing importance of SVOCs (Figure B7.3). However, the predicted increase is much smaller than the measured data. For example, the median effective SOA yields calculated from the chemical composition data only vary by a factor of 1.3 between Pre-LEV and ULEV vehicles versus a factor of 6 based on the measured SOA production. Although 26% of the NMOG remain uncharacterized, to explain the trends in measured

effective SOA yields the composition of this residual NMOG would need to vary radically across vehicle classes. Such large differences seem highly unlikely given the consistency in the large, characterized fraction.

SOA yields also depend on radical chemistry, especially the NO_x effects on the fate of peroxy radicals (5, 20-23), similar to the well-known ozone EKMA relationship. The available laboratory data reveal that the NO_x effects depend strongly on molecular structure. For example, aromatic compounds have much higher SOA yields under low- NO_x (high NMOG: NO_x) compared to high- NO_x conditions (low NMOG: NO_x) (20, 21, 24, 25). In comparison, SOA formation from alkanes appears to be less sensitive to NO_x than aromatics(26). However, NO_x effects have only been investigated for a small number of compounds. In addition, the majority of IVOC and SVOC emissions in gasoline-vehicle exhaust have not been resolved at the molecular level; aromatics, alkanes and likely other classes of compounds are in these emissions (15).

Although we added propene to the chamber to adjust the initial NMOG: NO_x (6), the experiments were performed across a wide range of initial NMOG: NO_x because of interferences associated with HONO and the chemiluminescence NO_x analyzer. These interferences affect the measurement of NO_2 not NO. Since NO_2 only contributed $6.6\% \pm 5.3\%$ of the NO_x emissions on a molar basis, we can make a robust estimate of the initial NMOG: NO_x using measured NO. These interferences were larger during experiments with low-emitting vehicles, creating a systematic trend in the initial

NMOG:NO_x across the fleet with 4.2 ± 1.0 , 8.4 ± 4.4 , 10.3 ± 4.3 , and 17.8 ± 20.3 for Pre-LEV, LEV, ULEV, and SULEV experiments, respectively.

The NMOG:NO_x evolved during the photo-oxidation phase of the experiments. Photolysis of HONO produced NO, which can react quickly with O₃ to form NO₂. Figure B7.4 shows that very low NO concentrations led to a rapid increase in ozone concentrations during LEV, ULEV and SULEV experiments. In contrast, relatively high NO levels were present in the chamber throughout every Pre-LEV experiment, which resulted in low ozone concentrations. This indicates important differences in the radical chemistry among experiments (Figure B7.4). The LEV, ULEV and SULEV experiments were likely conducted in a low-NO_x regime while the Pre-LEV experiments were conducted in a high-NO_x regime.

Our experiments provide us an opportunity to examine the importance of NMOG:NO_x in SOA formation from gasoline-vehicle exhaust, a dramatic complex mixture of organics compared to a small number of organic compounds investigated previously. To illustrate the importance of NMOG:NO_x, Figure 7.3A presents the effective SOA yield, defined as the measured SOA mass divided by the sum of reacted precursor mass (VOCs, IVOCs and SVOCs) at the end of each experiment, as a function of the initial NMOG:NO_x. There is a clear trend in the data, with effective yield increasing with increasing NMOG:NO_x. To quantify this trend, the data were binned by NMOG:NO_x and a curve (natural exponential) fit of the average value in each bin (red symbols). This fit indicates that the effective SOA yield increased from 0.06 to 0.46 as the NMOG:NO_x increased

from 4 to 10, after which the yield was approximately constant. This increase is at the high end of the NO_x dependence reported by single compound experiments (20, 21). This increase is important for predictions of atmospheric SOA formation as atmospheric $\text{NMOG}:\text{NO}_x$ is likely evolving into this increase range.

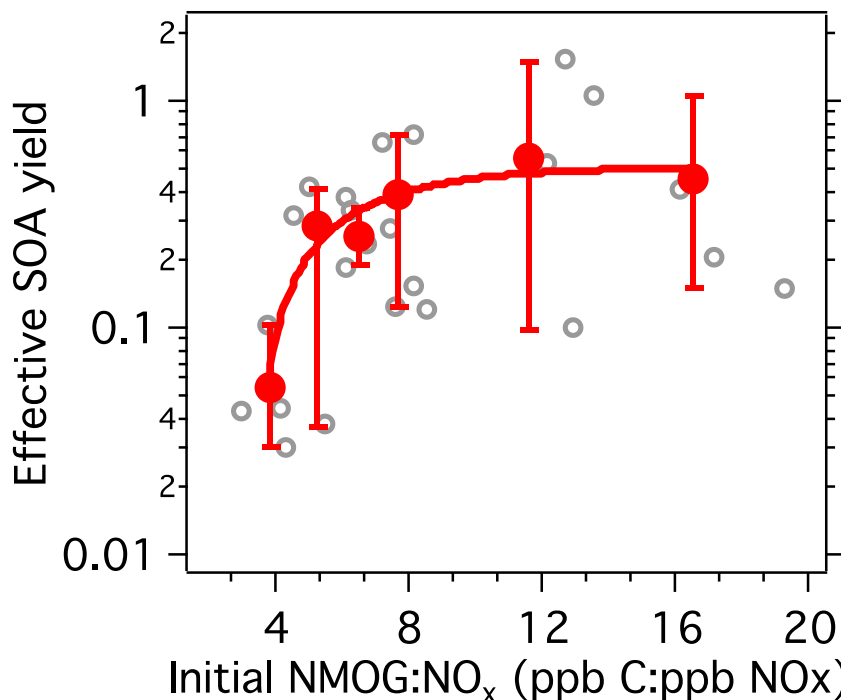


Figure 7.3. Effective SOA yield as a function of the initial $\text{NMOG}:\text{NO}_x$ during all photo-oxidation experiments with Pre-LEV, LEV and ULEV vehicles. The red points are averages and the vertical red bar indicates the maximum and minimum of effective SOA yields within each $\text{NMOG}:\text{NO}_x$ range.

As a final step in our analysis, we quantitatively compared the measurements to predictions of an SOA model (SI) to determine whether our analysis quantifies all SOA precursors and examine the importance of NO_x effects on SOA formation. Briefly, model inputs included measured precursor concentrations and OH exposure. We used yield data from the literature that accounts for both measured OA concentrations inside the chamber (gas-particle partitioning) and NO_x effects (high versus low $\text{NMOG}:\text{NO}_x$) (SI).

In Figure 7.4 we present model-measurement comparisons for high- and low-NO_x conditions. Both cases account for all measured precursors (VOCs, IVOCs, and SVOCs). The high-NO_x predictions substantially underestimate the measured SOA production with a median model-measurement ratio of 0.33. The exception is the high-NO_x pre-LEV data which have a model-measurement ratio of 2.5 ± 1.1 , consistent with a NO_x effect where Pre-LEV experiments had the lowest NMOG:NO_x among classes of vehicles. The low-NO_x predictions largely close the SOA mass balance for LEV and ULEV experiments conducted at high initial NMOG:NO_x with the median model-measurement ratio being 0.92. Therefore, SOA formation from gasoline-vehicle exhaust can be explained if one accounts for all precursors (VOCs, IVOCs, and SVOCs) and NO_x effects. The model calculations also confirm that the unexpectedly high effective SOA yields of low-emitting vehicles are likely due to high NMOG:NO_x during photo-oxidation experiments and not differences in SOA precursor emissions.

Figure 7.4 indicates that IVOCs and SVOCs are predicted to contribute one- to two-thirds of the predicted SOA under conditions of chamber experiments. This confirms the hypothesis of Jathar et al.(2) that unspciated NMOG are an important source of SOA precursors. However, we find that only a small fraction of the unspciated NMOG of Jathar et al.(2) – the now characterized IVOCs and SVOCs – comprises the vast majority of additional precursors. Furthermore, the effective SOA yields presented in Figure 7.3A show no positive correlation with the fraction of the residual NMOG, supporting the conclusion that the residual (uncharacterized) NMOG are not significant SOA precursors.

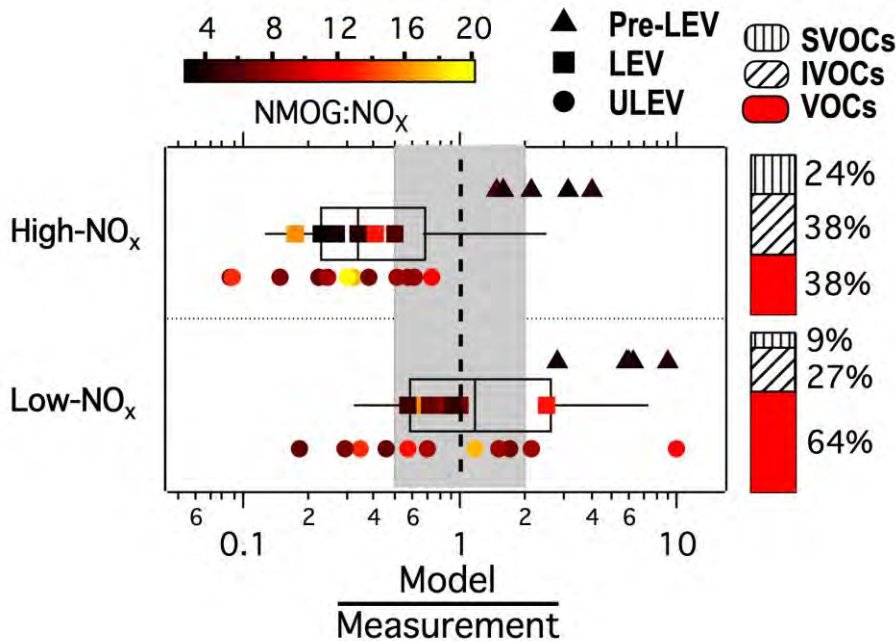


Figure 7.4. Comparison of distribution of predicted-to-measured SOA for high- and low-NO_x simulations. The box represents the 75th and 25th percentiles with the centerline being the median. The whiskers are the 90th and 10th percentiles. The symbols show the model-to-measurement-SOA ratios in individual experiments, color-coded by their initial NMOG:NO_x. The gray-shaded area indicates the range of the model-to-measurement-SOA ratio from 0.5 to 2 with the vertical dash line being the ratio of 1. The bars on the right present the average contribution of each class of SOA precursors to total predicted SOA production. SULEV data are not included because SOA formation comparable to the dynamic blank.

Our analysis demonstrates that increasingly stringent NMOG emissions standards have reduced SOA precursor emissions (Figure B7.3). This should reduce SOA production from gasoline-vehicle exhaust provided that the atmospheric NMOG:NO_x remains in the high-NO_x regime (Figure 7.2C). Notably, the single-ring aromatic (dominating SOA formation from VOCs) and IVOC emissions mirror the reductions in NMOG across vehicle classes (Figure B7.3). The exception is SVOC emissions; tightening NMOG emission standards is less effective at reducing SVOC emissions. This may be due to lubricating oil and not fuel being the major source of SVOC emissions (27). LEV and

ULEV vehicles have the same particulate-matter emission standard (11), which is also reflected by their similar POA emission factors (Figure B7.5).

7.3 Atmospheric Implications

The strong dependence of the SOA yield on the NMOG:NO_x can dramatically influence the effectiveness of gasoline-vehicle emission controls (and NMOG controls in general) with respect to SOA formation. Reducing NO_x will reduce nitrate aerosol, but these reductions will likely be offset to some extent by higher SOA. There is every reason to believe this same effect will play out in many other urban areas. In addition, although our analysis only considers the effect of the atmospheric NMOG:NO_x on on-road gasoline vehicle tailpipe emissions (a major source of SOA precursors in urban environments), similar trends likely apply to other sources. Our findings highlight the importance of an integrated emission control policy for NO_x and NMOGs in order to maximize benefits of recently promulgated tighter vehicle emission standards.

7.4 References:

1. P. L. Hayes et al., Organic aerosol composition and sources in Pasadena, California, during the 2010 CalNex campaign. *J. Geophys. Res.* **118**, 9233-9257 (2013).
2. S. H. Jathar et al., Unspeciated organic emissions from combustion sources and their influence on the secondary organic aerosol budget in the United States. *Proc. Natl. Acad. Sci. U. S. A.* **111**, 10473-10478 (2014).
3. B. C. McDonald, A. H. Goldstein, R. A. Harley, Long-Term Trends in California Mobile Source Emissions and Ambient Concentrations of Black Carbon and Organic Aerosol. *Environ. Sci. Technol.* **49**, 5178-5188 (2015).
4. M. Hallquist et al., The formation, properties and impact of secondary organic aerosol: current and emerging issues. *Atmos. Chem. Phys.* **9**, 5155-5236 (2009).
5. J. H. Kroll, J. H. Seinfeld, Chemistry of secondary organic aerosol: Formation and evolution of low-volatility organics in the atmosphere. *Atmos. Environ.* **42**, 3593-3624 (2008).

6. T. D. Gordon et al., Secondary organic aerosol formation exceeds primary particulate matter emissions for light-duty gasoline vehicles. *Atmos. Chem. Phys.* **14**, 4661-4678 (2014).
7. T. Liu et al., Secondary organic aerosol formation from photochemical aging of light-duty gasoline vehicle exhausts in a smog chamber. *Atmos. Chem. Phys.* **15**, 9049-9062 (2015).
8. E. Z. Nordin et al., Secondary organic aerosol formation from idling gasoline passenger vehicle emissions investigated in a smog chamber. *Atmos. Chem. Phys.* **13**, 6101-6116 (2013).
9. S. M. Platt et al., Secondary organic aerosol formation from gasoline vehicle emissions in a new mobile environmental reaction chamber. *Atmos. Chem. Phys.* **13**, 9141-9158 (2013).
10. A. A. May et al., Gas- and particle-phase primary emissions from in-use, on-road gasoline and diesel vehicles. *Atmos. Environ.* **88**, 247-260 (2014).
11. California Air Resources Board, "LEV III" Amendments to the California Greenhouse Gas and Criteria Pollution Exhaust and Evaporative Emission Standards and Test Procedures and to the On-Board Diagnostic System Requirements for Passenger Cars, Light-Duty Trucks, and Medium-Duty Vehicles, and to the Evaporative Emission Requirements for Heavy-Duty Vehicles. <http://www.arb.ca.gov/regact/2012/leviiiighg2012/levfrorev.pdf> (2012).
12. J. T. Scanlon, J. T. Willis, Calculation of Flame Ionization Detector Relative Response Factors Using the Effective Carbon Number Concept. *J. Chromatogr. Sci.* **23**, (1985).
13. A. A. May et al., Gas-Particle Partitioning of Primary Organic Aerosol Emissions: (2) Diesel Vehicles. *Environ. Sci. Technol.* **47**, 8288-8296 (2013).
14. Y. Zhao et al., Intermediate-Volatility Organic Compounds: A Large Source of Secondary Organic Aerosol. *Environ. Sci. Technol.* **48**, 13743-13750 (2014).
15. Y. Zhao et al., Intermediate Volatility Organic Compound Emissions from On-Road Gasoline Vehicles and Small Off-Road Gasoline Engines. *Environ. Sci. Technol.* **50**, 4554-4563 (2016).
16. J. J. Schauer, M. J. Kleeman, G. R. Cass, B. R. T. Simoneit, Measurement of emissions from air pollution sources. 5. C-1-C-32 organic compounds from gasoline-powered motor vehicles. *Environ. Sci. Technol.* **36**, 1169-1180 (2002).
17. N. M. Donahue, A. L. Robinson, S. N. Pandis, Atmospheric organic particulate matter: From smoke to secondary organic aerosol. *Atmos. Environ.* **43**, 94-106 (2009).
18. A. A. Presto, C. J. Hennigan, N. T. Nguyen, A. L. Robinson, Determination of Volatility Distributions of Primary Organic Aerosol Emissions from Internal Combustion Engines Using Thermal Desorption Gas Chromatography Mass Spectrometry. *Aerosol Sci. Technol.* **46**, 1129-1139 (2012).
19. A. H. Goldstein, I. E. Galbally, Known and unexplored organic constituents in the earth's atmosphere. *Environ. Sci. Technol.* **41**, 1514-1521 (2007).
20. A. W. H. Chan et al., Secondary organic aerosol formation from photooxidation of naphthalene and alkyl naphthalenes: implications for oxidation of intermediate volatility organic compounds (IVOCs). *Atmos. Chem. Phys.* **9**, 3049-3060 (2009).

21. N. L. Ng et al., Secondary organic aerosol formation from m-xylene, toluene, and benzene. *Atmos. Chem. Phys.* **7**, 3909-3922 (2007).
22. A. A. Presto, K. E. H. Hartz, N. M. Donahue, Secondary organic aerosol production from terpene ozonolysis. 2. Effect of NO_x concentration. *Environ. Sci. Technol.* **39**, 7046-7054 (2005).
23. J. Y. Zhang, K. E. H. Hartz, S. N. Pandis, N. M. Donahue, Secondary organic aerosol formation from limonene ozonolysis: Homogeneous and heterogeneous influences as a function of NO_x. *J. Phys. Chem. A* **110**, 11053-11063 (2006).
24. L. Hildebrandt, N. M. Donahue, S. N. Pandis, High formation of secondary organic aerosol from the photo-oxidation of toluene. *Atmos. Chem. Phys.* **9**, 2973-2986 (2009).
25. L. J. Li, P. Tang, D. R. Cocker, Instantaneous nitric oxide effect on secondary organic aerosol formation from m-xylene photooxidation. *Atmos. Environ.* **119**, 144-155 (2015).
26. C. D. Cappa et al., Application of the Statistical Oxidation Model (SOM) to Secondary Organic Aerosol formation from photooxidation of C-12 alkanes. *Atmos. Chem. Phys.* **13**, 1591-1606 (2013).
27. D. R. Worton et al., Lubricating Oil Dominates Primary Organic Aerosol Emissions from Motor Vehicles. *Environ. Sci. Technol.* **48**, 3698-3706 (2014).

8. Summary and Recommendations

8.1. Summary

The objective of this project was to quantify semivolatile and intermediate volatility organic compound (IVOC & SVOC) emissions and SOA formation from a small fleet of in-use vehicles, including SULEVs, GDI, late model larger non-SULEVs, and non-gasoline powered vehicles. Chassis dynamometer tests were done at the ARB Haagen-Smit Laboratory with a comprehensive set of measurements to quantify the primary emissions, including standard gases, PM mass, PM speciation (ions, OC/EC), SVOCs, and comprehensive speciation of volatile organic compounds (VOCs) including high time resolution for some VOCs using a proton transfer reaction mass spectrometer (PTR-MS). During a subset of the experiments, dilute exhaust was transferred into a smog chamber to quantify SOA formation under urban-like conditions. The combination of measurements and smog chamber experiments enable the evaluation of the effectiveness of the LEVIII standards for reducing motor vehicle emission contributions to ambient PM. We used multiple different complementary techniques to measure SVOC emissions, including state-of-the-art new instruments: a high resolution aerosol mass spectrometer (AMS) to measure particle-phase SVOC; a real-time instrument to quantify gas-and-particle SVOCs with 10-28 carbon atoms; and quartz filter and Tenax TA sorbent samples analyzed via thermal desorption and comprehensive two-dimensional GC with high resolution time of flight mass spectrometry (TD-GCxGC/HR-TOFMS).

Tailpipe emissions of regulated gas-phase pollutants (THC, CO, and NO_x) are lower from vehicles that meet more stringent emissions standards. In addition, there are no statistically significant differences in the composition of the speciated organics, including benzene, toluene, ethylbenzene, and xylenes (BTEX), between port-fuel injection (PFI) and GDI engine technologies. For vehicles certified to the same emissions standards, GDI engines had, on average, a factor of two higher particulate matter (PM) mass emissions compared to PFI engines. The difference is due to higher elemental carbon emissions from GDI vehicles. PM mass emissions from newer SULEV-certified GDIs are lower than older ULEV-certified GDIs suggesting improvements in GDI engine design. For our test fleet, the 16% decrease in CO₂ emissions from GDI vehicles was much greater than the potential climate forcing associated with higher EC emissions; thus, switching from PFI to GDI vehicles will likely lead to a reduction in net global warming. Real-time measurements were used to investigate the relative importance of cold-start versus hot-stabilized emissions. Hot-stabilized emissions have varying importance depending on species and may require a driving distance of 200 miles to equal the emissions from a single cold start. THC emissions are most sensitive to cold-start, followed by NO_x, CO and POA; elemental carbon emissions are the least sensitive to cold-start. Detailed quantification and characterization of IVOC emissions shows Tier 0 vehicles have about a factor of 10 higher emissions than PZEV vehicles, the composition of IVOC is relatively consistent across vehicle technologies, and 60% of IVOC mass is attributed to aromatic compounds. IVOC contribute, on average, 3% of THC emissions. Cold start IVOC emissions are between 2-6 times that of hot-running emissions, showing

a weaker cold start effect compared to VOCs. Predictions of potential SOA formation based solely on single ring aromatics and IVOC emissions give a consistent effective SOA yield of 10% across all vehicle categories, suggesting that the composition of emissions does not drive changes in SOA formation across vehicle classes. SVOC are emitted mainly as POA, have the same composition as the vehicles motor oil, correlate well with OC/EC measurements, and are dominated by cyclic aliphatic compounds. We investigated SOA formation from dilute, ambient-level exhaust from a subset of the fleet using a smog chamber. We measured lower SOA formation from newer vehicles that meet more stringent emissions standards than from older vehicles. SULEV vehicles had the lowest SOA production, comparable to that measured during dynamic blank experiments when the chamber was only filled with dilution air. Therefore, the gradual replacement of vehicles with newer vehicles that meet more stringent emissions standards should lead to lower SOA levels in California. However, we found a strongly nonlinear relationship between SOA formation and the VOC-to-NO_x ratio with the effective SOA yield for exhaust from gasoline vehicles a factor of 8 higher at low NO_x conditions. SOA formation from gasoline vehicle exhaust can be explained if one accounts for all precursors (VOCs, IVOCs, and SVOCs) and NO_x effects. The strong NO_x dependence also appears to explain higher effective yields measured from newer vehicles reported by previous studies. We investigated the implications of the strong NO_x dependence for the Los Angeles area. Although organic gas emissions from gasoline vehicles are expected to fall by almost 80% in Los Angeles over the next two decades, we predict there will be little to no reduction in SOA production from vehicle exhaust due to the rising atmospheric VOC-to-NO_x ratio. This highlights the importance of an integrated emission control policies for NO_x and organic gases.

The major conclusions of this work are that SULEV-certified vehicles have lower emissions and dramatically lower SOA production than vehicles meeting less-stringent emissions standards. SOA formation from gasoline vehicle exhaust can be quantitatively explained if one accounts for all precursors (VOCs, IVOCs, and SVOCs) and NO_x effects. However, the strong NO_x dependence of SOA formation means that there may be little to no reduction in SOA production from vehicle exhaust due to the rising atmospheric VOC-to-NO_x ratio.

8.2. Recommendations on future work

Recommendations for future study include characterization of the effects of different drive cycles on emissions and SOA production; characterization of emissions and SOA production from high-mileage SULEV-certified vehicles; quantification of emissions from non-vehicular sources such as petroleum based consumer products that are highly utilized in urban areas; quantification of SOA formation, including NO_x effects, from a comprehensive set of IVOCs, including different alkyl-benzenes; and incorporation of new emissions (especially IVOC and SVOC) into inventories and models.

GLOSSARY OF SYMBOLS AND ACRONYMS

BC Black carbon

CAFE Corporate average fuel economy

CO Carbon monoxide

CO₂ Carbon dioxide

CVS Constant volume sampler

EC Elemental carbon

GC-VUV-MS Gas chromatography with vacuum ultraviolet ionization mass spectrometry

GDI Gasoline direct injection

HR-tof-AMS High resolution time-of-flight aerosol mass spectrometer

IVOC intermediate-volatility organic compound

LEV Low emission vehicle

MY Model year

NMOG non-methane organic gas

NO_x Nitrogen oxides

O₃ Ozone

OA Organic aerosol

OC Organic carbon

OM Organic mass

PAH polycyclic aromatic hydrocarbon

PFI Port fuel injection

PM Particulate matter

POA Primary organic aerosol

PTR-MS Proton transfer reaction mass spectrometer

PZEV Partial zero emitting vehicle

rBC refractory black carbon

SOA Secondary organic aerosol

SP2 Single particle soot photometer

SULEV Super ultra-low emitting vehicle

THC Total hydrocarbons

UC Unified cycle

ULEV Ultra-low emitting vehicle

VOC Volatile organic compounds

Appendix A
Supplemental Material For Chapter 4

Table A1. Vehicle and test information for the current study.

* Hybrid Vehicle ** : GDI vehicle (otherwise PFI) *** :CNG vehicle

TEST_ID	ICLE_ID	T_TYPE	T_PHASE	DEL_YEAR	T_CLASS	STANDARD	VEHICLE
038708	20	UC	2	2012	PC**	ULEV	6733
038708	20	UC	3	2012	PC**	ULEV	6733
038708	20	UC	1	2012	PC**	ULEV	6733
038721	20	JB1B	1	2012	PC**	ULEV	6745
038722	20	JB1B	1	2012	PC**	ULEV	6761
038723	30	UC	1	2014	PC**	2SUL	1378
038723	30	UC	2	2014	PC**	2SUL	1378
038723	30	UC	3	2014	PC**	2SUL	1378
038724	31	UC	3	2012	PC**	ULEV	8310
038724	31	UC	1	2012	PC**	ULEV	8310
038724	31	UC	2	2012	PC**	ULEV	8310
038745	1	UC	1	2013	PC**	PZEV	8452
038745	1	UC	3	2013	PC**	PZEV	8452
038745	1	UC	2	2013	PC**	PZEV	8452
038747	23	UC	3	2013	PC**	ZEV*	902
038747	23	UC	2	2013	PC**	ZEV*	902
038747	23	UC	1	2013	PC**	ZEV*	902
038749	20	MAC4	1	2012	PC**	ULEV	6777
038750	30	UC	2	2014	PC**	2SUL	1390
038750	30	UC	3	2014	PC**	2SUL	1390
038750	30	UC	1	2014	PC**	2SUL	1390
038755	24	UC	2	2012	PC	PZEV	0832
038755	24	UC	3	2012	PC	PZEV	0832
038755	24	UC	1	2012	PC	PZEV	0832
038757	31	UC	3	2012	PC**	ULEV	8320
038757	31	UC	2	2012	PC**	ULEV	8320
038757	31	UC	1	2012	PC**	ULEV	8320
038760	24	UC	3	2012	PC	PZEV	0858
038760	24	UC	1	2012	PC	PZEV	0858
038760	24	UC	2	2012	PC	PZEV	0858
038763	24	JB1B	1	2012	PC	PZEV	0843
038797	23	UC	2	2013	PC**	ZEV*	913
038797	23	UC	3	2013	PC**	ZEV*	913
038797	23	UC	1	2013	PC**	ZEV*	913
038799	31	MAC4	1	2012	PC**	ULEV	8331
038801	35	UC	2	2013	PC**	JLEV	8303
038801	35	UC	3	2013	PC**	JLEV	8303
038801	35	UC	1	2013	PC**	JLEV	8303
1038820	35	UC	2	2013	PC**	ULEV	18314
1038820	35	UC	3	2013	PC**	ULEV	18314

Table A1. Vehicle and test information for the current study, continued.

TEST_ID	TEST_ID	TEST_TYPE	TEST_PHASE	MODEL_YEAR	VEH_CLASS	STANDARD	MILEAGE
1038820	35	UC	1	2013	PC**	ULEV	18314
1038821	18	UC	1	2008	PC	L2LEV	90406
1038821	18	UC	3	2008	PC	L2LEV	90406
1038821	18	UC	2	2008	PC	L2LEV	90406
1038822	36	UC	3	2013	PC**	L2ULV	19802
1038822	36	UC	1	2013	PC**	L2ULV	19802
1038822	36	UC	2	2013	PC**	L2ULV	19802
1038823	37	UC	2	2013	PC**	ULEV	23468
1038823	37	UC	3	2013	PC**	ULEV	23468
1038823	37	UC	1	2013	PC**	ULEV	23468
1038824	4	UC	3	2013	LDT	ULEV	24110
1038824	4	UC	2	2013	LDT	ULEV	24110
1038824	4	UC	1	2013	LDT	ULEV	24110
1038825	38	UC	3	2012	PC**	L2LEV	12943
1038825	38	UC	1	2012	PC**	L2LEV	12943
1038825	38	UC	2	2012	PC**	L2LEV	12943
1038827	27	UC	2	2013	PC**	L2ULV	21814
1038827	27	UC	1	2013	PC**	L2ULV	21814
1038827	27	UC	3	2013	PC**	L2ULV	21814
1038848	18	UC	2	2008	PC	L2LEV	90417
1038848	18	UC	3	2008	PC	L2LEV	90417
1038848	18	UC	1	2008	PC	L2LEV	90417
1038849	18	UC	1	2008	PC	L2LEV	90429
1038849	18	UC	2	2008	PC	L2LEV	90429
1038849	18	UC	3	2008	PC	L2LEV	90429
1038850	36	UC	3	2013	PC**	L2ULV	19821
1038850	36	UC	1	2013	PC**	L2ULV	19821
1038850	36	UC	2	2013	PC**	L2ULV	19821
1038853	21	UC	1	2014	PC**	PZEV	4483
1038853	21	UC	3	2014	PC**	PZEV	4483
1038853	21	UC	2	2014	PC**	PZEV	4483
1038854	21	MAC4	1	2014	PC**	PZEV	4494
1038862	28	UC	1	2013	PC**	L2SUL	28121
1038862	28	UC	2	2013	PC**	L2SUL	28121
1038862	28	UC	3	2013	PC**	L2SUL	28121
1038864	5	UC	3	2007	PC	L2SUL*	105707
1038864	5	UC	2	2007	PC	L2SUL*	105707
1038864	5	UC	1	2007	PC	L2SUL*	105707

Table A1. Vehicle and test information for the current study, continued

TEST_ID	TEST_ID	TEST_TYPE	TEST_PHASE	MODEL_YEAR	VEH_CLASS	STANDARD	MILEAGE
1038867	29	UC	1	2012	PC**	PZEV	13405
1038867	29	UC	2	2012	PC**	PZEV	13405
1038867	29	UC	3	2012	PC**	PZEV	13405
1038868	21	UC	3	2014	PC**	PZEV	4508
1038868	21	UC	1	2014	PC**	PZEV	4508
1038868	21	UC	2	2014	PC**	PZEV	4508
1038869	28	UC	2	2013	PC**	L2SUL	28132
1038869	28	UC	3	2013	PC**	L2SUL	28132
1038869	28	UC	1	2013	PC**	L2SUL	28132
1038870	9	MAC4	1	2003	PC	LEV	104571
1038871	9	MAC4	1	2003	PC	LEV	104586
1038883	12	UC	2	2014	M4	ULEV	15087
1038883	12	UC	1	2014	M4	ULEV	15087
1038883	12	UC	3	2014	M4	ULEV	15087
1038884	13	UC	1	2002	M4	TIER1	228442
1038884	13	UC	3	2002	M4	TIER1	228442
1038884	13	UC	2	2002	M4	TIER1	228442
1038885	5	UC	1	2007	PC	L2SUL*	105639
1038885	5	UC	2	2007	PC	L2SUL*	105639
1038885	5	UC	3	2007	PC	L2SUL*	105639
1038889	40	UC	3	2004	M4	ULEV	90432
1038889	40	UC	1	2004	M4	ULEV	90432
1038889	40	UC	2	2004	M4	ULEV	90432
1038890	40	MAC4	1	2004	M4	ULEV	90442
1038891	9	UC	1	2003	M3	LEV	104607
1038891	9	UC	2	2003	M3	LEV	104607
1038891	9	UC	3	2003	M3	LEV	104607
1038894	40	MAC4	1	2004	M4	ULEV	90456
1038901	14	UC	1	1990	PC	TIER0	121473
1038901	14	UC	2	1990	PC	TIER0	121473
1038901	14	UC	3	1990	PC	TIER0	121473
1038902	14	MAC4	1	1990	PC	TIER0	121552
1038903	13	MAC4	1	2002	M4	TIER1	228453
1038909	37	UC	2	2013	PC	ULEV	23514
1038909	37	UC	1	2013	PC	ULEV	23514
1038909	37	UC	3	2013	PC	ULEV	23514
1038911	9	UC	1	2003	M3	LEV	104619
1038912	14	UC	2	1990	PC	TIER0	121567
1038912	14	UC	3	1990	PC	TIER0	121567
1038912	14	UC	1	1990	PC	TIER0	121567

Table A1. Vehicle and test information for the current study, continued

TEST_ID	TEST_ID	TEST_TYPE	TEST_PHASE	MODEL_YEAR	VEH_CLASS	STANDARD	MILEAGE
1038915	37	UC	3	2013	PC**	ULEV	23494
1038915	37	UC	2	2013	PC**	ULEV	23494
1038916	37	MAC4	1	2013	PC**	ULEV	23480
1038917	4	UC	2	2013	LDT	ULEV	24182
1038917	4	UC	3	2013	LDT	ULEV	24182
1038918	4	UC	3	2013	LDT	ULEV	24136
1038918	4	UC	2	2013	LDT	ULEV	24136
1038919	4	MAC4	1	2013	LDT	ULEV	24147
1038920	21	UC	1	2014	PC**	PZEV	4526
1038920	21	UC	3	2014	PC**	PZEV	4526
1038920	21	UC	2	2014	PC**	PZEV	4526
1038922	15	MAC4	1	1990	M3	TIER1	59270
1038939	12	UC	2	2014	M4	ULEV	15107
1038939	12	UC	3	2014	M4	ULEV	15107
1038939	12	UC	1	2014	M4	ULEV	15107
1038945	4	UC	2	2013	LDT	ULEV	24170
1038945	4	UC	3	2013	LDT	ULEV	24170
1038945	4	UC	1	2013	LDT	ULEV	24170
1038947	36	UC	3	2013	PC**	L2ULV	19840
1038947	36	UC	1	2013	PC**	L2ULV	19840
1038947	36	UC	2	2013	PC**	L2ULV	19840
1038952	28	UC	3	2013	PC**	L2SUL	28152
1038952	28	UC	1	2013	PC**	L2SUL	28152
1038952	28	UC	2	2013	PC**	L2SUL	28152
1038961	33	UC	1	2007	PC***	L2LEV	19899
1038961	33	UC	2	2007	PC***	L2LEV	19899
1038961	33	UC	3	2007	PC***	L2LEV	19899
1038980	33	UC	1	2007	PC***	L2LEV	19910
1038980	33	UC	3	2007	PC***	L2LEV	19910
1038980	33	UC	2	2007	PC***	L2LEV	19910

Table A2. Composition of calibration standard for PTR-MS, concentrations in ppb.**Table III**

Compound	Concentration	Compound	Concentration
acetaldehyde	1006	benzene	1027
methanol	951	toluene	989
isoprene	962	m-Xylene	981
acetone	1008	b-pinene	515
acetonitrile	1035	3-carene	237
methacrolein	512	limonene	252
methyl vinyl ketone	482	dichlorobenzene	1012

Table A3. Test information for current study: total volume, CO, CO₂, and THC.**Table 2II**

TEST_ID	TEST_PHASE	VMIX [cf]	CO2 [g]	CO [g]	THC [g]
1038708	1	1861	581	1.330	0.140
1038708	2	6948	2684	58.767	0.156
1038708	3	1855	486	0.837	0.012
1038721	1	6459	2191	10.448	0.000
1038722	1	6425	2340	20.320	0.000
1038723	1	1849	794	1.140	0.322
1038723	2	6931	3174	1.168	0.000
1038723	3	1847	654	0.005	0.002
1038724	1	1861	718	3.530	0.312
1038724	2	6938	3030	4.574	0.024
1038724	3	1851	584	0.393	0.004
1038745	1	1857	744	1.136	0.087
1038745	2	6931	3073	9.083	0.000
1038745	3	1846	607	0.005	0.000
1038747	1	1867	501	1.296	0.280
1038747	2	6964	1698	2.501	0.013
1038747	3	1855	284	0.007	0.005
1038749	1	5077	2727	17.608	0.035
1038750	2	1860	854	1.244	0.140
1038750	3	6952	3256	1.223	0.000
1038750	1	1839	631	-0.016	0.002
1038755	2	1858	523	0.448	0.221
1038755	3	6964	1762	0.462	0.000
1038755	1	1855	310	0.004	0.003
1038757	1	1852	721	2.433	0.132
1038757	2	6918	3020	2.194	0.008
1038757	3	1846	593	0.261	0.004
1038760	1	2007	465	0.286	0.105
1038760	2	6965	1853	0.347	0.000
1038760	3	1846	308	0.006	0.002
1038763	1	6499	1879	0.355	0.011
1038797	1	1856	398	1.252	0.112
1038797	2	6959	2076	1.216	0.000
1038797	3	1848	356	0.069	0.003
1038799	1	5069	3263	18.467	0.062
1038801	1	1854	539	1.148	0.347
1038801	2	6931	2332	1.995	0.072
1038801	3	1845	441	0.323	0.028
1038820	1	1855	548	1.768	0.298

Table A3, continued. Test information for current study: total volume, CO, CO₂, and THC.

TEST ID	TEST PHASE	VMIX [cf]	CO ₂ [g]	CO [g]	THC [g]
1038820	2	6929	2288	1.827	0.092
1038820	3	1841	430	0.280	0.029
1038821	1	1851	1010	10.584	1.005
1038821	2	6886	3937	29.958	0.562
1038821	3	1834	784	6.214	0.214
1038822	1	1854	590	2.657	0.525
1038822	2	6909	2726	5.044	0.016
1038822	3	1849	494	0.634	0.016
1038823	1	1854	764	3.441	0.550
1038823	2	6934	3387	80.458	0.403
1038823	3	1842	607	1.426	0.021
1038824	1	1867	1181	8.195	0.841
1038824	2	6863	5006	4.060	0.006
1038824	3	1826	948	0.685	0.026
1038825	1	1848	621	2.648	0.258
1038825	2	6901	2571	32.111	0.151
1038825	3	1834	485	1.302	0.016
1038827	1	1848	559	6.609	0.639
1038827	2	6929	2402	16.466	0.135
1038827	3	1847	455	0.645	0.024
1038848	1	1850	992	10.186	1.091
1038848	2	6877	3929	30.272	0.559
1038848	3	1832	782	6.131	0.164
1038849	1	1848	979	17.659	1.171
1038849	2	6915	3974	37.748	0.607
1038849	3	1838	777	4.988	0.180
1038850	1	1868	637	2.513	0.303
1038850	2	6930	2693	2.718	0.023
1038850	3	1849	545	0.572	0.013
1038853	1	1853	664	2.003	0.141
1038853	2	6526	2641	1.636	0.000
1038854	1	5104	2908	2.342	0.000
1038862	1	1854	944	0.484	0.089
1038862	2	6944	3710	1.010	0.000
1038862	3	1845	726	0.038	0.002
1038864	1	1852	532	0.925	0.133
1038864	2	6926	1998	6.825	0.006
1038864	3	1843	322	0.268	0.010

Table A3, continued. Test information for current study: total volume, CO, CO₂, and THC.

TEST_ID	TEST_PHASE	VMIX [cf]	CO ₂ [g]	CO [g]	THC [g]
1038867	1	1853	713	1.395	0.137
1038867	2	6902	2876	29.033	0.060
1038867	3	1836	582	1.050	0.011
1038868	1	1852	660	1.361	0.123
1038868	2	6938	2865	1.274	0.000
1038868	3	1843	538	0.028	0.000
1038869	1	1847	962	0.479	0.071
1038869	2	6921	3804	1.931	0.006
1038869	3	1836	719	0.016	0.000
1038870	1	4957	6186	24.044	0.349
1038871	1	5130	6012	6.600	0.114
1038883	1	3243	1503	2.938	0.193
1038883	2	11975	6094	0.451	0.219
1038883	3	3153	1238	0.579	0.104
1038884	1	3231	1330	3.736	0.333
1038884	2	11865	5486	9.053	0.670
1038884	3	3142	1093	2.006	0.153
1038885	1	1829	466	1.442	0.384
1038885	2	6818	1881	6.925	0.010
1038885	3	1793	306	0.203	0.013
1038889	1	3237	1544	3.138	0.224
1038889	2	11747	6867	2.274	0.224
1038889	3	3125	1307	1.045	0.078
1038890	1	8926	6427	2.207	0.168
1038891	1	3317	1237	12.517	1.835
1038891	2	12410	5594	4.892	0.051
1038891	3	3307	1064	2.987	0.183
1038894	1	8900	6324	0.698	0.171
1038901	1	1855	804	9.350	1.982
1038901	2	6904	3644	5.463	0.521
1038901	3	1831	687	3.010	0.687
1038902	1	5160	4323	14.183	0.394
1038903	1	8960	5317	11.846	0.450
1038909	1	1860	785	4.691	0.646
1038909	2	6963	3280	30.574	0.242
1038909	3	1851	609	0.024	0.006
1038911	1	3314	1264	10.845	1.682
1038911	2	12407	5785	34.845	0.208
1038911	3	3304	1073	3.324	0.182

Table A3, continued. Test information for current study: total volume, CO, CO₂, and THC.

TEST_ID	TEST_PHASE	VMIX [cf]	CO ₂ [g]	CO [g]	THC [g]
1038912	1	1865	818	11.976	1.934
1038912	2	6917	3683	4.423	0.398
1038912	3	1846	684	4.087	0.611
1038915	1	2033	859	4.950	0.509
1038915	1	6961	3347	3.142	0.026
1038915	2	1848	650	1.303	0.013
1038916	3	5085	3424	7.650	0.052
1038917	1	1860	1154	9.236	0.813
1038917	2	6886	4921	5.308	0.040
1038917	3	1831	952	0.700	0.026
1038918	1	1858	1137	11.298	0.991
1038918	2	6894	5052	3.950	0.023
1038918	3	1832	966	1.001	0.024
1038919	1	5023	5314	5.974	0.052
1038920	1	1870	648	0.838	0.204
1038920	1	6974	2743	0.627	0.000
1038920	2	1848	522	0.008	0.000
1038922	3	9099	6046	72.902	3.125
1038939	1	3327	1530	3.685	0.337
1038939	2	12403	6068	0.263	0.153
1038939	3	3292	1198	0.024	0.032
1038945	1	1860	1189	7.731	0.662
1038945	2	6875	5064	6.365	0.072
1038945	3	1829	959	1.043	0.031
1038947	1	1858	613	2.136	0.337
1038947	2	6935	2720	2.544	0.032
1038947	3	1854	514	0.428	0.011
1038952	1	1860	922	0.499	0.152
1038952	2	6957	3596	1.034	0.000
1038952	3	1850	725	0.073	0.001
1038961	1	1855	478	0.277	0.273
1038961	2	6937	1992	5.517	0.000
1038961	3	1847	381	0.366	0.061
1038980	1	1855	489	0.338	0.323
1038980	2	6932	1970	3.887	0.000
1038980	3	1846	390	0.396	0.040

Table A4. Test information for current study: BTEX, ethane, and n-pentane.**Table 3II**

TEST_ID	TEST_PHASE	benzene	toluene	m-xylene	o-xylene	p-xylene	Ebenzene	Ethane	n-pentane
1038708	3	0.640	0.120	0.000	0.000	0.000	0.000	0.657	0.158
1038708	1	4.199	5.042	1.946	1.265	0.973	0.973	3.252	1.825
1038708	2	1.494	0.599	0.201	0.151	0.113	0.088	0.485	0.164
1038723	3	0.000	0.000	0.000	0.000	0.000	0.000	0.163	0.052
1038723	1	2.746	5.458	1.938	1.172	0.981	0.742	3.930	2.966
1038723	2	0.000	0.000	0.000	0.000	0.000	0.000	0.028	0.027
1038747	1	2.739	7.045	4.237	2.180	2.131	1.470	1.498	1.518
1038747	2	0.099	0.087	0.038	0.000	0.025	0.000	0.014	0.027
1038747	3	0.000	0.000	0.000	0.000	0.000	0.000	0.055	0.026
1038755	2	0.000	0.000	0.000	0.000	0.000	0.000	0.000	0.027
1038755	1	1.983	4.107	1.388	0.853	0.706	0.658	2.677	3.046
1038755	3	0.000	0.000	0.000	0.000	0.000	0.000	0.055	0.053
1038763	1	0.124	0.113	0.000	0.000	0.000	0.000	0.029	0.220
1038799	1	0.401	0.442	0.390	0.204	0.192	0.118	0.105	0.020
1038801	3	1.981	0.797	0.365	0.195	0.170	0.122	1.075	0.556
1038801	1	6.925	12.433	5.428	3.164	2.726	2.410	3.585	4.155
1038801	2	0.283	0.509	0.438	0.225	0.225	0.163	0.128	0.109
1038821	1	34.612	48.803	20.404	11.864	10.214	8.061	29.104	16.022
1038821	2	1.690	1.229	0.607	0.384	0.310	0.198	4.576	0.862
1038821	3	10.736	4.238	1.211	0.760	0.593	0.190	11.349	3.459
1038822	3	0.120	0.049	0.000	0.000	0.000	0.000	0.360	0.133
1038822	1	14.519	17.839	7.449	4.215	3.725	3.308	8.994	4.982
1038822	2	0.049	0.099	0.150	0.063	0.075	0.000	0.057	0.000
1038824	2	0.097	0.197	0.211	0.112	0.112	0.074	0.112	0.000
1038824	1	33.521	47.644	21.555	11.733	10.778	10.263	22.090	9.242
1038824	3	0.259	0.309	0.144	0.000	0.072	0.000	0.950	0.182
1038825	1	5.523	4.872	1.581	0.815	0.791	0.719	3.746	1.798
1038825	2	1.361	0.860	0.372	0.186	0.186	0.087	0.253	0.148
1038825	3	1.337	0.095	0.000	0.000	0.000	0.000	0.867	0.052
1038849	3	7.663	2.774	0.844	0.482	0.434	0.145	10.024	3.355
1038849	1	54.753	59.830	25.387	14.321	12.705	10.198	33.186	17.302
1038849	2	1.692	1.574	0.775	0.475	0.387	0.237	4.644	1.236
1038854	1	0.061	0.031	0.031	0.000	0.019	0.000	0.014	0.007
1038862	1	1.824	2.911	0.758	0.538	0.391	0.391	1.496	1.676
1038862	2	0.086	0.087	0.038	0.000	0.025	0.000	0.043	0.000
1038862	3	0.000	0.000	0.000	0.000	0.000	0.000	0.166	0.000
1038867	1	2.300	4.941	1.905	1.221	0.952	0.855	1.771	3.505
1038867	2	0.196	0.149	0.100	0.000	0.050	0.000	0.042	0.081
1038867	3	0.000	0.024	0.000	0.000	0.000	0.000	0.303	0.000

Table A4. Test information for current study: BTEX, ethane, and n-pentane.

TEST_ID	TEST_PHASE	benzene	toluene	m-xylene	o-xylene	p-xylene	Ebenzene	Ethane	n-pentane
1038870	1	1.649	1.559	0.613	0.364	0.303	0.219	1.018	0.574
1038891	2	0.373	0.377	0.157	0.000	0.090	0.000	0.304	0.122
1038891	1	40.224	104.897	58.947	33.764	29.473	25.399	21.360	20.360
1038891	3	24.682	7.486	1.952	1.345	0.954	0.000	6.782	3.302
1038901	3	15.134	28.419	13.394	7.964	6.697	5.955	17.639	13.471
1038901	2	1.455	1.682	0.860	0.548	0.424	0.386	2.768	0.962
1038901	1	37.994	101.668	53.304	30.734	26.652	23.026	26.876	24.489
1038902	1	1.045	1.169	0.624	0.378	0.309	0.265	1.093	0.425
1038909	2	1.979	1.305	0.501	0.238	0.251	0.188	0.227	0.041
1038909	3	0.047	0.024	0.000	0.000	0.000	0.000	0.136	0.000
1038909	1	20.634	35.506	18.395	10.650	9.197	6.995	9.597	7.527
1038916	1	0.104	0.123	0.124	0.062	0.062	0.043	0.035	0.000
1038917	3	0.475	0.360	0.169	0.000	0.073	0.000	0.904	0.263
1038917	2	0.293	0.358	0.274	0.137	0.137	0.100	0.169	0.095
1038917	1	34.118	53.432	23.834	14.276	11.917	11.941	21.078	7.801
1038919	1	0.187	0.262	0.215	0.117	0.104	0.061	0.202	0.060
1038920	2	0.049	0.050	0.063	0.000	0.025	0.000	0.000	0.000
1038920	1	5.671	7.775	3.723	1.911	1.862	1.396	1.832	3.809
1038920	3	0.047	0.000	0.000	0.000	0.000	0.000	0.000	0.000
1038922	1	10.580	16.293	8.363	4.665	4.187	4.076	6.065	3.080
1038945	1	26.592	38.828	16.606	9.451	8.303	8.034	19.118	5.948
1038945	3	0.427	0.432	0.169	0.000	0.097	0.000	1.371	0.211
1038945	2	0.427	0.456	0.261	0.149	0.137	0.099	0.366	0.095
1038947	1	6.448	7.726	2.702	1.655	1.339	1.217	7.115	2.488
1038947	2	0.086	0.111	0.137	0.075	0.075	0.000	0.099	0.000
1038947	3	0.118	0.000	0.000	0.000	0.000	0.000	0.327	0.000
1038952	1	1.765	2.387	0.875	0.486	0.438	0.340	1.129	1.427
1038952	3	0.000	0.000	0.000	0.000	0.000	0.000	0.219	0.000
1038952	2	0.074	0.037	0.000	0.000	0.000	0.000	0.028	0.000
1038980	1	0.119	0.000	0.000	0.000	0.000	0.000	8.545	0.000
1038980	2	0.000	0.025	0.000	0.000	0.000	0.000	0.071	0.000
1038980	3	0.000	0.000	0.000	0.000	0.000	0.000	0.109	0.000

Table A5. BTEX Composition Data from a previous study¹ used in combination with current data for Figure 4.2.

Test ID num.	Vehicle name	benzene	toluene	m-xylene	p-xylene	o-xylene
<u>1027872</u>	PreLEV-14	<u>5.04E-02</u>	<u>1.04E-01</u>	<u>2.93E-02</u>	<u>1.46E-02</u>	<u>1.52E-02</u>
1028029	PreLEV-10	1.56E-02	4.02E-02	1.68E-02	8.38E-03	8.39E-03
1027921	PreLEV-11	2.28E-02	4.39E-02	1.73E-02	8.63E-03	8.94E-03
1027920	PreLEV-8	1.02E-03	6.20E-04	1.35E-04	1.26E-04	5.80E-04
1032320	PreLEV-5	2.37E-02	6.12E-02	2.84E-02	1.42E-02	1.66E-02
1032392	PreLEV-4	4.82E-02	7.39E-02	3.49E-02	1.74E-02	1.95E-02
1032426	PreLEV-3	5.28E-02	5.91E-02	2.26E-02	1.13E-02	1.36E-02
1032444	PreLEV-2	1.75E-02	5.73E-02	2.76E-02	1.38E-02	1.63E-02
1032440	PreLEV-2	0.00E+00	0.00E+00	0.00E+00	0.00E+00	0.00E+00
1032389	PreLEV-3	0.00E+00	0.00E+00	0.00E+00	0.00E+00	0.00E+00
1032442	PreLEV-1	4.29E-02	6.73E-02	2.97E-02	1.48E-02	1.64E-02
1032443	PreLEV-9	2.22E-02	6.55E-02	3.91E-02	1.96E-02	2.26E-02
1032303	PreLEV-3	0.00E+00	0.00E+00	0.00E+00	0.00E+00	0.00E+00
1032445	PreLEV-15	3.09E-02	6.27E-02	2.97E-02	1.49E-02	1.68E-02
1028023	LEV1-25	5.30E-02	7.72E-02	2.56E-02	1.28E-02	1.21E-02
1027859	LEV1-1	1.45E-05	1.07E-03	2.14E-04	7.39E-05	1.72E-04
1027976	LEV1-8	0.00E+00	0.00E+00	0.00E+00	0.00E+00	0.00E+00
1027970	LEV1-26	7.94E-03	2.49E-02	1.18E-02	5.92E-03	6.05E-03
1027969	LEV1-19	0.00E+00	0.00E+00	0.00E+00	0.00E+00	0.00E+00
1027975	LEV1-17	2.20E-02	4.81E-02	2.06E-02	1.03E-02	1.06E-02
1028027	LEV1-16	7.37E-03	1.50E-02	7.65E-03	3.83E-03	4.20E-03
1027837	LEV1-1	1.28E-02	4.03E-02	2.10E-02	1.05E-02	1.23E-02
1028075	LEV1-19	8.09E-03	1.17E-02	5.05E-03	2.52E-03	2.54E-03
1027918	LEV1-6	1.61E-02	3.05E-02	1.38E-02	6.93E-03	8.18E-03
1032302	LEV1-2	4.33E-02	6.77E-02	3.12E-02	1.56E-02	1.73E-02
1032304	LEV1-2	3.98E-02	6.98E-02	3.15E-02	1.57E-02	1.71E-02
1032348	LEV1-3	6.81E-02	6.51E-02	3.36E-02	1.68E-02	1.79E-02
1032388	LEV1-21	3.63E-02	6.41E-02	3.12E-02	1.56E-02	1.75E-02
1032346	LEV1-3	3.26E-02	6.85E-02	3.10E-02	1.54E-02	1.76E-02
1032347	LEV1-3	8.56E-02	5.30E-02	3.47E-02	1.78E-02	2.25E-02
1023424	LEV1-21	0.00E+00	0.00E+00	0.00E+00	0.00E+00	0.00E+00
1032428	LEV1-9	0.00E+00	0.00E+00	0.00E+00	0.00E+00	0.00E+00
1032394	LEV1-24	0.00E+00	0.00E+00	0.00E+00	0.00E+00	0.00E+00
1032393	LEV1-4	2.93E-02	5.74E-02	2.63E-02	1.31E-02	1.46E-02
1032473	LEV1-2	5.54E-02	5.50E-02	4.18E-02	2.09E-02	2.43E-02

Table A5 continued.

Test ID num.	Vehicle name	benzene	toluene	m-xylene	p-xylene	o-xylene
1032436	LEV1-21	0.00E+00	0.00E+00	0.00E+00	0.00E+00	0.00E+00
1032435	LEV1-11	0.00E+00	0.00E+00	0.00E+00	0.00E+00	0.00E+00
1032434	LEV1-24	0.00E+00	0.00E+00	0.00E+00	0.00E+00	0.00E+00
1032472	LEV1-24	3.84E-02	6.71E-02	3.51E-02	1.75E-02	1.83E-02
1027977	LEV2-15	0.00E+00	0.00E+00	0.00E+00	0.00E+00	0.00E+00
1027973	LEV2-11	1.28E-02	4.14E-02	1.50E-02	7.51E-03	8.16E-03
1027905	LEV2-19	1.98E-02	2.77E-02	1.09E-02	5.40E-03	6.18E-03
1027978	LEV2-10	0.00E+00	0.00E+00	0.00E+00	0.00E+00	0.00E+00
1027908	LEV2-8	0.00E+00	0.00E+00	0.00E+00	0.00E+00	0.00E+00
1027906	LEV2-16	2.98E-02	4.50E-02	2.15E-02	1.07E-02	1.03E-02
1027852	LEV2-4	3.79E-02	7.32E-02	1.87E-02	9.36E-03	1.09E-02
1027867	LEV2-9	9.68E-03	2.11E-02	6.91E-03	3.45E-03	3.46E-03
1027907	LEV2-20	1.95E-02	4.46E-02	2.05E-02	1.03E-02	1.11E-02
1028021	LEV2-18	3.50E-03	5.99E-03	2.31E-03	1.14E-03	1.68E-03
1028022	LEV2-2	4.73E-02	7.65E-02	3.36E-02	1.67E-02	1.74E-02
1027863	LEV2-13	1.71E-02	3.18E-02	1.49E-02	7.58E-03	8.22E-03
1027971	LEV2-4	4.75E-02	6.36E-02	2.51E-02	1.27E-02	1.49E-02
1032282	LEV2-6	2.99E-02	4.54E-02	1.27E-02	1.27E-02	1.02E-02
1023305	LEV2-25	0.00E+00	0.00E+00	0.00E+00	0.00E+00	0.00E+00
1032310	LEV2-23	6.41E-02	6.38E-02	3.46E-02	1.71E-02	2.11E-02
1032309	LEV2-6	4.77E-02	7.71E-02	3.20E-02	1.61E-02	1.80E-02
1032321	LEV2-6	4.93E-02	8.11E-02	3.90E-02	1.94E-02	2.19E-02
1032342	LEV2-5	4.83E-02	7.34E-02	3.55E-02	1.77E-02	1.94E-02
1032351	LEV2-5	2.76E-02	4.89E-02	2.10E-02	1.06E-02	1.35E-02
1032345	LEV2-6	3.75E-02	5.82E-02	3.38E-02	1.70E-02	1.84E-02
1032360	LEV2-3	2.20E-02	4.71E-02	2.65E-02	1.36E-02	1.75E-02
1032343	LEV2-6	3.83E-02	5.32E-02	2.76E-02	1.38E-02	1.75E-02
1032383	LEV2-24	5.76E-02	6.57E-02	3.25E-02	1.62E-02	1.82E-02
1032359	LEV2-3	1.74E-02	7.33E-02	7.65E-02	3.84E-02	4.90E-02
1032283	LEV2-3	2.54E-02	3.96E-02	8.34E-03	8.34E-03	8.24E-03

Table A6. Vehicle data and emissions from a previous study¹ used in combination with current data for for Figure 4.4.

TEST_ID	Class	TEST_PHASE	MODEL_YEAR	MPG	HC_GM_MILE
1032302	LEV	1	1997	12.69	0.97
1032302	LEV	2	1997	22.12	0.02
1032302	LEV	3	1997	15.46	0.16
1032304	LEV	1	1997	11.95	1.20
1032304	LEV	2	1997	22.17	0.02
1032304	LEV	3	1997	15.25	0.13
1032309	LEV2	1	2011	10.36	0.49
1032309	LEV2	2	2011	17.98	0.04
1032309	LEV2	3	2011	12.78	0.06
1032310	LEV2	1	2011	12.93	0.31
1032310	LEV2	2	2011	23.70	0.00
1032310	LEV2	3	2011	15.29	0.02
1032320	T0	1	1990	12.57	1.70
1032320	T0	2	1990	22.18	0.06
1032320	T0	3	1990	15.48	0.38
1032321	LEV2	1	2011	10.29	0.71
1032321	LEV2	2	2011	18.46	0.02
1032321	LEV2	3	2011	11.92	0.05
1032322	LEV2	1	2012	10.84	0.12
1032322	LEV2	2	2012	20.04	0.01
1032322	LEV2	3	2012	13.91	0.01
1032342	LEV2	1	2011	14.22	0.30
1032342	LEV2	2	2011	24.03	0.02
1032342	LEV2	3	2011	16.84	0.01
1032346	LEV	1	1998	12.21	1.00
1032346	LEV	2	1998	21.49	0.01
1032346	LEV	3	1998	15.14	0.05
1032351	LEV2	1	2011	14.28	0.29
1032351	LEV2	2	2011	25.52	0.03
1032351	LEV2	3	2011	18.15	0.02
1032362	LEV	1	1998	11.83	1.09
1032362	LEV	2	1998	20.88	0.01
1032362	LEV	3	1998	14.96	0.07
1032382	LEV2	1	2012	17.47	0.10
1032382	LEV2	2	2012	29.16	0.00
1032382	LEV2	3	2012	21.02	0.01
1032383	LEV2	1	2012	9.71	0.46
1032383	LEV2	2	2012	17.36	0.02
1032383	LEV2	3	2012	12.75	0.01

Table A6 Continued.

TEST_ID	Class	TEST_PHASE	MODEL_YEAR	MPG	HC_GM_MILE
1032388	LEV	1	2001	13.79	0.71
1032388	LEV	2	2001	24.91	0.01
1032388	LEV	3	2001	18.08	0.13
1032392	T0	1	1989	18.78	2.51
1032392	T0	2	1989	30.09	0.27
1032392	T0	3	1989	24.74	0.41
1032393	LEV	1	1999	14.87	0.57
1032393	LEV	2	1999	27.14	0.03
1032393	LEV	3	1999	18.79	0.06
1032428	LEV	1	1994	8.92	6.53
1032428	LEV	2	1994	17.22	2.31
1032428	LEV	3	1994	10.73	3.11
1032435	LEV	1	1996	11.64	5.24
1032435	LEV	2	1996	19.79	1.87
1032435	LEV	3	1996	13.83	0.33
1032442	T0	1	1987	8.77	6.21
1032442	T0	2	1987	16.95	0.82
1032442	T0	3	1987	11.42	1.50
1032443	T0	1	1991	9.53	4.69
1032443	T0	2	1991	18.87	0.12
1032443	T0	3	1991	14.18	0.35
1032444	T0	1	1988	15.81	6.46
1032444	T0	2	1988	26.71	2.81
1032444	T0	3	1988	20.65	4.57
1032445	T0	1	1993	10.18	7.79
1032445	T0	2	1993	16.99	1.28
1032445	T0	3	1993	12.17	2.85
1032472	LEV	1	2002	6.70	2.20
1032472	LEV	2	2002	10.99	0.03
1032472	LEV	3	2002	7.94	0.14

Table A7. Vehicle data and emissions from a previous study¹ used in combination with current data for Figure 4.6.

TEST I	TEST PHAS	benzen	toluen	m-	p-	o-	ethan	n-
1032302	1	30.46	63.64	29.63	14.80	16.49	20.82	17.98
1032302	2	0.48	0.92	0.56	0.28	0.30	0.24	0.11
1032302	3	14.31	5.74	1.82	0.88	0.93	10.54	3.63
1032304	1	37.07	83.43	37.26	18.64	19.98	27.91	21.85
1032304	2	0.78	0.62	0.45	0.22	0.28	0.22	0.11
1032304	3	10.17	2.32	0.80	0.39	0.52	8.60	3.01
1032309	1	19.42	35.69	14.52	7.28	7.92	11.55	6.09
1032309	2	1.58	2.28	1.06	0.53	0.65	1.20	0.61
1032309	3	3.39	2.22	0.76	0.40	0.49	2.79	0.78
1032310	1	17.54	17.64	9.51	4.73	5.78	6.42	3.91
1032310	2	0.12	0.19	0.15	0.07	0.11	0.03	0.01
1032310	3	0.91	0.44	0.12	0.05	0.00	1.05	0.43
1032320	1	38.12	110.32	51.53	25.78	29.67	25.76	26.10
1032320	2	1.18	1.62	0.77	0.38	0.53	2.25	0.73
1032320	3	8.32	15.25	6.58	3.28	3.92	13.00	8.45
1032321	1	33.25	56.83	27.41	13.69	15.29	17.29	6.62
1032321	2	0.48	0.89	0.45	0.22	0.27	0.70	0.31
1032321	3	2.29	1.30	0.44	0.22	0.29	2.47	0.60
1032322	1	4.03	5.84	2.21	1.07	1.36	3.39	2.01
1032322	2	0.14	0.32	0.20	0.09	0.16	0.08	0.06
1032322	3	0.07	0.18	0.00	0.00	0.11	0.18	0.05
1032342	1	13.51	21.30	9.93	4.97	5.43	6.35	4.03
1032342	2	0.47	0.52	0.32	0.16	0.17	0.22	0.16
1032342	3	0.17	0.26	0.22	0.11	0.13	0.22	0.17
1032346	1	28.60	64.76	29.24	14.60	16.60	22.60	19.71
1032346	2	0.44	0.38	0.23	0.10	0.14	0.50	0.05
1032346	3	1.72	0.98	0.32	0.16	0.18	4.80	1.42
1032351	1	9.25	16.80	6.77	3.41	4.14	6.10	3.61
1032351	2	0.25	0.35	0.26	0.13	0.20	0.09	0.09
1032351	3	0.22	0.34	0.18	0.09	0.18	0.38	0.12
1032359	1	2.04	9.45	10.72	5.35	6.93	1.07	0.47
1032359	2	0.14	0.40	0.24	0.13	0.17	0.54	0.16
1032359	3	0.13	0.36	0.20	0.11	0.00	2.07	0.49
1032360	1	0.31	1.12	0.78	0.40	0.44	1.06	0.22
1032360	2	0.26	0.43	0.22	0.12	0.14	0.87	0.16
1032360	3	0.09	0.25	0.07	0.02	0.14	1.66	0.32
1032362	1	35.66	69.90	31.59	15.78	17.28	26.84	18.20
1032362	2	0.19	0.40	0.24	0.12	0.16	0.47	0.06
1032362	3	5.74	1.68	0.33	0.16	0.25	6.68	1.53

Table A7 Continued.

TEST_I D	TEST_PHAS E	benzen e	toluen e	m- xylen e	p- xylen e	o- xylen e	ethan e	n- pentan e
1032382	1	3.03	7.14	4.68	2.33	0.00	2.72	1.40
1032382	2	0.09	0.17	0.14	0.06	0.00	0.01	0.01
1032382	3	0.13	0.13	0.05	0.02	0.00	0.05	0.00
1032383	1	25.02	27.38	12.93	6.46	7.18	7.77	4.25
1032383	2	0.43	0.72	0.47	0.23	0.28	0.26	0.11
1032383	3	0.18	0.44	0.38	0.20	0.22	0.13	0.07
1032388	1	22.45	42.57	21.17	10.58	11.77	19.83	8.67
1032388	2	0.41	0.45	0.26	0.13	0.17	0.22	0.10
1032388	3	4.40	5.87	2.23	1.12	1.27	4.85	3.30
1032392	1	85.93	180.46	93.20	46.60	51.96	32.00	35.41
1032392	2	17.15	16.15	6.02	3.00	3.43	9.51	4.07
1032392	3	17.90	18.16	6.87	3.43	3.85	14.57	10.14
1032393	1	15.57	35.75	16.30	8.15	9.08	10.87	11.59
1032393	2	0.39	0.28	0.19	0.09	0.10	0.18	0.14
1032393	3	2.20	0.95	0.27	0.13	0.13	2.23	1.31
1032426	1	53.63	77.61	32.55	16.28	18.10	46.05	24.27
1032426	2	24.16	20.52	7.27	3.64	4.61	10.91	9.01
1032426	3	31.07	42.51	15.57	7.81	9.87	33.06	23.70
1032428	1	205.29	413.16	188.13	94.07	89.82	65.96	76.47
1032428	2	110.15	135.10	46.61	23.31	20.90	35.36	32.66
1032428	3	157.46	199.19	71.09	35.57	31.15	36.42	32.43
1032434	1	7.08	16.71	6.05	3.02	3.64	61.22	15.85
1032434	2	0.21	0.10	0.00	0.00	0.00	0.39	0.00
1032434	3	0.00	0.00	0.00	0.00	0.00	9.25	0.00
1032435	1	132.56	278.98	169.73	84.86	91.00	92.94	47.68
1032435	2	93.51	46.75	24.17	12.08	12.23	37.21	5.24
1032435	3	16.37	14.70	7.86	4.00	4.21	19.99	4.42
1032436	1	2.89	10.38	3.95	2.00	2.38	27.11	9.26
1032436	2	0.07	0.17	0.10	0.07	0.22	0.41	0.00
1032436	3	0.09	0.32	0.19	0.09	0.33	6.06	0.05
1032442	1	185.97	402.14	193.57	96.74	106.8 4	63.87	91.83
1032442	2	47.08	46.82	17.69	8.82	9.76	21.08	14.28
1032442	3	59.49	87.06	34.11	17.01	19.04	40.27	31.56
1032443	1	91.22	298.26	180.21	90.15	104.6 3	62.29	53.48
1032443	2	3.36	6.35	4.09	2.05	2.26	2.70	1.10
1032443	3	11.00	17.17	6.98	3.54	3.77	14.28	7.89

Table A7 continued

TEST_ID	TEST_PHASE	benzene	toluene	m-xylene	p-xylene	o-xylene	ethane	n-pentane
1032443	1	91.22	298.26	180.21	90.15	104.63	62.29	53.48
1032443	2	3.36	6.35	4.09	2.05	2.26	2.70	1.10
1032443	3	11.00	17.17	6.98	3.54	3.77	14.28	7.89
1032444	1	110.56	384.77	199.08	99.54	119.34	39.61	79.77
1032444	2	51.93	160.90	74.99	37.49	43.88	26.42	44.87
1032444	3	77.87	267.07	124.49	62.24	73.96	31.06	85.51
1032445	1	189.59	473.43	238.24	119.19	135.37	67.83	108.05
1032445	2	41.19	76.65	35.67	17.87	20.29	22.71	23.39
1032445	3	114.15	169.50	68.62	34.31	38.45	47.66	54.90
1032472	1	73.41	135.12	69.95	34.96	36.08	47.18	33.78
1032472	2	0.89	1.51	1.04	0.52	0.61	0.45	0.22
1032472	3	4.98	2.20	0.81	0.40	0.53	7.77	0.31
1032473	1	1.71	5.45	4.75	2.38	2.61	0.80	0.41
1032473	2	0.51	0.93	0.71	0.35	0.42	0.17	0.16
1032473	3	7.45	1.99	0.89	0.45	0.62	6.43	1.94

Table A8. Contribution of cold start for US drivers assuming driving patterns similar to the UC protocol.

% Contribution of Cold Start Emissions to the Average Driving Trip						
	THC	Benzene	Toluene	Xylenes	Ethane	n-Pentane
Average	0.94	0.93	0.94	0.94	0.93	0.96
Lower Quartile	0.72	0.8	0.87	0.77	0.83	0.87
Worst-Emitters	0.16	0.08	0.17	0.22	0.11	0.12

Table A9. Gasoline composition analysis.

Fraction		frac C	frac H		mass %		wt. C	wt. H
C4 P		0.827	0.173		0.5		0.4133	0.0867
C5 P		0.832	0.168		10.31		8.5814	1.7286
C6 P		0.836	0.164		9.86		8.2453	1.6147
C7 P		0.839	0.161		10.42		8.7428	1.6772
C8 P		0.841	0.159		10.41		8.7564	1.6536
C9 P		0.843	0.157		3.47		2.9245	0.5455
C10 P		0.844	0.156		1.37		1.1565	0.2135
C11+ P		0.845	0.155		2.4		2.0285	0.3715
C6 A		0.923	0.077		0.74		0.6827	0.0573
C7 A		0.912	0.088		5.13		4.6810	0.4490
C8 A		0.905	0.095		8		7.2404	0.7596
C9 A		0.899	0.101		6.65		5.9807	0.6693
C10 A		0.895	0.105		3.61		3.2304	0.3796
C11+ A		0.891	0.109		0.93		0.8288	0.1012
O/N		0.856	0.144		14.34		12.2789	2.0611
C5 cyc O		0.882	0.118		0.06		0.0529	0.0071
C6 cyc O		0.877	0.123		0.32		0.2807	0.0393
C7 cyc O		0.874	0.126		0.43		0.3759	0.0541
C8 cyc O		0.872	0.128		0.23		0.2005	0.0295
C9 cyc O		0.870	0.130		0.05		0.0435	0.0065
poly-N		0.869	0.131		0		0.0000	0.0000
MTBE		0.681	0.137		0		0.0000	0.0000
Ethanol		0.521	0.131		10.77		5.6155	1.4139
TAME		0.705	0.138		0		0.0000	0.0000
			Total %		100		82.3407	13.9187
					C/H Ratio		5.92	
					Wt% O		3.74	

Supplemental Figures

Comparison of PTR-MS and ARB-GC Results:
Bag 1 of UC Coldstart Tests

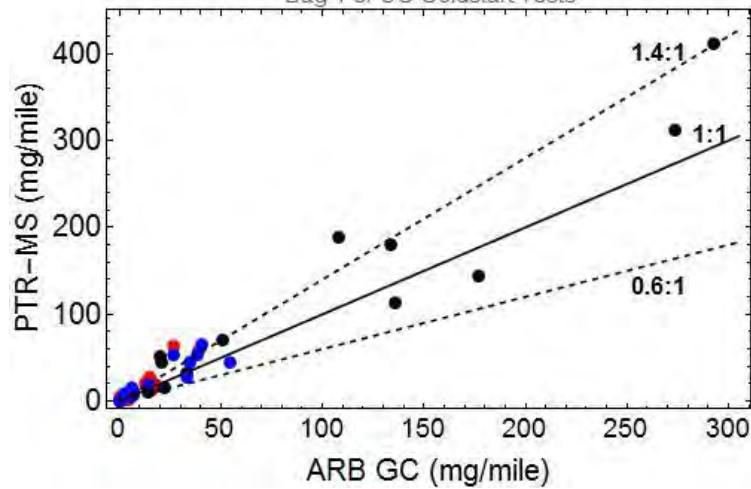


Figure A1. Comparisons of cold-start total BTEX (black), benzene (blue), and acetaldehyde (red) emissions as measured by PTR-MS and GC-FID. PTR-MS measurements for individual compounds are within 50% and BTEX as a group within 30% of GC-MS emissions.

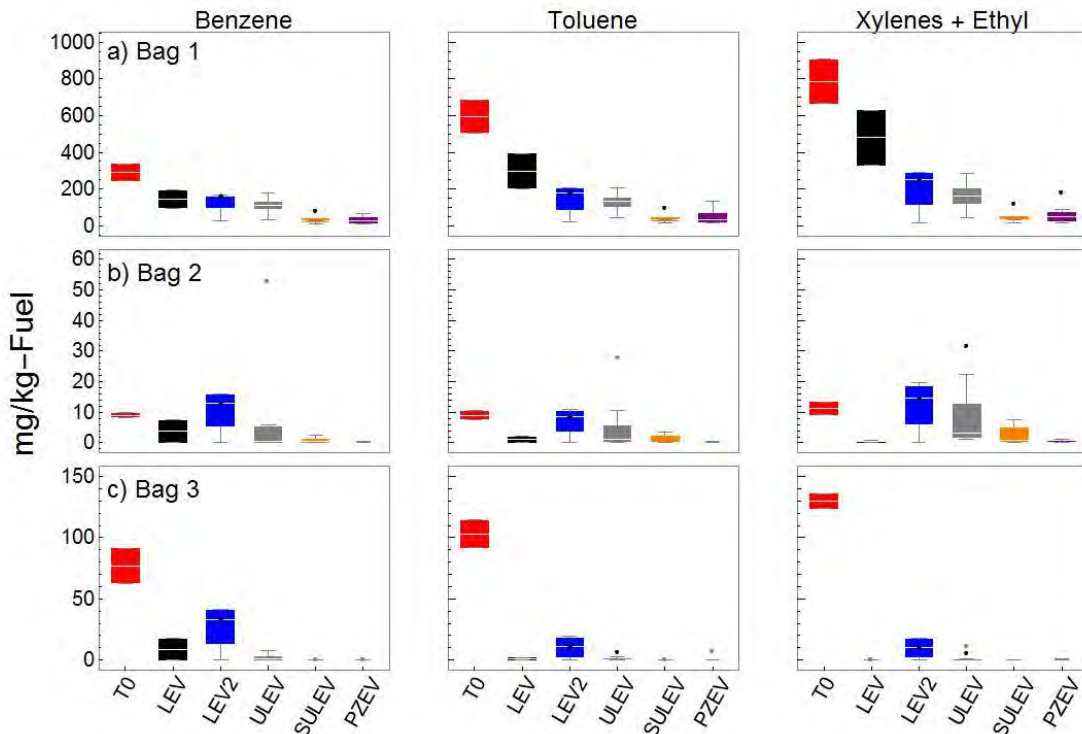


Figure A2. BTEX emission factors for all vehicle classes for bag 1 (a), bag 2 (b), and bag 3 (c) of the UC protocol, as measured by PTR-MS. Ethyl benzene is grouped with the xylenes. The central white lines on the box plots are median values; the edges of the boxes are the 25th and 75th percentiles; the whiskers extend to the most extreme data not considered outliers; and the solid black points are outliers.

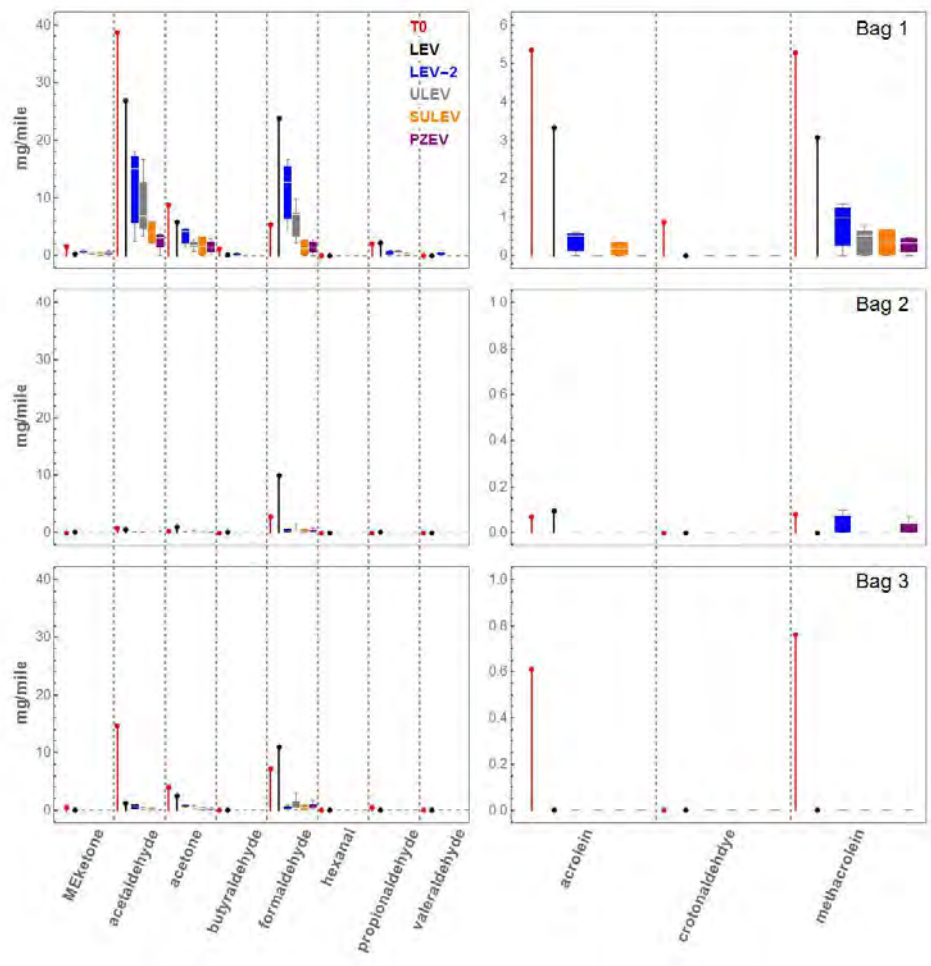


Figure A3. Emissions of ketones and aldehydes, measured by LC-MS in mg/mile.

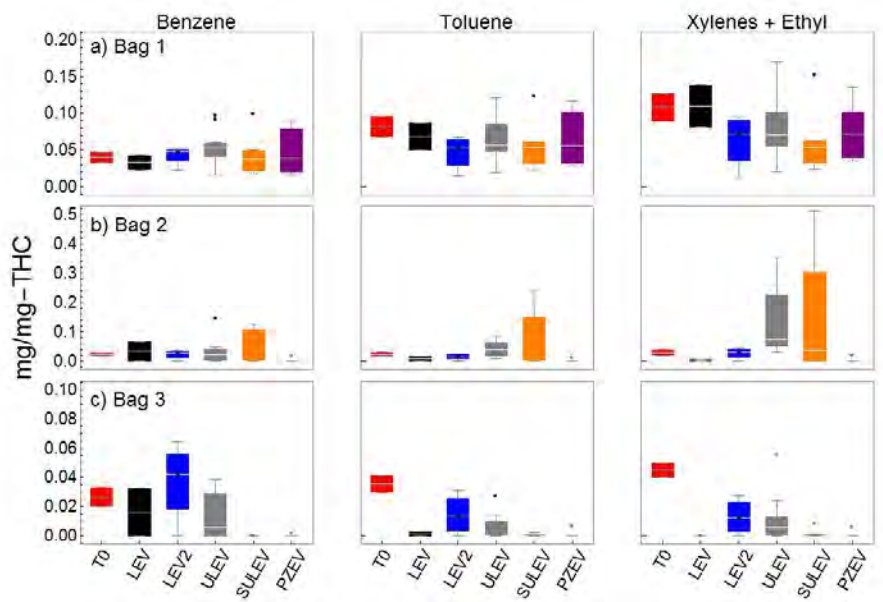


Figure A4. BTEX emissions normalized to NMOG emissions.

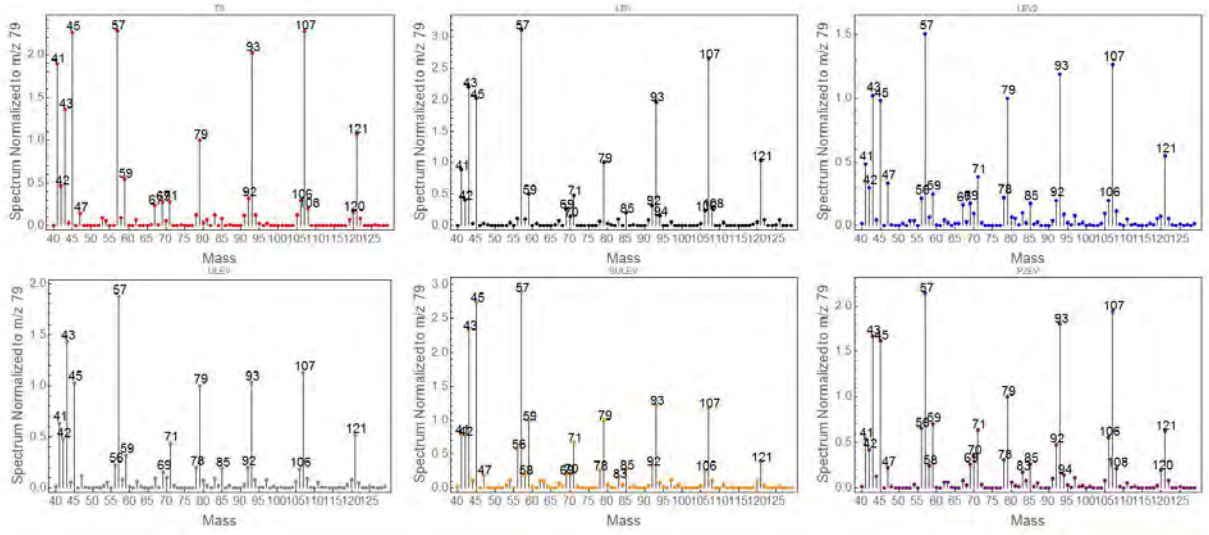


Figure A5. Average mass spectra for all classes of vehicles.

Appendix B Supplementary information for Chapter 5

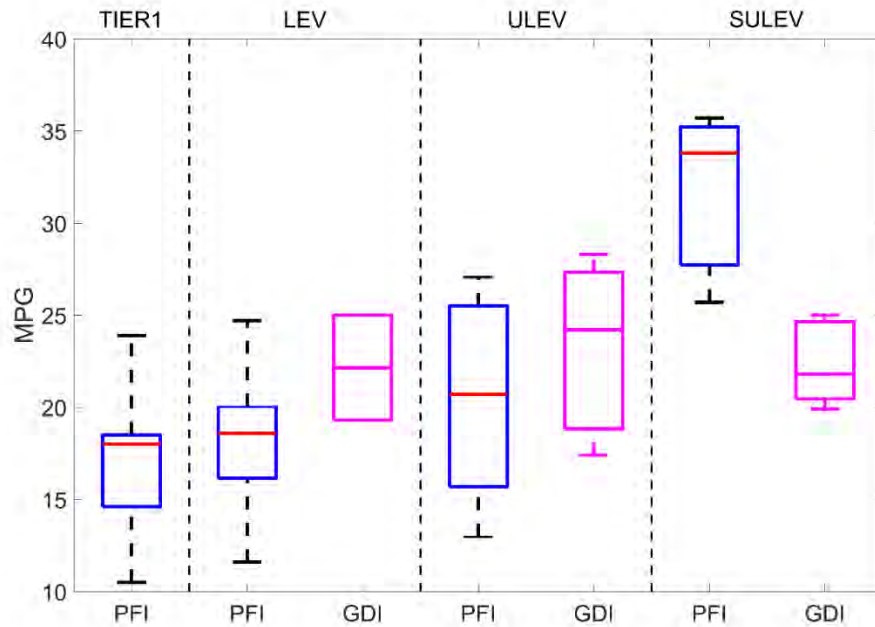


Figure B1: Fuel economy expressed in miles per gallon (MPG) as a function of vehicle categories. MPG was calculated using the amount of fuel burnt, the distance travelled, and the fuel density for each vehicle tested under the cold-start UC cycle. The data are presented as box-whiskers. Blue and magenta colors correspond to vehicles equipped with a PFI and a GDI engine respectively. SULEV PFI vehicles have higher fuel economy because most of the SULEV included in the analysis were equipped with a hybrid engine.

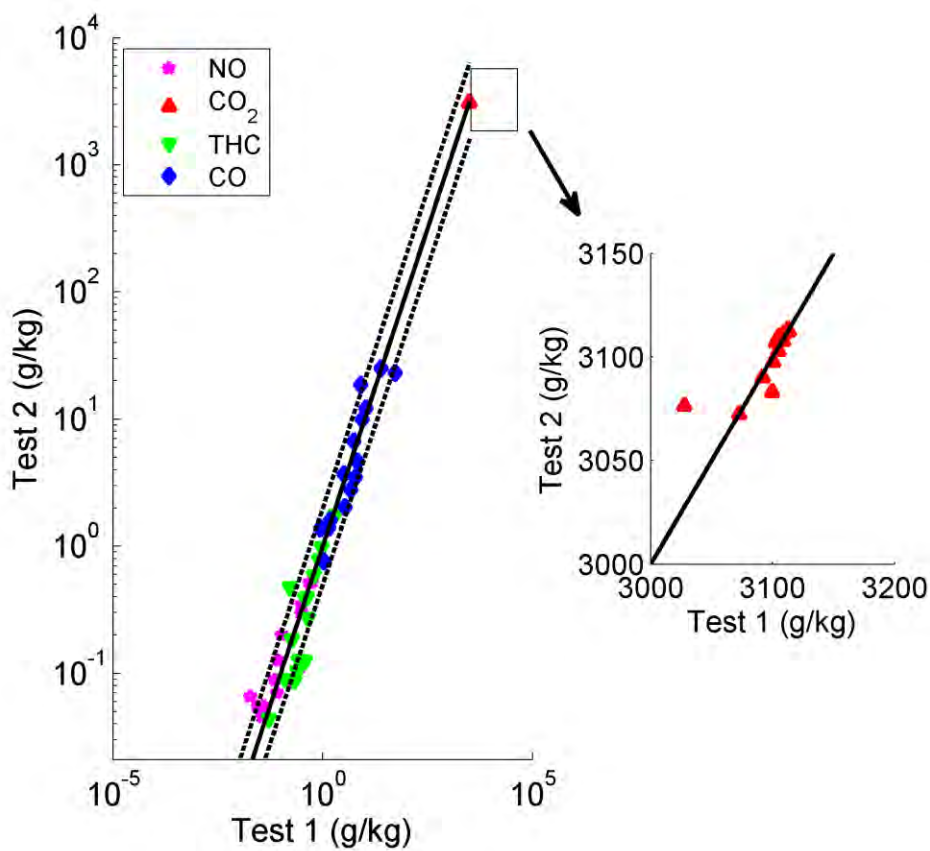


Figure B2: Experimental repeatability for gas-phase species including NO, CO₂, CO, and THC. The data are plotted as a scatter plot on log-log axes. The solid line indicates the 1:1 line and the two dotted lines correspond to the 2:1 and 1:2 lines.

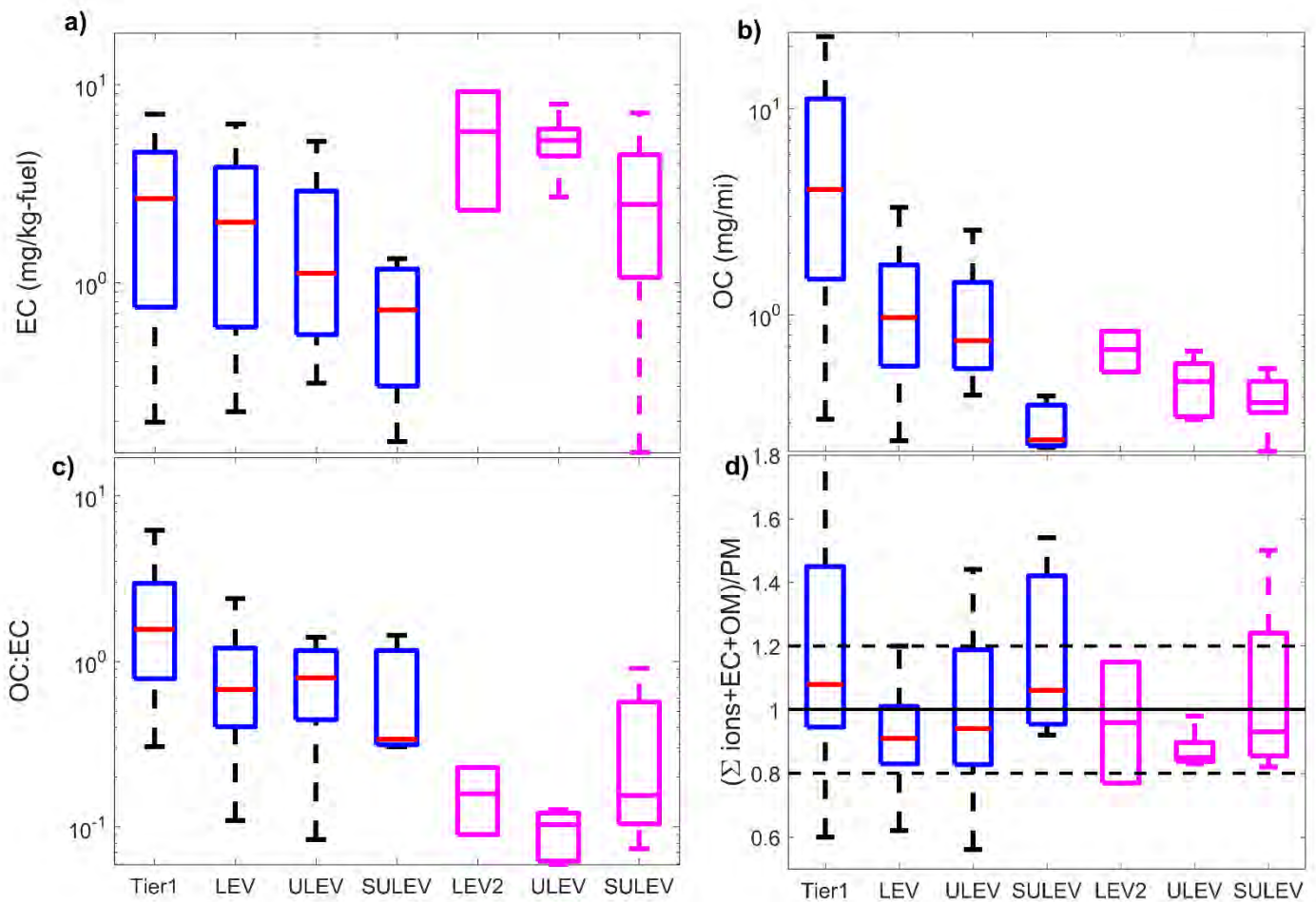


Figure B3: Particle emission factors for: a) elemental carbon (EC), b) organic carbon (OC), c) OC:EC ratio, and d) fraction of speciated particulate matter (PM) to gravimetric PM. For all vehicle categories good mass closure is achieved. The solid line indicates a ratio of unity, and the two dotted lines indicate a 20% deviation from the solid line. For all graphs blue and magenta box-whiskers represent vehicles equipped with a PFI and GDI engine technology respectively.

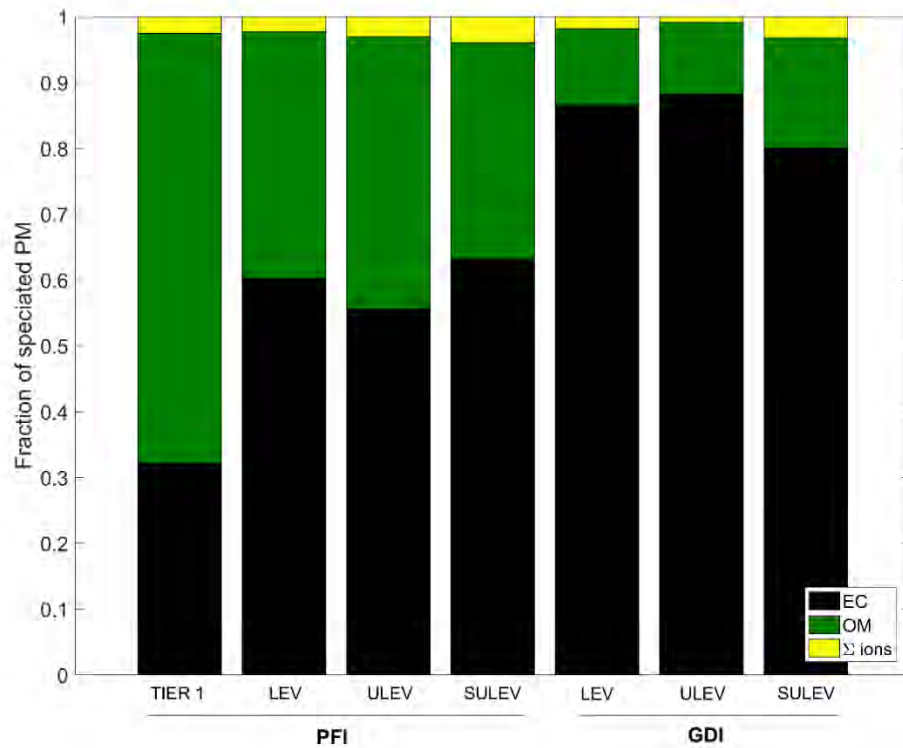


Figure B4: Fraction of elemental carbon (EC), organic carbon (OC), and sum of ions in total speciated PM as a function of vehicle categories. The fraction of EC in total speciated PM is increasing as we move towards newer vehicles. However, GDI vehicles are at the extreme with EC dominating PM.

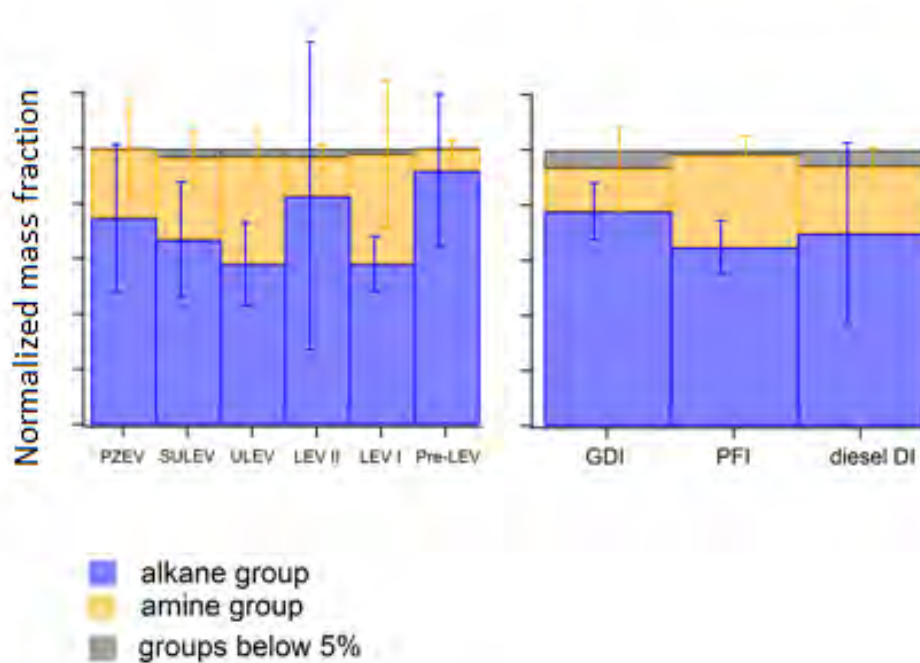


Figure B5: composition of primary organic aerosol (POA) as a function of emission certification and as a function of engine technology. Alkanes and amines dominate the composition of primary SOA, and POA composition is independent of emission standard and engine technology.

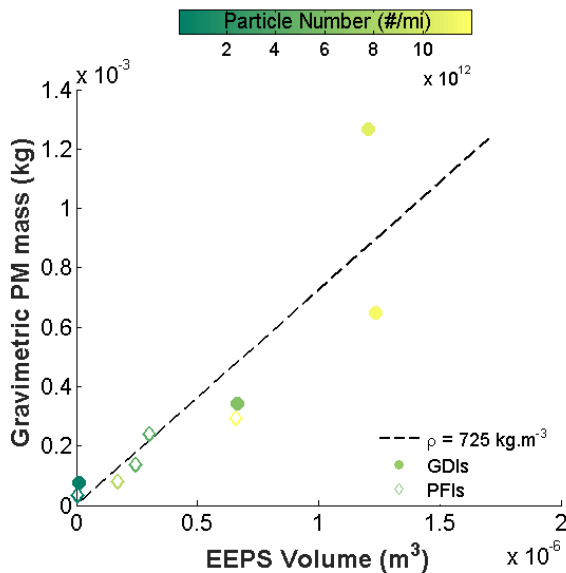


Figure B6: Scatter plot of particle volume (calculated from the EEPS number distribution assuming spherical particles) versus gravimetric PM mass for five PFI vehicles (open diamonds) and four GDI vehicles (filled circles). The dashed black line indicates a linear regression ($R^2=0.78$) whose slope corresponds to the effective density of 0.725 g cm^{-3} . Colors represent the total particle number emission factors for each vehicle tested.

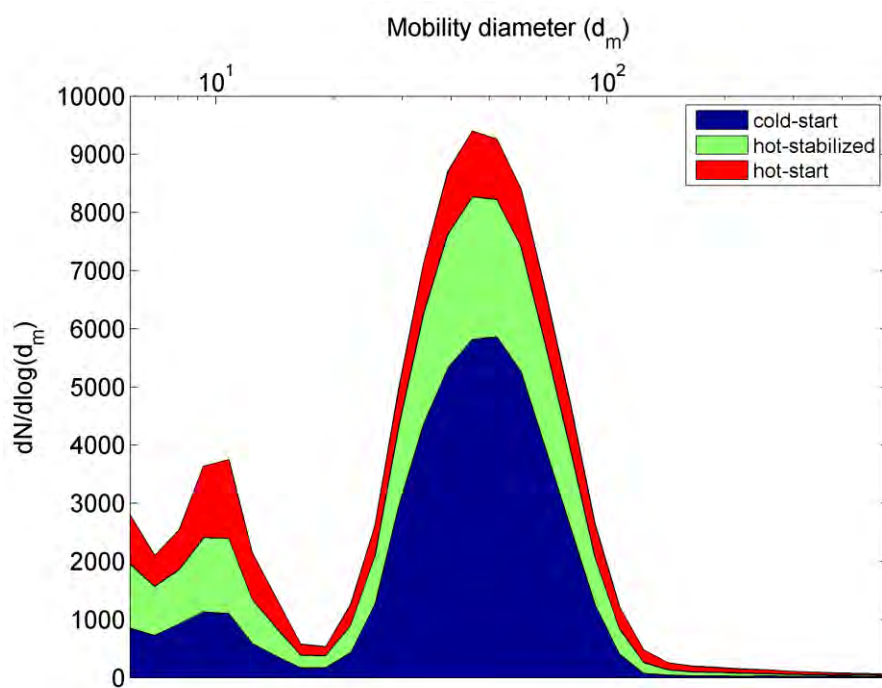


Figure B7: Particle number mobility size distributions emission factors presented as stacked area for a typical experiment. The x-axis is on a log scale. Blue, green, and red represent size distributions from cold-start, hot-stabilized, and hot-start respectively.

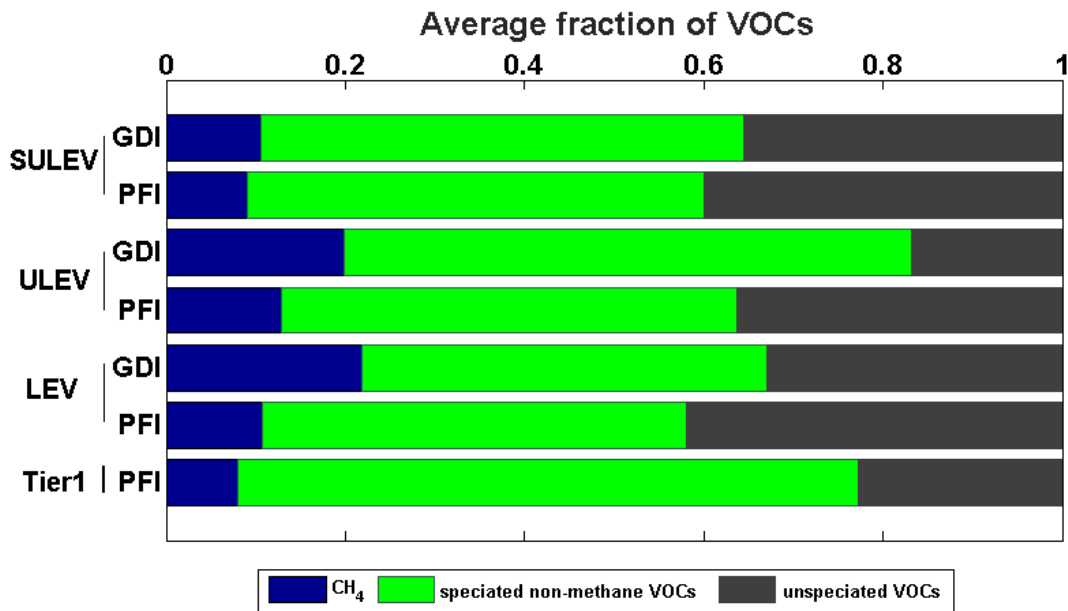


Figure B8: Average fraction of methane, speciated non-methane volatile organic compounds (VOCs) and unspciated VOCs (defined as the total organic gas minus the sum of speciated compounds) for different engine technologies and emissions certifications.

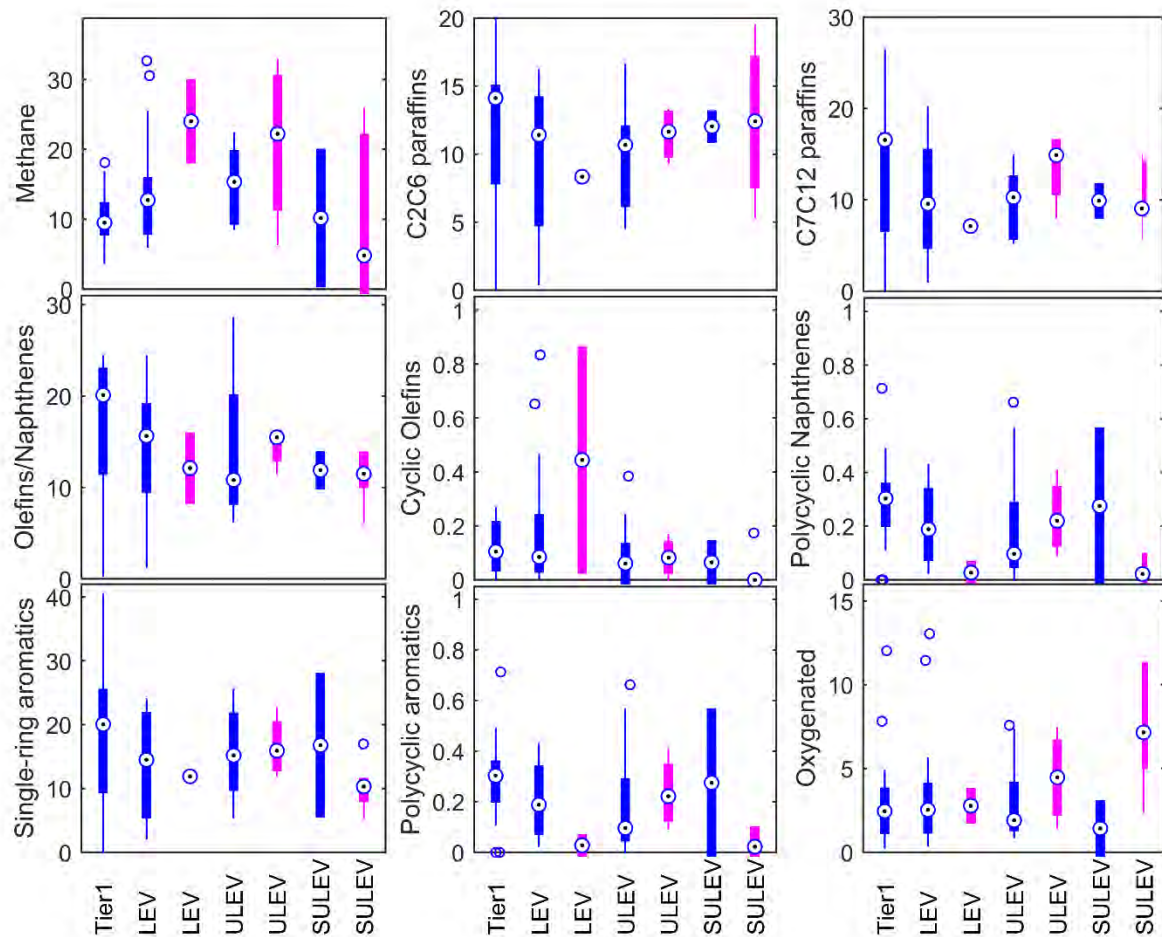


Figure B9: Detailed composition of speciated VOCs presented as a percentage of total organic gas (TOG) for methane, C2-C6 paraffins, C7-C12 paraffins, olefins/naphthenes, cyclic olefins, polycyclic naphthenes, single-ring aromatics, polycyclic aromatics, and oxygenated compounds. Blue and magenta box whiskers correspond to vehicles equipped with a PFI and GDI engine respectively.

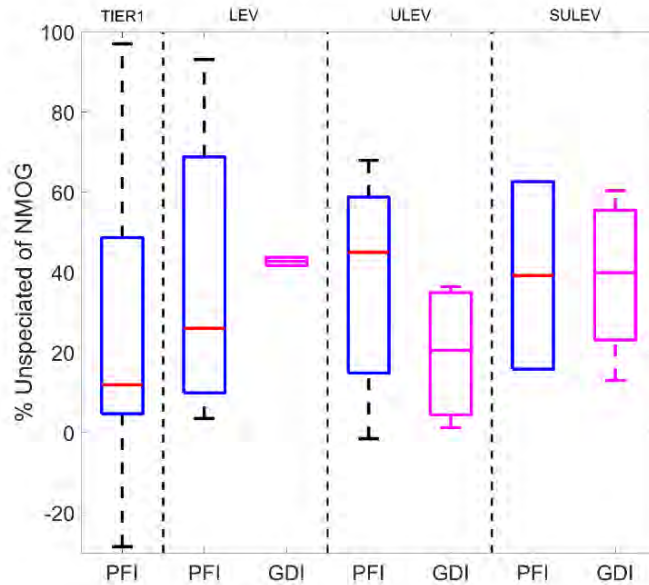


Figure B10: percentage of unspesiated VOCs as a percentage of speciated non-methane organic gas (NMOG), as a function of vehicle class. Data are presented as box-whisker plot. Blue and magenta colors correspond to vehicles equipped with a PFI and GDI engine respectively.

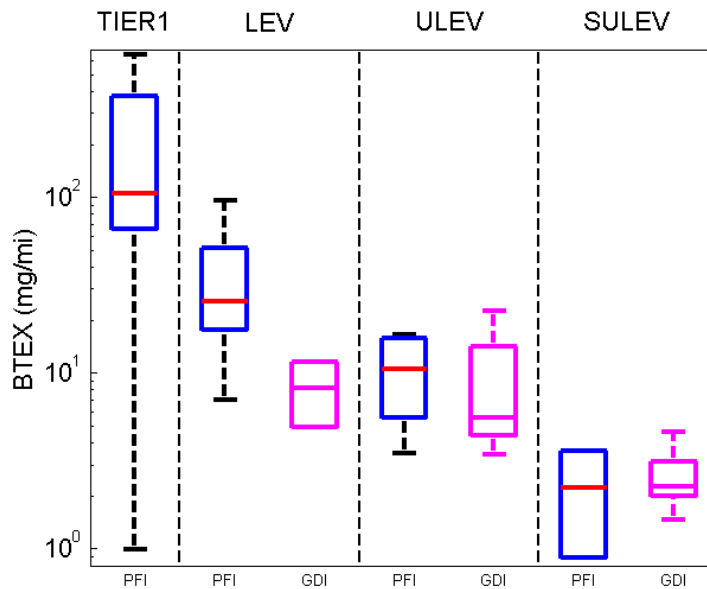


Figure B11: BTEX emission factors as a function of vehicle categories. Trends in BTEX mirror the decreasing behavior of THC with no significant differences between PFI and GDI vehicles.

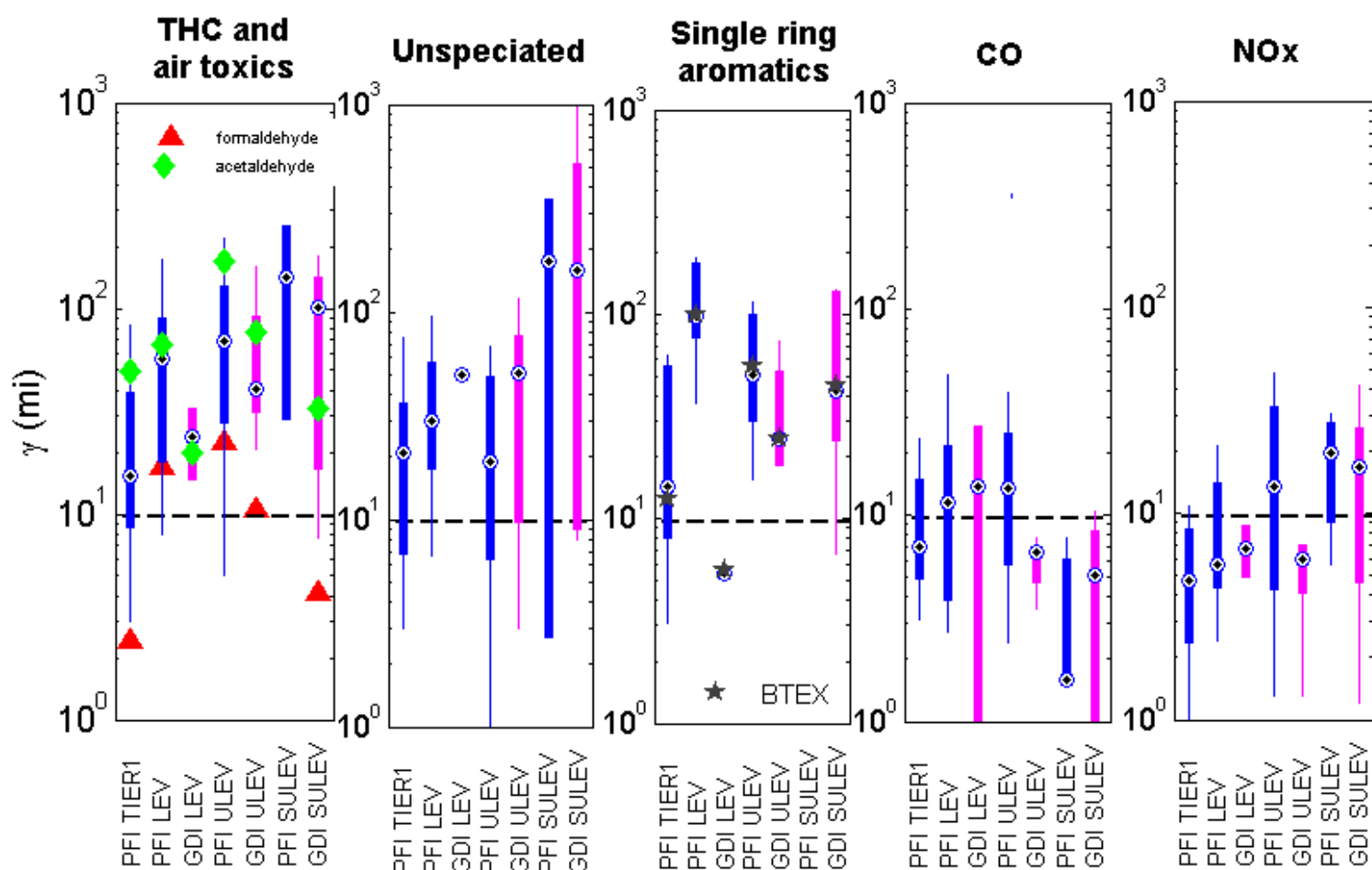


Figure B12: cold-start importance for different gas-phase pollutants as a function of emission certification and engine technology. a) γ for THC (shown as box-whisker) and median γ for formaldehyde (red triangle) and acetaldehyde (green diamond) b) γ for unspiciated (defined as total organic gas minus the sum of speciated compounds) c) γ values for single ring aromatics (box-whiskers) and median γ for BTEX (black star; box-whisker for BTEX mirrored the box-whiskers for single ring aromatics indicating that cold-start emission importance of single ring aromatics are driven by BTEX) d) γ for CO e) γ for NOx. The US average daily trip length of 9.8 miles is shown for reference as the horizontal dashed line.

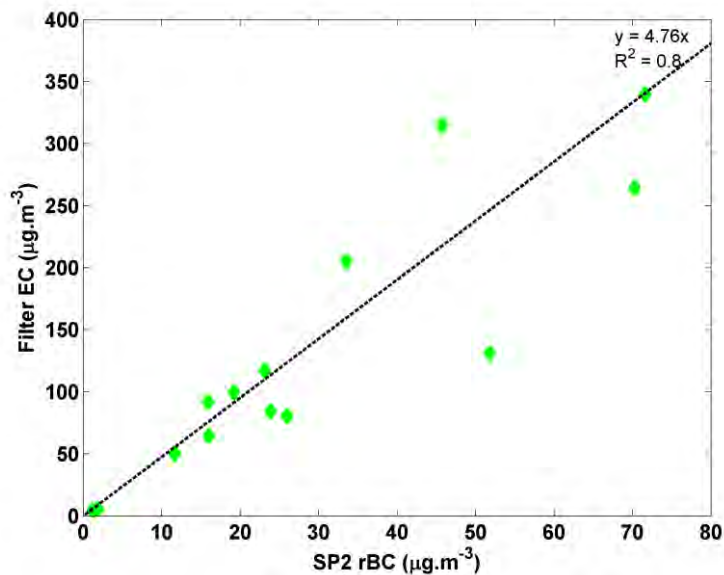


Figure B13: Comparison of filter EC and SP2 refractory BC (rBC) mass concentrations for all vehicle tested in the 2014 campaign. The dotted line indicates the line of best fit with SP2 underestimating filter mass concentrations by a factor of 5. The discrepancy between the two methods could be attributed to 1) coincidence errors in the SP2 due to high concentrations, 2) differences between operationally defined EC and rBC measured using different techniques.

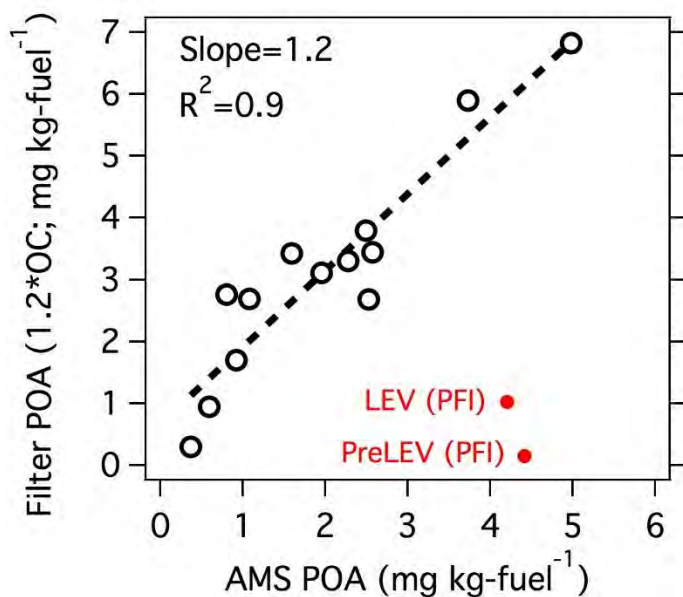


Figure B14: scatter plot of filter measured organic mass (defined as 1.2 times the organic carbon) fuel-based emission factors versus AMS measured primary organic aerosol (POA) fuel-based emission factors.

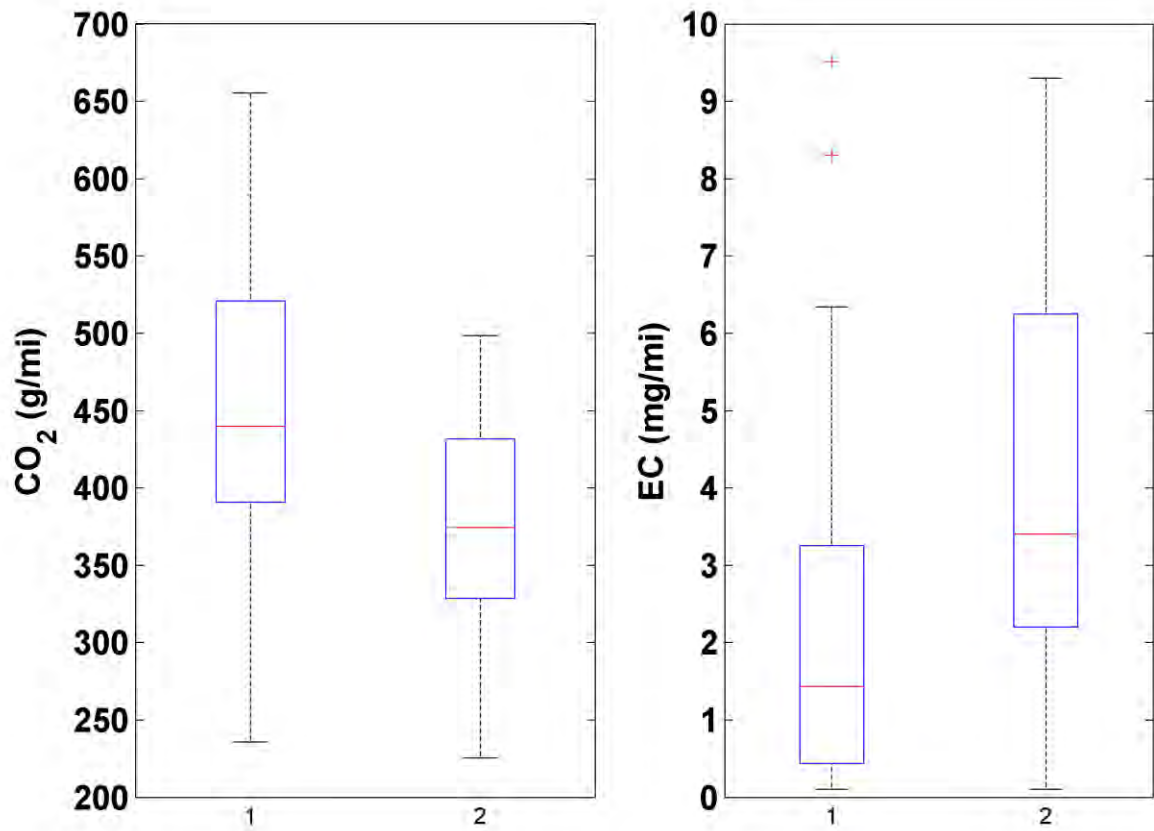


Figure B15: CO₂ and EC distance-based emission factors for vehicles equipped with PFI and GDI engines.

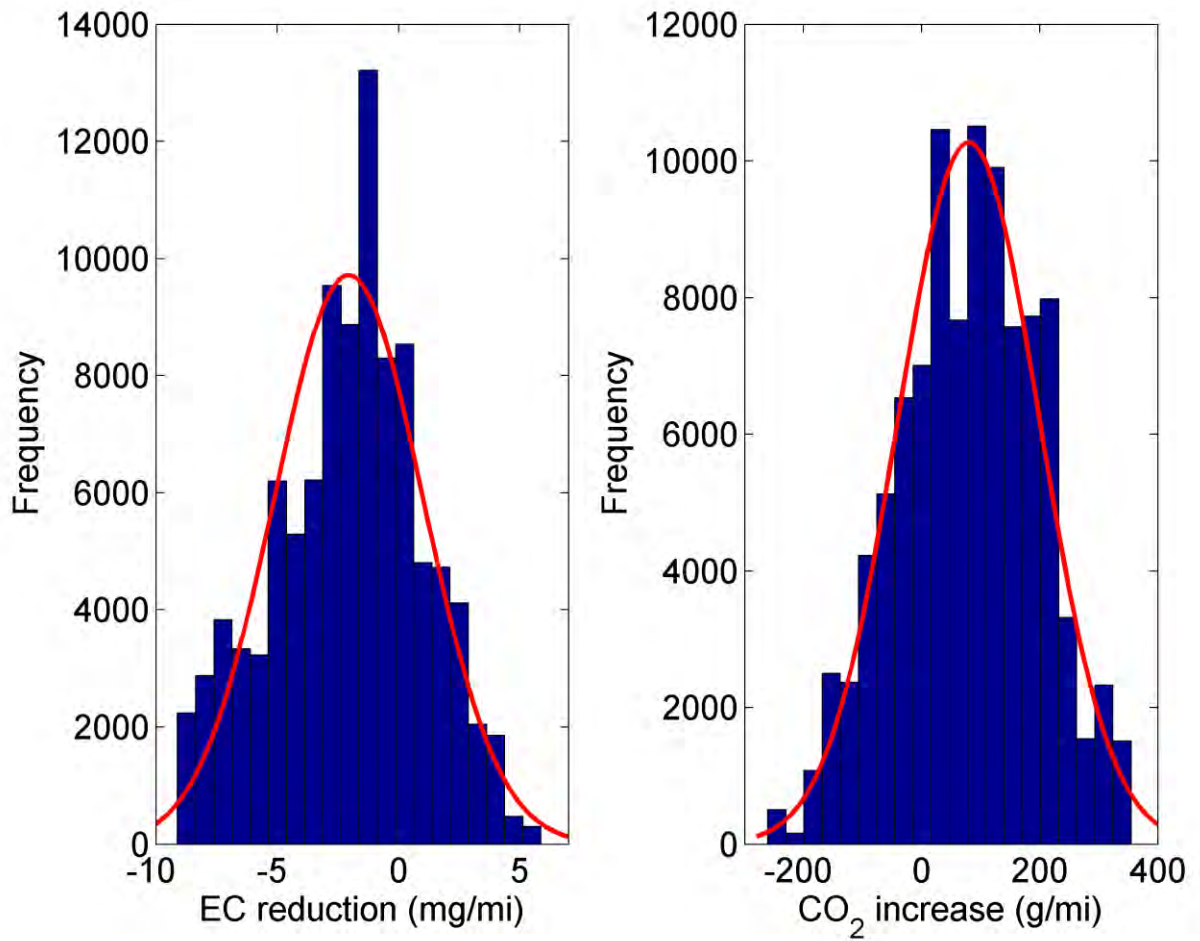


Figure B16: Monte Carlo (n=100000) simulation using data from Figure B13. The data compares the CO₂ increase of 57 g/mi from replacing a GDI vehicle by a PFI one, and the EC reduction of 2.1 mg/mi by replacing a GDI engine with a PFI one. These values were found by fitting normal distributions on the histograms (indicated by the red curves).

Table B1: Number of vehicles in each certification category for all vehicles reported in this study

Regulation	emission certification	Number of PFIs	Number of GDIs
Federal	Tier1	17	0
California	LEV1	20	0
	LEV2	10	2
	Total LEVs	30	2
	ULEV	17	5
	SULEV	3	8
	Total	67	15

Table B2 : Emissions Standards, FTP-75 (g/mi), 50,000 miles/5 years

Category	NMOG	CO	NO _x	PM	HCHO
TIER I	0.25	3.4	0.4	0.08	-
LEV 1	0.075	3.4	0.2	-	0.015
ULEV	0.04	1.7	0.2	-	0.008
LEV 2	0.075	3.4	0.05	-	0.015
L2ULV	0.04	1.7	0.05	-	0.008
SULEV/PZEV	-	-	-	-	-

Table B3: Gasoline fuel property and composition analysis

Property/ Fuel component	Units	Median Mass Value (%)
Density	g/mL	0.748
C4 paraffins	wt %	0.50
C5 paraffins	wt %	10.31
C6 paraffins	wt %	9.86
C7 paraffins	wt %	10.42
C8 paraffins	wt %	10.41
C9 paraffins	wt %	3.47
C10 paraffins	wt %	1.37
C11+ paraffins	wt %	2.40
Σ paraffins	wt %	48.74
C6 aromatics	wt %	0.74
C7 aromatics	wt %	5.13
C8 aromatics	wt %	8.00
C9 aromatics	wt %	6.65
C10 aromatics	wt %	3.61
C11+ aromatics	wt %	0.93
Σ aromatics	wt %	25.06
Olefins/ naphthenes	wt %	14.34
C5 cyclic olefins	wt %	0.06
C6 cyclic olefins	wt %	0.32
C7 cyclic olefins	wt %	0.43
C8 cyclic olefins	wt %	0.23
C9 cyclic olefins	wt %	0.05
Σ cyclic olefins	wt %	1.09
Polycyclic naphthenes	wt %	0.00
MTBE	wt %	0.00
Ethanol	wt %	10.77
TAME	wt %	0.00

Table B4: List of gasoline vehicles from 2014 campaign used in this study

1038901	UC	PC	1990	3.8	TIER0	18.0	121473
1038909	UC	PC	2013	2	ULEV	19.7	23514
1038911	UC	M3	2003	5.4	LEV	11.4	104619
1038912	UC	PC	1990	3.8	TIER0	17.9	121567
1038915	UC	PC	2013	2	ULEV	19.2	23494
1038917	UC	LDT	2013	5.3	ULEV	13.2	24182
1038918	UC	LDT	2013	5.3	ULEV	13.0	24136
1038920	UC	PC	2014	2.4	PZEV	23.8	4526
1038945	UC	LDT	2013	5.3	ULEV	12.9	24170
1038947	UC	PC	2013	1.6	L2ULV	24.2	19840
1038952	UC	PC	2013	3.6	L2SUL	17.8	28152

Table B5: List of gasoline vehicles used in previous campaigns

Test ID	Test Cycle	Vehicle Class	Model Year	Engine Size (L)	Certification	Fuel economy (mpg)	Odometer
1032322	Cold UC	PCa	2012	3.6	ULEV	17.4	9563
1032442	Cold UC	PC	1987	4.1	Tier I	14.6	197631
1032440, 1032444	Cold UC	PC	1988	1.6	Tier I	23.9	224758
1032303, 1032389, 1032426	Cold UC	M3	1990	5.0	Tier I	13.0	58586
1032392	Cold UC	PC	1989	1.3	Tier I	27.2	123085
1032320	Cold UC	PC	1991	3.8	LEV	19.4	118050
1028060	Cold UC	PC	1990	3.0	Tier I	18.5	
1027853	Cold UC	PC	1990	2.3	Tier I	18.1	
1027920	Cold UC	PC	1991	3.8	Tier I	18.5	
1032443	Cold UC	PC	1991	4.0	Tier I	16.4	144000
1028023	Cold UC	PC	1992	3.4	Tier I	15.7	
1027921	Cold UC	PC	1992	3.8	Tier I	18.0	
1028026	Cold UC	PC	1992	3.8	Tier I	18.4	
1027922	Cold UC	LDT	1992	5.7	Tier I	10.5	
1027872	Cold UC	PC	1993	4.9	Tier I	13.1	
1032445	Cold UC	T2	1993	4.3	Tier I	15.0	161476

Table B6: Light-duty gasoline vehicle emissions. Gas phase emissions in (g/mi), particle phase emissions (mg/mi)

Test ID	certific ation.	Engine tech.	Test Cycle	kg- Fuel/mi	MPG	CO2 (g/mi)	CO (g/mi)	NOx (g/mi)	NO (g/mi)	CH4 (g/mi)	NMHC (g/mi)	EC	OC	PM	Σ ions
1038708	SULEV	GDI	UC	0.112	23.6	340.97	5.539	0.015	0.010	0.009	0.019	1.73	0.391	2.918	0.186
1038723	L2SUL	GDI	UC	0.135	19.6	420.27	0.210	0.008	0.005	0.000	0.028	0.38	0.349	0.703	0.045
1038724	SULEV	GDI	UC	0.127	20.8	393.80	0.772	0.016	0.010	0.002	0.029	7.24	0.534	9.651	0.123
1038745	PZEV	GDI	UC	0.130	20.4	402.16	0.929	0.015	0.010	0.002	0.006	1.76	0.318	2.354	0.057
1038747	PZEV	GDI	UC	0.073	36.4	225.61	0.346	0.020	0.013	0.002	0.025	0.13	0.205	0.259	0.013
1038750	L2SUL	GDI	UC	0.138	19.1	430.96	0.223	0.010	0.006	0.000	0.012	n/a	n/a	n/a	n/a
1038755	PZEV	PFI	UC	0.076	34.9	235.88	0.083	0.002	0.001	0.000	0.020	0.15	0.225	0.298	0.032
1038757	SULEV	GDI	UC	0.127	20.9	394.05	0.444	0.014	0.009	0.001	0.012	n/a	n/a	n/a	n/a
1038760	PZEV	PFI	UC	0.077	34.5	238.79	0.058	0.008	0.005	0.001	0.009	n/a	n/a	n/a	n/a
1038797	PZEV	GDI	UC	0.083	32.0	257.18	0.231	0.011	0.007	0.001	0.009	n/a	n/a	n/a	n/a
1038801	ULEV	GDI	UC	0.097	27.3	301.06	0.315	0.048	0.031	0.003	0.038	8.04	0.476	10.462	0.046
1038820	ULEV	GDI	UC	0.096	27.7	296.86	0.352	0.043	0.028	0.003	0.035	n/a	n/a	n/a	n/a
1038821	L2LEV	PFI	UC	0.170	15.6	520.92	4.250	0.148	0.096	0.054	0.108	2.19	0.214	2.809	0.037
1038822	L2ULV	GDI	UC	0.112	23.7	346.35	0.758	0.015	0.010	0.008	0.042	5.22	0.309	6.702	0.034
1038823	ULEV	GDI	UC	0.143	18.5	432.44	7.757	0.064	0.041	0.030	0.058	8.61	0.879	11.514	0.087
1038824	ULEV	PFI	UC	0.209	12.6	648.56	1.176	0.009	0.006	0.012	0.067	2.49	3.816	7.408	0.079
1038825	L2LEV	GDI	UC	0.109	24.3	334.34	3.278	0.023	0.015	0.012	0.027	9.26	0.829	13.540	0.187
1038827	L2ULV	GDI	UC	0.101	26.2	310.56	2.156	0.007	0.004	0.014	0.059	2.72	0.324	3.629	0.044
1038848	L2LEV	PFI	UC	0.169	15.7	518.46	4.235	0.136	0.088	0.053	0.112	2.29	0.275	2.730	0.022
1038849	L2LEV	PFI	UC	0.170	15.5	520.93	5.490	0.150	0.097	0.056	0.122	n/a	n/a	n/a	n/a
1038850	L2ULV	GDI	UC	0.113	23.3	352.29	0.528	0.022	0.014	0.008	0.023	n/a	n/a	n/a	n/a
1038853	PZEV	GDI	UC	0.097	27.4	300.48	0.331	0.008	0.004	-0.001	0.013	3.60	0.506	n/a	0.129
1038862	L2SUL	GDI	UC	0.157	16.8	489.11	0.139	0.018	0.011	0.000	0.008	3.20	0.468	4.373	0.072

Test ID	Veh.	Engine tech.	Test Cycle	kg-Fuel/mi	MPG	CO2 (g/mi)	CO (g/mi)	NOx (g/mi)	NO (g/mi)	CH4 (g/mi)	NMHC (g/mi)	EC (mg/mi)	OC (mg/mi)	PM (mg/mi)	Σions (mg/mi)
1038864	L2SUL	PFI	UC	0.084	31.683	259.348	0.729	0.013	0.009	0.002	0.011	1.368	0.417	2.177	0.125
1038867	PZEV	GDI	UC	0.123	21.510	379.199	2.862	0.025	0.017	0.005	0.014	5.591	0.545	7.228	0.094
1038868	PZEV	GDI	UC	0.119	22.319	369.424	0.242	0.010	0.007	0.000	0.011	n/a	n/a	n/a	n/a
1038869	L2SUL	GDI	UC	0.160	16.544	498.580	0.221	0.022	0.014	0.000	0.007	n/a	n/a	n/a	n/a
1038885	L2SUL	PFI	UC	0.078	34.039	241.159	0.779	0.024	0.016	0.003	0.034	n/a	n/a	n/a	n/a
1038891	LEV	PFI	UC	0.232	11.446	717.657	1.854	0.116	0.074	0.015	0.173	0.502	0.425	1.235	0.088
1038901	TIER 0	PFI	UC	0.151	17.553	466.838	1.620	0.325	0.209	0.037	0.253	0.339	0.310	0.728	0.074
1038909	ULEV	GDI	UC	0.138	19.188	424.902	3.208	0.023	0.015	0.023	0.058	2.061	0.224	2.669	0.009
1038911	LEV	PFI	UC	0.240	11.065	738.443	4.456	0.135	0.083	0.021	0.167	n/a	n/a	n/a	n/a
1038912	TIER 0	PFI	UC	0.153	17.371	471.448	1.862	0.322	0.205	0.032	0.236	n/a	n/a	n/a	n/a
1038915	ULEV	GDI	UC	0.142	18.636	441.442	0.854	0.063	0.040	0.010	0.040	n/a	n/a	n/a	n/a
1038917	ULEV	PFI	UC	0.206	12.872	638.852	1.386	0.017	0.011	0.013	0.067	1.955	0.267	2.670	0.030
1038918	ULEV	PFI	UC	0.210	12.639	650.485	1.477	0.020	0.013	0.015	0.080	2.234	0.345	2.616	0.040
1038920	PZEV	GDI	UC	0.114	23.186	355.743	0.134	0.007	0.005	-0.001	0.018	2.421	0.270	3.121	0.039
1038945	ULEV	PFI	UC	0.211	12.546	655.543	1.376	0.023	0.015	0.013	0.056	4.471	0.983	7.406	0.121
1038947	L2ULV	GDI	UC	0.113	23.546	349.737	0.464	0.027	0.018	0.008	0.027	4.560	0.307	5.880	0.024
1038952	L2SUL	GDI	UC	0.153	17.309	476.627	0.146	0.012	0.008	0.000	0.014	3.241	0.249	3.818	0.033

Table B6: Light-duty gasoline vehicle emissions. Gas phase emissions in (g/mi), particle phase emissions (mg/mi)

Table 4II

TEST_ID	Test Cycle	(1-ME)benzene	(1-Mpropyl)benzene	(2-Mpropyl)benzene	1,2,3,4-tetraMbenzene	1,2,3,5-tetraMbenzene	1,2,3-triMbenzene	1,2,4,5-tetraMbenzene	1,2,4-triMCPentane
1038708	UC	0.000	0.000	0.096	0.000	0.000	0.214	0.000	0.150
1038723	UC	0.000	0.000	0.098	0.000	0.000	0.117	0.000	0.163
1038747	UC	0.000	0.000	0.000	0.000	0.000	0.555	0.000	0.272
1038755	UC	0.000	0.000	0.000	0.000	0.000	0.176	0.000	0.222
1038801	UC	0.138	0.000	0.139	0.000	0.139	1.181	0.000	0.377
1038821	UC	0.279	0.000	0.187	0.109	0.233	1.884	0.140	0.910
1038822	UC	0.193	0.000	0.121	0.000	0.145	0.554	0.121	0.430
1038824	UC	0.232	0.000	0.233	0.078	0.168	1.081	0.104	0.500
1038825	UC	0.000	0.000	0.000	0.000	0.000	0.121	0.000	0.152
1038827	UC	0.000	0.000	0.000	0.000	0.000	0.000	0.000	0.000
1038849	UC	0.373	0.000	0.266	0.094	0.708	2.648	0.203	1.409
1038862	UC	0.000	0.000	0.000	0.000	0.000	0.000	0.000	0.000
1038867	UC	0.000	0.000	0.000	0.000	0.000	0.131	0.000	0.229
1038891	UC	0.781	0.207	0.248	0.330	1.177	4.295	0.764	1.122
1038901	UC	1.448	0.281	2.378	0.509	2.473	7.316	1.315	3.330
1038909	UC	0.481	0.309	0.000	0.000	0.290	2.424	0.213	1.010
1038917	UC	0.233	0.000	0.364	0.065	0.196	1.219	0.143	0.422
1038920	UC	0.000	0.000	0.000	0.000	0.000	0.376	0.000	0.198
1038945	UC	0.152	0.000	0.500	0.000	0.179	0.863	0.102	0.373
1038947	UC	0.000	0.000	0.310	0.000	0.000	0.285	0.000	0.000
1038952	UC	0.000	0.000	0.000	0.000	0.000	0.000	0.000	0.000
1038980	UC	0.000	0.000	1.128	0.000	0.000	0.000	0.000	0.000

Table B7: Light-duty gasoline vehicle speciated VOC emissions. Values are reported as emission factors

Table B7: Light-duty gasoline vehicle speciated VOC emissions. Values are reported as emission factors

TEST_ID	Test Cycle	1,2,4-triMbenzene	1,2-butadiene	1,2-diBenzene	1,2-diM-3Ebenzene	1,2-diM-4Ebenzene	1,2-propadiene	1,3,5-triMXYhene	1,3,5-triMbenzene
1038708	UC	1.826	0.000	0.000	0.000	0.000	0.190	0.000	0.309
1038723	UC	0.603	0.000	0.000	0.000	0.000	0.000	0.000	0.233
1038747	UC	3.221	0.000	0.000	0.000	0.186	0.000	0.000	1.111
1038755	UC	0.776	0.000	0.000	0.000	0.000	0.000	0.000	0.282
1038801	UC	5.811	0.000	0.000	0.000	0.222	0.000	0.174	0.745
1038821	UC	8.084	0.125	0.000	0.000	0.311	1.688	0.163	0.138
1038822	UC	4.730	0.000	0.000	0.000	0.291	0.000	0.202	1.301
1038824	UC	5.938	0.065	0.000	0.000	0.323	0.901	0.000	1.979
1038825	UC	2.188	0.000	0.000	0.000	0.000	0.000	0.000	0.664
1038827	UC	0.000	0.000	0.000	0.000	0.000	0.000	0.000	0.000
1038849	UC	10.473	0.126	0.000	0.078	0.469	1.384	0.212	3.417
1038862	UC	0.588	0.000	0.000	0.000	0.000	0.000	0.000	0.000
1038867	UC	0.964	0.000	0.000	0.000	0.000	0.000	0.000	0.239
1038891	UC	18.577	0.146	0.269	0.186	1.632	0.000	0.561	5.220
1038901	UC	30.695	0.265	0.491	0.316	3.044	3.683	1.173	9.440
1038909	UC	9.925	0.000	0.000	0.000	0.561	0.000	0.505	3.135
1038917	UC	6.709	0.066	0.000	0.000	0.443	0.000	0.123	1.997
1038920	UC	1.647	0.000	0.000	0.000	0.000	0.000	0.000	0.635
1038945	UC	4.522	0.000	0.000	0.000	0.293	0.863	0.067	1.484
1038947	UC	2.408	0.000	0.000	0.000	0.000	0.451	0.000	0.451
1038952	UC	0.192	0.000	0.000	0.000	0.000	0.000	0.000	0.087
1038980	UC	0.160	0.000	0.000	0.000	0.000	0.000	0.000	0.000

Table B7: Light-duty gasoline vehicle speciated VOC emissions. Values are reported as emission factors

TEST_ID	Test Cycle	1,3-CYpentadiene	1,3-butadiene	1,3-butadiyne	1,3-di-n-propylbenzene	1,3-diEbenzene	1,3-diM-2Ebenzene	1,3-diM-4Ebenzene	1,3-diM-5Ebenzene
1038708	UC	0.000	1.488	0.000	0.000	0.000	0.000	0.000	0.000
1038723	UC	0.000	0.197	0.000	0.000	0.000	0.000	0.000	0.000
1038747	UC	0.000	0.300	0.000	0.000	0.000	0.000	0.186	0.335
1038755	UC	0.000	0.000	0.000	0.000	0.000	0.000	0.000	0.000
1038801	UC	0.000	1.257	0.000	0.000	0.000	0.000	0.194	0.360
1038821	UC	0.000	4.348	0.116	0.000	0.202	0.109	0.647	1.001
1038822	UC	0.000	1.586	0.000	0.000	0.170	0.000	0.242	0.460
1038824	UC	0.000	1.942	0.000	0.064	0.233	0.179	0.311	0.778
1038825	UC	0.000	1.024	0.000	0.000	0.000	0.000	0.000	0.000
1038827	UC	0.000	0.000	0.000	0.000	0.000	0.000	0.000	0.000
1038849	UC	0.000	3.869	0.000	0.079	0.297	0.188	0.853	1.456
1038862	UC	0.000	0.104	0.000	0.000	0.000	0.000	0.000	0.000
1038867	UC	0.000	0.220	0.000	0.000	0.000	0.000	0.000	0.000
1038891	UC	0.000	5.015	0.000	0.208	0.868	0.351	1.301	2.251
1038901	UC	0.000	13.481	0.164	0.441	1.490	1.040	2.518	4.585
1038909	UC	0.000	1.227	0.000	0.000	0.329	0.097	0.483	0.909
1038917	UC	0.000	1.694	0.000	0.000	0.300	0.091	0.365	0.743
1038920	UC	0.000	0.334	0.000	0.000	0.000	0.575	0.000	0.189
1038945	UC	0.000	2.102	0.000	0.000	0.204	0.089	0.255	0.549
1038947	UC	0.000	1.202	0.000	0.000	0.000	0.000	0.000	0.191
1038952	UC	0.000	0.106	0.000	0.000	0.000	0.000	0.000	0.000
1038980	UC	0.000	0.000	0.000	0.000	0.000	0.000	0.000	0.000

Table B7: Light-duty gasoline vehicle speciated VOC emissions. Values are reported as emission factors

TEST_ID	Test Cycle	1,4-diEbenzene	1,4-diM-2-Ebenzene	1-(diME)-2-Mbenzene	1-(diME)-3,5-diMbenzene	1-E-2-n-propylbenzene	1-E-tert-butyl-ether	1-M-2-(1-ME)benzene	1-M-2-Ebenzene
1038708	UC	0.000	0.000	0.000	0.000	0.000	0.000	0.000	1.103
1038723	UC	0.000	0.000	0.000	0.000	0.000	0.000	0.000	0.194
1038747	UC	0.000	0.223	0.000	0.000	0.000	0.000	0.000	0.814
1038755	UC	0.000	0.000	0.000	0.000	0.000	0.000	0.000	0.247
1038801	UC	0.000	0.222	0.000	0.000	0.000	0.000	0.000	1.567
1038821	UC	0.249	0.000	0.000	0.000	0.000	0.000	0.342	2.278
1038822	UC	0.170	0.291	0.000	0.000	0.000	0.000	0.121	1.084
1038824	UC	0.129	0.362	0.000	0.000	0.000	0.000	0.142	1.727
1038825	UC	0.000	0.000	0.000	0.000	0.000	0.000	0.000	0.145
1038827	UC	0.000	0.000	0.000	0.000	0.000	0.000	0.000	0.000
1038849	UC	0.359	0.000	0.000	0.000	0.000	0.000	0.297	3.006
1038862	UC	0.000	0.000	0.000	0.000	0.000	0.000	0.000	0.085
1038867	UC	0.000	0.000	0.000	0.000	0.000	0.000	0.000	0.196
1038891	UC	0.744	1.570	0.000	0.187	0.124	0.000	0.496	4.439
1038901	UC	2.201	3.157	0.229	0.282	0.194	0.000	0.911	9.076
1038909	UC	0.290	0.619	0.000	0.000	0.000	0.000	0.271	2.666
1038917	UC	0.182	0.430	0.000	0.000	0.000	0.000	0.130	1.854
1038920	UC	0.000	0.000	0.000	0.000	0.000	0.000	0.000	0.447
1038945	UC	0.115	0.293	0.000	0.000	0.000	0.000	0.102	1.437
1038947	UC	0.000	0.000	0.000	0.000	0.000	0.000	0.000	0.404
1038952	UC	0.000	0.000	0.000	0.000	0.000	0.000	0.000	0.000
1038980	UC	0.000	0.000	0.000	0.000	0.000	0.000	0.000	0.000

Table B7: Light-duty gasoline vehicle speciated VOC emissions. Values are reported as emission factors

TEST_ID	Test Cycle	1-M-2-n-butylbenzene	1-M-2-n-propylbenzene	1-M-3-(1-ME)benzene	1-M-3-Ebenzene	1-M-3-n-propylbenzene	1-M-4-(1-ME)benzene	1-M-4-ECYhexane	1-M-4-Ebenzene
1038708	UC	0.000	0.000	0.000	1.629	0.000	0.000	0.000	0.357
1038723	UC	0.000	0.000	0.000	0.350	0.000	0.000	0.000	0.117
1038747	UC	0.000	0.000	0.000	1.777	0.298	0.000	0.000	0.814
1038755	UC	0.000	0.000	0.000	0.459	0.000	0.000	0.000	0.318
1038801	UC	0.000	0.000	0.000	3.661	0.222	0.000	0.000	1.383
1038821	UC	0.000	0.140	0.109	4.678	0.358	0.000	0.000	2.082
1038822	UC	0.000	0.000	0.000	2.956	0.291	0.000	0.000	0.964
1038824	UC	0.000	0.104	0.104	4.195	0.285	0.000	0.000	1.936
1038825	UC	0.000	0.000	0.000	1.125	0.000	0.000	0.000	0.145
1038827	UC	0.000	0.000	0.000	0.000	0.000	0.000	0.000	0.000
1038849	UC	0.000	0.219	0.141	5.845	0.531	0.000	0.000	2.573
1038862	UC	0.000	0.000	0.000	0.188	0.000	0.000	0.000	0.000
1038867	UC	0.000	0.000	0.000	0.348	0.000	0.000	0.000	0.152
1038891	UC	0.456	0.661	0.372	10.667	1.508	0.227	0.130	4.686
1038901	UC	0.493	1.070	0.701	20.151	3.087	0.351	0.000	8.822
1038909	UC	0.155	0.290	0.251	5.900	0.735	0.135	0.242	2.668
1038917	UC	0.092	0.130	0.091	4.902	0.378	0.000	0.082	2.088
1038920	UC	0.000	0.000	0.000	0.941	0.142	0.000	0.000	0.424
1038945	UC	0.000	0.077	0.064	3.053	0.268	0.000	0.000	1.358
1038947	UC	0.000	0.000	0.000	1.172	0.000	0.000	0.000	0.451
1038952	UC	0.000	0.000	0.000	0.139	0.000	0.000	0.000	0.000
1038980	UC	0.000	0.000	0.000	0.000	0.000	0.000	0.000	0.000

Table B7: Light-duty gasoline vehicle speciated VOC emissions. Values are reported as emission factors

TEST_ID	Test Cycle	1-M-4-n-propylbenzene	1-MCYpentene	1-buten-3-yne	1-butene	1-butyne	1-heptene	1-hexene	1-nonene
1038708	UC	0.119	0.000	0.000	1.087	0.000	0.000	0.000	0.000
1038723	UC	0.000	0.000	0.000	0.511	0.000	0.000	0.000	0.000
1038747	UC	0.000	0.000	0.000	0.505	0.000	0.000	0.000	0.000
1038755	UC	0.000	0.000	0.000	0.778	0.000	0.000	0.000	0.000
1038801	UC	0.000	0.141	0.000	1.130	0.000	0.000	0.145	0.000
1038821	UC	0.000	0.079	0.075	3.631	0.000	0.000	0.260	0.081
1038822	UC	0.000	0.124	0.000	2.126	0.000	0.000	0.152	0.000
1038824	UC	0.000	0.119	0.138	4.286	0.000	0.000	0.230	0.081
1038825	UC	0.000	0.000	0.000	0.608	0.000	0.000	0.000	0.000
1038827	UC	0.000	0.000	0.000	0.000	0.000	0.000	0.000	0.000
1038849	UC	0.000	0.000	0.121	5.855	0.000	0.000	0.343	0.114
1038862	UC	0.000	0.000	0.000	0.251	0.000	0.000	0.000	0.000
1038867	UC	0.000	0.000	0.000	0.343	0.000	0.000	0.000	0.000
1038891	UC	0.475	0.232	0.200	5.245	0.000	0.000	0.237	0.259
1038901	UC	0.000	0.429	0.255	14.861	0.000	0.110	2.758	0.476
1038909	UC	0.116	0.000	0.000	1.839	0.000	0.000	0.141	0.202
1038917	UC	0.000	0.000	0.139	4.590	0.000	0.000	0.204	0.068
1038920	UC	0.000	0.145	0.000	0.519	0.000	0.000	0.000	0.000
1038945	UC	0.000	0.000	0.000	3.626	0.000	0.000	0.213	0.093
1038947	UC	0.000	0.462	0.000	1.247	0.000	0.000	0.000	0.000
1038952	UC	0.000	0.000	0.000	0.201	0.000	0.000	0.000	0.000
1038980	UC	0.000	0.000	0.000	0.000	0.000	0.000	0.000	0.000

Table B7: Light-duty gasoline vehicle speciated VOC emissions. Values are reported as emission factors

TEST_ID	Test Cycle	1-octene	1-pentene	1-propyne	1a,2a,3b-triMCPentane	2,2,3-triMbutane	2,2,4-triMheptane	2,2,4-triMhexane	2,2,4-triMpentane
1038708	UC	0.000	0.150	0.000	0.225	0.000	0.000	0.000	3.866
1038723	UC	0.000	0.347	0.000	0.000	0.000	0.000	0.000	4.242
1038747	UC	0.000	0.000	0.000	0.000	0.000	0.000	0.000	6.095
1038755	UC	0.000	0.000	0.000	0.000	0.000	0.000	0.000	3.885
1038801	UC	0.000	0.290	0.000	0.203	0.000	0.000	0.000	10.407
1038821	UC	0.081	0.553	2.323	0.325	0.183	0.000	0.000	17.694
1038822	UC	0.000	0.354	0.000	0.228	0.181	0.000	0.000	7.678
1038824	UC	0.000	0.473	0.734	0.216	0.166	0.137	0.096	7.184
1038825	UC	0.000	0.000	0.000	0.000	0.000	0.000	0.000	5.102
1038827	UC	0.000	0.000	0.000	0.000	0.000	0.000	0.000	0.000
1038849	UC	0.098	0.702	1.415	0.376	0.117	0.000	0.000	20.614
1038862	UC	0.000	0.000	0.000	0.000	0.000	0.000	0.000	1.425
1038867	UC	0.000	0.114	0.000	0.000	0.000	0.000	0.000	3.838
1038891	UC	0.000	0.993	0.987	0.626	0.220	0.000	0.811	23.191
1038901	UC	0.641	3.024	4.382	1.172	0.000	0.576	0.000	53.376
1038909	UC	0.000	0.283	0.000	0.546	0.000	0.000	0.144	13.805
1038917	UC	0.000	0.436	0.000	0.259	0.125	0.000	0.000	7.935
1038920	UC	0.000	0.000	0.000	0.124	0.000	0.000	0.000	4.218
1038945	UC	0.000	0.360	0.609	0.173	0.082	0.000	0.068	6.033
1038947	UC	0.000	0.224	0.522	0.000	0.000	0.000	0.000	2.919
1038952	UC	0.000	0.000	0.000	0.000	0.000	0.000	0.000	1.155
1038980	UC	0.000	0.000	0.000	0.000	0.000	0.000	0.000	0.000

Table B7: Light-duty gasoline vehicle speciated VOC emissions. Values are reported as emission factors

TEST_ID	Test Cycle	2,2,5-triMheptane	2,2,5-triMhexane	2,2-diM-octane	2,2-diMbutane	2,2-diMhexane	2,2-diMpentane	2,2-diMpropene	2,3,3-triMpentane
1038708	UC	0.000	0.863	0.000	0.000	0.000	0.000	0.000	0.000
1038723	UC	0.000	0.913	0.000	0.356	0.000	0.188	0.000	0.000
1038747	UC	0.000	1.738	0.000	0.000	0.000	0.000	0.000	0.000
1038755	UC	0.000	0.904	0.000	0.228	0.000	0.000	0.000	0.000
1038801	UC	0.000	3.106	0.000	0.821	0.000	0.000	0.000	0.000
1038821	UC	0.000	4.392	0.132	0.813	0.000	0.000	0.000	0.000
1038822	UC	0.000	2.109	0.000	0.726	0.000	0.000	0.000	0.000
1038824	UC	0.000	2.607	0.123	0.318	0.083	0.152	0.000	0.000
1038825	UC	0.000	1.561	0.000	0.233	0.000	0.000	0.000	0.000
1038827	UC	0.000	0.000	0.000	0.000	0.000	0.000	0.000	0.000
1038849	UC	0.000	5.334	0.199	1.025	0.000	0.333	0.000	0.000
1038862	UC	0.000	0.347	0.000	0.000	0.000	0.678	0.000	0.000
1038867	UC	0.000	0.975	0.000	0.445	0.000	0.000	0.000	0.000
1038891	UC	0.000	7.874	0.131	0.685	0.000	0.000	0.000	0.000
1038901	UC	0.000	16.175	0.669	2.158	0.504	0.261	0.000	9.224
1038909	UC	0.000	5.564	0.328	2.524	0.000	0.247	0.000	0.000
1038917	UC	0.000	2.606	0.083	0.251	0.000	0.000	0.000	0.000
1038920	UC	0.000	1.180	0.000	0.405	0.000	0.000	0.000	0.000
1038945	UC	0.000	1.872	0.068	0.191	0.000	0.082	0.000	0.000
1038947	UC	0.000	0.760	0.000	0.383	0.000	0.000	0.000	0.000
1038952	UC	0.000	0.000	0.000	0.000	0.000	0.000	0.000	0.000
1038980	UC	0.000	0.000	0.000	0.000	0.000	0.000	0.000	0.000

Table B7: Light-duty gasoline vehicle speciated VOC emissions. Values are reported as emission factors.

TEST_ID	Test Cycle	2,3,4-triMpentane	2,3,5-triMhexane	2,3-diM-1-butene	2,3-diM-2-pentene	2,3-diM-octane	2,3-diMbutane	2,3-diMheptane	2,3-diMhexane
1038708	UC	0.839	0.127	0.000	0.150	0.000	1.369	0.000	0.508
1038723	UC	1.060	0.145	0.000	0.000	0.000	1.255	0.000	0.457
1038747	UC	1.821	0.316	0.000	0.000	0.000	1.234	0.000	0.831
1038755	UC	1.019	0.000	0.000	0.000	0.000	1.821	0.000	0.641
1038801	UC	3.189	0.324	0.000	0.000	0.000	2.891	0.000	1.298
1038821	UC	5.046	0.496	0.146	0.179	0.363	6.710	0.000	2.718
1038822	UC	2.473	0.334	0.152	0.000	0.000	2.410	0.000	1.263
1038824	UC	2.106	0.412	0.189	0.162	0.302	2.527	0.206	1.363
1038825	UC	1.546	0.000	0.000	0.000	0.000	1.711	0.000	0.438
1038827	UC	0.000	0.000	0.000	0.000	0.000	0.000	0.000	0.000
1038849	UC	5.782	0.614	0.196	0.196	0.530	7.271	0.000	3.193
1038862	UC	0.402	0.000	0.000	0.000	0.000	0.570	0.000	0.183
1038867	UC	1.000	0.163	0.000	0.000	0.000	1.451	0.000	0.605
1038891	UC	7.900	1.426	0.281	0.000	0.394	6.634	0.000	4.329
1038901	UC	15.952	2.928	0.806	0.440	1.907	18.183	0.112	1.783
1038909	UC	5.389	1.006	0.121	0.000	0.184	3.931	0.000	2.674
1038917	UC	2.274	0.415	0.150	0.000	0.069	2.426	0.000	1.248
1038920	UC	1.207	0.176	0.000	0.000	0.000	1.670	0.000	0.654
1038945	UC	1.520	0.284	0.147	0.120	0.216	1.900	0.000	0.828
1038947	UC	0.914	0.127	0.000	0.000	0.000	1.021	0.000	0.406
1038952	UC	0.298	0.000	0.000	0.000	0.000	0.487	0.000	0.130
1038980	UC	0.000	0.000	0.000	0.000	0.000	0.000	0.000	0.000

Table B7: Light-duty gasoline vehicle speciated VOC emissions. Values are reported as emission factors

TEST_ID	Test Cycle	2,3-diMpentane	2,4,4-triM-1-pentene	2,4,4-triM-2-pentene	2,4,4-triMhexane	2,4-diM-1-pentene	2,4-diM-2-pentene	2,4-diM-octane	2,4-diMheptane
1038708	UC	3.076	0.000	0.000	0.000	0.000	0.000	0.000	0.178
1038723	UC	2.460	0.000	0.000	0.000	0.000	0.000	0.000	0.000
1038747	UC	4.166	0.000	0.000	0.000	0.194	0.000	0.000	0.198
1038755	UC	3.706	0.000	0.000	0.000	0.000	0.000	0.000	0.000
1038801	UC	7.639	0.000	0.203	0.000	0.000	0.000	0.000	0.206
1038821	UC	15.519	0.081	0.000	0.182	0.000	0.000	0.396	0.347
1038822	UC	5.838	0.000	0.253	0.180	0.000	0.000	0.000	0.231
1038824	UC	6.763	0.189	0.000	0.151	0.068	0.000	0.233	0.247
1038825	UC	4.310	0.000	0.000	0.000	0.000	0.000	0.000	0.000
1038827	UC	0.000	0.000	0.000	0.000	0.000	0.000	0.000	0.000
1038849	UC	17.649	0.000	0.000	0.249	0.000	0.000	0.547	0.431
1038862	UC	1.337	0.000	0.000	0.000	0.000	0.000	0.000	0.000
1038867	UC	3.708	0.000	0.000	0.000	0.000	0.000	0.000	0.000
1038891	UC	20.590	0.389	0.691	0.482	0.173	0.216	0.175	0.768
1038901	UC	45.808	0.623	0.128	0.949	0.202	0.000	0.520	2.353
1038909	UC	11.079	0.000	0.707	0.349	0.000	0.000	0.123	0.575
1038917	UC	6.876	0.000	0.259	0.166	0.000	0.000	0.000	0.538
1038920	UC	3.127	0.000	0.173	0.000	0.000	0.148	0.000	0.126
1038945	UC	5.247	0.000	0.000	0.122	0.067	0.000	0.149	0.190
1038947	UC	2.418	0.000	0.000	0.000	0.000	0.000	0.000	0.000
1038952	UC	0.841	0.000	0.000	0.000	0.000	0.000	0.000	0.000
1038980	UC	0.000	0.000	0.000	0.000	0.000	0.000	0.000	0.000

Table B7: Light-duty gasoline vehicle speciated VOC emissions. Values are reported as emission factors

TEST_ID	Test Cycle	2,4-diMhexane	2,4-diMpentane	2,5-diM-octane	2,5-diMhexane	2,6-diM-octane	2,6-diMheptane	2-M-1,3-butadiene	2-M-1-butene
1038708	UC	0.585	1.671	0.000	0.661	0.000	0.127	0.194	0.350
1038723	UC	0.707	1.605	0.000	0.707	0.000	0.000	0.000	0.225
1038747	UC	1.346	2.024	0.000	1.108	0.000	0.198	0.000	0.350
1038755	UC	0.717	1.967	0.000	0.981	0.000	0.000	0.180	0.296
1038801	UC	2.432	4.146	0.000	2.255	0.000	0.000	0.563	0.609
1038821	UC	3.944	8.501	0.132	3.652	0.149	0.413	0.095	0.845
1038822	UC	1.855	3.229	0.000	1.726	0.000	0.129	0.688	0.785
1038824	UC	1.734	3.379	0.110	1.734	0.096	0.316	0.617	1.420
1038825	UC	1.097	2.450	0.000	1.045	0.000	0.000	0.148	0.253
1038827	UC	0.000	0.000	0.000	0.000	0.000	0.000	0.000	0.000
1038849	UC	4.732	9.306	0.215	4.264	0.166	0.839	0.301	2.098
1038862	UC	0.311	0.000	0.000	0.292	0.000	0.000	0.105	0.108
1038867	UC	0.791	1.633	0.000	0.721	0.000	0.000	0.000	0.229
1038891	UC	6.340	10.159	0.372	5.516	0.241	0.417	0.650	2.288
1038901	UC	12.763	23.562	0.427	11.553	0.595	1.984	0.943	3.299
1038909	UC	3.867	5.692	0.123	3.661	0.184	0.287	0.216	0.727
1038917	UC	1.858	3.850	0.083	1.803	0.000	0.152	0.489	1.239
1038920	UC	0.906	1.841	0.000	0.780	0.000	0.000	0.192	0.272
1038945	UC	1.248	2.827	0.068	1.221	0.068	0.217	0.634	1.013
1038947	UC	0.685	1.247	0.000	0.609	0.000	0.000	0.315	0.474
1038952	UC	0.224	0.561	0.000	0.242	0.000	0.000	0.089	0.092
1038980	UC	0.000	0.000	0.000	0.000	0.000	0.000	0.000	0.000

Table B7: Light-duty gasoline vehicle speciated VOC emissions. Values are reported as emission factors

TEST_ID	Test Cycle	2-M-1-pentene	2-M-2-butene	2-M-2-hexene	2-M-2-pentene	2-M-indan	2-M-octane	2-M-t-3-hexene	2-Mbutane
1038708	UC	0.125	0.425	0.000	0.150	0.000	0.000	0.000	7.830
1038723	UC	0.000	2.921	0.000	0.143	0.000	0.000	0.000	7.779
1038747	UC	0.000	0.544	0.000	0.194	0.000	0.000	0.000	5.242
1038755	UC	0.000	0.852	0.000	0.185	0.000	0.000	0.000	11.398
1038801	UC	0.203	1.014	0.000	0.406	0.000	0.000	0.000	18.504
1038821	UC	0.195	0.887	0.000	0.537	0.123	0.000	0.000	39.628
1038822	UC	0.278	1.164	0.000	0.456	0.000	0.000	0.152	14.086
1038824	UC	0.216	1.893	0.000	0.514	0.115	0.000	0.311	13.799
1038825	UC	0.000	0.481	0.000	0.228	0.000	0.000	0.000	8.371
1038827	UC	0.000	0.000	0.000	0.000	0.000	0.000	0.000	0.000
1038849	UC	0.261	1.050	0.000	0.588	0.169	0.000	0.000	43.841
1038862	UC	0.000	0.215	0.000	0.000	0.000	0.000	0.000	3.430
1038867	UC	0.000	0.297	0.000	0.137	0.000	0.000	0.000	9.066
1038891	UC	0.540	3.130	0.130	0.950	0.712	0.000	0.216	31.403
1038901	UC	0.989	2.473	0.000	1.649	1.278	0.000	0.385	91.325
1038909	UC	0.162	1.071	0.202	0.384	0.171	0.000	0.000	19.091
1038917	UC	0.245	1.757	0.000	0.572	0.180	0.000	0.068	10.480
1038920	UC	0.000	0.494	0.000	0.222	0.000	0.000	0.000	9.864
1038945	UC	0.160	1.306	0.000	0.387	0.113	0.000	0.000	8.049
1038947	UC	0.000	0.599	0.000	0.175	0.000	0.000	0.000	7.131
1038952	UC	0.000	0.183	0.000	0.000	0.000	0.000	0.000	3.110
1038980	UC	0.000	0.000	0.000	0.000	0.000	0.000	0.000	0.069

Table B7: Light-duty gasoline vehicle speciated VOC emissions. Values are reported as emission factors

TEST_ID	Test Cycle	2-Mheptane	2-Mhexane	2-Mnonane	2-Mpentane	2-Mpropene	2-butyne	3,3-diM-1-butene	3,3-diM-octane
1038708	UC	1.408	1.096	0.431	3.268	3.846	0.000	0.000	0.000
1038723	UC	0.645	2.001	0.352	3.012	1.430	0.000	0.000	0.000
1038747	UC	1.069	2.143	1.262	3.384	1.672	0.000	0.000	0.000
1038755	UC	0.679	1.967	0.376	4.439	1.668	0.000	0.000	0.000
1038801	UC	2.107	4.609	2.092	7.286	3.521	0.000	0.000	0.000
1038821	UC	3.519	7.869	2.678	16.994	9.926	0.000	0.098	0.165
1038822	UC	1.675	3.539	1.155	6.419	4.328	0.000	0.000	0.154
1038824	UC	1.720	3.808	1.629	6.467	7.693	0.000	0.068	0.151
1038825	UC	0.438	2.148	0.759	3.829	2.835	0.000	0.000	0.000
1038827	UC	0.000	0.000	0.000	0.000	0.000	0.000	0.000	0.000
1038849	UC	4.276	9.392	3.650	18.525	12.920	0.000	0.163	0.265
1038862	UC	0.238	0.660	0.000	1.932	0.539	0.000	0.000	0.000
1038867	UC	0.721	1.703	0.348	4.414	0.846	0.000	0.000	0.000
1038891	UC	5.318	11.165	4.664	17.306	13.039	0.000	0.194	0.482
1038901	UC	10.468	23.577	9.681	45.377	28.383	0.000	0.696	1.171
1038909	UC	3.888	7.373	2.542	11.241	5.129	0.000	0.000	0.307
1038917	UC	1.692	3.823	1.672	6.880	7.069	0.000	0.000	0.138
1038920	UC	0.755	1.841	0.551	4.184	1.211	0.000	0.000	0.000
1038945	UC	1.486	2.864	1.404	4.801	6.303	0.000	0.093	0.095
1038947	UC	0.584	1.502	0.455	2.528	2.768	0.000	0.000	0.000
1038952	UC	0.205	0.673	0.000	1.219	0.494	0.000	0.000	0.000
1038980	UC	0.000	0.000	0.000	0.205	0.000	0.000	0.000	0.000

Table B7: Light-duty gasoline vehicle speciated VOC emissions. Values are reported as emission factors

TEST_ID	Test Cycle	3,3-diMhexane	3,3-diMpentane	3,4-diM-1-pentene	3,4-diMhexane	3,5-diMheptane	3-E-2-pentene	3-Epentane	3-M-1-butene
1038708	UC	0.000	0.000	0.000	0.153	0.178	0.000	0.000	0.125
1038723	UC	0.000	0.104	0.000	0.104	0.166	0.000	0.000	0.123
1038747	UC	0.000	0.198	0.000	0.198	0.356	0.000	0.198	0.000
1038755	UC	0.000	0.000	0.000	0.189	0.000	0.000	0.000	0.000
1038801	UC	0.000	0.237	0.000	0.265	0.412	0.000	0.296	0.232
1038821	UC	0.000	0.382	0.146	0.595	0.826	0.000	0.481	0.472
1038822	UC	0.000	0.284	0.127	0.335	0.540	0.000	0.336	0.380
1038824	UC	0.000	0.345	0.081	0.385	0.577	0.000	0.331	0.487
1038825	UC	0.000	0.000	0.000	0.000	0.000	0.000	0.000	0.127
1038827	UC	0.000	0.000	0.000	0.000	0.000	0.000	0.000	0.000
1038849	UC	0.000	0.467	0.147	0.582	1.387	0.000	0.583	0.653
1038862	UC	0.000	0.000	0.000	0.000	0.000	0.000	0.000	0.000
1038867	UC	0.000	0.140	0.000	0.186	0.163	0.000	0.140	0.114
1038891	UC	0.000	0.000	0.000	1.121	1.930	0.194	0.925	0.863
1038901	UC	0.000	2.287	0.549	2.817	3.575	0.110	2.274	2.657
1038909	UC	0.185	0.454	0.141	0.926	1.314	0.000	0.598	0.303
1038917	UC	0.125	0.250	0.068	0.347	0.609	0.000	0.320	0.558
1038920	UC	0.000	0.000	0.000	0.226	0.201	0.000	0.151	0.124
1038945	UC	0.000	0.177	0.000	0.217	0.406	0.000	0.231	0.373
1038947	UC	0.000	0.153	0.000	0.000	0.152	0.000	0.127	0.175
1038952	UC	0.000	0.000	0.000	0.000	0.000	0.000	0.000	0.000
1038980	UC	0.000	0.000	0.000	0.000	0.000	0.000	0.000	0.000

Table B7: Light-duty gasoline vehicle speciated VOC emissions. Values are reported as emission factors

TEST_ID	Test Cycle	3-M-1-hexene	3-M-1-pentene	3-M-c-2-hexene	3-M-c-2-pentene	3-M-octane	3-M-t-2-pentene	3-M-t-3-hexene	3-MCYpentene
1038708	UC	0.000	0.000	0.000	0.000	0.304	0.125	0.000	0.000
1038723	UC	0.000	0.000	0.000	0.102	0.166	0.000	0.000	0.000
1038747	UC	0.000	0.000	0.000	0.000	0.632	0.000	0.000	0.000
1038755	UC	0.000	0.000	0.000	0.222	0.226	0.000	0.000	0.000
1038801	UC	0.000	0.000	0.000	0.145	0.765	0.000	0.000	0.000
1038821	UC	0.000	0.342	0.000	0.374	1.807	0.000	0.000	0.381
1038822	UC	0.000	0.152	0.000	0.202	0.951	0.127	0.000	0.000
1038824	UC	0.000	0.297	0.000	1.109	0.934	0.000	0.068	0.409
1038825	UC	0.000	0.000	0.000	0.000	0.154	0.000	0.000	0.000
1038827	UC	0.000	0.000	0.000	0.000	0.000	0.000	0.000	0.000
1038849	UC	0.000	0.457	0.000	0.392	2.198	0.000	0.000	0.446
1038862	UC	0.000	0.000	0.000	0.000	0.000	0.000	0.000	0.000
1038867	UC	0.000	0.114	0.000	0.000	0.302	0.000	0.000	0.000
1038891	UC	0.000	0.237	0.302	0.453	3.071	0.281	0.108	0.000
1038901	UC	0.513	0.751	0.000	5.612	5.754	0.000	0.165	1.055
1038909	UC	0.000	0.000	0.141	0.323	2.176	0.141	0.000	0.000
1038917	UC	0.000	0.123	0.123	0.163	1.010	0.191	0.000	0.000
1038920	UC	0.000	0.000	0.000	0.000	0.402	0.000	0.000	0.000
1038945	UC	0.000	0.253	0.000	0.280	0.596	0.000	0.000	0.312
1038947	UC	0.000	0.000	0.000	0.125	0.279	0.000	0.000	0.146
1038952	UC	0.000	0.000	0.000	0.000	0.000	0.000	0.000	0.000
1038980	UC	0.000	0.000	0.000	0.000	0.000	0.000	0.000	0.000

Table B7: Light-duty gasoline vehicle speciated VOC emissions. Values are reported as emission factors

TEST_ID	Test Cycle	3-Mheptane	3-Mhexane	3-Mpentane	4-M-1-pentene	4-M-c-2-pentene	4-M-indan	4-M-octane	4-M-t-2-hexene
1038708	UC	0.763	1.721	2.293	0.000	0.000	0.000	0.406	0.000
1038723	UC	0.769	1.543	2.071	0.000	0.000	0.000	0.311	0.000
1038747	UC	1.227	2.222	2.229	0.000	0.000	0.000	1.027	0.000
1038755	UC	0.905	1.967	2.960	0.000	0.000	0.000	0.301	0.000
1038801	UC	2.452	4.846	4.851	0.000	0.000	0.000	1.879	0.000
1038821	UC	4.720	8.958	11.499	0.163	0.000	0.000	2.477	0.000
1038822	UC	1.804	3.771	4.267	0.127	0.000	0.000	1.363	0.000
1038824	UC	2.271	3.682	4.326	0.108	0.000	0.000	1.305	0.108
1038825	UC	0.413	2.321	2.326	0.000	0.000	0.000	0.283	0.000
1038827	UC	0.000	0.000	0.000	0.000	0.000	0.000	0.000	0.000
1038849	UC	5.699	9.938	12.324	0.229	0.000	0.000	3.137	0.000
1038862	UC	0.292	0.000	1.011	0.000	0.000	0.000	0.128	0.000
1038867	UC	0.954	1.796	2.909	0.000	0.000	0.000	0.464	0.000
1038891	UC	6.351	11.908	11.882	0.216	0.000	0.163	4.255	0.173
1038901	UC	14.207	24.591	30.952	0.971	0.000	0.259	7.706	0.440
1038909	UC	4.464	7.765	7.803	0.182	0.000	0.000	3.038	0.000
1038917	UC	1.927	4.059	4.709	0.000	0.000	0.000	1.412	0.000
1038920	UC	0.855	2.431	2.674	0.000	0.000	0.000	0.603	0.000
1038945	UC	1.781	2.923	3.680	0.080	0.000	0.000	0.772	0.000
1038947	UC	0.787	1.502	2.271	0.000	0.000	0.000	0.329	0.000
1038952	UC	0.224	0.561	0.862	0.000	0.000	0.000	0.093	0.000
1038980	UC	0.000	0.000	0.171	0.000	0.000	0.000	0.000	0.000

Table B7: Light-duty gasoline vehicle speciated VOC emissions. Values are reported as emission factors

TEST_ID	Test Cycle	4-M-t-2-pentene	4-Mheptane	5-M-indan	CYhexane	CYhexene	CYpentane	CYpentene	ECYhexane
1038708	UC	0.000	0.229	0.000	0.400	0.000	0.200	0.000	0.000
1038723	UC	0.000	0.146	0.000	0.531	0.000	0.286	0.000	0.000
1038747	UC	0.000	0.435	0.000	0.855	0.000	0.272	0.000	0.000
1038755	UC	0.000	0.264	0.000	0.741	0.000	0.445	0.000	0.000
1038801	UC	0.000	0.531	0.000	0.000	0.000	0.551	0.225	0.174
1038821	UC	0.179	1.411	0.107	2.886	0.159	1.630	0.458	0.277
1038822	UC	0.000	0.644	0.143	0.000	0.148	0.557	0.344	0.253
1038824	UC	0.149	0.661	0.115	1.351	0.132	0.595	1.103	0.216
1038825	UC	0.127	0.181	0.000	0.000	0.000	0.228	0.148	0.000
1038827	UC	0.000	0.000	0.000	0.000	0.000	0.000	0.000	0.000
1038849	UC	0.180	1.696	0.154	3.426	0.175	1.801	0.873	0.359
1038862	UC	0.000	0.000	0.000	0.000	0.000	0.126	0.000	0.000
1038867	UC	0.000	0.302	0.000	0.617	0.000	0.343	0.000	0.000
1038891	UC	0.950	2.110	0.692	0.000	0.337	1.490	0.524	0.648
1038901	UC	1.282	4.200	1.175	8.523	1.002	5.532	1.726	1.099
1038909	UC	0.000	1.604	0.190	2.526	0.099	0.828	0.393	0.606
1038917	UC	0.123	0.666	0.180	1.199	0.106	0.558	1.363	0.245
1038920	UC	0.000	0.327	0.000	0.000	0.000	0.321	0.144	0.000
1038945	UC	0.107	0.434	0.126	0.813	0.078	0.373	0.919	0.147
1038947	UC	0.000	0.228	0.000	0.549	0.000	0.274	0.145	0.000
1038952	UC	0.000	0.000	0.000	0.000	0.000	0.110	0.000	0.000
1038980	UC	0.000	0.000	0.000	0.000	0.000	0.000	0.000	0.000

Table B7: Light-duty gasoline vehicle speciated VOC emissions. Values are reported as emission factors

TEST_ID	Test Cycle	ECYpenta ne	Ebenzen e	Ethane	M-tert- butyl- ether	MCYhexa ne	MCYpent ane	MEketon e	Methane
1038708	UC	0.000	1.559	7.172	0.000	0.649	1.954	0.000	0.000
1038723	UC	0.000	0.599	3.470	0.000	0.694	1.573	0.642	0.000
1038747	UC	0.000	2.207	2.487	0.000	0.855	2.022	1.381	0.000
1038755	UC	0.000	0.947	3.932	0.000	0.926	2.594	0.000	0.000
1038801	UC	0.000	4.165	6.280	0.000	1.362	4.147	0.557	0.000
1038821	UC	0.000	6.223	47.132	0.000	4.576	10.083	0.734	0.000
1038822	UC	0.000	3.233	9.540	0.000	1.746	3.594	0.355	0.000
1038824	UC	0.000	5.638	12.453	0.000	1.879	4.028	0.413	0.000
1038825	UC	0.000	1.341	6.426	0.000	0.563	2.025	0.611	0.000
1038827	UC	0.000	0.000	0.000	0.000	0.000	0.000	0.251	0.000
1038849	UC	0.000	7.720	49.029	0.000	4.963	10.575	0.601	0.000
1038862	UC	0.000	0.272	1.367	0.000	0.323	0.826	0.000	0.000
1038867	UC	0.000	0.757	2.105	0.000	0.868	2.011	0.482	0.000
1038891	UC	0.216	11.968	14.288	0.000	4.954	11.573	0.611	0.000
1038901	UC	0.000	22.942	46.498	0.000	11.351	27.405	1.601	0.000
1038909	UC	0.141	6.589	8.974	0.000	4.385	6.154	0.958	0.000
1038917	UC	0.000	6.706	12.291	0.000	1.553	4.031	0.286	0.000
1038920	UC	0.000	1.333	1.748	0.000	0.964	1.977	0.948	0.000
1038945	UC	0.000	4.518	11.937	0.000	1.360	3.069	0.375	0.000
1038947	UC	0.000	1.180	7.900	0.000	0.848	1.521	0.694	0.000
1038952	UC	0.000	0.243	1.106	0.000	0.183	0.641	0.214	0.000
1038980	UC	0.000	0.000	11.990	0.000	0.000	0.000	0.346	0.000

Table B7: Light-duty gasoline vehicle speciated VOC emissions. Values are reported as emission factors

TEST_ID	Test Cycle	Mpropane	acetaldehyde	acetone	acrolein	benzaldehyde	benzene	butyraldehyde	c-1,2-dimethylcyclohexane
1038708	UC	0.122	4.170	2.103	0.301	0.000	15.102	0.000	0.000
1038723	UC	0.338	5.323	4.768	0.275	0.000	2.218	0.275	0.000
1038747	UC	0.242	9.383	3.111	0.000	0.000	5.178	0.000	0.000
1038755	UC	0.230	0.000	0.000	0.000	0.000	2.855	0.000	0.000
1038801	UC	0.240	5.074	2.559	0.000	0.512	12.312	0.078	0.232
1038821	UC	0.858	11.493	4.795	0.390	1.770	36.970	0.387	0.211
1038822	UC	0.341	7.452	6.012	0.000	0.815	14.651	0.337	0.304
1038824	UC	0.265	9.471	2.608	0.000	0.156	18.005	0.215	0.149
1038825	UC	0.052	3.698	2.967	0.000	0.268	16.624	0.173	0.000
1038827	UC	0.000	5.729	2.008	0.000	0.980	0.000	0.328	0.000
1038849	UC	0.868	13.258	3.972	0.316	1.809	47.779	0.316	0.245
1038862	UC	0.186	1.477	0.000	0.000	0.000	1.696	0.000	0.000
1038867	UC	0.307	4.267	2.104	0.000	0.000	3.279	0.000	0.000
1038891	UC	0.134	15.107	7.465	1.892	1.900	31.843	0.453	1.015
1038901	UC	0.626	43.443	11.025	4.659	5.786	45.923	1.047	0.806
1038909	UC	0.167	6.004	4.027	0.000	0.654	27.540	0.000	0.687
1038917	UC	0.183	6.927	1.592	0.000	0.310	19.443	0.000	0.341
1038920	UC	0.154	3.258	4.103	0.000	0.000	5.796	0.000	0.124
1038945	UC	0.110	7.036	1.269	0.000	0.529	15.535	0.000	0.093
1038947	UC	0.155	5.584	2.055	0.000	0.000	6.959	0.000	0.000
1038952	UC	0.000	0.552	0.271	0.000	0.000	1.634	0.000	0.000
1038980	UC	0.174	0.351	0.401	0.000	0.000	0.156	0.000	0.000

Table B7: Light-duty gasoline vehicle speciated VOC emissions. Values are reported as emission factors

TEST_ID	Test Cycle	c-1,3-diMcyhexane	c-1,3-diMcyheptane	c-1-M-3-ECYpentane	c-2-butene	c-2-heptene	c-2-hexene	c-2-octene	c-2-pentene
1038708	UC	0.175	0.375	0.000	0.300	0.000	0.000	0.000	0.000
1038723	UC	0.163	0.388	0.000	0.306	0.000	0.000	0.000	0.163
1038747	UC	0.272	0.505	0.000	0.272	0.000	0.000	0.000	0.000
1038755	UC	0.222	0.593	0.000	0.408	0.000	0.000	0.000	0.259
1038801	UC	0.493	0.811	0.000	0.464	0.000	0.000	0.000	0.232
1038821	UC	1.321	2.566	0.000	1.512	0.098	0.146	0.000	0.537
1038822	UC	0.607	0.987	0.000	0.911	0.000	0.000	0.000	0.304
1038824	UC	0.608	1.109	0.000	2.812	0.081	0.149	0.000	0.487
1038825	UC	0.127	0.329	0.000	0.253	0.000	0.000	0.000	0.000
1038827	UC	0.000	0.000	0.000	0.000	0.000	0.000	0.000	0.000
1038849	UC	1.507	2.807	0.000	2.634	0.114	0.180	0.000	0.637
1038862	UC	0.090	0.180	0.000	0.108	0.000	0.000	0.000	0.000
1038867	UC	0.251	0.503	0.000	0.183	0.000	0.000	0.000	0.137
1038891	UC	1.964	3.087	0.000	2.094	0.302	0.000	0.000	0.756
1038901	UC	3.819	7.268	0.000	6.037	0.568	0.696	0.000	2.089
1038909	UC	1.637	1.758	0.000	1.172	0.121	0.000	0.000	0.283
1038917	UC	0.640	1.008	0.000	2.942	0.000	0.409	0.000	0.422
1038920	UC	0.297	0.445	0.000	0.247	0.000	0.148	0.000	0.124
1038945	UC	0.413	0.773	0.000	2.440	0.067	0.133	0.000	0.347
1038947	UC	0.224	0.424	0.000	0.499	0.000	0.000	0.000	0.175
1038952	UC	0.000	0.183	0.000	0.110	0.000	0.000	0.973	0.000
1038980	UC	0.000	0.000	0.000	0.000	0.000	0.000	0.000	0.000

Table B7: Light-duty gasoline vehicle speciated VOC emissions. Values are reported as emission factors

TEST_ID	Test Cycle	c-3-hexene	crotonald ehdye	ethanol	ethene	ethyne	formalde hyde	hexanal	indan
1038708	UC	0.000	0.000	0.000	21.147	1.136	84.812	0.000	0.164
1038723	UC	0.000	0.000	0.000	9.763	0.000	6.744	0.000	0.000
1038747	UC	0.000	0.000	0.000	8.398	0.686	5.355	0.000	0.328
1038755	UC	0.000	0.000	0.000	9.931	0.172	0.000	0.000	0.000
1038801	UC	0.203	0.000	0.000	18.181	3.738	5.840	0.000	0.326
1038821	UC	0.000	0.000	27.114	71.351	25.969	12.424	0.000	0.624
1038822	UC	0.228	0.000	0.000	37.587	10.736	12.939	0.000	0.403
1038824	UC	0.000	0.000	15.875	50.473	5.534	4.378	0.000	0.696
1038825	UC	0.000	0.000	0.000	15.464	0.798	4.543	0.000	0.000
1038827	UC	0.000	0.000	0.000	0.000	0.000	7.270	0.000	0.000
1038849	UC	0.000	0.000	23.896	86.189	12.159	12.208	0.000	1.289
1038862	UC	0.000	0.000	0.000	4.883	0.100	0.000	0.000	0.000
1038867	UC	0.000	0.000	0.000	5.241	0.297	2.510	0.000	0.000
1038891	UC	0.302	0.000	76.290	63.207	14.215	49.864	0.000	1.899
1038901	UC	0.000	0.629	46.311	153.960	34.634	23.473	0.000	3.312
1038909	UC	0.121	0.000	14.464	38.232	3.432	6.821	0.000	1.410
1038917	UC	0.000	0.000	13.232	52.518	4.197	5.069	0.000	0.956
1038920	UC	0.000	0.000	0.000	8.476	0.459	9.974	0.000	0.162
1038945	UC	0.000	0.000	9.523	45.039	5.147	5.070	0.000	0.562
1038947	UC	0.000	0.000	0.000	23.840	9.328	22.923	0.000	0.140
1038952	UC	0.000	0.000	0.000	4.577	0.221	0.869	0.000	0.000
1038980	UC	0.000	0.000	0.000	1.111	0.000	1.996	0.000	0.000

Table B7: Light-duty gasoline vehicle speciated VOC emissions. Values are reported as emission factors

TEST_ID	Test Cycle	m-tolualdehyde	m-xylene	methacrolein	methanol	n-butane	n-decane	n-dodecane	n-heptane
1038708	UC	0.000	3.292	0.000	21.920	0.502	0.000	0.000	0.714
1038723	UC	0.000	1.565	0.550	0.000	0.508	0.000	0.000	0.917
1038747	UC	0.000	6.771	1.496	0.000	0.403	0.276	0.000	1.508
1038755	UC	0.000	1.998	0.000	0.000	0.883	0.000	0.000	1.135
1038801	UC	0.000	10.063	0.000	0.000	1.711	0.265	0.000	3.129
1038821	UC	0.000	16.707	0.633	0.000	3.507	0.314	0.000	5.495
1038822	UC	0.000	8.333	0.493	0.000	2.229	0.257	0.000	2.299
1038824	UC	0.000	12.121	0.000	0.000	0.840	0.315	0.067	2.456
1038825	UC	0.000	4.247	0.710	0.000	0.824	0.000	0.000	1.247
1038827	UC	0.000	0.000	0.000	0.000	0.000	0.000	0.000	0.000
1038849	UC	0.314	20.373	0.854	0.000	3.392	0.739	0.000	6.385
1038862	UC	0.000	0.714	0.000	0.000	0.223	0.000	0.000	0.403
1038867	UC	0.000	2.320	0.388	0.000	0.726	0.000	0.000	1.166
1038891	UC	0.350	29.224	1.443	0.000	2.818	0.985	0.153	8.138
1038901	UC	2.915	52.646	4.778	14.967	4.962	2.287	0.278	15.682
1038909	UC	0.000	17.367	0.488	0.000	0.375	0.656	0.000	5.579
1038917	UC	0.000	13.759	0.357	0.000	1.495	0.263	0.000	2.794
1038920	UC	0.000	3.984	0.193	0.000	5.466	0.125	0.000	1.311
1038945	UC	0.000	9.630	0.408	0.000	0.428	0.162	0.000	1.864
1038947	UC	0.000	3.572	0.503	0.000	0.749	0.152	0.000	0.891
1038952	UC	0.000	0.624	0.000	0.000	0.436	0.634	0.000	0.336
1038980	UC	0.000	0.000	0.000	0.000	2.061	0.000	0.000	0.000

Table B7: Light-duty gasoline vehicle speciated VOC emissions. Values are reported as emission factors

TEST_ID	Test Cycle	n-hexane	n-nonane	n-octane	n-pentane	n-pentylbenzene	n-propylbenzene	n-undecane	naphthalene
1038708	UC	2.344	0.228	0.407	3.069	0.000	0.119	0.304	0.000
1038723	UC	2.029	0.208	0.416	2.595	0.000	0.000	0.000	0.000
1038747	UC	2.667	0.474	0.950	2.614	0.000	0.370	0.000	0.000
1038755	UC	2.960	0.000	0.453	4.742	0.000	0.000	0.000	0.000
1038801	UC	5.000	0.383	1.606	6.185	0.000	0.359	0.000	0.488
1038821	UC	11.449	1.128	2.546	16.511	0.000	0.681	0.115	0.645
1038822	UC	4.164	0.514	1.237	4.999	0.000	0.386	0.128	0.732
1038824	UC	4.728	0.591	1.308	4.922	0.000	0.528	0.137	0.173
1038825	UC	2.570	0.000	0.284	2.913	0.000	0.000	0.000	0.000
1038827	UC	0.000	0.000	0.000	0.000	0.000	0.000	0.000	0.000
1038849	UC	12.668	1.605	3.397	18.921	0.000	0.980	0.199	0.879
1038862	UC	0.974	0.000	0.164	1.163	0.000	0.000	0.000	0.000
1038867	UC	2.247	0.163	0.512	3.620	0.000	0.000	0.000	0.000
1038891	UC	13.305	1.908	4.439	11.560	0.187	2.322	0.612	0.671
1038901	UC	31.619	3.862	8.349	32.412	0.282	4.268	1.621	0.285
1038909	UC	6.493	1.273	2.921	6.177	0.000	1.135	0.184	0.764
1038917	UC	4.956	0.567	1.331	4.633	0.000	0.584	0.166	0.149
1038920	UC	2.716	0.301	0.604	3.635	0.000	0.165	0.000	0.000
1038945	UC	3.470	0.393	0.909	3.531	0.000	0.406	0.149	0.073
1038947	UC	1.728	0.253	0.432	2.412	0.000	0.000	0.000	0.670
1038952	UC	0.838	0.000	0.130	1.017	0.000	0.000	0.000	0.000
1038980	UC	0.069	0.000	0.000	0.000	0.000	0.000	0.000	0.000

Table B7: Light-duty gasoline vehicle speciated VOC emissions. Values are reported as emission factors

TEST_ID	Test Cycle	o-xylene	p-xylene	propane	propene	propionaldehyde	styrene	t-1,2-dimethylpentane	t-1,3-dimethylhexane
1038708	UC	2.280	1.734	0.515	8.096	0.370	0.787	0.250	0.175
1038723	UC	0.947	0.792	0.764	3.452	0.496	0.095	0.266	0.102
1038747	UC	3.274	3.471	0.504	3.771	0.000	0.253	0.505	0.194
1038755	UC	1.227	1.017	0.454	4.484	0.000	0.000	0.408	0.185
1038801	UC	5.603	5.082	0.416	8.711	0.550	1.007	0.695	0.377
1038821	UC	9.894	8.382	1.383	28.605	0.704	2.211	1.837	0.952
1038822	UC	4.558	4.166	0.637	12.554	0.705	0.799	0.810	0.456
1038824	UC	6.545	6.084	0.565	24.202	0.458	1.006	0.825	0.406
1038825	UC	2.147	2.123	0.780	6.647	0.127	0.838	0.253	0.000
1038827	UC	0.000	0.000	0.000	0.000	0.328	0.000	0.000	0.000
1038849	UC	11.670	10.202	1.660	35.767	0.601	1.860	2.070	1.071
1038862	UC	0.374	0.397	0.435	1.580	0.000	0.000	0.000	0.000
1038867	UC	1.081	1.160	0.295	2.590	0.115	0.000	0.366	0.160
1038891	UC	16.543	14.639	0.701	34.334	1.345	2.284	2.612	1.187
1038901	UC	30.802	26.291	1.727	89.518	2.058	5.859	5.123	2.707
1038909	UC	9.760	8.684	0.466	14.453	0.469	0.844	1.536	0.970
1038917	UC	8.085	6.873	0.456	24.223	0.453	0.898	0.872	0.436
1038920	UC	1.824	1.949	0.000	3.262	0.000	0.161	0.395	0.124
1038945	UC	5.433	4.844	0.363	19.903	0.519	0.894	0.573	0.280
1038947	UC	2.124	1.818	0.601	7.706	0.366	0.324	0.299	0.200
1038952	UC	0.346	0.312	0.058	1.483	0.040	0.000	0.000	0.000
1038980	UC	0.000	0.000	0.951	0.000	0.077	0.000	0.000	0.000

Table B7: Light-duty gasoline vehicle speciated VOC emissions. Values are reported as emission factors

TEST_ID	Test Cycle	t-1,3-diMCPentane	t-1,3-pentadiene	t-1,4-diMCPentane	t-1-M-3-ECYPentane	t-2-butene	t-2-heptene	t-2-hexene	t-2-octene
1038708	UC	0.300	0.000	0.125	0.150	0.375	0.000	0.000	0.000
1038723	UC	0.531	0.000	0.000	0.123	0.388	0.000	0.000	0.000
1038747	UC	0.544	0.000	0.000	0.272	0.350	0.000	0.000	0.000
1038755	UC	0.482	0.000	0.000	0.000	0.704	0.000	0.000	0.000
1038801	UC	0.898	0.000	0.203	0.348	0.637	0.000	0.000	0.145
1038821	UC	2.250	0.000	0.309	0.569	1.935	0.000	0.309	0.146
1038822	UC	1.038	0.148	0.228	0.405	1.088	0.000	0.000	0.177
1038824	UC	0.973	0.092	0.216	0.406	2.907	0.068	0.257	0.135
1038825	UC	0.355	0.000	0.000	0.000	0.431	0.000	0.000	0.000
1038827	UC	0.000	0.000	0.000	0.000	0.000	0.000	0.000	0.000
1038849	UC	2.473	0.000	0.376	0.637	3.304	0.000	0.343	0.000
1038862	UC	0.197	0.000	0.000	0.000	0.162	0.000	0.000	0.000
1038867	UC	0.411	0.000	0.114	0.160	0.229	0.000	0.000	0.000
1038891	UC	3.346	0.168	0.626	1.252	2.871	0.216	0.583	0.367
1038901	UC	6.262	0.303	1.568	2.558	7.810	0.458	1.338	0.733
1038909	UC	1.738	0.000	0.667	0.788	1.486	0.000	0.222	0.263
1038917	UC	1.117	0.066	0.218	0.422	2.602	0.068	0.272	0.136
1038920	UC	0.470	0.000	0.148	0.173	0.371	0.000	0.124	0.000
1038945	UC	0.680	0.091	0.160	0.280	2.173	0.000	0.200	0.093
1038947	UC	0.349	0.969	0.000	0.150	0.574	0.000	0.000	0.000
1038952	UC	0.146	0.000	0.000	0.000	0.146	0.000	0.000	0.000
1038980	UC	0.000	0.000	0.000	0.000	0.000	0.000	0.000	0.000

Table B7: Light-duty gasoline vehicle speciated VOC emissions. Values are reported as emission factors

TEST_ID	Test Cycle	t-2-pentene	t-3-heptene	t-3-hexene	t-4-octene	toluene	valeraldehyde
1038708	UC	0.200	0.000	0.000	0.000	9.186	0.000
1038723	UC	0.286	0.000	0.000	0.000	4.408	0.000
1038747	UC	0.233	0.000	0.233	0.000	11.522	0.000
1038755	UC	0.371	0.000	0.000	0.000	5.912	0.000
1038801	UC	0.435	0.000	0.000	0.000	19.012	0.000
1038821	UC	0.976	0.000	0.195	0.000	39.795	0.365
1038822	UC	0.506	0.000	0.127	0.228	18.177	0.000
1038824	UC	0.825	0.162	0.162	0.000	25.779	0.000
1038825	UC	0.177	0.000	0.000	0.000	11.136	0.000
1038827	UC	0.000	0.000	0.000	0.000	0.000	0.000
1038849	UC	1.013	0.000	0.212	0.000	47.360	0.000
1038862	UC	0.108	0.000	0.000	0.000	2.456	0.000
1038867	UC	0.251	0.000	0.000	0.000	5.339	0.000
1038891	UC	1.317	0.389	0.000	0.194	54.228	0.000
1038901	UC	3.665	0.605	1.008	0.000	102.702	0.000
1038909	UC	0.445	0.000	0.000	0.000	35.452	0.000
1038917	UC	0.708	0.163	0.163	0.109	29.863	0.000
1038920	UC	0.222	0.000	0.000	0.000	7.762	0.000
1038945	UC	0.547	0.000	0.120	0.000	21.965	0.000
1038947	UC	0.324	0.000	0.000	0.000	8.262	0.000
1038952	UC	0.110	0.000	0.000	0.000	1.891	0.000
1038980	UC	0.000	0.000	0.000	0.000	0.232	0.000

Table B7: Light-duty gasoline vehicle speciated VOC emissions. Values are reported as emission factors

Appendix C
Supplementary Information for Chapter 6

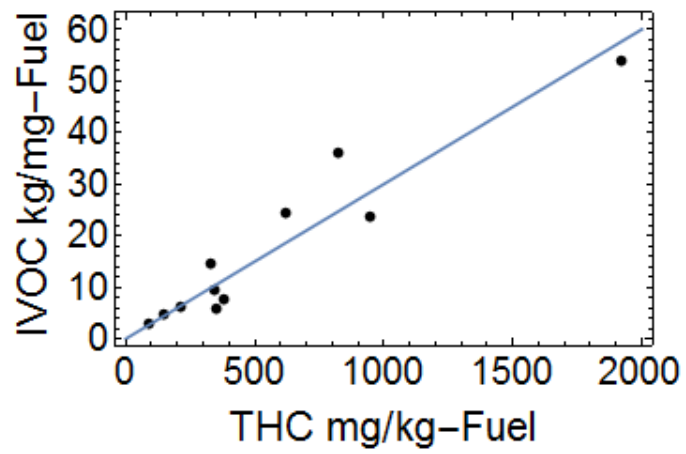


Figure C1. Correlation of IVOC and THC emissions. The best fit line has a slope of 0.03 with an R^2 of 0.89.

Table C1. Table of IVOC composition by volatility.

Test ID	Vehicle ID	Carbon # Bin	Emission factor in mg/kg-Fuel							
			12	13	14	15	16	17	18	
1038867	29	Aliphatic	0.95	0.52	0.52	0.13	0.04	<DL	<DL	<DL
		SRA	0.85	0.31	0.04	0.03	0.04	<DL	<DL	<DL
		Polar	2.16	0.34	0.09	0.02	0.03	0.03	0.10	0.02
1038920	21	Aliphatic	0.1848	0.01386	0.01134	<DL	<DL	<DL	<DL	<DL
		SRA	0.61	<DL	<DL	<DL	<DL	<DL	<DL	<DL
		Polar	0.255	0.03876	0.01479	<DL	<DL	<DL	<DL	<DL
1038862	28	Aliphatic	0.31	0.39	0.23	0.07	0.05	0.01	<DL	<DL
		SRA	0.46	0.18	0.07	<DL	<DL	<DL	<DL	<DL
		Polar	0.87	0.15	0.09	0.01	0.02	0.06	0.08	0.06
1038864	5	Aliphatic	0.44	0.41	0.20	0.00	0.04	<DL	<DL	<DL
		SRA	1.26	0.26	<DL	<DL	<DL	<DL	<DL	<DL
		Polar	1.44	0.64	0.04	0.05	0.02	0.03	0.04	0.03
1038801	35	Aliphatic	1.04	0.35	0.13	<DL	<DL	<DL	<DL	<DL
		SRA	2.33	0.54	<DL	<DL	<DL	<DL	<DL	<DL
		Polar	2.33	0.72	0.03	0.05	0.01	0.02	0.06	<DL
1038827	27	Aliphatic	6.96	3.08	1.09	0.12	0.05	<DL	<DL	<DL
		SRA	11.52	2.85	0.10	0.01	0.03	<DL	<DL	<DL
		Polar	2.90	1.67	0.33	0.09	0.05	0.05	0.11	<DL
1038823	37	Aliphatic	3.78	4.00	1.98	0.14	0.08	<DL	<DL	<DL
		SRA	9.10	2.84	<DL	<DL	<DL	<DL	<DL	<DL
		Polar	0.94	1.14	0.21	0.26	0.02	0.01	0.02	<DL

Table C1. Table of IVOC composition by volatility.

			Emission factor in mg/kg-Fuel							
1038945	4									
		Aliphatic	2.03	1.51	0.53	0.12	0.03	<DL	<DL	<DL
		SRA	3.74	0.84	0.02	<DL	<DL	<DL	<DL	<DL
		Polar	3.11	2.21	0.03	0.18	0.04	0.03	0.11	<DL
1038848	18									
		Aliphatic	3.16	2.67	1.13	0.22	0.32	<DL	<DL	<DL
		SRA	5.45	2.35	<DL	<DL	<DL	<DL	<DL	<DL
		Polar	4.42	2.82	0.40	0.23	0.07	0.22	0.14	0.19
1038825	38									
		Aliphatic	0.77	0.64	0.28	0.07	0.05	<DL	<DL	<DL
		SRA	1.09	0.31	<DL	<DL	<DL	<DL	<DL	<DL
		Polar	1.37	0.53	0.21	0.20	0.06	<DL	<DL	<DL
1038891	9									
		Aliphatic	4.53	3.70	4.56	2.87	0.88	0.06	<DL	<DL
		SRA	4.08	1.43	1.02	0.05	0.42	0.68	0.02	<DL
		Polar	6.61	3.84	1.05	0.94	0.15	0.23	0.18	<DL
1038901	14									
		Aliphatic	5.87	8.24	4.19	1.33	0.24	0.11	0.02	<DL
		SRA	12.19	7.86	0.62	0.00	0.64	1.29	0.30	<DL
		Polar	1.88	6.49	1.37	1.04	0.11	0.05	0.27	<DL

Appendix D
Supporting Information for Chapter 7
Reducing Secondary Organic Aerosol Formation from Gasoline Vehicle Exhaust

This supporting Information includes methods used to characterize the primary emissions, determine the SOA production and predict SOA production of measured SOA precursors. This supporting information also includes 6 figures and 2 tables involved in the discussions.

Test Fleet, Fuel and Test Cycle in this Chapter

Tailpipe emissions from on-road gasoline vehicles and their SOA production have been investigated during dynamometer testing at the California Air Resources Board's (CARB) Haggen-Smit Laboratory. The test fleet consisted of 60 on-road gasoline vehicles, spanning a wide range of model years and aftertreatment technologies. All of these vehicles have been tested for primary emissions. A subset of these vehicles (n=25) was tested for SOA formation in a smog chamber. Table B7.1 summarizes the information of the test fleet, primary emissions measurements and photo-oxidation experiments. The detailed description of the experimental setup and procedure has been provided elsewhere [Gordon et al., 2014; May et al., 2014]. Only a brief discussion is provided here.

For discussion, the 60 tested vehicles were categorized into four groups based on emission certification standards as 14 Pre-LEV vehicles (Tier0 and Tier1), 18 LEV vehicles (transitional low emission vehicles and low emission vehicles) and 19 ULEV vehicles (Ultra-low emission vehicles) and 9 SULEV vehicles (Super ultra-low and partial zero emission vehicles). The SULEV category includes both port and direct injection vehicles (Table B7.1). There are 6 vehicles whose specific emission standards were unknown. We have classified them as LEV vehicles if there are certificated as LEV I vehicles (n=3) and classified them as ULEV vehicles if these vehicles were certificated as LEV II vehicles (n=3). Our categorization reflects reductions in emissions due to the tightening of emissions standards (Fig. B3).

All vehicles were tested over a cold-start Unified Cycle (UC) using the same California commercial summer gasoline fuel. The UC is designed to mimic driving in the Southern California. The UC consists of three bags, similar to the Federal Test Procedure (FTP)-75, but is a more aggressive cycle with higher speeds, higher acceleration, fewer stops and less idling time. Two of these vehicles were also tested over a hot-start UC.

Quantification of IVOCs and SVOCs

IVOCs and SVOCs were characterized for a subset of vehicles [Y. Zhao et al., 2016] (Table B7.1). In brief, IVOCs and SVOCs were collected by sampling the dilute exhaust from the CVS through a quartz filter immediately followed by two adsorbent tubes (Gerstel 6 mm OD, 4.5 mm ID glass tube filled with ~290 mg of Tenax[®] TA), all connected in series. This sampling train was housed inside a temperature-controlled box, maintained at ~47°C mimicking the CFR86 protocol. Both adsorbent tubes and the quartz filters were analyzed by gas chromatography-mass spectrometry (GC/MS) (Agilent, 6890 GC/5975 MS) equipped with a Gerstel thermal desorption and injection system (Gerstel, Baltimore, MD) and a capillary column (Agilent HP-5MS, 30 m × 0.25 mm). The thermal desorption temperature was 275 °C for adsorbent tubes and 300 °C for quartz filters. The detailed description of quantification of IVOCs can be found elsewhere [Y. Zhao et al., 2016; Y. Zhao et al., 2014].

In this study, IVOCs were defined as the compounds in the retention-time range of C₁₂~C₂₂ n-alkanes desorbed from adsorbent tubes. The total IVOCs in each sample were quantified by binning the total ion chromatogram acquired during GC/MS analysis of the

adsorbent tube into 11 bins based on the retention time of C₁₂~C₂₂ n-alkanes. Each bin was centered at one n-alkane and defined the “B_n” bin where “n” was the carbon number of the n-alkane in that bin. The amount of IVOCs in each bin was determined by the total ion signal in that bin divided by the response factor of the n-alkane in that bin.

Speciation analysis of IVOCs was performed. Fifty-seven individual species, including n-alkanes, b-alkanes, cyclic alkanes and aromatics, were quantified. In sum, these compounds only accounted for 16±6% of total IVOCs [Y. Zhao et al., 2016]. The unspciated IVOCs, defined as the difference between total IVOCs and spciated IVOCs, were composed of a complex mixture of co-eluted compounds, which cannot be resolved on a molecular basis through the traditional GC/MS analysis. This material is often referred to as an unresolved complex mixture (UCM). These unspciated IVOCs were classified into unspciated b-alkanes and unspciated cyclic compounds in each retention-time based bin based on their mass spectra [Y. Zhao et al., 2016; Y. Zhao et al., 2014]. We present the emission factors of spciated IVOCs, unspciated b-alkanes and cyclic compounds in each of 11 bins.

SVOCs were defined as the compounds collected on quartz filters and two adsorbent tubes in the retention time range of C₂₃~C₃₂ n-alkanes. SVOCs desorbed from the quartz filters were quantified using the same approach as the one for IVOCs.

A different approach was used for quantification of SVOCs desorbed from adsorbent tubes. SVOCs desorbed from adsorbent tubes were quantified using m/z 57, instead of

the total ion signal, because of substantial interference of products from the reactions of NO_x and adsorbent Tenax TA [Kleno et al., 2002] on the total ion signal in this SVOC retention-time range and difficulty to separate the interference from signals produced by organics in tailpipe emissions. However, interference of these products on the signal of m/z 57 was negligible. In addition, the signal of m/z 57 was detected across the retention time range of SVOCs.

SVOCs desorbed from adsorbent tubes were quantified by binning the chromatogram of m/z 57 into 10 bins based on the retention time of $\text{C}_{23}\sim\text{C}_{32}$ n-alkanes with each bin centered at one n-alkane. The mass of m/z 57 in each bin was calculated using the response factor of m/z 57 determined by the n-alkane. The mass of m/z 57 in each bin was converted to total organics by assuming the fraction of m/z 57 in that bin to be same as the average fraction of m/z 57 in the same bin of SVOCs desorbed from quartz filters.

We did not characterize the chemical composition of SVOCs in this study. However, SVOCs are likely dominated by cyclic alkanes[Worton et al., 2014].

The emissions of speciated VOCs, IVOCs and SVOCs were not measured for all of tests (Table B7.1). However, the strong correlations of NMOG to speciated VOCs and IVOCs have been found and NMOG emissions have been quantified for all tests. For example, the linear regression yields the slope of 0.2 and $R^2=0.93$ for single-ring aromatic compounds versus NMOG and 0.04 and $R^2=0.92$ for IVOCs versus NMOG. For experiments where quantification of these precursors was not performed, emissions of

speciated VOCs and IVOCs are estimated based on NMOG emissions and the chemical composition of speciated VOCs and IVOCs is assumed to be same as the average chemical composition of measured VOCs and IVOCs.

SVOCs are a major component of POA and likely attributed to the lubricant oil[Worton et al., 2014], differing from single-ring aromatics and IVOCs originating from gasoline fuel. Measured SVOC emissions show the similar trend to POA emissions (Fig. B3D, Fig. B5), although a strong correlation was not found between SVOC and POA emissions. The SVOCs for the tests without SVOC measurements were estimated based on the median ratio between measured SVOCs and POA in each class of vehicles (0.85 for Pre-LEV, 1.25 for LEV, 1.19 for ULEV). POA was the organics collected by a bare quartz filter. For SULEV vehicles, the median SVOC-to-POA ratio for ULEV vehicles was used as ULEV and SULEV vehicles were new and met the same PM emission standard[CARB, 2012].

Vapor Wall Loss and Condensation Sink

The wall losses of condensable vapors during the smog-chamber experiments could lead to the underestimate of SOA production, which, in turn, underestimate the effective SOA yield[Zhang et al., 2014]. Although it is difficult to quantify the vapor wall losses, the consistency in vapor wall losses for experiments conducted in the same smog chamber can be assessed through the condensation sink of suspended particles. To examine whether higher effective SOA yields for LEV and ULEV vehicles than Pre-LEV vehicles

were caused by lower organic vapor wall losses, we have calculated the condensation sink caused by suspended particles for organic vapors following the approach of Saleh et al.[Saleh et al., 2013] and Trump et al.[Trump et al., 2014]. A smaller condensation sink of suspended particles indicates a larger fraction of organic vapors losing to the walls compared to their condensation onto suspended particles[Saleh et al., 2013].

To be conservative, we calculated the condensation sink of suspended particles at the end of photo-oxidation experiments, when the particle number concentration was lowest. The measured particle size distribution was used in the calculation. We assumed a mass accommodation coefficient of unity and an average molecular weight of organic vapors of 200 g/mol.

The average condensation sink in experiments for Pre-LEV vehicles ($0.44 \pm 0.33 \text{ min}^{-1}$) was comparable to the averages for LEV ($0.57 \pm 0.33 \text{ min}^{-1}$), ULEV vehicles ($0.39 \pm 0.19 \text{ min}^{-1}$) and SULEV vehicles ($0.37 \pm 0.23 \text{ min}^{-1}$). These comparisons indicate that higher effective SOA yields for LEV and ULEV vehicles than Pre-LEV vehicles were not due to the biases caused by organic vapor wall losses.

In this present study, we estimated the wall losses of condensable vapors by assuming that condensable vapors maintain equilibrium with both suspended and wall-bound particles (Method#1) to calculate SOA production. To evaluate performance of this method#1 in accounting for the vapor wall losses, we also estimated the condensable vapor losses to chamber walls by assigning a condensation sink to the chamber walls.

The condensation sink of the chamber walls was assumed to be in the range of 0.1 to 0.14 min⁻¹[Krechmer et al., 2016] (Method#2), which was determined using an 8 m³ smog chamber, similar to the size of our chamber. We assumed the accommodation coefficients of 0.1 and 1 for suspended particles.

Figure B7.6 compares SOA production after correcting for vapor wall losses calculated through the method#1 and #2 in a photo-oxidation experiment for a ULEV vehicle. Saleh et al.[Saleh et al., 2013] has reported a mass accommodation coefficient of order 0.1 for the SOA produced during alpha-pinene ozonolysis. The comparisons in Figure B7.6 show that our approach of determining SOA production (method#1) well accounts for vapor wall losses if the published condensation sink of the chamber walls[Krechmer et al., 2016] is applicable to our chamber.

Estimating SOA Production from VOCs, IVOCs and SVOCs

SOA production (ΔM) from a quantified SOA precursor (HC_i) over a period (Δt) is predicted by:

$$\Delta M = [HC_i] \times (1 - e^{-k_{OH,i} \times [OH] \times \Delta t}) \times Y_i$$

Where $[HC_i]$ is the initial concentration of a compound i in the chamber ($\mu\text{g m}^{-3}$); $k_{OH,i}$ is the OH reaction rate constant (25°C, molecules cm^{-3}); $[OH]$ is the concentration of hydroxyl radicals; Y_i is the SOA yield. The total SOA production is the sum of the SOA production from each compound. To estimate SOA production during each photo-oxidation experiment, the OH exposure ($[OH] \times \Delta t$) was calculated based on the decay of butanol-d₉ or aromatics for experiments with no addition of butanol-d₉. The SOA yield for each compound was derived based on published results from chamber experiments

and the wall-loss corrected OA concentration in the end of each experiment in this study. A detailed discussion of assigning surrogates to compounds, whose SOA yields have not investigated through photo-oxidation experiments, can be found elsewhere [Chan et al., 2009; Y. Zhao et al., 2016; Y. Zhao et al., 2014]. A brief description is provided below.

SOA Production from VOCs. Speciated VOCs considered as SOA precursors included benzene, ARO1, ARO2 and ALK5. The speciated VOCs included in ARO1, ARO2 and ALK5 were determined based on definitions given in the lumped SARPC-07 mechanisms [Carter, 2010]. The SOA yields for estimation of SOA from VOCs were derived from published CMAQ parameters in Carlton et al. [Carlton et al., 2010]. Some of the speciated VOCs in ARO1 and ARO2 were likely quantified as IVOCs. These speciated VOCs were removed from ARO1 and ARO2 to avoid double counting of the SOA precursors based on their retention time indices, although they accounted for less than 1%, on average, of species in ARO1 and ARO2.

SOA production from IVOCs. Estimation of SOA production from IVOCs follows the approach of Zhao et al. [Y. Zhao et al., 2016; Y. Zhao et al., 2014]. For speciated IVOCs, the OH rate constants are either taken from the literature [Atkinson and Arey, 2003] or calculated based on the structure-reactivity relationship [Kwok and Atkinson, 1995]. SOA yields are derived for each compound based on published results from photo-oxidation experiments [Cappa et al., 2013; Chan et al., 2009; Hunter et al., 2014; Lim and Ziemann, 2009; Presto et al., 2010]. For unspciated IVOCs, surrogate compounds are assigned to unspciated b-alkanes and unspciated cyclic compounds in each of 11

retention-time based bins to represent their OH rate constants and SOA yields (Table B7.2). The selection of surrogate compounds has accounted for the effects of molecular structure and volatility on OH reaction rate constants and SOA yields [Y. Zhao et al., 2016; Y. Zhao et al., 2014].

Both aromatic compounds and cyclic alkanes have been indicated as major contributors to unspciated cyclic compounds[Y. Zhao et al., 2016]. Therefore, two types of surrogate compounds (n-alkanes or naphthalenes) are used to bound the estimates of the SOA production from unspciated cyclic compounds. SOA production from unspciated cyclic compounds in this present study is considered as the average of SOA production estimated using n-alkanes and naphthalenes as surrogate compounds.

SOA production from SVOCs. SVOCs are a group of compounds defined based on the retention time of C₂₃~C₃₂ n-alkanes [Y. Zhao et al., 2015] and are likely dominated by cyclic alkanes [Worton et al., 2014]. In this study, SVOCs are considered as one lumped component with its SOA yield and OH reaction rate constant represented by the C₂₃ n-alkane.

Estimating SOA yields under high- and low-NO_x conditions. The SOA yields for VOCs (benzene, ARO1, ARO2 and ALK5) under high-NO_x conditions are derived based on results from Ng et al. [Ng et al., 2007] and Carlton et al. [Carter, 2010]. The SOA yields for IVOCs and SVOCs under high-NO_x conditions are derived based on results

from Chan et al. [Chan et al., 2009], Lim and Ziemann [Lim and Ziemann, 2009], Presto et al. [Presto et al., 2010] and Hunter et al. [Hunter et al., 2014].

The SOA yields for single-ring aromatic compounds and naphthalenes under low-NO_x conditions do not depend on the OA concentration [Chan et al., 2009; Ng et al., 2007].

There is limited data on the SOA yield for alkanes at low-NO_x conditions. Cappa et al. [Cappa et al., 2013] and Loza et al. [Loza et al., 2014] reported SOA yields for four C₁₂ alkanes (dodecane, 2-methyleundecane, cyclododecane and n-hexylcyclohexane) under low-NO_x conditions. No other data is available to derive the SOA yields under low-NO_x conditions for alkanes with larger carbon number, which are a major contributor to both IVOCs [Y. Zhao et al., 2016] and SVOCs [Worton et al., 2014]. For these four alkanes, the SOA yields at the OA concentration of 10 µg/m³ are similar under high- and low-NO_x conditions, except for cyclododecane [Cappa et al., 2013]. Cyclic alkanes in IVOC and SVOC range likely dominated by cyclic alkanes with one or more rings and one or more branched alkyl side chains [Gentner et al., 2012; Worton et al., 2014]. Alk5 is dominated by n- and b-alkanes (Figure 7.2A). Therefore, we assume that SOA yields for alkanes do not have NO_x dependence (they are the same for low and high NO_x conditions).

Effective SOA Yield. The effective SOA yield in each experiment is calculated using the measured SOA divided by the reacted SOA precursors, including VOCs (benzene, ARO1, ARO2 and ALK5), IVOCs and SVOCs at the end of the experiment. The chemical composition of SOA precursors is accounted for in the calculations through OH

rate constants of individual compounds and lumped components. The OH rate constants used for individual species and lumped components have been discussed above.

References:

- Atkinson, R., and J. Arey (2003), Atmospheric degradation of volatile organic compounds, *Chem. Rev.* (Washington, DC, U. S.), 103(12), 4605-4638.
- Cappa, C. D., X. Zhang, C. L. Loza, J. S. Craven, L. D. Yee, and J. H. Seinfeld (2013), Application of the Statistical Oxidation Model (SOM) to Secondary Organic Aerosol formation from photooxidation of C-12 alkanes, *Atmos. Chem. Phys.*, 13(3), 1591-1606.
- CARB (2012), California Air Resources Board, "LEV III" Amendments to the California Greenhouse Gas and Criteria Pollution Exhaust and Evaporative Emission Standards and Test Procedures and to the On-Board Diagnostic System Requirements for Passenger Cars, Light-Duty Trucks, and Medium-Duty Vehicles, and to the Evaporative Emission Requirements for Heavy-Duty Vehicles. <http://www.arb.ca.gov/regact/2012/leviiiighg2012/levfrorev.pdf>, edited.
- Carlton, A. G., P. V. Bhave, S. L. Napelenok, E. D. Edney, G. Sarwar, R. W. Pinder, G. A. Pouliot, and M. Houyoux (2010), Model Representation of Secondary Organic Aerosol in CMAQv4.7, *Environ. Sci. Technol.*, 44(22), 8553-8560.
- Carter, W. P. L. (2010), Development of the SAPRC-07 chemical mechanism, *Atmos. Environ.*, 44(40), 5324-5335.
- Chan, A. W. H., K. E. Kautzman, P. S. Chhabra, J. D. Surratt, M. N. Chan, J. D. Crouse, A. Kurten, P. O. Wennberg, R. C. Flagan, and J. H. Seinfeld (2009), Secondary organic aerosol formation from photooxidation of naphthalene and alkylnaphthalenes: implications for oxidation of intermediate volatility organic compounds (IVOCs), *Atmos. Chem. Phys.*, 9(9), 3049-3060.
- Gentner, D. R., et al. (2012), Elucidating secondary organic aerosol from diesel and gasoline vehicles through detailed characterization of organic carbon emissions, *Proc. Natl. Acad. Sci. U. S. A.*, 109(45), 18318-18323.
- Gordon, T. D., et al. (2014), Secondary organic aerosol formation exceeds primary particulate matter emissions for light-duty gasoline vehicles, *Atmos. Chem. Phys.*, 14(9), 4661-4678.
- Hunter, J. F., A. J. Carrasquillo, K. E. Daumit, and J. H. Kroll (2014), Secondary Organic Aerosol Formation from Acyclic, Monocyclic, and Polycyclic Alkanes, *Environmental Science and Technology*, 48, 10227-10234.
- Kleno, J. G., P. Wolkoff, P. A. Clausen, C. K. Wilkins, and T. Pedersen (2002), Degradation of the adsorbent Tenax TA by nitrogen oxides, ozone, hydrogen peroxide, OH radical, and limonene oxidation products, *Environ. Sci. Technol.*, 36(19), 4121-4126.
- Krechmer, J. E., D. Pagonis, P. J. Ziemann, and J. L. Jimenez (2016), Quantification of Gas-Wall Partitioning in Teflon Environmental Chambers Using Rapid Bursts of Low-Volatility Oxidized Species Generated in Situ, *Environ. Sci. Technol.*, 50(11), 5757-5765.
- Kwok, E. S. C., and R. Atkinson (1995), Estimation of Hydroxyl Radical Reaction-Rate Constants for Gas-Phase Organic-Compounds Using a Structure-Reactivity Relationship - an Update, *Atmos. Environ.*, 29(14), 1685-1695.
- Lim, Y. B., and P. J. Ziemann (2009), Effects of Molecular Structure on Aerosol Yields from OH Radical-Initiated Reactions of Linear, Branched, and Cyclic Alkanes in the Presence of NO_x, *Environ. Sci. Technol.*, 43(7), 2328-2334.

Loza, C. L., et al. (2014), Secondary organic aerosol yields of 12-carbon alkanes, *Atmos. Chem. Phys.*, 14(3), 1423-1439.

May, A. A., et al. (2014), Gas- and particle-phase primary emissions from in-use, on-road gasoline and diesel vehicles, *Atmos. Environ.*, 88, 247-260.

Ng, N. L., J. H. Kroll, A. W. H. Chan, P. S. Chhabra, R. C. Flagan, and J. H. Seinfeld (2007), Secondary organic aerosol formation from m-xylene, toluene, and benzene, *Atmos. Chem. Phys.*, 7(14), 3909-3922.

Presto, A. A., M. A. Miracolo, N. M. Donahue, and A. L. Robinson (2010), Secondary Organic Aerosol Formation from High-NO_x Photo-Oxidation of Low Volatility Precursors: n-Alkanes, *Environ. Sci. Technol.*, 44(6), 2029-2034.

Saleh, R., N. M. Donahue, and A. L. Robinson (2013), Time Scales for Gas-Particle Partitioning Equilibration of Secondary Organic Aerosol Formed from Alpha-Pinene Ozonolysis, *Environ. Sci. Technol.*, 47(11), 5588-5594.

Trump, E. R., I. Riipinen, and N. M. Donahue (2014), Interactions between atmospheric ultrafine particles and secondary organic aerosol mass: a model study, *Boreal Environment Research*, 19(5-6), 352-362.

Worton, D. R., G. Isaacman, D. R. Gentner, T. R. Dallmann, A. W. H. Chan, C. Ruehl, T. W. Kirchstetter, K. R. Wilson, R. A. Harley, and A. H. Goldstein (2014), Lubricating Oil Dominates Primary Organic Aerosol Emissions from Motor Vehicles, *Environ. Sci. Technol.*, 48(7), 3698-3706.

Zhang, X., C. D. Cappa, S. H. Jathar, R. C. McVay, J. J. Ensberg, M. J. Kleeman, and J. H. Seinfeld (2014), Influence of vapor wall loss in laboratory chambers on yields of secondary organic aerosol, *Proc. Natl. Acad. Sci. U. S. A.*, 111, 5802-5807.

Zhao, Y., N. T. Nguyen, A. A. Presto, C. J. Hennigan, A. A. May, and A. L. Robinson (2015), Intermediate Volatility Organic Compound Emissions from On-Road Diesel Vehicles: Chemical Composition, Emission Factors, and Estimated Secondary Organic Aerosol Production, *Environ. Sci. Technol.*, 49(19), 11516-11526.

Zhao, Y., N. T. Nguyen, A. A. Presto, C. J. Hennigan, A. A. May, and A. L. Robinson (2016), Intermediate Volatility Organic Compound Emissions from On-Road Gasoline Vehicles and Small Off-Road Gasoline Engines, *Environ. Sci. Technol.*, 50, 4554-4563.

Zhao, Y., C. J. Hennigan, A. A. May, D. S. Tkacik, J. A. de Gouw, J. B. Gilman, W. C. Kuster, A. Borbon, and A. L. Robinson (2014), Intermediate-Volatility Organic Compounds: A Large Source of Secondary Organic Aerosol, *Environ. Sci. Technol.*, 48(23), 13743-13750.

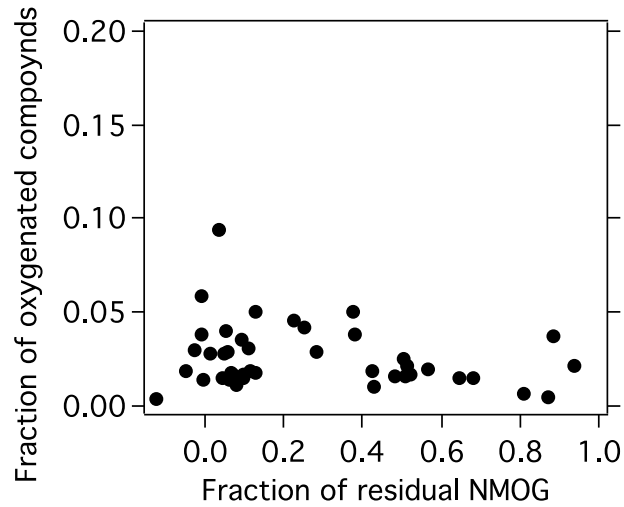


Figure D7.1. Fraction of total oxygenated compounds in NMOG as a function of the fraction of the residual NMOG. The data points here only include tests in which all measurements of VOCs, IVOCs, SVOCs and oxygenated compounds have been carried out.

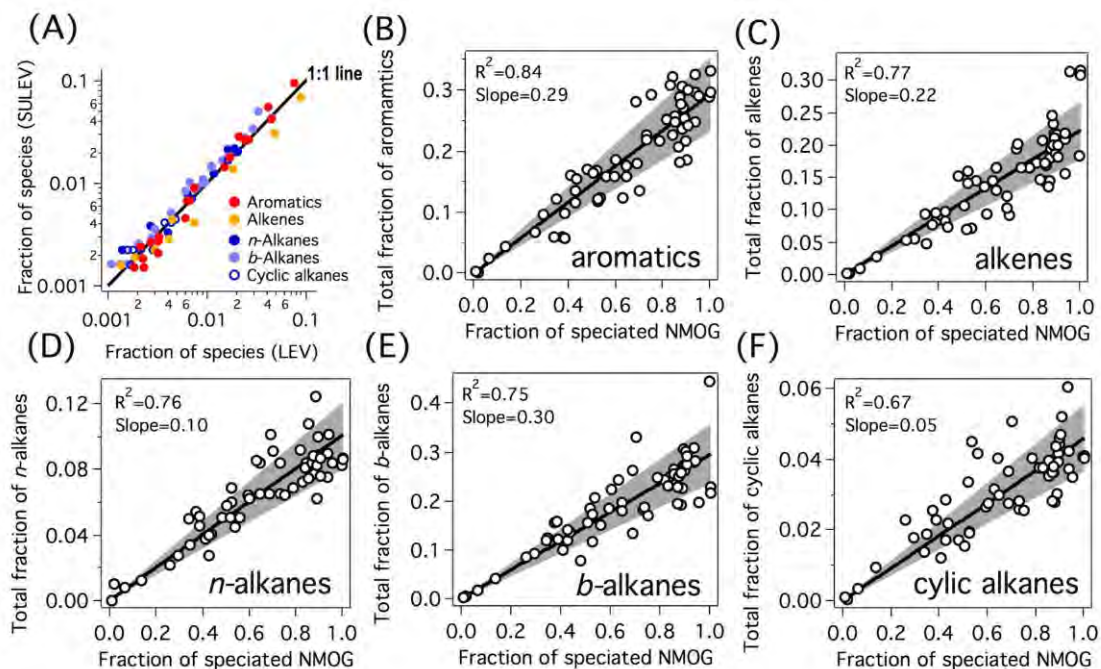


Figure D7.2. (A) Comparison between a SULEV vehicle and a LEV vehicle for their speciated VOCs. The fraction of speciated VOCs in total NMOG is 35% for the SULEV vehicle and 91% for the LEV vehicle. This comparison includes 66 species in total speciated VOCs, including 20 aromatic compounds, 12 alkenes, 9 *n*-alkanes, 28 *b*-alkanes and 11 cyclic alkanes, showing the consistency in the composition of the organic emissions between vehicles in spite of the fractions of speciated VOCs. (B)-(F) Correlation of total speciated VOCs with the sum of species in each major component: (B) single-ring aromatics (SRA), (C) alkenes, (D) *n*-alkanes, (E) *b*-alkanes and (F) cyclic alkanes. All data are presented as their fractions in total NMOGs. Each symbol represents one test. The grey-shaded area in (B)-(F) indicates the 20% range of the slope. The strong correlations showed in (B)-(F) further support the conclusion that the chemical composition of speciated VOCs is consistent across all tests.

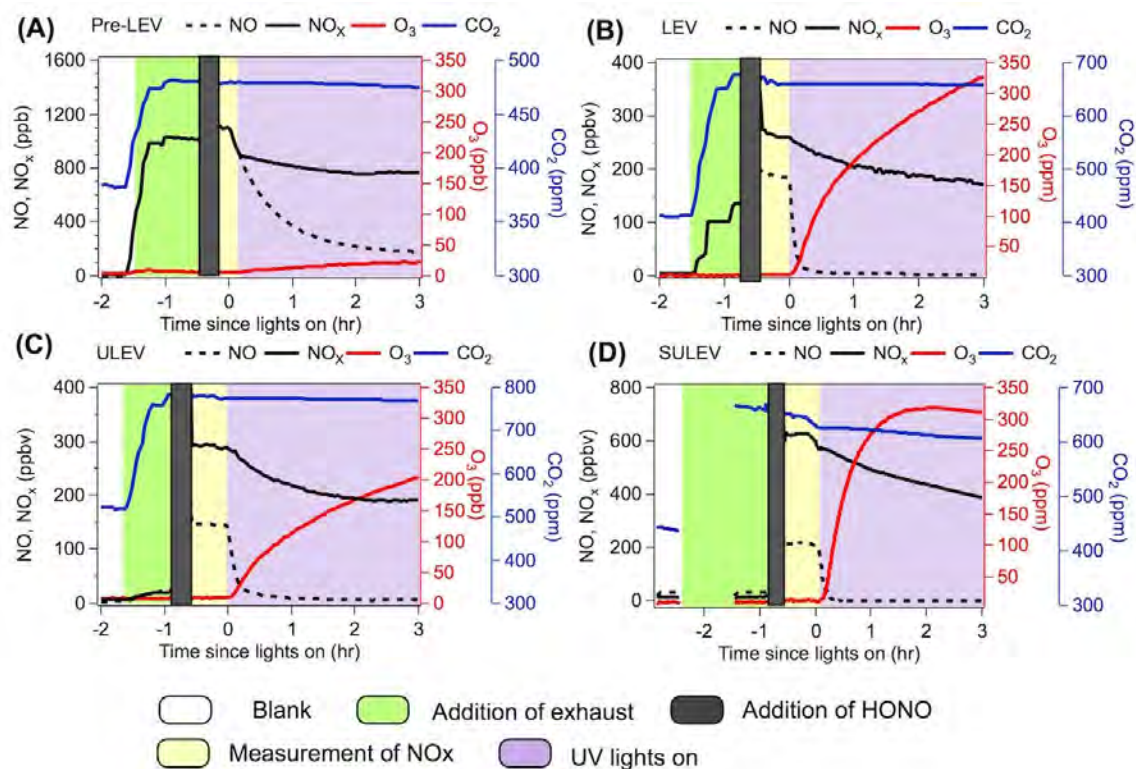


Figure D7.3. Time series of gases during chamber experiments. The addition of exhaust was not observed during the experiments with SULEV vehicles because the gas monitors were sampling from a potential aerosol mass reactor during addition of exhaust into the chamber. The concentrations of gases in the exhaust were still measured before the UV lights were turned on to initiate the photo-oxidation.

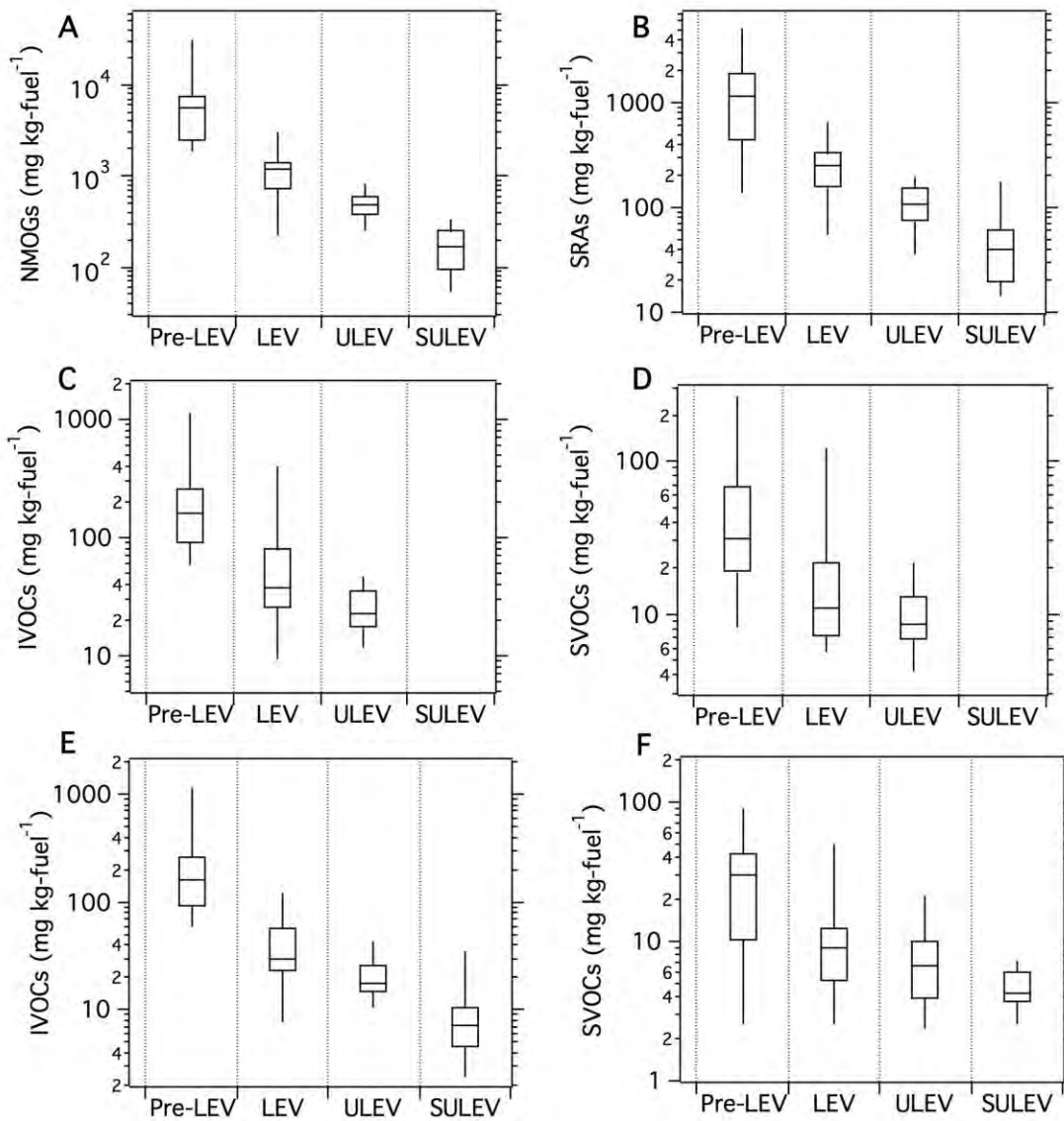


Figure D7.4. NMOG and SOA precursor emission factors for all tested vehicles. The boxes represent the 75th and 25th percentiles with the centerline being the median. The whiskers are the 90th and 10th percentiles. Table B7.1 compiled the measurements of SOA precursors (Single-ring aromatic compounds (SRA), IVOCs and IVOCs) conducted for each test. The SOA production from SRAs accounts for 98%±2% under high-NO_x conditions and 99%±1% of predicted SOA production from speciated VOCs. (A)~(D) present the measured data. (E) and (F) present the combination of measured and estimated data of IVOCs and SVOCs.

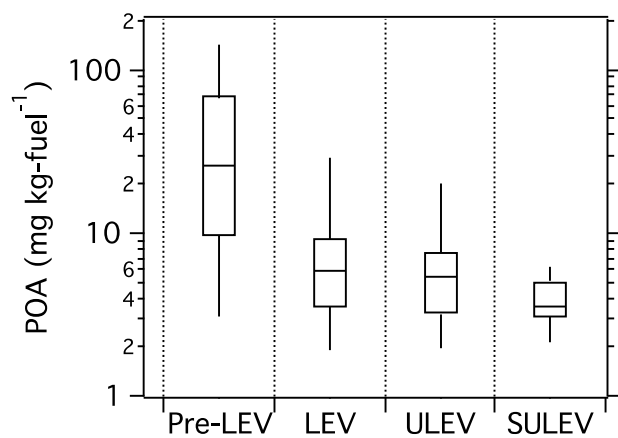


Figure D7.5. POA emission factors for all tested vehicles. POA is defined as the organics collected by a bare quartz filter.

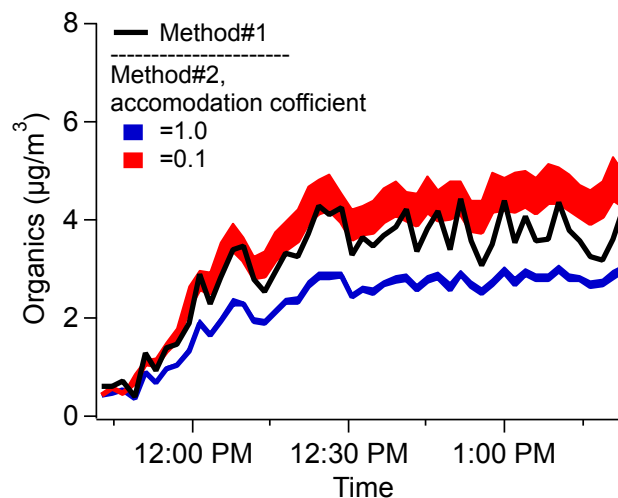


Figure D7.6. SOA production calculated using different approaches to correct for vapor wall losses in a photo-oxidation experiment for a ULEV vehicle. Method#1 assumes that condensable vapors maintain equilibrium with both suspended and wall-bound particles. Method#2 estimates the vapor wall losses based on the condensation sink of suspended particles and chamber walls. The mass accommodation coefficients of 0.1 and 1 are used for suspended particles in Method#2. The shaded areas indicate the estimated SOA production range when the condensation sink of the chamber walls is between 0.10 and 0.14 min^{-1} for each mass accommodation coefficient.

Table D7.1. Summary of the test fleet and measurements.

Test ID ¹	Vehicle name	Vehicle class ²	Model year	Engine size (L)	Certification	Fuel Economy (MPG)	Test cycle	Note ³
1027837	PreLEV-1	PC	1996	2.7	Tier I	20.01	Cold UC	a,b,c
1027852	ULEV-13	LDT	2010	3.6	ULEV; Tier II	15.61	Cold UC	a,b,c
1027859	PreLEV-1	PC	1996	2.7	Tier I	20.39	Cold UC	a,b
1027863	ULEV-3	PC	2008	1.6	LEV2, ULEV; Tier II, Bin 5	25.54	Cold UC	a,b,c
1027872	PreLEV-7	PC	1993	4.9	Tier I	13.09	Cold UC	a,b,c
1027905	ULEV-6	PC	2009	2	LEV2, ULEV; Tier II, Bin 5	19.75	Cold UC	a,b,c
1027906	LEV-13	PC	2008	3.6	LEV2; Tier II, Bin 5	18.59	Cold UC	a,b
1027907	ULEV-8	PC	2009	2.4	LEV2, ULEV	18.75	Cold UC	a,b,c
1027908	LEV-17	PC	2004	2.2	LEV2; Tier II, Bin 8	24.68	Cold UC	b,c
1027918	LEV-10	PC	2003	3.5	LEV1, NLEV	18.31	Cold UC	a,b,c
1027920	PreLEV-13	PC	1991	3.8	Tier I	18.46	Cold UC	a,b,c
1027921	PreLEV-6	PC	1992	3.8	Tier I	17.97	Cold UC	a,b,c
1027969	LEV-3	PC	2000	3.5	LEV1	18.81	Cold UC	b,c
1027970	ULEV-1	PC	2003	1.8	LEV1, ULEV	26.78	Cold UC	a,b,c
1027971	ULEV-13	LDT	2010	3.6	ULEV; Tier II	15.78	Cold UC	a,b,c,d
1027973	ULEV-2	PC	2005	1.8	LEV2, ULEV; Tier II, Bin 5	26.23	Cold UC	a,b,c
1027975	LEV-2	LDT	1999	4	LEV1, NLEV	16.39	Cold UC	a,b
1027976	PreLEV-3	PC	1994	1.9	LEV1; Tier I	21.67	Cold UC	b,c
1027977	ULEV-4	PC	2008	2.7	LEV2	17.78	Cold UC	b,c
1027978	LEV-12	LDT	2005	2.7	LEV2; Tier II, Bin 5	19.31	Cold UC	b
1028021	ULEV-5	LDT	2009	5.7	Tier II	13.78	Cold UC	a,b,c
1028022	ULEV-7	LDT	2008	4.2	LEV2	15.44	Cold UC	a,b,d

Test ID ¹	Vehicle name	Vehicle clasB2	Model year	Engine size (L)	Certification	Fuel Economy (MPG)	Test cycle	NoteB3
1028023	PreLEV-2	PC	2003	3	LEV1; Tier I	17.31	Cold UC	a,b,c
1028027	LEV-1	PC	1998	1.8	LEV1, TLEV	27.31	Cold UC	a,b
1028029	PreLEV-5	PC	1992	3.4	Tier I	15.70	Cold UC	a,b
1028075	LEV-3	PC	2000	3.5	LEV1	20.12	Cold UC	a,b,c
1032282	SULEV-2	PC	2012	2	PZEV	16.05	Cold UC	a,b
1032283	ULEV-10	PC	2012	3.6	ULEV	19.62	Cold UC	a,b,d
1032302	LEV-4	PC	1997	3	LEV	19.34	Cold UC	a,b,c
1032303	PreLEV-10	PC	1990	5	Tier I	13.06	Cold UC	b,c,d
1032304	LEV-4	PC	1997	3	LEV	19.21	Cold UC	a,b,c,d
1032309	ULEV-16	PC	2011	3.6	LEV2, ULEV	15.76	Cold UC	a,b,c,d
1032310	ULEV-9	PC	2011	n/a	LEV2, ULEV	20.38	Cold UC	a,b
1032320	LEV-18	PC	1991	3.8	LEV	19.36	Cold UC	a,b,c
1032321	ULEV-14	PC	2011	2	ULEV	15.92	Cold UC	a,b,c,d
1032342	ULEV-14	PC	2011	2	ULEV	21.09	Cold UC	a,b,c,d
1032346	LEV-7	PC	1998	3	LEV	18.78	Cold UC	a,b,d
1032351	ULEV-14	PC	2011	2	ULEV	22.30	Cold UC	a,b,d
1032360	ULEV-11	PC	2008	3.5	LEV2	20.44	Hot UC	a,b,c,d
1032383	ULEV-11	PC	2008	3.5	LEV2	15.24	Cold UC	a,b,c
1032388	LEV-5	PC	2001	2.2	LEV	21.81	Cold UC	a,b,c
1032392	PreLEV-11	PC	1989	1.3	Tier I	27.21	Cold UC	a,b,c
1032393	LEV-9	PC	1999	2	TLEV	23.57	Cold UC	a,b,c,d
1032394	LEV-6	PC	2002	5.7	LEV	N/A	Cold UC	b,c
1032428	LEV-11	N/A	N/A	N/A	N/A	N/A	Cold UC	b,c
1032440	PreLEV-9	PC	1988	1.6	Tier I	24.12	Cold UC	b,c,d

Test ID ¹	Vehicle name	Vehicle clasB2	Model year	Engine size (L)	Certification	Fuel Economy (MPG)	Test cycle	NoteB3
1032442	PreLEV-4	PC	1987	4.1	Tier I	14.58	Cold UC	a,b,c
1032443	PreLEV-14	PC	1991	4	Tier I	16.45	Cold UC	a,b,c
1032444	PreLEV-9	PC	1988	1.6	Tier I	23.78	Cold UC	a,b,c
1032445	PreLEV-8	LDT	1993	4.3	Tier I	14.98	Cold UC	a,b,c
1032472	LEV-6	PC	2002	5.7	LEV	9.72	Cold UC	a,b,c
1032473	LEV-4	PC	1997	3	LEV	19.05	Hot UC	a,b,d
1038708	SULEV-3	PC (GDI)	2012	2	SULEV	23.76	Cold UC	a
1038723	SULEV-8	PC (GDI)	2014	3.5	LEV2, SULEV	19.84	Cold UC	a,d
1038724	SULEV-9	PC (GDI)	2012	2.4	SULEV	21.08	Cold UC	d
1038747	SULEV-4	PC (GDI)	2013	1.4	PZEV	36.72	Cold UC	a,d
1038755	SULEV-5	PC	2012	2.5	PZEV	35.17	Cold UC	a,d
1038801	ULEV-17	PC (GDI)	2013	1.6	ULEV	27.50	Cold UC	a,d
1038821	LEV-14	PC	2008	3.9	LEV2 LEV	15.80	Cold UC	a
1038822	ULEV-18	PC (GDI)	2013	1.6	LEV2, ULEV	23.66	Cold UC	a,d
1038824	ULEV-12	LDT	2013	5.3	ULEV	12.78	Cold UC	a
1038825	LEV-16	PC (GDI)	2012	1.6	LEV2, LEV	24.48	Cold UC	a,d
1038827	ULEV-15	PC (GDI)	2013	2	LEV2, ULEV	26.32	Cold UC	a
1038848	LEV-14	PC	2008	3.9	LEV2, LEV	15.76	Cold UC	d
1038849	LEV-14	PC	2008	3.9	LEV2, LEV	15.64	Cold UC	a
1038853	SULEV-1	PC (GDI)	2014	2.4	PZEV	6.92	Cold UC	d
1038862	SULEV-6	PC (GDI)	2013	3.6	LEV2, SUL	16.86	Cold UC	a,d
1038867	SULEV-7	PC (GDI)	2012	2.4	PZEV	21.55	Cold UC	a,d
1038891	LEV-8	M3	2003	5.4	LEV	11.43	Cold UC	a,d
1038901	PreLEV-12	PC	1990	3.8	TIER0	17.65	Cold UC	a,d

Test ID ¹	Vehicle name	Vehicle clasB2	Model year	Engine size (L)	Certification	Fuel Economy (MPG)	Test cycle	NoteB3
1038909	ULEV-19	PC (GDI)	2013	2	ULEV	19.42	Cold UC	a
1038917	ULEV-12	LDT	2013	5.3	ULEV	12.93	Cold UC	a
1038918	ULEV-12	LDT	2013	5.3	ULEV	12.73	Cold UC	d
1038920	SULEV-1	PC (GDI)	2014	2.4	PZEV	23.39	Cold UC	a,d
1038945	ULEV-12	LDT	2013	5.3	ULEV	12.60	Cold UC	a
1038947	ULEV-18	PC (GDI)	2013	1.6	LEV2, ULEV	23.81	Cold UC	a,d
1038952	SULEV-6	PC (GDI)	2013	3.6	LEV2, SULEV	17.52	Cold UC	a,d
1038980	LEV-15	PC	2007	1.8	LEV2, LEV	25.18	Cold UC	a

¹ The tests with their test IDs ranging 1027837 to 1032473 have been reported in May et al. (2), Zhao et al. (3), and Gordon et al. (1). The tests with test IDs ranging from 1038708 to 1038980 were newly conducted with a focus on newer vehicles (ULEV and SULEV).

² PC: passenger car; LDT: light-duty truck; GDI: gasoline direct injection

³ Note: Different measurements have been carried out for each test: "a" refers to speciated analysis of NMOGs; "b" and "c" refer to quantification of IVOCs and SVOCs; and "d" refers to photo-oxidation experiments

Table D7.2. Surrogate compounds for predicting SOA production from unspciated IVOCs.
Table D7.2a. Surrogate compounds (n-alkanes) used for OH reaction rate constants ($\text{cm}^3 \text{ molec}^{-1} \text{ s}^{-1}$) and SOA yields of unspciated IVOC bins for the IVOC-cyclic case.

Bin#	OH rate constant	Surrogate compounds for SOA yields	
		Unspciated b-alkanes	Unspciated cyclic compounds (IVOC-cyclic)
B12	C12	C10	C12
B13	C13	C11	C13
B14	C14	C12	C14
B15	C15	C13	C15
B16	C16	C14	C16
B17	C17	C15	C17
B18	C18	C16	C18
B19	C19	C17	C19
B20	C20	C18	C20
B21	C21	C19	C21
B22	C22	C20	C22

Table D7.2b. Surrogate compounds (n-alkanes and naphthalenes) for OH reaction rate constants ($\text{cm}^3 \text{ molec}^{-1} \text{ s}^{-1}$) and SOA yields of unspciated cyclic compounds in each IVOC bin for the IVOC-aromatic case.

Bin#	OH rate constant	Unspciated cyclic compounds (IVOC-aromatic)
B12	Naphthalene	Naphthalene
B13	C1-naphthalene	2-Methylnaphthalene
B14	C2-naphthalene	1,2-Dimethylnaphthalene
B15	C3-naphthalene	C15
B16	C4-naphthalene	C16
B17	C17	C17
B18	C18	C18
B19	C19	C19
B20	C20	C20
B21	C21	C21
B22	C22	C22